MONASH University

Biased Allosteric Modulators of Metabotropic Glutamate Receptor 5

Kathy Sengmany

Bachelor of Pharmacy (Hons)

A thesis submitted for the degree of Doctor of Philosophy at
Monash University in 2018
Drug Discovery Biology, Monash Institute of Pharmaceutical Sciences

Copyright notice

Table of Contents

Abstract

The metabotropic glutamate receptor subtype 5 ($mGlu_5$) is a Class C G protein-coupled receptor (GPCR) widely expressed throughout the central nervous system (CNS), and subsequently implicated in various CNS disorders. Newer paradigms in drug design have targeted allosteric binding sites within GPCRs, sites topographically distinct from orthosteric sites. This allows for greater selectivity between receptor subtypes and temporal fine-tuning of receptor activity. The tractability of $mGlu_5$ as a CNS drug target has seen a rise in $mGlu_5$ allosteric ligands – broadly classified as positive, negative and neutral allosteric modulators or ligands. However, with increased understanding of both drug and receptor pharmacology, these classifications remain insufficient to capture the full scope of ligand activity. Herein underlies the notion of signalling bias, whereby binding of a ligand may emphasise or diminish distinct receptor signalling pathways at the exclusion of others. Therefore, each ligand has a characteristic signalling fingerprint, in which a unique receptor conformation is achieved upon ligand binding. Further, probe dependence, where the cooperativity of the allosteric ligand may be influenced by the choice of orthosteric ligand studied in conjunction, provides another layer of complexity in understanding full drug pharmacology.

Current classifications of $mGlu_5$ allosteric ligands are based largely on their modulatory actions on the canonical signalling pathway of intracellular calcium mobilisation. However, increasing evidence suggests pleotropic coupling of the $mGlu_5$ receptor, suggesting the potential of unappreciated signalling bias of allosteric ligands. The first two studies (Chapter 2 and 3) aim to determine the signalling fingerprint of various chemically and pharmacologically diverse $mGlu_5$ allosteric

modulators, to test the hypothesis that these compounds display biased agonism and/or modulation. $mGlu_5$ allosteric ligands broadly categorised as PAMs or NAMs were assessed at calcium mobilisation, inositol phosphate-1 (IP_1) accumulation and extracellular-signal regulated kinases (ERK) 1/2 phosphorylation in both recombinant systems and cortical cultures. Biased agonism and modulation was determined via robust pharmacological quantification using the method proposed by Kenakin *et al.* 2012, and the operational model of allosteric modulation, and shown to be operative with $mGlu_5$ allosteric ligands in both recombinant and neuronal cell systems.

Following on from the first study in Chapter 2, the structural basis of $mGlu_5$ ligand bias was investigated through point mutations within the PAM allosteric binding pocket. In Chapter 4, seven distinct mutations, chosen based on alterations to affinity and efficacy of select PAMs in calcium signalling (Gregory *et. al.,* 2013), were assessed. Four $mGlu_5$ allosteric ligands, displaying distinct signalling fingerprints, were evaluated at calcium mobilisation, IP_1 accumulation and ERK1/2 phosphorylation against the orthosteric ligand DHPG. Signalling fingerprints were quantified at each mutation and provided insight into key residues involved in ligand-receptor interactions.

The final study of this thesis (Chapter 5) focused on $mGlu_5$ modulation of the co-localised transient receptor potential cation channel subfamily V member 1 (TRPV1) calcium responses in rat dorsal root ganglion (DRG) neurons. Within the peripheral system, $mGlu_5$ localisation in DRG is implicated in both inflammatory and neuropathic pain, with injury within nerves, spinal cord or peripheral tissues resulting in the release of glutamate from sensory neurons. Modulation of endovanilloid-

mediated TRPV1 responses were assessed following pre-incubation with $mGlu_5$ ligand, via calcium imaging. Four hour pre-incubation with glutamate, DHPG, and several allosteric ligands did not show significant effects on calcium responses generated by the prototypical TRPV1 agonist capsaicin, as well as the endovanilloids, anandamide, oleoylethanolamide and *N*-arachidonoyl dopamine. Despite these findings, the interaction between $mGlu_5$ and TRPV1 warrants further study to greater understand the relationship between the two receptors.

The work presented within this thesis has increased the understanding of $mGlu_5$ allosteric ligand activity, highlighting the need to assess multiple signalling endpoints, rather than simply the canonical pathway, to encapsulate full ligand activity. With increased understanding of receptor structure, and the associated conformations linked to various signalling endpoints, there remains the exciting possibility of designing therapies with increased receptor subtype selectivity, but also selectivity for desired signalling endpoints at the target receptor.

Declaration

This thesis contains no material which has been accepted for the award of any other degree or diploma at any university or equivalent institution and that, to the best of my knowledge and belief, this thesis contains no material previously published or written by another person, except where due reference is made in the text of the thesis.

Signature: 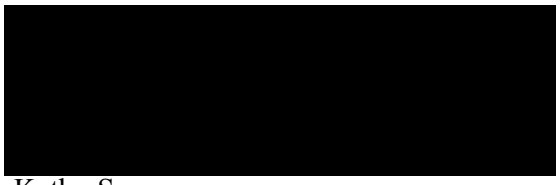

Print Name: Kathy Sengmany

Date: 26 March 2018

Publications during enrolment

Sengmany, K., Gregory, K. J., 2016. Metabotropic glutamate receptor subtype 5: molecular pharmacology, allosteric modulation and stimulus bias. Br J Pharmacol 173, 3001-3017.

Sengmany, K., Singh, J., Stewart, G. D., Conn, P. J., Christopoulos, A., Gregory, K. J., 2017. Biased allosteric agonism and modulation of metabotropic glutamate receptor 5: Implications for optimizing preclinical neuroscience drug discovery. Neuropharmacology 115, 60-72.

Sengmany K., Gregory K.J. (2018) Drugs to Tune Up Glutamatergic Systems: Modulators of Glutamate Metabotropic Receptors. In: Parrot S., Denoroy L. (eds) Biochemical Approaches for Glutamatergic Neurotransmission. Neuromethods, vol 130. Humana Press, New York, NY

Thesis including published works declaration

I hereby declare that this thesis contains no material which has been accepted for the award of any other degree or diploma at any university or equivalent institution and that, to the best of my knowledge and belief, this thesis contains no material previously published or written by another person, except where due reference is made in the text of the thesis.

This thesis includes three original papers published in peer reviewed journals. The core theme of the thesis is "Biased Allosteric Modulators of Metabotropic Glutamate Receptor 5". The ideas, development and writing up of all the papers in the thesis were the principal responsibility of myself, the student, working within the Drug Discovery Biology theme under the supervision of Dr Karen Gregory and Professor Arthur Christopoulos.

The inclusion of co-authors reflects the fact that the work came from active collaboration between researchers and acknowledges input into team-based research.

In the case of Chapters 1, 2 and 3 my contribution to the work involved the following:

Thesis Chapter	Publication Title	Status	Nature and % of student contribution	Co-author name(s) Nature and % of Co-author's contribution*	Co-author (s), Monash student Y/N*
Chapter 1	Metabotropic glutamate receptor subtype 5: molecular pharmacology, allosteric modulation and stimulus bias	Published	Wrote and proofed the manuscript (60%)	KJG co-wrote and proofed the manuscript (40%)	No
Chapter 1	Drugs to Tune Up Glutamatergic Systems: Modulators of Glutamate Metabotropic Receptors	Published	Wrote and proofed the manuscript (80%)	KJG co-wrote and proofed the manuscript (20%)	No

Chapter 2	Biased allosteric agonism and modulation of metabotropic glutamate receptor 5: Implications for optimizing preclinical neuroscience drug discovery	Published	Performed the majority of experiments, analysed and interpreted data, wrote and proofed the manuscript. (80%)	1) JS performed VU0360172 interaction experiments (2%) 2) GDS optimised and aided culturing of cortical neurons (1%) 3) PJC provided allosteric ligands (1%) 4) AC (6%) and 5) KJG (10%) conceived and supervised the project, performed data analysis and wrote the manuscript.	Yes No No No No
Chapter 3	Kinetic and system bias as drivers of biased metabotropic glutamate receptor 5 allosteric modulation	For submission	Designed and performed experiments, analysed and interpreted data, wrote and proofed the manuscript (70%).	1) SA performed interaction experiments and aided neuron culture (10%), 2) SDH aided culturing of cortical neurons and performed a selection of experiments (5%) 3) TW select performed radioligand binding experiments (0.5%) 4) PJC provided allosteric ligands (0.5%) 5) LTM (0.5%) 6) AC (2%) 7) KL (4%) 8) KJG (7.5%) conceived and/or supervised the study and co-written and edited the manuscript	No No Yes No No No No No

I have renumbered sections of submitted or published papers in order to generate a consistent presentation within the thesis.

Student signature: [redacted] **Date:** 24-March-2018

The undersigned hereby certify that the above declaration correctly reflects the nature and extent of the student's and co-authors' contributions to this work. In instances where I am not the responsible author I have consulted with the responsible author to agree on the respective contributions of the authors.

Main Supervisor signature: [redacted] **Date:** 24-March-2018

Acknowledgements

Firstly, I would like to thank my supervisors Dr Karen J Gregory and Professor Arthur Christopoulos, as well as my University of Nottingham supervisor A/Prof Steve Alexander, for their guidance and support throughout my PhD.

I would also like to thank my thesis panel members: Dr Michelle Halls, Professor David Adams, Dr Christopher Langmead and Dr Elva Zhao for their expertise throughout my candidature. I would like to acknowledge Professor Jeffery Conn and Vanderbilt University for the provision of $mGlu_5$ compounds used within this thesis.

This thesis would not have been possible without the financial support of the Australian Postgraduate Award and the generous Vaughan Williams top up scholarship provided by Monash University.

I would further like to extend my thanks to the Class C group – in particular, Sabine Albold, Shane Hellyer and Amy Chen, for their practical support and discussions of all experimental matters, and Dr Katie Leach for her extensive GPCR expertise.

Finally, to my friends and family, thank you for your unwavering support throughout the four years. Especially to Eevon Moo and Sheng Yu for being my family in Melbourne, and Peter Gowler for being my family in Nottingham.

Abbreviations

7TMs	seven transmembrane-spanning domains
AEA	anandamide
ANOVA	analysis of variance
BSA	bovine serum albumin
cAMP	cyclic adenosine monophosphate
CDPPB	3-Cyano-*N*-(1,3-diphenyl-1*H*-pyrazol-5-yl)benzamide
CPPHA	*N*-(4-chloro-2-[(1,3-dioxo-1,3-dihydro-2*H*-isoindol-2-yl)methyl]phenyl)-2-hydroxybenzamide
CGRP	calcitonin-gene-related-peptide
CHO	Chinese hamster ovary
CNS	central nervous system
cpd	compound
CPCCOEt	7-(hydroxyimino)cyclopropa[*b*] chromen-1a-carboxylate ethyl ester
DAG	diacylglcerol
DFB	((3-Fluorophenyl)methylene)hydrazone-3-fluorobenzaldehyde
DHPG	(*S*)-3,5-dihydroxyphenylglycine
dipraglurant	6-fluoro-2-[4-(2-pyridinyl)-3-butyn-1-yl]-Imidazo[1,2-a]pyridine
DMEM	Dulbecco's modified Eagle's medium
DPFE	1-(4-(2,4-difluorophenyl)piperazin-1-yl)-2-((4-fluorobenzyl)oxy)ethanone
DRG	dorsal root ganglion
eCa^{2+}	extracellular calcium
ECL	extracellular loop
ELISA	enzyme-linked immunosorbent assay
ERK1/2	extracellular signal-regulated kinase 1/2
FBS	foetal bovine serum
Fenobam	1-(3-chlorophenyl)-3-[(2e)-1-methyl-4-oxoimidazolidin-2-ylidene]urea
GDNF	glial cell line-derived neurotropic factor
GPCR	G protein-coupled receptor

GPT	glutamic pyruvic transaminase
GRK	G protein receptor kinase
HBSS	Hank's balanced salt solution
HEK293A	human embryonic kidney 293 adherent
iCa^{2+}	intracellular calcium
IMS	industrial methylated spirits
IP_1	inositol monophosphate
IP_3	inositol triphosphate
LTD	long-term depression
LTP	long-term potentiation
MAPK	mitogen-activated protein kinases
mGlu	metabotropic glutamate receptor
$mGlu_5$	metabotropic glutamate receptor subtype 5
min	minutes
MPEP	2-Methyl-6-(phenylethynyl)pyridine
M-5MPEP	2-[2-(3-methoxyphenyl)ethynyl]-5-methylpyridine
MTEP	2-methyl-4-(pyridin-3-ylethynyl)thiazole
mTOR	mammalian target of rapamycin
NADA	*N*-arachidonoyl-dopamine
NAL	neutral allosteric ligand
NAM	negative allosteric modulator
NCFP	*N*-(4-chloro-2-[(1,3-dioxoisoindolin-2-yl)methyl)phenyl)picolinamide]
NGF	nerve growth factor
NMDA	N-methyl-d-aspartate
OEA	oleoylethanolamide
Opti-MEM	Opti- modified Eagle's medium
PAM	positive allosteric modulator
PBS	phosphate-buffered saline
pERK1/2	extracellular signal-regulated kinases 1/2 phosphorylation
PI3K	phosphoinositide 3 kinase
PKA	protein kinase A
PKC	protein kinase C

PLC	phospholipase C
RT	room temperature
TM	transmembrane
TRPV1	transient receptor potential cation channel subfamily V member 1
VFT	Venus flytrap
VU0360172	*N*-cyclobutyl-6-((3-fluorophenyl)ethynyl)picolinamide
VU0366058	2-(1,3-benzoxazol-2-ylamino)-4-(4-fluorophenyl)pyrimidine-5-carbonitrile
VU0366248	N-(3-Chloro-2-fluorophenyl)-3-cyano-5-fluoro-benzamide
VU0403602	*N*-cyclobutyl-5-((3-fluorophenyl)ethynyl)picolinamide
VU0409106	3-Fluoro-*N*-(4-methyl-2-thiazolyl)-5-(5-pyrimidinyloxy)benzamide.
VU0424465	*(R)*-5-((3-fluorophenyl)ethynyl)-*N*-(3-hydroxy-3-methylbutan-2-yl)picolinamide
VU0405398	(5-((3-fluorophenyl)ethynyl)pyridin-2-yl)(3-hydroxyazetidin-1-yl)methanone
VU0409551	((4-fluorophenyl)(2-(phenoxymethyl)-6,7-dihydrooxazolo[5,4-*c*]pyridin-5(4*H*)-yl)methanone)
VU29	*N*-(1,3-diphenyl-1*H*-pyrazolo-5-yl)-4-nitrobenzamide
WT	wild type

Chapter 1

General Introduction

Sections adapted from published works:

Chapter section	**Published work**
1.1. Glutamate and the metabotropic glutamate receptor subtype 5	Sengmany, K., Gregory, K. J., 2016. Metabotropic glutamate receptor subtype 5: molecular pharmacology, allosteric modulation and stimulus bias. Br J Pharmacol 173, 3001-3017.
1.2. Pharmacological agents targeting $mGlu_5$ receptors	Sengmany, K., Gregory, K. J., 2016. Metabotropic glutamate receptor subtype 5: molecular pharmacology, allosteric modulation and stimulus bias. Br J Pharmacol 173, 3001-3017. Sengmany K., Gregory K.J. (2018) Drugs to Tune Up Glutamatergic Systems: Modulators of Glutamate Metabotropic Receptors. In: Parrot S., Denoroy L. (eds) Biochemical Approaches for Glutamatergic Neurotransmission. Neuromethods, vol 130. Humana Press, New York, NY
1.3. Allosteric modulation of mGlu receptors	Sengmany K., Gregory K.J. (2018) Drugs to Tune Up Glutamatergic Systems: Modulators of Glutamate Metabotropic Receptors. In: Parrot S., Denoroy L. (eds) Biochemical Approaches for Glutamatergic Neurotransmission. Neuromethods, vol 130. Humana Press, New York, NY
1.4. Biased agonism and modulation	Sengmany K., Gregory K.J. (2018) Drugs to Tune Up Glutamatergic Systems: Modulators of Glutamate Metabotropic Receptors. In: Parrot S., Denoroy L. (eds) Biochemical Approaches for Glutamatergic Neurotransmission. Neuromethods, vol 130. Humana Press, New York, NY
1.5. CNS disorders linked to an altered glutamatergic system	Sengmany K., Gregory K.J. (2018) Drugs to Tune Up Glutamatergic Systems: Modulators of Glutamate Metabotropic Receptors. In: Parrot S., Denoroy L. (eds) Biochemical Approaches for Glutamatergic Neurotransmission. Neuromethods, vol 130. Humana Press, New York, NY

1.1. Glutamate and the metabotropic glutamate receptor subtype 5

1.1.1. Characterisation of glutamate receptors

Glutamate is the main excitatory neurotransmitter in the brain, providing the balance to the major inhibitory neurotransmitter GABA in neuronal synaptic interplay. Until the mid-1980s, glutamate was thought to act solely via a family of ligand-gated ion channels, the ionotropic glutamate receptors comprised of three subtypes: N-methyl-D-aspartate (NMDA), α-amino-3-hydroxy-5-methyl-4-isoxazoleproprionic acid (AMPA) and kainate. It was not until this neurotransmitter was shown to stimulate inositol phosphate, that the first G protein-coupled metabotropic glutamate (mGlu) receptor was cloned (Houamed et al., 1991; Masu et al., 1991). Eight mGlu subtypes, belonging to the Class C family of G protein-coupled receptors (GPCRs) have since been characterised and are subdivided based on signal transduction mechanisms, pharmacology and sequence homology (Niswender and Conn, 2010). Group I consists of $mGlu_1$ and $mGlu_5$ that preferentially activate phospholipase C (PLC) via $G_{q/11}$ coupling. Group II, $mGlu_2$ and $mGlu_3$, and Group III, $mGlu_4$, $mGlu_6$, $mGlu_7$ and $mGlu_8$ couple to $G_{i/o}$ and adenylate cyclase inhibition (Niswender and Conn, 2010).

1.1.2. $mGlu_5$ in physiology

Widely expressed within postsynaptic densities (PSDs) throughout the cortex, striatum, hippocampus, caudate nucleus and nucleus accumbens, and in astrocytes, glia and peripheral sensory neurons (Crawford et al., 2000; Shigemoto et al., 1993; Walker et al., 2001), $mGlu_5$ is crucial for synaptic plasticity and neuronal development (Ballester-Rosado et al., 2010; Black et al., 2010; Bortolotto et al., 2005;

Chen et al., 2012; Fendt and Schmid, 2002; Galik et al., 2008; Hamilton et al., 2014; Jia et al., 1998; She et al., 2009; Wijetunge et al., 2008; Xiao et al., 2013; Xu et al., 2009). Through the study of $mGlu_5$ knockout animal models, this receptor has been implicated in the pathology or as a therapeutic target for numerous CNS disorders, including: psychosis and schizophrenia (Brody et al., 2004; Chen et al., 2010; Kinney et al., 2003), motor control (Ribeiro et al., 2014), anxiety and depression (Inta et al., 2013; Li et al., 2006), reward and addiction (Bird et al., 2010; Chesworth et al., 2013; Eiler et al., 2011; Olsen et al., 2010; Stoker et al., 2012), appetite and energy homeostasis (Bradbury et al., 2005) and pain (Galik et al., 2008; Kolber et al., 2010). The immense therapeutic potential in targeting the $mGlu_5$ receptor has been extensively summarised (Gregory et al., 2013c; Lindsley and Stauffer, 2013; Noetzel et al., 2012; Palucha-Poniewiera et al., 2013; Pilc et al., 2013), with candidates entering clinical trials for anxiety, depression and Fragile X syndrome with varying successes and failures (Emmitte, 2013; Jaeschke et al., 2015; Levenga et al., 2011; Lindemann et al., 2015; Pecknold et al., 1982; Porter et al., 2005b; Wieronska and Pilc, 2013). As discussed in detail below, $mGlu_5$ promiscuously couples to various G proteins and interacts with complex and dynamic protein scaffolding complexes, such that our understanding of signal transduction mechanisms remains convoluted.

1.1.3. Signal transduction of $mGlu_5$

Preferentially coupled to $G\alpha_{q/11}$, $mGlu_5$ activation leads to activation of phospholipase C (PLC) and production of inositol-1,4,5-triphosphate (IP_3) and diacylglycerol (DAG), and subsequently mobilisation of intracellular calcium (Abe et al., 1992). Calcium, in combination with DAG, leads to the activation of protein kinase C (PKC), phospholipase A_2 (PLA_2), mitogen-activated protein kinases (MAPK) and the

modulation of ion channels (Conn and Pin, 1997; Hermans and Challiss, 2001; Ribeiro et al., 2010a) (Figure 1.1). Activation of this canonical signalling pathway is linked to various cell processes including synaptic plasticity (Borgdorff and Choquet, 2002; Gerrow and Triller, 2010; Kato et al., 2012). In addition to G_q coupling, $mGlu_5$ has also been demonstrated to couple to G_s in HEK293 cells (Francesconi and Duvoisin, 1998) and is linked to cyclic adenosine monophosphate (cAMP) formation in LLC-PK1 cells and oocytes (Joly et al., 1995). However, when expressed in CHO cells or astrocytes, no agonist-stimulated increases in cAMP accumulation were observed (Abe et al., 1992; Balazs et al., 1997; Ribeiro et al., 2010a), suggesting that $mGlu_5$ promiscuous G protein coupling is cell-type dependent.

Downstream of G protein coupling, agonist stimulation of $mGlu_5$ leads to phosphorylation of extracellular-signal regulated kinases 1 and 2 (ERK1/2) (Hu et al., 2007; Thandi et al., 2002) and p38 MAPK (Peavy and Conn, 1998; Rush et al., 2002). Interestingly, $mGlu_5$-mediated phosphorylation of ERK1/2 has been reported to be independent of PKC, phosphoinositide 3-kinase (PI3K) and calcium (Peavy and Conn, 1998; Thandi et al., 2002). Additional evidence has implicated Homer 1b/c scaffolding protein (Mao et al., 2005), epidermal growth factor receptor tyrosine kinase, proline-rich tyrosine kinase 2 (Pyk2) and Src activation in coupling $mGlu_5$ to ERK1/2 phosphorylation (Nicodemo et al., 2010; Peavy et al., 2001; Thandi et al., 2002; Wang et al., 2007). $mGlu_5$-mediated ERK1/2 phosphorylation leads to activation of downstream transcription factors including Elk-1, cAMP response element binding-protein (CREB) and c-Jun, which regulate gene expression involved in long term depression (LTD) (Gallagher et al., 2004; Rush et al., 2002; Wang et al., 2007). Group I mGlu receptor activation of PI3K, Akt and mammalian target of rapamycin (mTOR) (Chan et al., 1999; Hou and Klann, 2004) has also been

implicated in LTD. It is the interplay between ERK-MAPK and PI3K-mTOR pathways through which group I mGlu receptors mediate synaptic plasticity, resulting in de novo protein synthesis and late-phase LTD (Waung and Huber, 2009). In addition to complex acute signalling outcomes, regulatory processes triggered by $mGlu_5$ activation show a similar level of intricacy.

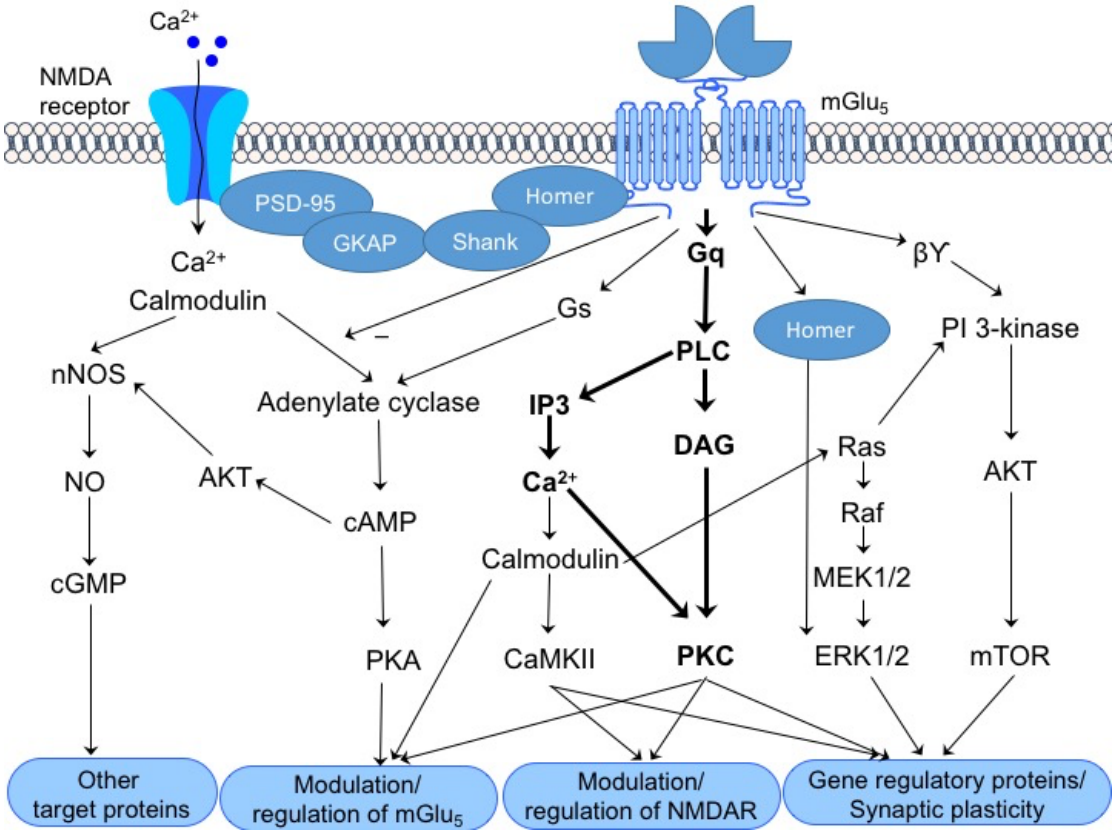

Fig 1.1. Activation of $mGlu_5$ receptors triggers diverse distinct and converging signalling pathways. The group I mGlu receptor family preferentially couples to G_q, leading to activation of the canonical PLC–IP_3–DAG–Ca^{2+} pathway (bold). As reviewed in the text, $mGlu_5$ receptors promiscuously couple to other G proteins as well as alternate second messengers and kinases via mechanisms that can be independent of Ca^{2+}mobilisation. Protein–protein interactions with scaffolding and regulatory proteins (blue ovals) add further diversity: integrating different signalling pathways, directly mediating interactions between $mGlu_5$ receptors and ion channels such as the NMDA receptor and regulating the activity of the $mGlu_5$ receptor itself. As an additional level of complexity, the signalling pathways and effectors stimulated by $mGlu_5$ receptor activation also show considerable cell type dependence. From: Sengmany, K., Gregory, K. J., 2016. Metabotropic glutamate receptor subtype 5: molecular pharmacology, allosteric modulation and stimulus bias. Br J Pharmacol 173, 3001-3017.

1.1.4. Regulation of $mGlu_5$ signalling

Signal transduction arising from $mGlu_5$ is tightly controlled by the phosphorylation status of the receptor. The frequency of glutamate-induced intracellular calcium oscillations is governed by a 'dynamic uncoupling' mechanism where the receptor undergoes rapid cycles of phosphorylation and dephosphorylation (Bradley and Challiss, 2011; Kawabata et al., 1996; Nash et al., 2002). The major mediator of $mGlu_5$ phosphorylation and subsequent desensitisation of $mGlu_5$ signalling is PKC, although other kinases also play a role such as G protein-coupled receptor kinases (GRK), tyrosine kinases and Ca^{2+}/calmodulin-dependent protein kinase II (reviewed in detail: (Mao et al., 2008)). The phosphorylation status of $mGlu_5$ regulates interactions with other proteins. Trafficking and signalling of $mGlu_5$ is regulated by calmodulin that is mediated via interactions with the C terminus (Choi et al., 2011). PKC phosphorylation of $mGlu_5$ inhibits calmodulin binding (Lee et al., 2008), and facilitates Seven in Absentia Homolog 1A (Siah-1A) binding, promoting endocytosis and receptor down-regulation via ubiquitination-dependent mechanisms (Kammermeier and Ikeda, 2001; Ko et al., 2012; Moriyoshi et al., 2004). Calmodulin binding sites also partially overlap with that of Norbin, a neuronal protein that binds $mGlu_5$ to promote cell surface expression and signalling (Wang et al., 2009). Another key adaptor protein that regulates $mGlu_5$ function and expression is the Homer family (Ango et al., 2002; Brakeman et al., 1997; Kammermeier and Worley, 2007; Lv et al., 2014; Tu et al., 1999; Xiao et al., 1998). Of note, Homer interactions with $mGlu_5$ are enhanced by receptor phosphorylation mediated by cyclin-dependent kinase 5 (Orlando et al., 2009), and disruption of Homer scaffolding has been implicated in various disease states (Matosin and Newell, 2013; Ronesi et al., 2012). Recently, $mGlu_5$ was also shown to be a target of PKA phosphorylation, with $mGlu_5$

phosphorylation levels being linked to elevated intracellular cAMP levels (Uematsu et al., 2015). Collectively, these data highlight the critical role $mGlu_5$ phosphorylation plays in regulating receptor function; however, not all mechanisms rely on phosphorylation.

For example G protein-coupled receptor kinase 2 (GRK2) mediates $mGlu_5$ desensitisation and internalisation (Sorensen and Conn, 2003) via a mechanism that can be phosphorylation independent (Ribeiro et al., 2009). Functioning as a clarthrin adaptor, GRK2 is able to facilitate internalisation in a β-arrestin independent manner (Shiina et al., 2001). Indeed, GRK2 overexpression was also shown to increase clathrin recruitment to $mGlu_5$, leading to increased agonist-stimulated desensitisation and internalisation (Ribeiro et al., 2009). Thus, there is much diversity in both the cellular responses and regulatory mechanisms triggered by $mGlu_5$ activation and this diversity extends further to modulation of the response to other glutamate receptors.

1.1.5. $mGlu_5$ interactions with other receptors

1.1.5.1. Modulation of other glutamatergic receptors

Activation of group I mGlu receptors modulates the activity of various ion channels, in particular the NMDA and AMPA ionotropic glutamate receptors (Homayoun et al., 2004; Kato et al., 2012; Nakamoto et al., 2007). Mechanisms of modulation include activation of downstream second messengers, kinases and direct protein-protein interactions (Benquet et al., 2002; Collett and Collingridge, 2004; Gao et al., 2013; Homayoun et al., 2004; Moutin et al., 2012; Ribeiro et al., 2010a). The overall response of an individual cell to glutamate is highly integrated. For example, NMDA receptor activation is involved in early phase synaptic plasticity, with rapid calcium

influx leading to modulation of AMPA receptor trafficking (Borgdorff and Choquet, 2002). The modulation of ionotropic receptors by $mGlu_5$ and vice versa is complex. For example, $mGlu_5$ activation positively modulates the NMDA receptor through increasing open channel probability, with PKC-dependent Src signalling, and stabilisation of a Homer-Shank protein anchor implicated (Benquet et al., 2002; Kotecha et al., 2003; Lu et al., 1999; Tu et al., 1999). In contrast, $mGlu_5$ activation inhibits NMDA receptor-mediated activation of adenylate cyclase, resulting in reduced cAMP and neuronal nitric oxide synthase (nNOS) activity, signal transduction mechanisms that are involved in NMDA receptor-mediated excitotoxicity (Llansola and Felipo, 2010). The relationship between ionotropic receptors and $mGlu_5$ has resulted in extensive efforts to design therapies targeting $mGlu_5$ in particular for the treatment of CNS disorders related to NMDA receptor dysfunction (Conn et al., 2008; Matosin and Newell, 2013; Veerman et al., 2014). Indeed, targeting $mGlu_5$ represents a promising approach to overcome NMDA receptor dysfunction while avoiding excitotoxicity associated with direct stimulation of NMDA receptors.

In addition to modulating ionotropic glutamate receptors, $mGlu_5$ is known to partner with the $mGlu_1$ receptor. In the hippocampus, chemically-induced long term depression (LTD) is partially blocked by antagonists of either receptor, a combination of both $mGlu_1$ and $mGlu_5$ antagonists is required to completely block the response (Volk et al., 2006). This is in spite of the fact that genetic deletion of $mGlu_5$ alone is sufficient to prevent (*S*)-3,5-dihydroxyphenylglycine (DHPG) induced LTD (Huber et al., 2001), supporting the hypothesis that heterodimerisation plays a role. The mechanisms underlying this remain to be fully elucidated, with both $mGlu_1$/$mGlu_5$

heterodimerisation and synergistic signalling (independent of heterodimerisation) proposed (Doumazane et al., 2011; Goudet et al., 2005; Romano et al., 1996; Sevastyanova and Kammermeier, 2014b). Collectively, it is clear that, where expressed, $mGlu_5$ is integral in the interplay of receptors involved in the overall cellular response to glutamate.

1.1.5.2. $mGlu_5$ modulation of ion channels and other GPCRs

In addition to modulating glutamatergic receptors, $mGlu_5$ activation influences the function of other ion channels and GPCRs. In HEK293 cells and isolated cortical neurons, $mGlu_5$ activation inhibits N-type and P/Q-type calcium channels in a voltage-dependent manner, with both βγ subunits of $G_{i/o}$ and Homer scaffolding proteins involved (Kammermeier et al., 2000; McCool et al., 1998). In hippocampal neurons, $mGlu_5$ activation facilitates L-type voltage-dependent calcium channel dependent depolarisation via the opening of calcium-induced calcium release-coupled cation channels (Kato et al., 2012). Within the periphery, $mGlu_5$, located in the dorsal root ganglia, is implicated in both inflammatory and neuropathic pain, with injury to nerves, spinal cord or peripheral tissues resulting in the release of glutamate from primary afferent neurons (Valerio et al., 1997; Walker et al., 2001). In these tissues, $mGlu_5$ is co-localised with the non-selective cation channel transient receptor potential vanilloid subtype 1 (TRPV1) enhancing the activity of TRPV1 channels via DAG formation (Kim et al., 2009; Varney and Gereau, 2002). Recent work suggests that $mGlu_5$ mediated potentiation of TRPV1 is biphasic, transiently potentiating TRPV1-mediated inward currents but inhibiting voltage-gated calcium channels (Masuoka et al., 2015). The mechanism mediating these two different responses remains to be elucidated.

Co-localisation of $mGlu_5$ with multiple GPCRs has functional consequences on the signalling and/or pharmacology of the individual GPCR (Brown et al., 2012a; Schroder et al., 2009). For example, co-stimulation or blockade of $mGlu_5$ and adenosine A_{2A} receptors results in synergistic effects, however, the mechanisms mediating the cross-talk between these receptors appear to be dependent on the brain region studied (Domenici et al., 2004; Ferre et al., 2002; Nishi et al., 2003; Tebano et al., 2006; Tebano et al., 2005). Intriguingly, this synergy between $mGlu_5$ and adenosine A_{2A} has been proposed to involve the formation of heteromers (Ferre et al., 2002; Rodrigues et al., 2005). In fact, in addition to heteromers with $mGlu_1$ mentioned above, $mGlu_5$ heterodimerises with numerous GPCRs, including the calcium-sensing receptor (Gama et al., 2001) and μ-opioid receptor (Schroder et al., 2009). Furthermore, $mGlu_5$, adenosine A_{2A} and D_2 dopamine receptors are thought to form higher order oligomers (Cabello et al., 2009), capable of changing the pharmacological properties of a heteromer 'subunit' (Ferre et al., 1999; Popoli et al., 2001). It is clear that the signalling pathways triggered and interacting proteins modulated by $mGlu_5$ activation are complex and highly dependent on the cellular and tissue context. Therefore it is perhaps not surprising that ligand pharmacology can differ depending on the system under exploration.

1.2. Pharmacological agents targeting $mGlu_5$ receptors

1.2.1. Orthosteric ligands

As highlighted earlier, $mGlu_5$ receptors are implicated in various neuronal processes and selective $mGlu_5$ drugs are attractive putative therapies for numerous CNS disorders. Traditional drug discovery strategies have targeted the endogenous ligand binding (orthosteric) site to activate or block receptor activity. Several group I mGlu

selective ligands have been discovered (Table 1.1) with DHPG prevailing as the most commonly utilised group I mGlu selective pharmacological tool (reviewed in: (Brauner-Osborne et al., 2007). However, high affinity/potency and $mGlu_5$ selective orthosteric ligands have remained elusive, likely due to the fact that the orthosteric site is highly conserved across the mGlu family. The complete activation or inhibition of receptor responses achieved by orthosteric ligands also presents an additional liability, as such compounds lack the delicate balance on neurotransmission, which may lead to undesirable or adverse effects. Thus, many research groups have turned their focus to targeting allosteric binding sites that are topographically distinct from the orthosteric site (Christopoulos and Kenakin, 2002; Leach et al., 2007).

1.2.2. Allosteric ligands

Traditional drug development has largely focused on understanding the endogenous (orthosteric) ligand binding pocket and designing small molecules to bind competitively to either activate or block the desired receptor. However, a greater understanding of G protein-coupled receptor (GPCR) structure and conformational dynamism has allowed a paradigm shift toward designing drugs that bind to alternate pockets distinct from the orthosteric binding site (Lagerstrom and Schioth, 2008). These topographically distinct pockets are referred to as allosteric sites. Simultaneous receptor occupation with an allosteric ligand can modulate the binding of, or response to, an endogenous ligand, a property referred to as cooperativity (Christopoulos and Kenakin, 2002). Positive allosteric modulators (PAMs) enhance, while negative allosteric modulators (NAMs) diminish orthosteric agonist binding/efficacy (Figure 1.2). Neutral allosteric ligands (NALs) bind to allosteric sites without altering orthosteric agonist activity/binding. In addition, allosteric modulators may also

possess intrinsic efficacy (either inverse or positive) in their own right, such compounds are classified first on the basis of the allosteric effect followed by intrinsic efficacy, for e.g. PAM-agonists, NAM-inverse agonists (Christopoulos et al., 2014). Discovery efforts for mGlu receptor allosteric modulators have been particularly fruitful over the past two decades. A wealth of different chemotypes comprising the full spectrum of allosteric ligand pharmacology is now available (Table 1.1, Figure 1.3).

Advantages of allosteric ligands are three-fold; first, allosteric sites generally show lower sequence conservation than orthosteric pockets, allowing for greater selectivity between receptor subtypes. Second, as pure allosteric modulators require orthosteric agonist to have an effect there is an inherent potential to fine-tune receptor activity in a temporal and spatially refined manner, that simply cannot be achieved by a synthetic orthosteric ligand (Keov et al., 2011). However, pure allosteric modulators that have no intrinsic activity and require endogenous neurotransmitter may also present as a disadvantage. For example, in disease states that have a diminished endogenous neurotransmitter levels, such as dopamine loss in Parkinson's disease (Kalia and Lang, 2015), pure allosteric modulators may not have efficacy. Third, the cooperativity between allosteric modulators and orthosteric ligands is saturable, and thus there is reduced risk in the case of overdose. Overall, targeting allosteric binding pockets offers a promising and viable option to develop CNS therapeutics with desirable outcomes and minimal adverse effects.

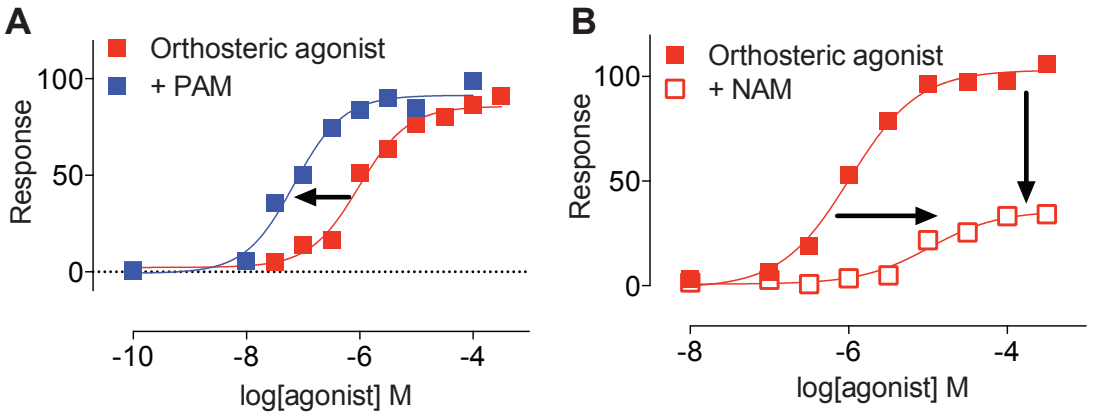

Fig 1.2. Two example simulations of allosteric interactions detected using a functional response to orthosteric agonist. It should be noted, however, that there are numerous manifestations of allosteric interactions via alterations in affinity and/or efficacy. **A**) In the presence of a positive allosteric modulator (PAM) orthosteric agonist potency is increased, shifting to the left ($\alpha\beta>1$). **B**) The presence of a negative allosteric modulator (NAM) decreases the potency of orthosteric agonist ($0<\alpha\beta<1$), and may also diminish the agonist maximal response. From: Sengmany K., Gregory K.J. (2018) Drugs to Tune Up Glutamatergic Systems: Modulators of Glutamate Metabotropic Receptors. In: Parrot S., Denoroy L. (eds) Biochemical Approaches for Glutamatergic Neurotransmission. Neuromethods, vol 130. Humana Press, New York, NY.

Table 1.1. Molecular pharmacology and therapeutic potential of select mGlu ligands.

Nonselective mGlu ligands					
Compound	**Chemical Name**	**Target**	**Activity**	**Therapeutic/biological significance**	**Reference**
L-glutamate	*(S)*-1-aminopropane-1,3-dicarboxylic acid	$mGlu_{1\text{-}3,5}$ > $mGlu_{4,6\text{-}8}$	Orthosteric agonist	Pharmacological tool	(Conn and Pin, 1997; Niswender and Conn, 2010)
(1*S*,3*R*)-ACPD	(1*S*,3*R*)-1-Aminocyclopentane-1,3-dicarboxylic acid	$mGlu_{1\text{-}3,5}$ > $mGlu_{4,6\text{-}8}$	Orthosteric agonist	Pharmacological tool	(Conn and Pin, 1997; Niswender and Conn, 2010)
Group I mGlu ligands					
(S)-3,5-DHPG	(*S*)-3,5-Dihydroxyphenylglycine	$mGlu_{1/5}$	Orthosteric agonist	Pharmacological tool	(Conn and Pin, 1997; Niswender and Conn, 2010; Wisniewski and Car, 2002)
L-quisqualate	(2S)-2-amino-3-(3,5-dioxo-1,2,4-oxadiazolidin-2-yl)propanoic acid	$mGlu_{1/5}$ #	Orthosteric agonist	Pharmacological tool	(Conn and Pin, 1997; Niswender and Conn, 2010)
FITM	4-fluoro-*N*-(4-(6-(isopropylamino)pyrimidin-4-yl)thiazol-2-yl)-*N*-methylbenzamide	$mGlu_1$	NAM	Pharmacological tool	(Wu et al., 2014)
HTL14242	(3-Chloro-5-[6-(5-fluoropyridin-2-yl)pyrimidin-4-yl]benzonitrile)	$mGlu_5$	NAM	Lead compound	(Christopher et al., 2015)
CPPHA	*N*-[4-Chloro-2-[(1,3-dihydro-1,3-dioxo-2*H*-isoindol-2-yl)methyl]phenyl]-2-hydroxybenzamide	$mGlu_5$ > $mGlu_1$> $mGlu_{4/8}$	PAM: IP_1, iCa^{2+} Agonist: pERK1/2	Pharmacological tool, second site PAM	(Chen et al., 2008)
CPCCOEt	7-(Hydroxyimino)cyclopropa[*b*]chromen-1a-carboxylate ethyl ester	$mGlu_1$	NAM	Pain	(Brauner-Osborne et al., 1999; Gasparini et al., 2001)
MPEP	2-Methyl-6-(phenylethynyl)pyridine hydrochloride	$mGlu_5$ > $mGlu_4$	NAM: iCa^{2+}, pERK1/2 Inverse agonist: IP_1	Anxiety, depression, pain, addiction, PD	(Bradley et al., 2011; Chen et al., 2007; Gasparini et al., 1999a; Gregory et al., 2012; Rovira et al., 2015)
JNJ16259685	3,4-dihydro-2H-pyrano[2,3]b quinolin-7-yl)(cis-4-methoxycyclohexyl) methanone	$mGlu_1$	NAM	Pain	(Mabire et al., 2005)
CDPPB	3-Cyano-*N*-(1,3-diphenyl-1*H*-pyrazol-5-yl)benzamide	$mGlu_5$	Agonism: IP_1>pERK1/2>>iCa^{2+} [a]	Psychosis	(Lindsley et al., 2004; Sengmany et al., 2017)
VU0360172	N-cyclobutyl-6-((3-fluorophenyl)ethynyl)nicotinamide	$mGlu_5$	Agonism: IP_1>pERK1/2[a] PAM: iCa^{2+}	Psychosis	(Rodriguez et al., 2010a; Sengmany et al., 2017)

DPFE	1-(4-(2,4-difluorophenyl)piperazin-1-yl)-2-((4-fluorobenzyl)oxy)ethanone	$mGlu_5$	Agonism: IP_1>>iCa^{2+}; biphasic pERK1/2[a]	Psychosis, cognition	(Gregory et al., 2013a; Sengmany et al., 2017)
VU0424465	5-[2-(3-fluorophenyl)ethynyl]-N-[(2R)-3-hydroxy-3-methylbutan-2-yl]pyridine-2-carboxamide	$mGlu_5$	Agonism: IP_1>pERK1/2>>iCa^{2+} [a]	Seizures	(Rook et al., 2013; Sengmany et al., 2017)
VU0403602	N-cyclobutyl-5-((3-fluorophenyl)ethynyl)picolinamide	$mGlu_5$	Agonism: IP_1>pERK1/2>>iCa^{2+} [a]	Metabolite causes seizures	(Bridges et al., 2013; Sengmany et al., 2017)
fenobam	*N*-(3-Chlorophenyl)-*N*'-(4,5-dihydro-1-methyl-4-oxo-1*H*-imidazol-2-yl)urea	$mGlu_5$ #	NAM	Anxiety, depression, addiction, pain	(Berry-Kravis et al., 2009; Jacob et al., 2009; Montana et al., 2011; Pecknold et al., 1982; Porter et al., 2005a; Watterson et al., 2013; Wieronska and Pilc, 2013)
basimglurant	(2-chloro-4-[1-(4-fluoro-phenyl)-2,5-dimethyl-1H-imidazol-4-ylethynyl]-pyridine)	$mGlu_5$	NAM	Major depressive disorder	(Quiroz et al., 2016)
mavoglurant	Methyl (3aR,4S,7aR)-4-hydroxy-4-[2-(3-methylphenyl)ethynyl]-3,3a,5,6,7,7a-hexahydro-2H-indole-1-carboxylate	$mGlu_5$	NAM	FXS, PD, Huntington's disease	(Bailey et al., 2016; Berry-Kravis et al., 2016; Dore et al., 2014; Trenkwalder et al., 2016)
CTEP	2-chloro-4-((2,5-dimethyl-1-(4-(trifluoromethoxy)phenyl)-1H-imidazol-4-yl)ethynyl)pyridine	$mGlu_5$	NAM	FXS	(Dolen et al., 2007; Michalon et al., 2012; Yan et al., 2005)
VU0477573	N,N-diethyl-5-((3-fluorophenyl)ethynyl)picolinamide	$mGlu_5$	limited NAM	Anxiety	(Nickols et al., 2016)
Group II mGlu ligands					
LY354740	(1S,2S,5R,6S)-2-aminobicyclo[3.1.0]hexane-2,6-dicarboxylate monohydrate	$mGlu_{2/3}$	Orthosteric agonist	Psychosis, anxiety, addiction	(Cartmell et al., 1999; Conn and Jones, 2009; Schoepp et al., 2003)
LY379268	(1*R*,4*R*,5*S*,6*R*)-4-Amino-2-oxabicyclo[3.1.0]hexane-4,6-dicarboxylic acid	$mGlu_{2/3}$	Orthosteric agonist	Psychosis	(Cartmell et al., 1999)
LY341495	(2*S*)-2-Amino-2-[(1*S*,2*S*)-2-carboxycycloprop-1-yl]-3-(xanth-9-yl) propanoic acid	$mGlu_{2/3}$	Orthosteric antagonist	Psychosis	(Cartmell et al., 1999)
BINA	3'-[[(2-Cyclopentyl-2,3-dihydro-6,7-dimethyl-1-oxo-1*H*-inden-5-yl)oxy]methyl]-[1,1'-biphenyl]-4-carboxylic acid	$mGlu_2$	PAM	Psychosis, anxiety	(Jin et al., 2010; Muguruza et al., 2016)
LY487379	N-(4-(2-methoxyphenoxy)phenyl)-N-(2,2,2-trifluoroethylsulfonyl)-pyrid-3-ylmethylamine	$mGlu_2$	PAM	Psychosis	(Muguruza et al., 2016)

Group III mGlu ligands					
ACPT-I	(1*S*,3*R*,4*S*)-1-Aminocyclopentane-1,3,4-tricarboxylic acid	Group III	Orthosteric agonist	Pain	(Jalan-Sakrikar et al., 2014)
LSP4–2022	(2S)-2-amino-4-(([4-(carboxymethoxy)phenyl] (hydroxy)methyl)-(hydroxy)phosphoryl)butanoic acid	$mGlu_4$	Orthosteric agonist	Pain	(Goudet et al., 2008; Jalan-Sakrikar et al., 2014; Vilar et al., 2013)
PHCCC	*N*-Phenyl-7-(hydroxyimino)cyclopropa[*b*]chromen-1a-carboxamide	$mGlu_4$ >$mGlu_1$	PAM: iCa^{2+}>GIRK[b]	Pain, Parkinson's disease	(Battaglia et al., 2006; Goudet et al., 2008; Maj et al., 2003; Marino et al., 2003; Vilar et al., 2013)
VU0155041	*cis*-2-[[(3,5-Dichlorophenyl)amino]carbonyl]cyclohexane carboxylic acid	$mGlu_4$	PAM	Parkinson's disease	(Bennouar et al., 2013; Jones et al., 2011; Le Poul et al., 2012)
ADX88178	4-methyl-N-[5-methyl-4-(1H-pyrazol-4-yl)-1,3-thiazol-2-yl]pyrimidin-2-amine	$mGlu_4$	PAM	Parkinson's disease	(Bennouar et al., 2013; Jones et al., 2011; Le Poul et al., 2012)
AF21934	(1S,2R)-2-[(aminooxy)methyl]-N-(3,4-dichlorophenyl)cyclohexane-1-carboxamide	$mGlu_4$	PAM	Anxiety, Parkinson's disease	(Bennouar et al., 2013; Jones et al., 2011; Le Poul et al., 2012)

[a] bias relative to DHPG

[b] bias relative to glutamate

has activity at non-mGlu receptors (ionotropic glutamate receptors for L-quisqualate, A_3 adenosine receptors for fenobam).

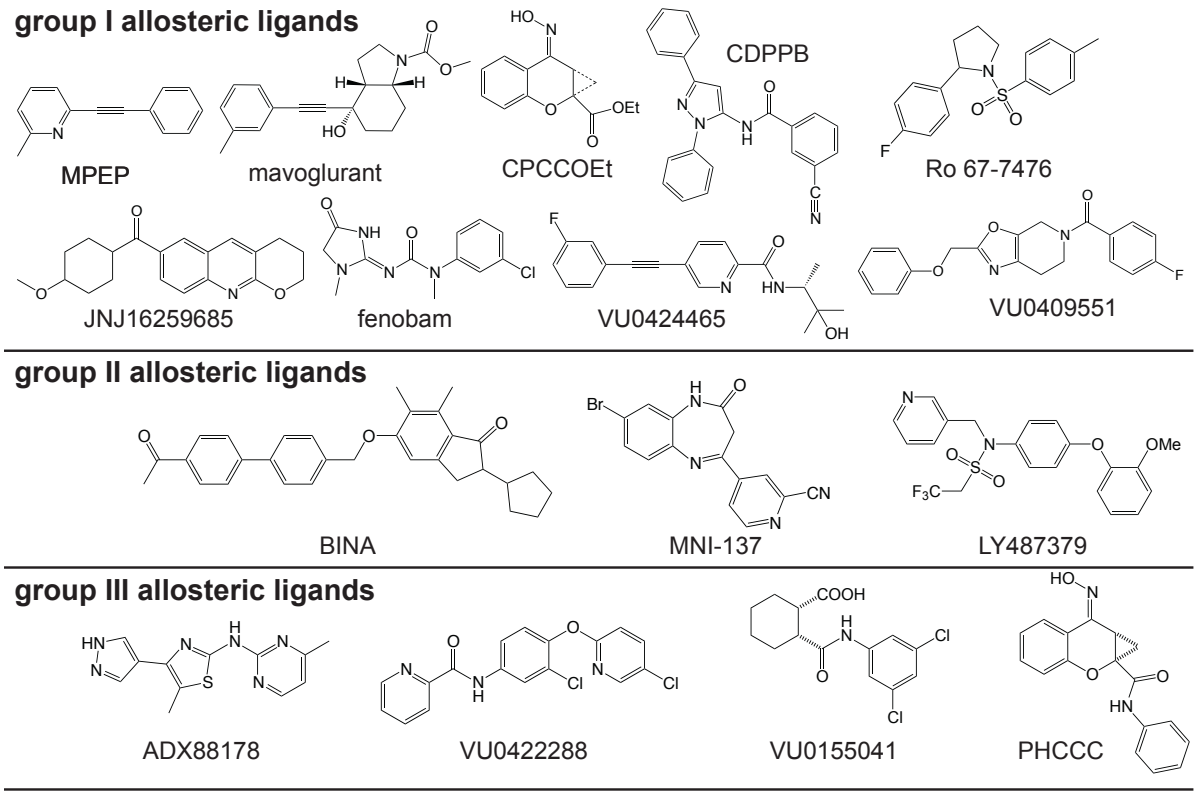

Fig. 1.3. Structures of select mGlu allosteric modulators. Figure from: Sengmany K., Gregory K.J. (2018) Drugs to Tune Up Glutamatergic Systems: Modulators of Glutamate Metabotropic Receptors. In: Parrot S., Denoroy L. (eds) Biochemical Approaches for Glutamatergic Neurotransmission. Neuromethods, vol 130. Humana Press, New York, NY.

1.3. Allosteric modulation of mGlu receptors

1.3.1. Quantifying allosteric interactions

As alluded to earlier, allosteric modulators can influence both orthosteric ligand affinity and efficacy, which has the capacity to result in complex pharmacological profiles. Multiple models have emerged to facilitate quantification of GPCR allosteric interactions. The simplest model to describe the influence of an allosteric modulator on the binding on an orthosteric ligand to its receptor is the allosteric ternary complex model (ATCM) (Hall, 2000; Kenakin, 2004, 2009). The simultaneous occupation of a receptor by two ligands influences affinity, denoted by the cooperativity factor α, and is governed by ligand concentrations, equilibrium dissociation constants K_A and K_B of orthosteric (A) and allosteric (B) ligands respectively (Ehlert, 1988; Leach et al., 2007) (Figure 1.4). Affinity modulation is reciprocal, the binding of an allosteric ligand stabilises receptor conformations that increase or decrease orthosteric ligand affinity and vice versa. Increasingly, it has become apparent that allosteric interactions may also influence GPCR activation states, in addition to, or exclusive of, effects on affinity. In order to accommodate allosteric modulation of efficacy the simple ATCM was extended to an allosteric two-state model, and the now widely applied operational model of allosterism (Hall, 2000; Leach et al., 2007). The operational model of allosterism amalgamates the ATCM and Black and Leff's operational model of agonism (Black and Leff, 1983). Within this framework the effect of an allosteric ligand on both orthosteric agonist affinity (α) and efficacy (β) is accommodated (Leach et al., 2007) (Figure 1.4). PAMs are defined as having a cooperativity ($\alpha\beta$) value greater than 1, NAMs, a cooperativity value between 0 and 1, and NALs are defined as having neutral cooperativity ($\alpha\beta = 1$). It is important to note that an allosteric modulator may influence affinity and efficacy to different

degrees and in different directions (Price et al., 2005). Furthermore, there is the potential that cooperativity drives subtype selectivity rather than affinity. For example, MPEP is an $mGlu_5$ NAM of glutamate efficacy for iCa^{2+} mobilisation and ERK1/2 phosphorylation, and DHPG/quisqualate mediated IP_1 accumulation (Bradley et al., 2011; Chen et al., 2007; Gasparini et al., 1999b; Gregory et al., 2012). On the other hand, MPEP is an $mGlu_4$ PAM-agonist of L-AP4 mediated iCa^{2+} mobilisation (Rovira et al., 2015). The operational model of allosterism allows for delineation of effects on affinity versus efficacy. Further, intrinsic allosteric agonist efficacy is also accommodated as denoted by τ_B (Christopoulos et al., 2014; Keov et al., 2011). For the mGlu receptors this is an important consideration since for multiple chemotypes and at multiple subtypes, allosteric agonist activity is evident (Bradley et al., 2011; Domin et al., 2015; Gregory et al., 2013c; Gregory et al., 2012; Jalan-Sakrikar et al., 2014; Mitsukawa et al., 2005; Rook et al., 2015). Thus rigorous quantification of allosteric ligands remains pertinent to accurately define pharmacology of mGlu allosteric ligands and facilitate comparisons between chemotypes and targets (Christopoulos et al., 2014).

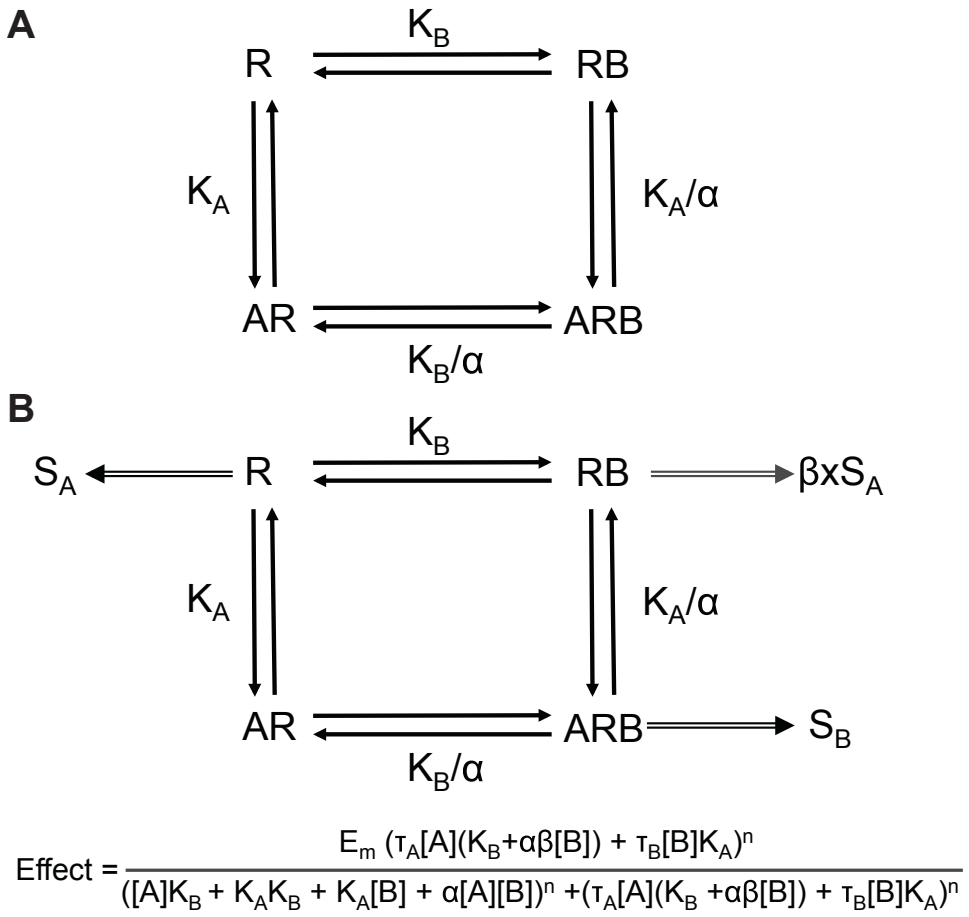

$$\text{Effect} = \frac{E_m\,(\tau_A[A](K_B+\alpha\beta[B]) + \tau_B[B]K_A)^n}{([A]K_B + K_AK_B + K_A[B] + \alpha[A][B])^n + (\tau_A[A](K_B + \alpha\beta[B]) + \tau_B[B]K_A)^n}$$

Fig 1.4. Ternary complex and operational models for G protein-coupled receptor allostery. A) The simplest framework to describe allosteric interactions is the ATCM, where an orthosteric ligand (A) and allosteric modulator (B) can simultaneously bind to a receptor (R) influencing the respective equilibrium dissociation constants (K_A and K_B), as described by the cooperativity factor α. **B**) To describe effects on efficacy, the ATCM was incorporated in to Black and Leff's operational model of agonism. The change in stimulus response coupling (S_A) in the presence of allosteric modulator is described by the scaling factor β. Intrinsic allosteric agonist efficacy is also accommodated. From: Sengmany K., Gregory K.J. (2018) Drugs to Tune Up Glutamatergic Systems: Modulators of Glutamate Metabotropic Receptors. In: Parrot S., Denoroy L. (eds) Biochemical Approaches for Glutamatergic Neurotransmission. Neuromethods, vol 130. Humana Press, New York, NY.

1.3.2 Validation and detection of allosteric modulators

In addition to application of analytical models to quantify allosteric interactions, robust experimental approaches are required to define and validate allosteric interactions. Radioligand binding assays are commonly used to verify allosteric agonist binding of a studied ligand. This is readily done for $mGlu_1$, $mGlu_2$ and $mGlu_5$, where allosteric radioligands have been developed (Cosford et al., 2003a; Gasparini et al., 2002; Kohara et al., 2005; Lavreysen et al., 2003), such that novel allosteric ligands can be validated via inhibition binding assays. Allosteric ligand affinity can be directly determined from inhibition binding assays via application of the standard Cheng-Prusoff equation (Cheng and Prusoff, 1973). For many GPCRs the gold-standard approach to definitively demonstrate an allosteric mechanism is through demonstration of affinity modulation between an unlabeled allosteric ligand and radiolabelled orthosteric ligand using dissociation kinetic binding assays (Gregory et al., 2010). A change in ligand dissociation rate from the receptor when simultaneously occupied is unambiguously demonstrative of an allosteric interaction. For mGlu receptors the prevailing approach has been to determine changes in orthosteric radioligand affinity (e.g. [^{3}H]quisqualate for Group I mGlu receptors, and [^{3}H]LY354740 for Group II mGlu receptors) rather than kinetics (Lavreysen et al., 2003; Lundstrom et al., 2011; Schaffhauser et al., 2003). The $mGlu_5$ PAMs, [(3-fluorophenyl)methylene]hydrazone-3-fluorobenzaldehyde (DFB) and 3-cyano-*N*-(1,3-diphenyl-1*H*-pyrazol-5-yl)benzamide (CDPPB), however, enhance $mGlu_5$ orthosteric agonist affinity (quisqualate) in rat cortical astrocytes (Bradley et al., 2011), while $mGlu_2$ PAMs also enhance affinity of several orthosteric ligands including glutamate and LY354740 (Johnson et al., 2005). Affinity modulation has also been shown with [^{3}H]quisqualate and [^{3}H]DCG-IV by $mGlu_1$ and $mGlu_2$ PAMs respectively (Knoflach

et al., 2001; Schaffhauser et al., 2003). Furthermore, several mGlu allosteric ligands are thought to be efficacy-only modulators, including the $mGlu_5$ PAM CDPPB (with glutamate), the $mGlu_5$ NAM MPEP and $mGlu_1$ NAM CPCCOEt (Hemstapat et al., 2006; Kinney et al., 2005; Litschig et al., 1999; Pagano et al., 2000). Functional assays are required to detect and validate allosteric modulation of efficacy.

Allosteric efficacy modulation can be determined via cell-based functional assays (Melancon et al., 2012). Rapid screening of small allosteric molecules commonly involves administration of allosteric ligand at varying concentrations, with either an EC_{20} orthosteric agonist concentration for PAMs, or an EC_{80} (submaximal) orthosteric agonist concentration for NAMs (Melancon et al., 2012). Orthosteric agonist concentrations are chosen to allow for clear determination of modulatory activity, as enhancement of a small response, or reduction of a large response allows for ease of classification as either a PAM or NAM respectively. A "triple add" paradigm has more recently surpassed the "single add" protocol, as it allows for simultaneous screening for agonist, PAM and NAM activity for receptor measures that are detected in real-time (Melancon et al., 2012). In this protocol, compounds are first added, followed by a second addition of orthosteric agonist EC_{20}, and a third addition of orthosteric agonist EC_{80}. Agonist activity is determined through the first addition, and PAM or NAM activity is determined through the second and third addition of orthosteric ligand respectively (Melancon et al., 2012). These experimental paradigms provide a quick snapshot of prospective modulators via a potency determination. It is important to consider that modulator potency is a composite measure of allosteric modulator affinity, affinity and efficacy cooperativity, and intrinsic agonist activity. Furthermore, modulator potency is also dependent upon the orthosteric agonist

concentration (Gregory et al., 2012; Lindsley et al., 2016). PAM activity may manifest as an increase in agonist potency that approaches a limit as defined by cooperativity and/or an increase in the maximal agonist response (Kenakin, 2004; Niswender and Conn, 2010). Conversely, NAM activity will manifest as a progressive right shift in agonist potency that reaches a limit and/or a depression in the agonist maximal response (Kenakin, 2004; Niswender and Conn, 2010). It should be noted, however, that under hemi-equilibrium conditions, competitive antagonists display a NAM modality – thus appropriate assay conditions are necessary to clearly delineate ligand activity. The magnitude and direction of the shifts in agonist potency correspond to cooperativity whereas the concentrations over which these effects happen are related to modulator affinity. In addition to the saturable nature of allosteric ligand interactions, determination of allosteric binding sites provides a second level of validation for an allosteric mechanism of action.

1.3.3. Structural basis of mGlu allosteric modulation

In addition to sharing the common 7TM typical of all GPCRs, Class C receptors have a large extracellular N-terminal domain, widely known as the Venus flytrap (VFT) domain. Early homology modeling against bacterial periplasmic amino acid binding proteins, such as the leucine/isoleucine/valine binding protein (LIVBP), suggested the N-terminal domain comprised two distinct lobes that closed around glutamate upon ligand binding (Costantino and Pellicciari, 1996; O'Hara et al., 1993). Subsequently, several mGlu VFT domain crystal structures have definitively localised the glutamate orthosteric binding site within this domain (Kunishima et al., 2000; Muto et al., 2007). Of note, receptors with only the soluble N-terminal region retain their ability to bind mGlu agonists (Goudet et al., 2004; Okamoto et al., 1998; Rondard et al., 2006;

Suzuki et al., 2007), highlighting the presence of the orthosteric binding pocket within the VFT. Consistent with these findings, modeling suggests glutamate binding to only one VFT is required for conformational changes to induce a receptor activation (Pin and Duvoisin, 1995). Linking the N-terminal region to the 7TM is the cysteine rich domain (CRD) with four disulfide bridges (Muto et al., 2007; Romano et al., 2001; Romano et al., 1996). The CRD is crucial in signal transduction from the VFT to the 7TM upon orthosteric ligand binding (Muto et al., 2007; Rondard et al., 2006). In addition to glutamate, select divalent cations, such as calcium and magnesium, have been shown to bind within the VFT and consequently modulate receptor responses (Francesconi and Duvoisin, 2004; Kubo et al., 1998). To date, however, the majority of mGlu allosteric ligands bind to the 7TM domain (discussed below).

1.3.3.1. Common allosteric site within 7TM domain

Early mGlu receptor chimeras where the VFT of different subtypes were interchanged, provided invaluable information on localisation of allosteric ligand binding sites. CPCCOEt was validated as an allosteric modulator via $mGlu_1$ and calcium sensing receptor chimera (Brauner-Osborne et al., 1999), as well as chimeras with other mGlu subtypes (Gasparini et al., 2001). Numerous mGlu chimeras were consequently used to characterise the binding of a diverse range of mGlu allosteric ligands to the 7TM domain (Knoflach et al., 2001; Maj et al., 2003; Pagano et al., 2000; Suzuki et al., 2007). In addition, truncated receptor constructs also offered insight into allosteric binding locations, with the use of "headless" mGlu receptors – that is, mGlu receptors lacking the extracellular N-terminus that retaining a functional 7TM and C-terminus capable of coupling to intracellular effectors (Goudet et al., 2004). In these modified $mGlu_{1/5}$ receptors, PAMs were agonists, and NAMs were

inverse agonists (Goudet et al., 2004; Suzuki et al., 2007), highlighting the fact that these ligands bind within the 7TM, rather than VFT. Subsequently, multiple site-directed mutagenesis based studies primarily focused on group I receptors demonstrated that residues within the top third of TM3, TM5, TM6 and TM7 were critical for mGlu allosteric ligand interactions within a proposed common allosteric site across the entire Class C GPCR family (Leach and Gregory, 2017; Malherbe et al., 2006; Malherbe et al., 2003; Sheffler et al., 2011).

Recently, x-ray crystal structures of 7TM domains of human $mGlu_1$ and $mGlu_5$ receptor, in complex with the $mGlu_1$ NAM FITM (Wu et al., 2014) and $mGlu_5$ NAMs mavoglurant (Dore et al., 2014) and HTL14242 (Christopher et al., 2015) confirmed the location of the proposed mGlu common allosteric binding pocket, otherwise known as the MPEP binding pocket (Figure 1.5A-B). The $mGlu_5$ mavoglurant/HTL14242 allosteric binding pocket resides between TM2, TM3, TM5, TM6 and TM7, and has a restricted ~ 7Å entrance into the helical bundle due to anchoring of extracellular loop 2 across the top of the 7TMs (Dore et al., 2014) (Figure 1.4C). The FITM binding pocket in $mGlu_1$ overlaps with that observed in $mGlu_5$, but is located higher within the 7TMs (Figure 1.5A), these differences likely allow subtype selective targeting between group I mGlu receptors (Wu et al., 2014). Further, these studies revealed new structural insights into the overall architecture of Class C GPCR 7TM region and activation mechanisms. For example, water was crystallised in the bottom of the $mGlu_5$/mavoglurant and $mGlu_5$/HTL14242 structures coordinated with residues previously shown to engender switches in allosteric modulator pharmacology (Christopher et al., 2015; Dore et al., 2014; Gregory et al.,

2013b). These NAM co-crystal structures have opened up the possibility of rational discovery approaches informed by structural information.

The $mGlu_5$ allosteric pocket, in particular, is found between TM2, TM3, TM5, TM6 and TM7 and comprises two chambers linked by a narrow channel (Christopher et al., 2015; Dore et al., 2014). The alkyne linker, a common chemical motif amongst several $mGlu_5$ allosteric ligands, extends through the narrow channel between Tyr659, Ser809, Val806 and Pro655 – with Ser809 and Ser805 providing hydrogen bonding with available hydroxyl substituents adjacent the alkyne substituent (Christopher et al., 2015; Dore et al., 2014). Toward the top chamber of the binding pocket, a large hydrophobic region is able to accommodate the saturated bicyclic structure of mavoglurant (Dore et al., 2014). Mutation of Trp784 within this hydrophobic pocket was shown to abolish MPEP binding (Malherbe et al., 2003), while alanine substitution led to increased DFB-mediated potentiation (Muhlemann et al., 2006). This Trp784 residue corresponds to the highly conserved "toggle switch" $FxxCWxP^{6.50A}$ motif in other class A receptors, highlighting it's potential importance in stabilisation of active and inactive receptor states (Nygaard et al., 2009).

A key allosteric interaction with $mGlu_5$ and 3-methyl substituent of mavoglurant occurs within the deeper section of the allosteric binding pocket. Ligand binding interactions in this region involve the formation of a hydrogen bond network with a water molecule and residues Tyr659, Thr781 and Ser809 (Dore et al., 2014). Thr781 has direct hydrogen bond interactions with the water molecule, while the Ser809 interactions with mavoglurant and Ser805 mentioned above provides a kink in TM7 such that carbonyl of Ser809 is oriented to hydrogen bond with the water molecule.

This region has been implicated in the modality of cooperativity, with Ala substitutions of Thr781 (Thr780 rat) and Ser809 (Ser808 rat) switching PAM pharmacology to NAM or NAL (Gregory et al., 2013b).

Adjacent to this water network, the 3-methylphenyl ring of mavoglurant lies between Ala810 and Pro655 within the deepest section of the allosteric binding pocket. Mutations of either of these residues have resulted in loss of appreciable [^{3}H]MPEP radioligand binding (Malherbe et al., 2003; Pagano et al., 2000), as well as significant loss of affinity and/or efficacy for several acetylene scaffold PAMs (Gregory et al., 2013b; Gregory et al., 2012). Further, substitutions in the 3-fluorophenyl position of the $mGlu_5$ PAM 3,3'-difluorobenzaldeazine (DFB) with methoxy and chloro groups resulted in switches in pharmacology to a NAM and NAL respectively (O'Brien et al., 2003), while mutations of either of these residues resulted in abolishment of DFB PAM activity (Muhlemann et al., 2006). Interestingly, while Ser809 and Thr781 involved in the water network are conserved between mGlu subtypes, Ala810 and Pro655 are non-conserved. This suggests the first two residues may be involved in global allosteric ligand activity, while allosteric chemical scaffolds may be manipulated to target the latter two residues to increase subtype selectivity. The effect of select mutations within the $mGlu_5$ allosteric binding pocket is summarised in table 1.2.

Comparing the $mGlu_5$ crystal structure to that of $mGlu_1$, the allosteric pockets are shown to overlap, although the $mGlu_1$ NAM 4-fluoro-*N*-(4-(4-(isopropylamino)pyrimidin-4-yl)thiazol-2-yl)-*N*-methylbenzamide (FITM) binds higher within the allosteric site – comparable to the orthosteric site of class A GPCRs

(Latek et al., 2012). Phenylalkylamine allosteric modulators of the class C calcium sensing receptor (CaSR) have also been suggested to bind to a corresponding FITM site, with hydrogen bonding with the key reside Glu837 in TM7 occurring within both receptors (Leach and Gregory, 2017). The structurally distinct CaSR PAM AC265347, however, binds deeper within 7TM, analogous to mavoglurant binding with $mGlu_5$ (Leach et al., 2016) – thus the group I mGlu crystal structures allows for potential translation into understanding ligand-binding mechanisms of structurally related Class C GPCRs.

Despite the recent crystallisation success within the mGlu receptor family, there remains the caveat of these structures being static crystals in an inactive (NAM-bound) state. Thus, while providing invaluable insight into allosteric ligand binding, there are limitations in predictions involving receptor activation and cooperativity. Nonetheless, the crystal structures of mGlu receptors offer vital information on key residues and interactions involved not only in ligand binding, but also allosteric binding sites within related GPCRs.

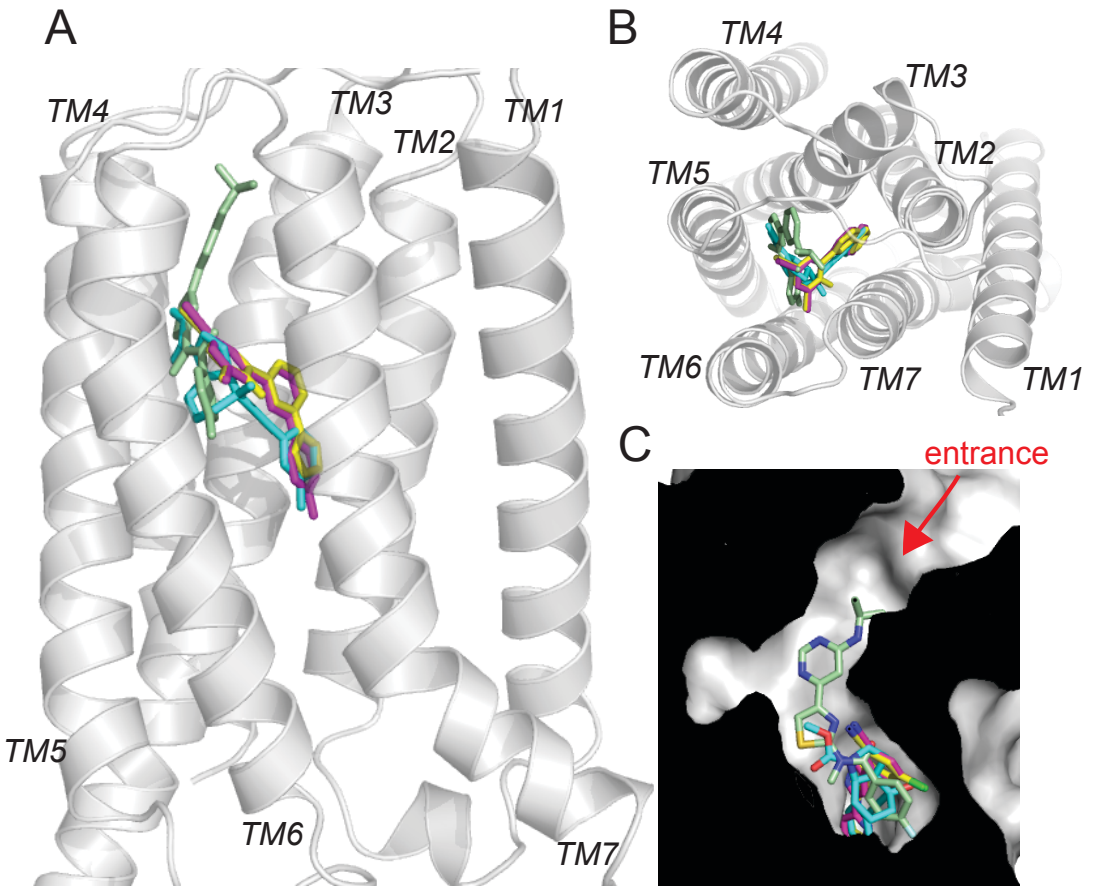

Fig. 1.5. Recent crystal structures provide new insights into allosteric modulator binding within mGlu receptors. A) Alignment of $mGlu_1$ (PDB ID: 4OR2) and $mGlu_5$ 7TM crystal structures (PDB ID's: 4OO9, 5CGC, 5CGD) reveals the overlapping binding cavity. For clarity the backbone of 4OO9 only is shown in cartoon, ligands are depicted in sticks: green is FITM; cyan is mavoglurant; yellow (5CGC) and magenta (5CGD) are HTL14242. **B**) Top-down view of the binding pocket (panel A rotated 90°). **C)** Slice through of the protein surface reveals the narrow entrance. (Figure made by K. J. Gregory for Sengmany K., Gregory K.J. (2018) Drugs to Tune Up Glutamatergic Systems: Modulators of Glutamate Metabotropic Receptors. In: Parrot S., Denoroy L. (eds) Biochemical Approaches for Glutamatergic Neurotransmission. Neuromethods, vol 130. Humana Press, New York, NY.)

1.3.3.2. Secondary allosteric sites

At least one other secondary allosteric binding pocket within $mGlu_5$, distinct from the well-characterised MPEP site, was proposed with the discovery of the $mGlu_5$ PAM CPPHA, and its derivative NCFP, that have no effect or an allosteric interaction with the common site $mGlu_5$ allosteric radioligand [^{3}H]methoxyPEPy (Noetzel et al., 2013; O'Brien et al., 2004). Mutagenesis studies supported a lack of interaction with the common MPEP site, and identified a single residue in TM1 that influenced CPPHA potentiation (Chen et al., 2008) as well as the related compound NCFP (Noetzel et al., 2013). Further, high throughput screening resulted in the discovery of another class of $mGlu_5$ with a benzamine scaffold with subsequent optimisation leading to the $mGlu_5$ PAM VU0357121 and the first non-MPEP site NAL VU0365396 (Hammond et al., 2010). Radioligand binding studies also suggest a binding site distinct from that of MPEP, whereas mutagenesis studies were inconsistent with CPPHA site, but suggested overlap with the common allosteric site (Hammond et al., 2010). A third $mGlu_5$ PAM, VU0400100, is also proposed to bind to a site distinct from the common/MPEP site (Rodriguez et al., 2010b). Recently, a fourth ligand, XAP044, an $mGlu_7$ selective NAM, was discovered that binds allosterically within the VFT (Gee et al., 2014). The presence of different 'druggable' allosteric pockets opens up the possibility of engendering unique pharmacological profiles through stabilisation of different receptor conformations.

Table 1.2. Summary of select mutagenesis-based studies of $mGlu_5$ allosteric site

Mutant	Location	Effect	Reference
I580V (r) A582P (r)	TM1 TM1	• No effect on CPPHA potentiation in iCa^{2+} mobilisation	(Chen et al., 2008)
F585I (r)	TM1	• Reduced CPPHA affinity and potentiation, no effect on VU29 or MPEP affinity and cooperativity in iCa^{2+} mobilisation	(Chen et al., 2008; Gregory et al., 2013b; Gregory et al., 2012)
C630M (r)	TM2	• No effect on CPPHA potentiation in iCa^{2+} mobilisation	(Chen et al., 2008)
T632A (h)	TM2	• No effect on 2-BisPEB, 3-BisPEB, 4-BisPEB and MPEP potency in iCa^{2+} mobilisation	(Mølck et al., 2012)
T632P (h)	TM2	• Increased 2-BisPEB and MPEP potency, no effect on 3-BisPEB and 4-BisPEB potency in iCa^{2+} mobilisation	(Mølck et al., 2012)
L634F (r)	TM2	• No effect on CPPHA potentiation in iCa^{2+} mobilisation	(Chen et al., 2008)
R647A (r)	TM3	• Decreased [^{3}H]fenobam and [^{3}H]MPEP affinity • No effect on MPEP or acetylene PAM affinity, no effect on DFB potentiation in iCa^{2+} mobilisation • No effect on fenobam and MTEP potency in iCa^{2+} mobilisation	(Gregory et al., 2014; Gregory et al., 2013b; Malherbe et al., 2006; Muhlemann et al., 2006)
R648E (h)	TM3	• Decreased 2-BisPEB, 3-BisPEB and MPEP potency, no effect on 4-BisPEB potency in iCa^{2+} mobilisation	(Mølck et al., 2012)
I650A (r)	TM3	• No change in MPEP, acetylene PAM functional affinity or cooperativity in iCa^{2+} mobilisation	(Gregory et al., 2013b)
I651V (h)	TM3	• No effect on [^{3}H]MPEP binding	(Pagano et al., 2000)
I651F (h)	TM3	• Decrease in 2-BisPEB, 3-BisPEB, 4-BisPEB and MPEP potency in iCa^{2+}	(Mølck et al., 2012)
P654S (r)	TM3	• Decreased fenobam, MTEP, MPEP potency, no effect on DFB potentiation in iCa^{2+} mobilisation • Decreased VU0405398, VU0414051, MPEP affinity in iCa^{2+} mobilisation • Abolished [^{3}H]fenobam binding, decreased [^{3}H]MPEP binding	(Gregory et al., 2013b; Malherbe et al., 2006; Malherbe et al., 2003; Muhlemann et al., 2006)

P654F (r)	TM3	• Reduced affinity of MPEP, VU0403602, VU0415051, VU0405386 and VU0405398 in iCa^{2+} mobilisation • Abolished VU0360173 potentiation in iCa^{2+} mobilisation	(Gregory et al., 2013)
Y658V (r)	TM3	• Abolished [^{3}H]MPEP and [^{3}H]fenobam binding • Increased fenobam potency, reduced MPEP affinity, no effect on DFB and VU0465731 potentiation in iCa^{2+} mobilisation • Reduced affinity of VU0424465, VU0405398 and VU0430644 in iCa^{2+} mobilisation • Abolished VU0360172, VU0403602, VU0360173, VU0415051 and VU0405386 potentiation in iCa^{2+} mobilisation • VU0405398 and VU0430644 switch from PAM to NAM in iCa^{2+} mobilisation	(Gregory et al., 2013b; Gregory et al., 2012; Malherbe et al., 2006; Malherbe et al., 2003; Muhlemann et al., 2006; Turlington et al., 2013)
Y658F (r)	TM3	• Reduced [^{3}H]fenobam affinity and potency, no effect on DFB iCa^{2+} potentiation or [^{3}H]MPEP binding	(Malherbe et al., 2006; Malherbe et al., 2003; Muhlemann et al., 2006)
Y659F (h)	TM3	• No effect on 2-BisPEB, 3-BisPEB or MPEP potency in iCa^{2+}, increased 4-BisPEB potency	(Mølck et al., 2012)
Y659A (h)	TM3	• Decreased 2-BisPEB and MPEP potency, abolished NAM activity of 3-BisPEB and and 4-BisPEB in iCa^{2+} mobilisation	(Mølck et al., 2012)
V739M (r)	TM5	• No effect on CPPHA and MPEP affinity or cooperativity in iCa^{2+} mobilisation	(Chen et al., 2008; Gregory et al., 2013b)
P742S (r)	TM5	• Reduced MPEP, VU0360172, VU0403602, VU0405386 affinity, increased cooperativity of acetylene PAMs in iCa^{2+} mobilisation	(Gregory et al., 2013b)
L743V (r)	TM5	• No effect on [^{3}H]fenobam affinity or potency • Reduced [^{3}H]MPEP affinity and potency	(Malherbe et al., 2006; Malherbe et al., 2003)
N746A (r)	TM5	• Reduced VU0403602 and VU0415051 affinity • No change in MPEP, VU0360172, VU0405398 and VU0405386 affinity	(Gregory et al., 2013b)
T780A (r)	TM6	• Reduced affinity of MPEP, VU0424465, VU0403602, VU0415051, VU0465731, VU0430644, VU0405386 • Abolished [^{3}H]fenobam binding, reduced fenobam potency • Reduced [^{3}H]MPEP affinity and potency	(Gregory et al., 2013b; Malherbe et al., 2006; Malherbe et al., 2003;

		• Abolished DFB, VU0360173 and VU0360172 potentiation • VU0415051 switch from PAM to NAM	Muhlemann et al., 2006; Turlington et al., 2013)
W784A (r)	TM6	• Increased DFB and nicotinamide cooperativity • Decreased VU0403602 affinity, but no effect on affinity of other acetylene PAMs • Abolished [^{3}H]fenobam binding, and reduced fenobam potency	(Gregory et al., 2013b; Malherbe et al., 2006; Muhlemann et al., 2006; Turlington et al., 2014)
F787A (r)	TM6	• Abolished [^{3}H]fenobam and [^{3}H]MPEP binding • Reduced fenobam and MPEP potency • DFB switch PAM to NAM	(Malherbe et al., 2006; Malherbe et al., 2003; Muhlemann et al., 2006)
V788A (r)	TM6	• Reduced MPEP affinity in iCa^{2+} mobilisation • Increased affinity of VU0360173 VU0405398, VU0415051 and VU0405386 in iCa^{2+} mobilisation	(Gregory et al., 2013b)
Y791A (r)	TM6	• Reduced DFB potentiation, and fenobam and MPEP potency at iCa^{2+} mobilisation • Reduced [^{3}H]fenobam and [^{3}H]MPEP affinity	(Malherbe et al., 2006; Malherbe et al., 2003; Muhlemann et al., 2006)
M801T (r)	TM7	• Abolished DFB potentiation • No change in fenobam, VU29, CDPPB activity in iCa^{2+} mobilisation	(Chen et al., 2007; Malherbe et al., 2006; Malherbe et al., 2003; Muhlemann et al., 2006)
S808A (r)	TM7	• Reduced affinity of MPEP, VU0424465, VU0403602, and VU0465731 • No change in affinity of VU0360172, VU0415051, VU0405398, VU0430644 or VU0405386 • VU0405398 and VU0430644 switch from PAM to NAM • VU0405386 switch from PAM to NAL	(Gregory et al., 2013b; Turlington et al., 2013)
S808T (r)	TM7	• Reduced MPEP, VU0415051 and VU0403602 affinity in iCa^{2+} • No effect on VU0360172, VU0360173, VU0405398 and VU0405386 affinity	(Gregory et al., 2013b)
A809G (r)	TM7	• Decreased affinity of MPEP, VU0403602, VU0415051, VU0405398 and VU0405386	(Gregory et al., 2013b)
A809V (r)	TM7	• Abolished [^{3}H]MPEP, [^{3}H]methoxyPEPy and [^{3}H]fenobam radioligand binding	(Chen et al., 2008; Gregory et

		• Reduced affinity of MPEP, VU29, VU0403602, VU0360172, VU0405386 and VU0415051 • Reduced potency of MPEP and fenobam • Reduced DFB potentiation and abolished VU0360173 and VU0405398 potentiation • No effect on CPPHA potentiation	al., 2013b; Gregory et al., 2012; Malherbe et al., 2006; Muhlemann et al., 2006)
A810G (h)	TM7	• Loss of [^{3}H]M-MPEP binding	(Pagano et al., 2000)
A810V (h)	TM7	• Abolished [^{3}H]M-MPEP binding • Reduced MPEP, 2-BisPEB and 4-BisPEB potency • Abolished 3-BisPEB inhibition in iCa^{2+} mobilisation	(Mølck et al., 2012; Pagano et al., 2000)

1.3.4. Complexities of allosteric modulation

While allosteric modulation provides a valuable avenue in targeting and pharmacologically manipulating select GPCRs, complexities arise from translating findings from a controlled *in vitro* environment to physiologically relevant systems, preclinical models and to patients. First, mGlu receptors are obligate homodimers, however, may also exist as heteromers, or higher order oligomers, within native systems (Conn and Pin, 1997). Heteromers and oligomers often have vastly different receptor pharmacology to the individual monomers (Prinster et al., 2005). Functional heteromers have been shown with a combination of group II and III mGlu receptors (Doumazane et al., 2011; Kammermeier, 2012; Sevastyanova and Kammermeier, 2014a; Yin et al., 2014), between group I mGlu receptors, $mGlu_5$/calcium-sensing receptor (Gama et al., 2001), $mGlu_5$/μ-opioid receptor (Schroder et al., 2009) and $mGlu_5$/adenosine A_{2A} receptor (Ferre et al., 2002; Rodrigues et al., 2005). The presence of functional heteromers can perturb allosteric modulator pharmacology. For example, PHCCC, a prototypical $mGlu_4$ PAM, potentiates glutamate activity at $mGlu_4$/$mGlu_4$ homomers but not $mGlu_{2/4}$ heteromers, whereas the structurally distinct $mGlu_4$ PAM, VU0155041, modulates both $mGlu_4$ homomers and $mGlu_{2/4}$ heteromers (Yin et al., 2014). As a result, PHCCC does not modulate $mGlu_4$ activity at cortico-striatal synapses due to the presence of $mGlu_2$/$mGlu_4$ heteromers (Yin et al., 2014). Small molecule drug discovery programs often screen initial drug hits at a single target, therefore the presence of heteromers in native systems may result in unanticipated effects. If the relationship between mGlu and other receptors can be understood, the intricacies between individual receptor "subunits" may offer a unique avenue of drug development. Indeed, this concept has been manipulated with the $mGlu_5$ and μ-opioid receptor, where application of the $mGlu_5$ NAM, MPEP, reduced

μ-opioid receptor internalisation, phosphorylation and desensitisation in response to agonist (Schroder et al., 2009). Targeting $mGlu_5$ and μ-opioid receptors in tandem may provide a means to maximise efficacy of current opioid therapies with reduced tolerance, an adverse effect commonly seen with morphine and its derivatives (Williams et al., 2013). However, receptor heteromerisation, and indeed receptor cross-talk, remains a variable in drug design that must be accounted for, as drugs are taken from *in vitro* studies to the complex physiological environment.

Localisation of ligand binding, whether on intracellular or on plasma membrane-bound receptors provides another potential therapeutic target in drug development. Increasing evidence has shown the presence of $mGlu_5$ on intracellular membranes (Jong et al., 2009; Kumar et al., 2008; Purgert et al., 2014), thus leading to the notion of location bias, where differential activation of a signaling cascades may be observed in discrete regions of the cell. $mGlu_5$ receptors are in fact, mostly found intracellularly, within inner and outer nuclear membranes, as well as within the endoplasmic reticulum (Hubert et al., 2001; Kumar et al., 2008). Intracellular $mGlu_5$ receptors are oriented (N-terminus is within the lumen of the organelle, and C-terminus located within the cytoplasm) such that identical second messenger proteins are available to these receptors (Jong et al., 2014). The difference, however, lies in receptor activation. Only agonists that are able to diffuse, or be actively transported across the plasma membrane are able to activate intracellular receptors (Jong et al., 2005). Moreover, diverse physiological outcomes may be location dependent, for example, intracellular and cell surface $mGlu_5$ receptors mediate JNK, Ca^{2+}/CaMK and CREB phosphorylation, whereas activation of only intracellular receptors leads to pERK1/2 and pElk-1 (Jong et al., 2009). In the striatum, intracellular but not plasma

membrane $mGlu_5$ mediates activation of ERK1/2, and the transcription factors Elk-1 and Arc, that are critical for synaptic plasticity (Jong et al., 2009; Kumar et al., 2012). Hippocampal $mGlu_5$-dependent synaptic plasticity can be influenced by receptor compartmentalisation, where intracellular $mGlu_5$ mediates LTD and plasma membrane $mGlu_5$ mediates both LTD and LTP (Jong et al., 2005; Purgert et al., 2014). Thus, in targeting intracellular receptors, drug design may also need to consider formulations that allow delivery to intracellular compartments.

At the level of the ligand, complexities arise from the steep structure activity relationships (SAR) commonly observed with mGlu allosteric ligands (Wood et al., 2011). "Molecular switches" have been observed where small changes in chemical structure result in dramatic changes in cooperativity, e.g. a PAM arising from a NAM scaffold or vice versa (Wood et al., 2011). In phenylethynyl pyrimidine chemotypes, different methyl substitutions converted an $mGlu_5$ partial antagonist to either a NAM or PAM respectively (Sharma et al., 2009) or a NAM to NAL (Rodriguez et al., 2005a), while modifications of $mGlu_5$ PAM ADX-472373 resulted in NAMs, PAMs and partial agonists (Lamb et al., 2011). Moreover, small changes in chemical structure can result in changes in mGlu subtype selectivity (Sheffler et al., 2012; Wood et al., 2011). Thus, the complexities of mGlu allosteric modulator SAR remain a challenge in medicinal chemistry efforts to optimise lead compounds and highlight the need to delineate affinity and cooperativity rather than potency to best understand allosteric modulator SAR.

Ultimately, the key difference between currently marketed central nervous system (CNS) drugs, which act largely via orthosteric agonism or antagonism, and allosteric

modulators, is the potential to maintain receptor physiology, rather than be completely silenced or switched on (Christopoulos and Kenakin, 2002; Leach et al., 2007; Melancon et al., 2012). Therefore allosteric modulators may maintain favorable neurotransmitter tone within the CNS environment. A further level of specificity as well as complexity is presented with the emerging drug action paradigm of biased agonism, where agonist and/or allosteric modulators dictate different functional outcomes through interactions at the same receptor.

1.4. Biased agonism and modulation

Biased agonism describes the phenomenon where the binding of either orthosteric or allosteric ligands results in different effector coupling and signaling profiles in a ligand dependent fashion (Galandrin et al., 2016; Luttrell, 2014) (Figure 1.6). Bias can be manifested as ligand-dependent alterations in archetypal G protein coupling and second-messenger activation, to internalisation, desensitisation, compartmentalisation and even receptor oligomerisation (Galandrin et al., 2016; Luttrell, 2014). The underlying molecular basis for biased agonism is thought to be ligand-induced stabilisation of distinct subsets of receptor conformations resulting in different signaling fingerprints (Kenakin and Christopoulos, 2013; Kenakin et al., 2012). As mentioned earlier, pleiotropic coupling in mGlu receptors is gaining greater appreciation. It is clear that assessment of ligand activity in a single functional assay is insufficient to understand the full scope of drug pharmacology. Indeed, biased agonism is operative for orthosteric ligands of $mGlu_1$ $mGlu_4$, $mGlu_7$ and $mGlu_8$ receptors (Emery et al., 2012; Hathaway et al., 2015; Jalan-Sakrikar et al., 2014). Interestingly, comparison of different endogenous orthosteric $mGlu_1$ agonists revealed glutaric acid and succinic acid were biased toward sustained ERK1/2 phosphorylation

and cytoprotection versus phosphoinositide (PI) hydrolysis relative to glutamate, which coupled more strongly to PI hydrolysis over pERK1/2 and cytoprotection (Emery et al., 2012). The concept of biased endogenous ligands may explain apparent biological redundancies in activating mGlu receptors. Indeed, this notion has been explored with the existence of multiple somatostatin and opioid endogenous ligands (Thompson et al., 2014), with each endogenous ligand potentially stabilising distinct receptor conformations to engender different physiological effects.

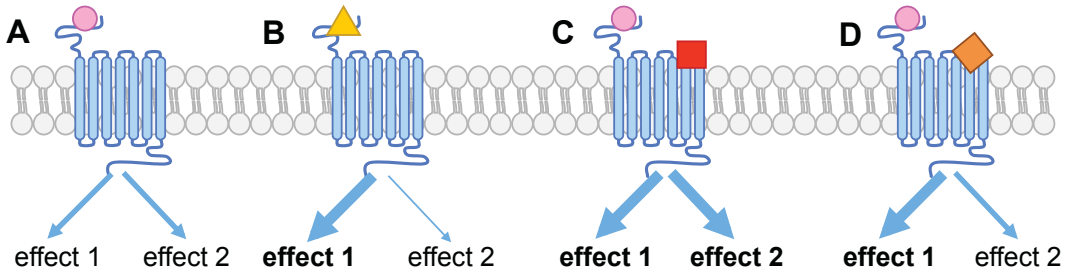

Fig 1.6. Biased agonism and modulation of receptor responses. Receptor activation by different agonists (**A** & **B**) can result in different pharmacological profiles. **C**) Binding of an allosteric modulator may modulate coupling to all pathways to a similar extent. **D**) Binding of a biased modulator will differentially modulate different signaling pathways. From: Sengmany, K., Gregory, K. J., 2016. Metabotropic glutamate receptor subtype 5: molecular pharmacology, allosteric modulation and stimulus bias. Br J Pharmacol 173, 3001-3017.

Biased agonism, however, is not limited to orthosteric ligands. Comparison of relative efficacies of $mGlu_5$ PAM-agonists with that of glutamate revealed that select allosteric agonists also display bias - for instance, toward ERK1/2 phosphorylation over intracellular Ca^{2+} mobilisation, the opposite profile to glutamate (Gregory et al., 2012). Extending on from individual signalling pathways, VU0409551, a PAM of glutamate-mediated calcium mobilisation, was shown to lack efficacy in modulating NMDA receptor currents or NMDA receptor-dependent synaptic plasticity in *in vitro* electrophysiological preparations (Rook et al., 2015), while VU0424465, an $mGlu_5$

PAM-agonist has seizure liability mediated via $mGlu_5$ (Rook et al., 2013). The ability of VU0409551 to engender a different biased agonism fingerprint relative to VU0424465 may underlie *in vivo* efficacy in antipsychotic and cognition models coupled with improved safety profiles (Gregory et al., 2013a; Rook et al., 2015). It remains to be determined whether biased allosteric agonists will translate to novel therapeutics with improved therapeutic efficacy and safety profiles.

Direct activation of receptors may not be desirable within the CNS environment. Related to biased agonism, there is the potential for allosteric ligands to differentially modulate different signaling pathways stimulated by an orthosteric agonist, a phenomenon referred to as biased modulation. Biased modulation may manifest as different degrees of cooperativity with the same orthosteric agonist, or a different apparent affinity of an allosteric modulator for a receptor, depending on response measured (Cook et al., 2015). For $mGlu_5$, biased modulation is evident between iCa^{2+} and ERK1/2 phosphorylation in recombinant cells and cortical astrocyte and neuron cultures (Gregory et al., 2012; Zhang et al., 2005). Biased modulation has the potential to result in distinct physiological effects. For example, the second-site $mGlu_5$ PAM NCFP did not potentiate hippocampal synaptic plasticity, but did potentiate DHPG-induced depolarisation in subthalamic nucleus neurons (Noetzel et al., 2013). Beyond $mGlu_5$, a pan-group III mGlu potentiator (VU0422288) was recently disclosed that has different degrees of cooperativity with glutamate at $mGlu_7$ in an assay dependent manner (Jalan-Sakrikar et al., 2014). The prevalence and therapeutic potential of biased agonism and/or modulation is only beginning to be realised. If signaling fingerprints can be linked to a desired therapeutic outcome, in the future it may be possible to rationally design mGlu allosteric ligands that tailor receptor

activity toward therapeutic effects and avoid adverse effects. However, the possibility of biased agonism and/or modulation also raises additional complexity when investigating mGlu allosteric modulators.

Allosteric interactions by their nature are sensitive to the two ligands that simultaneously occupy the receptor, a phenomenon referred to as probe dependence. Probe dependence describes observations that the magnitude and direction of cooperativity can change depending upon which orthosteric ligand is used to detect an allosteric interaction (Suratman et al., 2011; Valant et al., 2012). Probe dependence is a key consideration when moving from a recombinant system, where glutamate may be readily used as an orthosteric ligand due to the controlled nature of receptor expression, toward a native system, where the presence of various glutamatergic receptors and transporters may confound results if glutamate is used. Probe dependence is operative in Group III mGlu, with two pan-group III mGlu PAMs showing differing degrees of affinity and efficacy cooperativity depending on the orthosteric agonist utilised (Jalan-Sakrikar et al., 2014). Despite the complexity and potential pitfalls, biased agonism and/or modulation offer the potential to fine-tune glutamatergic signaling to the level of intracellular effectors that may be altered in disease.

1.5. CNS disorders linked to an altered glutamatergic system

As glutamate is the main excitatory neurotransmitter in the brain, it is unsurprising that changes in either CNS glutamate levels (Auer et al., 2000; Hashimoto et al., 2007; Kaiser et al., 2005; Sanacora et al., 2012), or the function of glutamate receptors (Amalric, 2015; Bruno et al., 2001; Conn, 2003; Nicoletti et al., 2011a; Nicoletti et al., 2015; Spooren et al., 2003; Spooren et al., 2001) are associated with several CNS disorders. A plethora of mGlu allosteric modulators show promise as novel therapeutics for a variety of CNS disorders (table 1.1). With greater understanding of the full scope of drug action, allosteric drug development has the potential to move toward greater specificity and selectivity for desired therapeutic receptor endpoints, minimising both off- and on-target adverse effects.

1.5.1. Schizophrenia

Schizophrenia is a debilitating disease comprising of three symptom classes: positive (hallucinations, delusions, paranoia), negative (depression, anhedonia) and cognitive (working memory deficits, inability to plan or anticipate outcomes). Current therapeutic options are generally dopamine receptor antagonists, however, these drugs offer minimal relief of negative and cognitive symptoms, and can be associated with severe extrapyramidal side effects (Noetzel et al., 2012). The glutamatergic system is implicated in the undertreated pathophysiology of schizophrenia. For example, all three symptom clusters are evident in rodent models treated with the non-specific NMDA receptor antagonist phencyclidine (PCP) (Morris et al., 2005) – it should be noted however, that rodent models of schizophrenia may be limited to only certain aspects of the disease, and may not fully encompass all positive and negative symptoms. Nonetheless, further evidence of the influence of the glutamatergic system

in schizophrenia, ketamine, an NMDA receptor antagonist, produced psychosis in healthy human volunteers, closely resembling the thought disorders observed in symptomatic schizophrenia (Adler et al., 1999). Glutamatergic dysfunction in schizophrenia is postulated to arise from NMDA receptor hypofunction on GABAergic interneurons within the cortical and subcortical circuits within the brain (Marek et al., 2010) and as such, enhancing glutamatergic tone is a potential therapeutic option (Wieronska et al., 2016). While the aforementioned evidence suggests NMDA receptor function enhancement is a viable objective in schizophrenia treatment, this receptor's fast-acting ionotropic properties may reduce its potential as a therapeutic target due to the risk of excitotoxicity (Serafini et al., 2013). Metabotropic glutamate receptors are slower acting and modulate activity of ionotropic glutamate receptors (Matosin and Newell, 2013), therefore offering an attractive therapeutic strategy.

1.5.1.1. $mGlu_5$ PAMs in the treatment of schizophrenia

$mGlu_5$ activation positively modulates the NMDA receptor through increasing open channel probability, via PKC-dependent Src signaling, and stabilisation of the Homer-Shank protein anchor (Lu et al., 1999; Tu et al., 1999). Interestingly, NMDA receptor activation is suggested to be involved in early phase synaptic plasticity, with rapid calcium influx leading to modulation of AMsPA receptor trafficking (Borgdorff and Choquet, 2002). This relationship between ionotropic and metabotropic glutamate receptors has resulted in extensive efforts in designing therapies targeting $mGlu_5$ to treat CNS disorders related to NMDA receptor dysfunction. Knockout rodent models have highlighted the close correlation between $mGlu_5$ and schizophrenia-like symptoms or psychosis, with $mGlu_5$ knock out mice (Gould et al., 2016) showing

consistent deficits in prepulse inhibition relative to wild-type controls (reviewed in (Wieronska et al., 2016)

Promisingly, selective $mGlu_5$ PAMs have efficacy in preclinical models of antipsychotic-like effects. CDPPB was the first selective $mGlu_5$ modulator to reverse the multidimensional aspects associated with psychosis: amphetamine induced hyperlocomotion, prepulse inhibition and cognitive deficits (Horio et al., 2013; Kinney et al., 2005). Several other selective $mGlu_5$ PAMs have since been shown to be efficacious in rodent models of psychosis (Gregory et al., 2013a; Rodriguez et al., 2010a; Rook et al., 2015). In addition to promising preclinical efficacy, select $mGlu_5$ PAMs and PAM-agonists have been associated with adverse effect liability. VU0424465, a robust PAM-agonist, did not produce any antipsychotic effects, but rather resulted in dose-dependent seizures (Rook et al., 2013), while 4-fluorophenyl((2R,5S)-5-[5-(5-fluoropyridin-2-yl)-1,2,4-oxadiazol-3-yl]-2-methylpiperidin-1-yl)methanone (5PAM523), an $mGlu_5$ PAM with little/no agonism, had anti-psychotic-like effects, however, 5PAM523 also caused neurotoxicity in rats (Parmentier-Batteur et al., 2014). Interestingly, another $mGlu_5$ PAM-agonist, VU0403602, dose-dependently reversed amphetamine-induced hyperlocomotion, however, produced time-dependent seizures and forelimb asymmetry (Bridges et al., 2013). VU0403602 adverse effects were attributed to an active metabolite, thereby highlighting the importance of understanding not only drug pharmacodynamics, but also pharmacokinetic profiles within the living system (Bridges et al., 2013). Recently, the $mGlu_5$ PAM VU0409551 was shown to be a biased ligand, differentially activating/modulating different signaling pathways and lacked the ability to potentiate $mGlu_5$ modulation of NMDA receptor currents (Rook et al., 2015). Despite the

absence of NMDA receptor modulation, VU0409551 had anti-psychotic-like and cognition-enhancing effects in preclinical rodent models, potentially negating the role of NMDA receptors in $mGlu_5$ PAM efficacy (Rook et al., 2015). Nonetheless, targeting $mGlu_5$ receptors may prove fruitful in designing therapies for this schizophrenia that treat both psychosis and cognition impairments.

1.5.1.2. Other mGlu ligands in the treatment of schizophrenia

Group II mGlu receptors are implicated as potential therapeutic targets due to autoreceptor properties and localisation within the limbic and forebrain regions associated with schizophrenia (Wright et al., 2013). Preclinical studies showed normalisation of a PCP-induced rat model of hyperlocomotion, working memory, and stereotypy by the $mGlu_{2/3}$ agonist LY354740, with a favorable adverse effect profile and minimal effects on spontaneous activity or dopamine neurotransmission (Moghaddam and Adams, 1998). The related $mGlu_{2/3}$ agonist LY379268 also ameliorated amphetamine-induced hyperlocomotion evoked by PCP, with minimal adverse effects, which was reversed by the selective $mGlu_{2/3}$ antagonist LY341495 (Cartmell et al., 1999). While agonism may provide therapeutic effect, group II mGlu receptor PAMs may provide a greater safety profile due to fine-tuning, rather than direct receptor activation. Indeed, the $mGlu_2$ selective PAMs, LY487379 and BINA, have behavioral effects similar to $mGlu_{2/3}$ agonists in PCP- and amphetamine-induced mouse models of hyperlocomotion and prepulse inhibition (Muguruza et al., 2016) Thus, the preclinical studies of Group II mGlu agonists and PAMs show great promise in the treatment of this multifaceted disease.

1.5.2. Anxiety and depression

Generalised anxiety and major depressive disorder remain a large burden, not only on the individual, but on society and the economy as a whole (Kessler et al., 2009). Current therapies include benzodiazepines, tricyclic antidepressants and serotonergic agents; however, these therapies are associated with adverse effects such as dry mouth, constipation, diarrhea and dizziness (Tham et al., 2016). These adverse effects may be attributed to the general "dirty" nature of current drugs (Galling et al., 2015; Woods et al., 1992), with many of the adverse effects linked to unwanted anti-cholinergic effects (Tham et al., 2016). Thus, there remains a clear need for more efficacious therapeutics, with greater selectivity and minimal off-target effects. Altered glutamate levels within the brains of patients with anxiety and depression (Auer et al., 2000; Hashimoto et al., 2007) have implicated mGlu receptors as potential targets in the treatment of these disorders (Chaki et al., 2013; Chojnacka-Wojcik et al., 2001).

1.5.2.1. $mGlu_5$ NAMs in the treatment of anxiety and depression

As NMDA receptor overactivity is implicated in anxiety and depression (Valenti et al., 2002), $mGlu_5$ presents as an attractive drug target due to its ability to modulate NMDA receptor activity. In support of this hypothesis, $mGlu_5$ knockout mice have reduced depressive symptoms relative to their wild-type counterparts, despite a paradoxical increase in anxiety (Inta et al., 2013; Li et al., 2006). Inta and colleagues suggest this may be the result of general ablation of $mGlu_5$, resulting in altered neurogenesis (Inta et al., 2013). Nevertheless, the prototypical $mGlu_5$ NAM MPEP is both anxiolytic and antidepressive in preclinical studies (Belozertseva et al., 2007; Li et al., 2006; Schulz et al., 2001; Spooren et al., 2000). Furthermore, MPEP improved

the antidepressive effects of imipramine, a currently marketed tricyclic antidepressant, suggesting synergistic efficacy in targeting multiple CNS neurotransmitters (Li et al., 2006). $mGlu_5$ NAMs from multiple chemical scaffolds also show efficacy in decreasing mouse marble burying, a behavioral model of anxiolytic drug activity (Felts et al., 2013; Mueller et al., 2012; Rodriguez et al., 2010a). Fenobam is an $mGlu_5$ NAM, which was originally discovered as a non-benzodiazepine anxiolytic, with clinical efficacy in a small double-blind, placebo-controlled study with fewer adverse effects reported relative to diazepam control (Pecknold et al., 1982; Porter et al., 2005a; Wieronska and Pilc, 2013). Safety and efficacy of basimglurant, an $mGlu_5$ NAM, as an adjunct treatment of major depressive disorder was recently assessed in a phase IIb trial. Basimglurant had anti-depressive effects in all secondary outcomes, with good tolerability, however, the primary outcome measure of clinician-reported changes in depression, were not met (Quiroz et al., 2016). While promising, it should be noted that select $mGlu_5$ NAMs, such as fenobam and MPEP, are associated with cognitive impairments and psychotomimetic-like effects (Gregory et al., 2013c). It has been postulated that one means to overcome $mGlu_5$ NAM adverse effect liability is via the development of "partial" NAMs, which have limited cooperativity, such that even at full receptor occupancy by the NAM, a degree of glutamate agonist activity is retained (Gould et al., 2016; Nickols et al., 2016). A number of partial $mGlu_5$ NAMs have now been discovered that have anxiolytic and anti-addiction efficacy (Gould et al., 2016; Nickols et al., 2016), and promisingly are devoid of psychotomimetic-like effects or cognitive deficits (Gould et al., 2016). Therefore, development of “partial” or NAMs with limited cooperativity may provide greater control in modulating glutamatergic neurotransmission to yield a broader therapeutic index.

1.5.2.2. Other mGlu ligands in the treatment of anxiety

Group II mGlu agonists display anxiolytic effects in preclinical rodent models (Swanson et al., 2005), with LY354740 increasing open-arm time in a mouse behavioral model of anxiety without the adverse effect of sedation associated with benzodiazepines (Schoepp et al., 2003). LY354740 also showed clinical efficacy in the treatment of panic attacks and generalised anxiety disorder with a favorable adverse effect profile (Schoepp et al., 2003). Despite its promise in the preclinical setting, LY354740 activates both $mGlu_2$ and $mGlu_3$ receptors, and hence does not allow differentiation of subtype activity (Conn and Jones, 2009). The design of subtype selective PAMs has paved the way for greater selectivity of pharmacological interventions (Conn and Jones, 2009). Positive allosteric modulators derived from BINA and LY487379 (Galici et al., 2005; Galici et al., 2006; Johnson et al., 2005), with increased selectivity toward $mGlu_2$, exhibit anxiolytic effects (Galici et al., 2006). Therefore, $mGlu_2$ selective PAMs are a novel treatment strategy for the treatment of anxiety.

1.5.3. Addiction

While dopamine, within the reward neurocircuitry of the brain, is implicated in addiction, glutamate may play a pivotal role in both development and maintenance of addiction (Tzschentke and Schmidt, 2003). The glutamatergic system is highly integrated and thus able to modulate the dopaminergic reward system, with glutamatergic projections observed in key dopaminergic brain areas such as the ventral tegmental area and nucleus accumbens (Christie et al., 1987; Gorelova and Yang, 1997). Knockout of $mGlu_5$ ameliorates preclinical models of addiction, such as operant sensation seeking, extinction and reinstatement (Bird et al., 2010; Chesworth

et al., 2013; Chiamulera et al., 2001; Eiler et al., 2011; Olsen et al., 2010; Stoker et al., 2012). In preclinical models, fenobam attenuated drug-seeking behavior in rats and reduced cocaine-induced behavioral sensitisation (Huang et al., 2015; Watterson et al., 2013). $mGlu_5$ NAMs show preclinical efficacy in relapse and reinstatement of amphetamine, cocaine, nicotine and alcohol addictions (Olive, 2009), and thus provide attractive pharmacological options in targeting the multiple facets of addiction. In addition, Group II mGlu receptors are expressed within brain regions associated with reward and addiction (Liechti et al., 2007). Nicotine self-administration down-regulates Group II mGlu receptor expression, thus, up-regulation of these receptors may offer relief from addiction (Liechti et al., 2007). Indeed, $mGlu_{2/3}$ agonists LY354740 and LY379268 decreased nicotine self-administration and cue-reinstatement, although tolerance to LY379268 quickly developed, highlighting the malleable and highly adaptable CNS environment (Helton et al., 1997; Liechti et al., 2007). Administration of the $mGlu_2$ PAM AZD8529 in rodent models of abstinence reduced relapse of methamphetamine administration and cue-seeking behavior (Caprioli et al., 2015), while similar effects were observed with the $mGlu_2$ PAM BINA and cocaine addiction (Jin et al., 2010). Thus, there is much promise in fine-tuning glutamatergic neurotransmission for the treatment of addictive disorders.

1.5.4. Pain and inflammation

Chronic or neuropathic pain has been associated with dysfunction of several mGlu receptors (Woolf and Salter, 2000). Group I mGlu receptors are located within dorsal root ganglia, the spinal cord, and brain regions associated with pain sensation and transmission (Crawford et al., 2000; Martin et al., 1992; Walker et al., 2001), with group I knockout mice displaying decreased pain responses (Galik et al., 2008; Kolber

et al., 2010). The $mGlu_1$ selective NAM JNJ16259685 produced analgesia in a rodent model of formalin-induced hyperalgesia (Mabire et al., 2005), while an $mGlu_1$ antagonist produced analgesia in a spinal nerve ligation assay (Bennett et al., 2012). Fenobam also produced similar effects, with favorable activity in mouse models of pain and importantly, did not induce tolerance after chronic administration (Jacob et al., 2009; Montana et al., 2011). Interestingly, while the analgesia is thought to arise from central pathways, peripherally injected MPEP, into an inflamed rat hind paw, was more effective than intracerebroventricular or intrathecal administration to attenuate hyperalgesia (Walker et al., 2001). Thus, targeting peripheral mGlu receptors represent yet another avenue in which to design drugs that act directly to the site of injury or inflammation.

In addition to group I receptors, $mGlu_4$ is an attractive target for pain and inflammation. $mGlu_4$ is located within spinal neuronal terminals and unmyelinated C-fibers, and $mGlu_4$ deletion produced hypersensitivity to noxious stimuli (Vilar et al., 2013). Group III agonists including the $mGlu_4$ selective agonist LSP4-2022, as well as the mGlu4 PAM PHCCC reduced hyperalgesia without affecting healthy controls (Goudet et al., 2008; Vilar et al., 2013). Current analgesics are suboptimal and associated with tolerance (Jamison and Mao, 2015), there remains a need for better pain therapeutics, which may be addressed through targeting mGlu receptors.

1.5.5. Autism Spectrum Disorders

Fragile X Syndrome (FXS) is a genetic disorder where mutations silence the *Fmr1* gene, which encodes fragile X mental retardation protein (FMRP), and is one of the most common inherited causes of autism spectrum disorders (ASD) and mental

retardation (Garber et al., 2008). FMRP is an RNA binding protein involved mRNA translation, its absence leads to impaired synaptic plasticity (Garber et al., 2008). Phenotypically, patients present with autistic-like behaviors and cognitive deficits ranging from poor working memory to impaired executive function and social skills (Garber et al., 2008). The glutamatergic system has been heavily implicated in this disorder, with rodent models of FXS showing an imbalance in long-term depression and long-term activation, resulting in disturbed glutamatergic synaptic plasticity and abnormal neuronal growth (Bear et al., 2004; Huber et al., 2002; Irwin et al., 2002; Nimchinsky et al., 2001). $mGlu_5$ hyperactivity is suggested to play a significant role in FXS pathophysiology, and hence $mGlu_5$ negative modulation may be a therapeutic option (Bear et al., 2004). Indeed, $mGlu_5$ NAMs MPEP and CTEP rescue multiple aspects of the FXS phenotype in numerous rodent models (Dolen et al., 2007; Michalon et al., 2012; Yan et al., 2005). These promising preclinical studies led to recent clinical trials. Fenobam was tested in an open-label pilot study for the treatment of FXS, where no clinically significant adverse effects were observed (Berry-Kravis et al., 2009). Another $mGlu_5$ NAM, mavoglurant, improved behavioral symptoms in FXS in two phase IIb trials, however, primary outcome measures were not met (Berry-Kravis et al., 2016). Of note, primary outcomes were parental observations of patients, and hence were potentially subjective (Bailey et al., 2016). Despite this, mavoglurant has a predictable and tolerable adverse effect profile (Bailey et al., 2016; Berry-Kravis et al., 2016), and may instruct further development of $mGlu_5$ NAMs to remedy glutamatergic hyperactivity in FXS.

Tuberous sclerosis complex (TSC) is a genetic disorder affecting multiple organ systems, with up to 95% of patients experiencing CNS involvement including

epilepsy, intellectual disability and autism spectrum disorders (Sahin, 2012). Malfunction of the *TSC1* and *TSC2* genes results in the loss of the hamartin-tuberin complex, and subsequent aberration in mTOR signaling, protein synthesis and neuronal development (Kwiatkowski and Manning, 2005; Wullschleger et al., 2006). Unlike FXS, TSC rodent models display deficiencies in mGlu mediated long-term depression (LTD) (Auerbach et al., 2011; Chevere-Torres et al., 2012), thus leading to enhancement of mGlu receptors being a tractable therapy in this disease. Pretreatment of hippocampal slices with the $mGlu_5$ PAM CDPPB in TSC mouse models restored LTD to wild type levels, and normalised protein synthesis (Auerbach et al., 2011). CDPPB also reversed the cognitive and behavioral deficits in the TSC mouse models (Auerbach et al., 2011). Thus, targeting $mGlu_5$ receptors, through inhibition or enhancement informed by the underlying pathophysiology, provides potential therapies in the treatment of both FXS and TSC respectively.

1.5.6. Parkinson's disease

Parkinson's disease (PD) is characterised by bradykinesia, rigidity and tremors arising from the aggregation of Lewy bodies and loss of dopaminergic innervation within the substantia nigra (Kalia and Lang, 2015). Current treatment for PD involves replacement of dopaminergic input through administration of the dopamine precursor L-3,4-dihydroxyphenylalanine (L-DOPA), however, with long term therapy up to 80% of patients experience L-DOPA induced dyskinesias (LID) (Bastide et al., 2015). Evidence suggests LID may arise from deranged synaptic plasticity, or 'pathological' long-term potentiation, between dopaminergic and glutamatergic inputs within the nigrostriatal pathway (Calabresi et al., 2000; Picconi et al., 2012), and as such, current treatments for LID involve NMDA antagonism by amantadine (Fox et al., 2011).

There remains a need for more efficacious treatments for both PD and LID, without the adverse motor and cognitive effects seen with L-DOPA and amantadine.

1.5.6.1. $mGlu_5$ NAMs in the treatment of PD and LID

Elevated $mGlu_5$ receptor expression has been reported in the striatum of patients of PD and in 1-methyl-4-phenyl-1,2,3,6-tetrahydropyridine (MPTP)-lesioned non-human primates with dyskinesias (Ouattara et al., 2011). Treatment with MPEP in conjunction with L-DOPA produced an L-DOPA sparing effect, reducing the overall incidence of LID (Morin et al., 2013a; Morin et al., 2013b). Further, fenobam treatment in rodent and non-human primate models of PD reduced peak-dose dyskinesias (Rylander et al., 2010). The immense potential of $mGlu_5$ targeted PD and LID therapies have been summarised in (Litim et al., 2017). Mavoglurant was assessed in the treatment of LID in two phase II trials, however, failed to meet the primary outcome of antidyskinetic activity, with a greater adverse effect profile relative to placebo (Trenkwalder et al., 2016). Despite lack of clinical trial success to date, $mGlu_5$ allosteric ligands remain viable options in the treatment of PD and LID, and may find a role in synergistic therapies to reduce L-DOPA doses.

1.5.6.2. $mGlu_4$ PAMs in the treatment of PD and LID

$mGlu_4$ receptors are widely expressed throughout brain regions involved in the pathophysiology of PD, including the basal ganglia, hippocampus and cerebellum (Duty, 2010; Nicoletti et al., 2011b). Administration of the group III selective mGlu agonists into the substantia nigra reversed akinesia in rodent models of PD, while also providing neuroprotection against 6-hydroxydopamine lesions (Austin et al., 2010; Lopez et al., 2012). The selective $mGlu_4$ PAM PHCCC also reversed reserpine-

induced akinesia and was protective against neuronal degeneration in rodents (Battaglia et al., 2006; Marino et al., 2003). Haloperidol-induced catalepsy was also reversible by the $mGlu_4$ PAMs VU0155041, ADX88178, AF21934 with the absence of LID adverse effects (Bennouar et al., 2013; Jones et al., 2011; Le Poul et al., 2012). Interestingly, both $mGlu_4$ PAMs ADX88178 and AF21934 showed synergistic effects with administration of L-DOPA, such that the therapeutic dose of L-DOPA may be reduced, thereby reducing the risk of LID (Bennouar et al., 2013; Le Poul et al., 2012). Thus, $mGlu_4$ PAMs in conjunction with current therapies may provide a novel therapeutic strategy to reduce adverse effects while maximising therapeutic effects.

1.6. Scope of thesis

In various preclinical models of CNS disorders, mGlu allosteric ligands have demonstrated promising efficacy profiles. Unfortunately, the limited examples of mGlu allosteric ligands that have progressed into phase II clinical trials have yet to demonstrate efficacy. To address this disconnect between animal models and human trials, there remains a need to evaluate the full scope of mGlu allosteric modulator activity in a pharmacological robust and thorough manner. Indeed progression into preclinical and clinical models based solely on pharmacological assessment at one or two receptor endpoints precludes the prediction of adverse outcomes along diverse receptor endpoints. Conversely, abandonment of potential lead compounds due to lack of efficacy at the single studied receptor pathway results in immense loss of prospective therapeutics.

Thus, this thesis aims to provide a deeper understanding of $mGlu_5$ allosteric ligands through rigorous characterisation of agonism and allosterism, with the aim of assessing the presence of $mGlu_5$ allosteric ligand bias. We hypothesise that the studied ligands display unappreciated bias at multiple $mGlu_5$ receptor endpoints. Sixteen $mGlu_5$ allosteric ligands were assessed at $mGlu_5$ mediated iCa^{2+} mobilisation, IP_1 accumulation and ERK1/2 phosphorylation in both recombinant and mouse embryonic cortical neurons. Nuances in kinetics and systems context were also probed, in order to provide a greater picture of ligand pharmacology.

The study was extended to assess the structural basis of $mGlu_5$ allosteric agonism, whereby ligands were assessed in $mGlu_5$ receptors containing single point mutations within the allosteric binding pocket. The effect of these mutations on select $mGlu_5$

orthosteric and allosteric agonists was compared relative to wild-type receptors to determine the importance of selected residues in activation of iCa^{2+}, IP_1 or pERK1/2 receptor endpoints.

As mentioned above, in physiologically relevant systems, $mGlu_5$ is known to interact with numerous other receptors, including the nonselective cation channel TRPV1. However, the effect of allosteric modulation of $mGlu_5$ on TRPV1 is unknown. For the final study in this thesis, we assessed effects of $mGlu_5$ ligand incubation on TRPV1 mediated calcium responses in rat dorsal root ganglia neurons of several endogenous TRPV1 agonists. Modulation of TRPV1 responses provides a potential therapeutic avenue in the treatment of both acute and chronic pain.

Ultimately, by understanding how different mGlu-stimulated signaling pathways are linked to pathology and therapeutic efficacy, it may be possible to develop biased mGlu modulators that normalise defective signaling cascades and avoid target-mediated adverse effects. It is clear that modulators of glutamatergic neurotransmission show immense potential in a wide range of CNS disorders, not only as prospective therapies, but also pharmacological tools in understanding the complexities of metabotropic glutamate receptor activity in health and disease.

Chapter 2

Biased allosteric agonism and modulation of metabotropic glutamate receptor 5: implications for optimizing preclinical neuroscience drug discovery

Kathy Sengmany, Junaid Singh, Gregory D Stewart, P Jeffrey Conn, Arthur Christopoulos, Karen J Gregory

Neuropharmacology **115**: 60-72, March 2017

Neuropharmacology 115 (2017) 60–72

Contents lists available at ScienceDirect

Neuropharmacology

journal homepage: www.elsevier.com/locate/neuropharm

Biased allosteric agonism and modulation of metabotropic glutamate receptor 5: Implications for optimizing preclinical neuroscience drug discovery

Kathy Sengmany [a], Junaid Singh [a], Gregory D. Stewart [a], P. Jeffrey Conn [b], Arthur Christopoulos [a, **], Karen J. Gregory [a, *]

[a] Drug Discovery Biology, Monash Institute of Pharmaceutical Sciences and Department of Pharmacology, Monash University, Parkville, VIC, Australia
[b] Vanderbilt Center for Neuroscience Drug Discovery, Vanderbilt University Medical Center, Nashville, TN, USA

ARTICLE INFO

Article history:
Received 22 February 2016
Received in revised form
30 June 2016
Accepted 1 July 2016
Available online 5 July 2016

Chemical compounds studied in this article:
Glutamate (L-glutamic acid PubChem CID: 33032)
DHPG (PubChem CID: 108001)
VU0424465 (PubChem CID: 53384864)
VU0403602 (PubChem CID: 53384878)
VU29 (PubChem CID: 11610682)
VU0360172 (PubChem CID: 53318624)
CDPPB (PubChem CID: 11245456)
DPFE (PubChem CID: 16663278)
VU0405398 (PubChem CID: 70789303)

Keywords:
Biased agonism
Positive allosteric modulator
Stimulus bias
Metabotropic glutamate receptor 5

ABSTRACT

Allosteric modulators, that exhibit no intrinsic agonist activity, offer the advantage of spatial and temporal fine-tuning of endogenous agonist activity, allowing the potential for increased selectivity, reduced adverse effects and improved clinical outcomes. Some allosteric ligands can differentially activate and/or modulate distinct signaling pathways arising from the same receptor, phenomena referred to as 'biased agonism' and 'biased modulation'. Emerging evidence for CNS disorders with glutamatergic dysfunction suggests the metabotropic glutamate receptor subtype 5 ($mGlu_5$) is a promising target. Current $mGlu_5$ allosteric modulators have largely been classified based on modulation of intracellular calcium (iCa^{2+}) responses to orthosteric agonists alone. We assessed eight $mGlu_5$ allosteric modulators previously classified as $mGlu_5$ PAMs or PAM-agonists representing four distinct chemotypes across multiple measures of receptor activity, to explore their potential for engendering biased agonism and/or modulation. Relative to the reference orthosteric agonist, DHPG, the eight allosteric ligands exhibited distinct biased agonism fingerprints for iCa^{2+} mobilization, IP_1 accumulation and ERK1/2 phosphorylation in HEK293A cells stably expressing $mGlu_5$ and in cortical neuron cultures. VU0424465, DPFE and VU0409551 displayed the most disparate biased signaling fingerprints in both HEK293A cells and cortical neurons that may account for the marked differences observed previously for these ligands *in vivo*. Select $mGlu_5$ allosteric ligands also showed 'probe dependence' with respect to their cooperativity with different orthosteric agonists, as well as biased modulation for the magnitude of positive cooperativity observed. Unappreciated biased agonism and modulation may contribute to unanticipated effects (both therapeutic and adverse) when translating from recombinant systems to preclinical models.

This article is part of the Special Issue entitled 'Metabotropic Glutamate Receptors, 5 years on'.

1. Introduction

In recent years, the metabotropic glutamate receptor subtype 5 ($mGlu_5$), a G protein-coupled receptor (GPCR) ubiquitously expressed throughout the brain, has emerged as a promising drug target for multiple central nervous system (CNS) disorders, including schizophrenia, autism, Parkinson's disease and depression (Gregory et al., 2013c; Niswender and Conn, 2010). Drug design efforts for $mGlu_5$ are largely focused on targeting allosteric sites, that is, receptor binding sites topographically distinct from that of the endogenous ligand. Allosteric ligands offer the promise of increasing receptor selectivity, maximizing therapeutic effects and minimizing adverse effects. Further, modulation of orthosteric agonists by allosteric ligands without intrinsic agonism, allows for spatiotemporal fine-tuning of receptor responses – a favorable therapeutic mechanism within the complex CNS environment (Christopoulos and Kenakin, 2002; Leach et al., 2007; Melancon et al., 2012). Allosteric ligands that enhance receptor responses are called positive allosteric modulators (PAMs), while some

* Corresponding author. 381 Royal Parade, Parkville, VIC, 3052, Australia.
** Corresponding author. 381 Royal Parade, Parkville, VIC, 3052, Australia.
E-mail addresses: Kathy.sengmany@monash.edu (K. Sengmany), junaidsingh1@gmail.com (J. Singh), greg.stewart@monash.edu (G.D. Stewart), jeff.conn@vanderbilt.edu (P.J. Conn), arthur.christopoulos@monash.edu (A. Christopoulos), karen.gregory@monash.edu (K.J. Gregory).

http://dx.doi.org/10.1016/j.neuropharm.2016.07.001
0028-3908/

Abbreviations

cAMP	cyclic adenosine monophosphate
CDPPB	3-Cyano-*N*-(1,3-diphenyl-1*H*-pyrazol-5-yl)benzamide
CNS	central nervous system
CPCCOEt	7-(hydroxyimino)cyclopropa[*b*] chromen-1a-carboxylate ethyl ester
DHPG	(*S*)-3,5-dihydroxyphenylglycine
DMEM	Dulbecco's modified Eagle's medium
DPFE	1-(4-(2,4-difluorophenyl)piperazin-1-yl)-2-((4-fluorobenzyl)oxy)ethanone
eCa^{2+}	extracellular calcium
ERK1/2	extracellular signal-regulated kinases 1 and 2
FBS	fetal bovine serum
GPCR	G protein-coupled receptor
GPT	glutamic pyruvic transaminase
HBSS	Hank's Balanced Salt Solution
HEK293A	human embryonic kidney 293
iCa^{2+}	intracellular calcium
IP1	inositol 1-phosphate
$mGlu_5$	metabotropic glutamate receptor subtype 5
MPEP	2-Methyl-6-(phenylethynyl)pyridine
mTOR	mammalian target of rapamycin
NAL	neutral allosteric ligand
NAM	negative allosteric modulator
Opti-MEM	Opti-modified Eagle's medium
PAM	positive allosteric modulator
PI3K	phosphoinositide 3-kinase
VU0360172	*N*-cyclobutyl-6-((3-fluorophenyl)ethynyl) picolinamide
VU0403602	*N*-cyclobutyl-5-((3-fluorophenyl)ethynyl) picolinamide
VU0424465	(*R*)-5-((3-fluorophenyl)ethynyl)-*N*-(3-hydroxy-3-methylbutan-2-yl)picolinamide
VU0405398	(5-((3-fluorophenyl)ethynyl)pyridin-2-yl) (3-hydroxyazetidin-1-yl)methanone
VU0409551	((4-fluorophenyl) (2-(phenoxymethyl)-6,7-dihydrooxazolo[5,4-*c*]pyridin-5(4*H*)-yl) methanone)
VU29	*N*-(1,3-diphenyl-1*H*-pyrazolo-5-yl)-4-nitrobenzamide

allosteric compounds may also activate the receptor in the absence of endogenous ligand (PAM-agonists). Similar to orthosteric agonists, PAM-agonists do not have the benefit of temporal control of receptor activity. Allosteric ligands that diminish endogenous responses are termed negative allosteric modulators (NAMs), and those that neither increase nor decrease responses are referred to as neutral allosteric ligands (NALs) (Gentry et al., 2015). Discovery efforts for $mGlu_5$ allosteric modulators have been particularly fruitful. Diverse modulator chemotypes recognize the 'MPEP' site, an allosteric pocket located within the receptor's seven transmembrane bundle (Dore et al., 2014; Gregory et al., 2013b, 2014; Wu et al., 2014). Of note, $mGlu_5$ PAMs (classified based on glutamate stimulation of $mGlu_5$-intracellular Ca^{2+} (iCa^{2+}) mobilization in recombinant cells) have demonstrated efficacy in preclinical models of psychosis and cognition enhancement (Kinney et al., 2005; Rodriguez et al., 2010; Gregory et al., 2013a). However, recent studies have also reported adverse effects for select $mGlu_5$ enhancers, such as seizure activity induced by VU0424465 (a PAM-agonist for $mGlu_5$ mediated iCa^{2+} mobilization) (Rook et al., 2013) and neurotoxicity in rats treated with 5PAM523 (a pure PAM for $mGlu_5$-iCa^{2+} mobilization stimulated by glutamate) (Parmentier-Batteur et al., 2014).

It has also become increasingly evident that, like many GPCRs, the $mGlu_5$ receptor is pleiotropically coupled, activating multiple signaling pathways. In particular, while the receptor is predominantly coupled to G_q and subsequent changes in intracellular calcium (iCa^{2+}) mobilization, $mGlu_5$ couples to iCa^{2+}-independent signaling pathways, such as extracellular signal-regulated kinases (ERK) 1 and 2 phosphorylation, cAMP, mTOR/PI3K, and can interact with, and modulate the activity of, other GPCRs and ion channels (Sengmany and Gregory, 2015). It is conceivable therefore that $mGlu_5$ activation by chemically diverse ligands may engender unique receptor conformations, such that the receptor favors distinct subsets of physiological responses. This concept is known as 'biased agonism' (Kenakin and Christopoulos, 2013). Biased agonism offers the opportunity to design drugs that are tailored to activate the desired complement of receptor responses linked to therapeutic outcomes while avoiding those linked to adverse effects. Biased agonism is operative for orthosteric agonists at the related Group I $mGlu_1$ receptor between G-protein and β-arrestin pathways in both recombinant and natively expressing cells (Emery et al., 2010, 2012; Hathaway et al., 2015). Several studies have suggested that $mGlu_5$ biased agonism may be linked to distinct physiological responses (Gregory et al., 2012, 2013a; Noetzel et al., 2013; Zhang et al., 2005). However, the vast majority of $mGlu_5$ allosteric modulators have been classified as PAMs, PAM-agonists, NAMs or NALs, based on modulation of glutamate-mediated iCa^{2+} mobilization alone. To date, there have been no rigorous analyses of the $mGlu_5$ signaling fingerprints of diverse allosteric modulators across different pathways. It is possible that preferential activation or inhibition of distinct $mGlu_5$ signaling pathways could lead to different behavioral and/or toxicological outcomes.

One means to avoid the neurotoxicity and seizure liability associated with certain $mGlu_5$ PAM and/or PAM-agonists (Rook et al., 2013; Parmentier-Batteur et al., 2014) and retain antipsychotic and pro-cognitive effects may be via the development of biased $mGlu_5$ modulators (Rook et al., 2015). Moreover, hitherto unappreciated bias may contribute to observations that markedly different doses of the same modulator are required for efficacy in different preclinical behavioral models. For example, DPFE, an $mGlu_5$ PAM-agonist of glutamate-mediated iCa^{2+} mobilization and ERK1/2 phosphorylation in HEK293A cells, required vastly different doses to elicit cognition-enhancement versus reversal of amphetamine-induced hyperlocomotion in rats (Gregory et al., 2013a). Therefore, in the current study, we undertook the first rigorous analysis of $mGlu_5$ bias for diverse PAMs in both HEK293A cells and primary cortical neuron cultures. Allosteric ligands were selected based on i) known interaction at the 'MPEP' allosteric site, ii) previous classification as PAMs or PAM-agonists in iCa^{2+} assays and iii) existing data in preclinical behavioral models. Propensity for biased allosteric agonism was determined relative to the orthosteric agonist DHPG across four signaling pathways that were amenable to assessment in both recombinant and neuronal cell cultures. We demonstrate that $mGlu_5$ allosteric modulators display biased agonism and cooperativity, providing proof-of-concept that the development of biased $mGlu_5$ allosteric modulators may be a means to tailor enhancement of $mGlu_5$ activity to elicit therapeutically beneficial effects, such as anti-psychotic and cognition enhancement, while avoiding adverse effects.

2. Materials and methods

2.1. Materials

Dulbecco's modified Eagle's medium (DMEM), Neurobasal and Opti-modified Eagle's medium (Opti-MEM), Fluo-4-AM and antibiotics were purchased from Invitrogen (Carlsbad, CA). Fetal bovine serum (FBS) was purchased from Thermo Electron Corporation (Melbourne, Australia). IP-One HTRF® assay kit was purchased from Cisbio Assays, Genesearch (Arundel, QLD, Australia) and AlphaScreen detection beads were from PerkinElmer Life and Analytical Sciences. Select allosteric modulators *N*-cyclobutyl-5-((3-fluorophenyl)ethynyl)picolinamide (VU0403602), *N*-cyclobutyl-6-((3-fluorophenyl) ethynyl)picolin-amide (VU0360172), *(R)*-5-((3-fluorophenyl)ethynyl)-*N*-(3-hydroxy-3-methylbutan-2-yl)picolinamide (VU0424465), 1-(4-(2,4-difluorophenyl)piperazin-1-yl)-2-((4-fluorobenzyl)oxy) ethanone (DPFE), (5-((3-fluorophenyl)ethynyl)pyridin-2-yl) (3-hydroxyazetidin-1-yl)methanone (VU0405398) (4-fluorophenyl) (2-(phenoxymethyl)-6,7-dihydrooxazolo[5,4-*c*]pyridin-5(4*H*)-yl) methanone (VU0409551) were synthesized at Vanderbilt Centre for Neuroscience Drug Discovery as described previously (Gregory et al., 2012, 2013a; Rook et al., 2013; Bridges et al., 2013; Rodriguez et al., 2010; Rook et al., 2015). *N*-(1,3-Diphenyl-1*H*-pyrazolo-5-yl)-4-nitrobenzamide (VU29), 3-Cyano-*N*-(1,3-diphenyl-1*H*-pyrazol-5-yl) benzamide (CDPPB) and 7-(Hydroxyimino)cyclopropa[*b*]chromen-1a-carboxylate ethyl ester (CPCCOEt) were purchased from Tocris Bioscience (Melbourne, Australia). Unless stated otherwise, all other reagents were purchased from Sigma-Aldrich (St. Louis, MO) and were of analytical grade.

2.2. Animals

All animal experiments and procedures were approved by the Monash Institute of Pharmaceutical Sciences Animal Ethics Committee (Protocol no. MIPS.2014.37). Asmu:Swiss outbred 8-week female wild-type mice were provided by the Monash Animal Research Platform (Clayton, Victoria, Australia). Time-mated females were humanely sacrificed and E16 embryos were recovered for primary cell culture.

2.3. Cell culture

HEK293A cells stably expressing wild-type rat $mGlu_5$ at low levels (HEK293A-$mGlu_5$-low), equivalent to those observed in primary cortical astrocytes (Noetzel et al., 2012) were maintained at 5% CO_2, 37 °C in DMEM supplemented with 5% FBS, 16 mM HEPES and 500 μg/mL G418. The day before assays, cells were seeded onto poly-D-lysine coated, clear-bottom 96-well plates in assay medium (glutamine-free DMEM supplemented with 5% dialyzed FBS, 16 mM HEPES and 500 μg/mL G418) at a density of 40,000 cells/well, unless otherwise specified.

2.4. Primary cell culture

E16 Asmu:Swiss wild-type mice were decapitated, cortices dissected and neurons mechanically dissociated in Hank's Balanced Salt Solution (HBSS; KCl 5.33 mM, KH_2PO_4 0.44 mM, $NaHCO_3$ 4.17 mM, NaCl 137.93 mM, Na_2HPO_4 0.34 mM, D-glucose 5.56 mM). Cortical neurons were then immediately plated on poly-D-lysine, FBS-coated clear-bottom 96-well plates in Neurobasal media, supplemented with 2 mM L-glutamine, 1 × B-27®, 50 U/mL penicillin, 50 μg/mL streptomycin, 1.25 μg/mL Fungizone® Antimycotic, at a density of 100 000 cells/well. Plates were maintained at 37 °C and 5% CO_2 for 5–7 days before experimentation, to allow growth of neurons.

2.5. Intracellular calcium mobilization

Intracellular calcium flux was measured as a change in fluorescence of the Ca^{2+} indicator dye, Fluo-4-AM, using a FlexStation I or III as described previously using a double-add paradigm, where allosteric ligands were added 1 min prior to orthosteric agonist (Gregory et al., 2012), with the exception of allosteric agonists, which were added simultaneously with orthosteric compound to avoid confounding effects of desensitization. Intracellular calcium mobilization was measured at room temperature (RT) for HEK293A-$mGlu_5$-low cells and at 37 °C for cortical neurons. For extracellular Ca^{2+}-free experiments, $CaCl_2$ was omitted from Ca^{2+} assay buffer (HBSS as above, with 2.5 mM probenecid, pH 7.4) and also supplemented with 1 mM EDTA. A 5-point smoothing function was applied to the raw fluorescence traces and peak fluorescence values (within 60 s post-addition of ligand) normalized to the maximal response to either glutamate (HEK293A cells) or DHPG (cortical neurons).

2.6. Inositol monophosphate (IP_1) accumulation assay

HEK293A-$mGlu_5$-low or cortical neurons were washed with PBS and incubated for 1 h at 37 °C with stimulation buffer (HBSS as above, with 20 mM HEPES, 30 mM $LiCl_2$, 1.2 mM $CaCl_2$, pH 7.4) before compound addition. After 1 h incubation, cells were lysed with Lysis Buffer (HTRF® IP-one assay kit) and IP_1 levels determined using the HTRF® IP-one assay kit as per manufacturer's instructions and fluorescence measured using the PHERAstar. Data were expressed as either fold over basal, or as a percentage of the maximal DHPG response.

2.7. ERK1/2 phosphorylation

Receptor-mediated ERK1/2 phosphorylation was determined using an AlphaScreen-based ERK SureFire kit as described previously (Gregory et al., 2012). Cells were serum-starved using DMEM supplemented with 16 mM HEPES, for a minimum of 4 h for cortical neurons, and 6 h for recombinant cells. In HEK293A-$mGlu_5$-low cells, the peak time for $mGlu_5$-mediated ERK phosphorylation by all compounds was 5–7 min (Gregory et al., 2012; Rook et al., 2015), while in cortical neurons, DPFE and VU0405398 peaked at 5 min, and all remaining modulators and DHPG peaked at 20 min (Supplementary Information). For interaction experiments in cortical neurons, allosteric modulators or vehicle were added 1 min prior to 20 min stimulation with DHPG. Assays were terminated by aspiration of ligand-containing medium and addition of 50 μL/well lysis buffer. Following 5 min shaking, 4 μL of lysate was transferred to a white 384 well ProxiPlate (PerkinElmer). Under low-light conditions, 7 μL AlphaScreen detection mixture (1:7 (v/v) activation buffer: reaction buffer; with 1:240 (v/v) acceptor and donor beads) was added to each well and incubated 1.5 h at 37 °C. AlphaScreen signal was measured using an Envision with standard AlphaScreen settings. Data were expressed as fold over basal levels of phosphorylated ERK.

2.8. Data analysis

Agonist-concentration response curves were fitted to a variable four-parameter logistic equation:

$$y = \frac{bottom + (top - bottom)}{(1 + 10^{(logEC_{50} - Log[A])n}} \quad (1)$$

where bottom and top are lower and upper plateau levels of the concentration response curve respectively, n is the Hill coefficient,

[A] is the molar concentration of agonist, and EC_{50} is the agonist concentration required to produce a half maximal response between top and bottom values (potency).

Allosteric modulation of glutamate or DHPG-mediated responses were fitted to the operational model of allosterism (Leach et al., 2007):

$$Effect = \frac{E_m(\tau_A[A](K_B + \alpha\beta[B]) + \tau_B[B]K_A)^n}{([A]K_B + K_AK_B + K_A[B] + \alpha[A][B])^n + (\tau_A[A](K_B + \alpha\beta[B]) + \tau_B[B]K_A)^n} \quad (2)$$

where [A] and [B] are the molar concentrations of orthosteric agonist, glutamate or DHPG, and allosteric modulator respectively. K_A and K_B are the equilibrium dissociation constants of the orthosteric agonist and allosteric modulator respectively, and α represents affinity cooperativity and β is a scaling factor that denotes the magnitude of effect an allosteric modulator has on the efficacy to an orthosteric agonist. Parameters τ_A and τ_B represent the respective ligand's intrinsic ability to activate the receptor, while E_m and n represent the maximal system response and the transducer slope respectively. K_A values for orthosteric agonists were constrained to affinity estimates previously determined from inhibition binding assays (Gregory et al., 2012). Affinity cooperativity (α) was assumed to be neutral as validated previously (Gregory et al., 2012) and thus constrained to a value of 1, allowing estimates of β as a measure of cooperativity, that is the magnitude of effect a modulator has on orthosteric agonist potency and/or efficacy.

Biased agonism was quantified using an operational model of agonism (Kenakin et al., 2012):

$$Y = basal + \frac{(Em - basal)\left(\frac{\tau}{K_A}\right)^n [A]^n}{[A]^n\left(\frac{\tau}{K_A}\right)^n + \left(1 + \frac{[A]}{K_A}\right)^n} \quad (3)$$

where [A] is the agonist concentration, E_m is the maximal response of the system, n is the transducer slope, and τ is the coupling efficiency of the agonist as defined by R_T/K_E, where R_T is the receptor number and K_E if the coupling efficiency of the system. From this equation the transduction coefficient $\log(\tau/K_A)$ a composite of both affinity and efficacy can be derived, which describes agonism and bias for a given pathway. A normalized transduction coefficient, $\Delta\log(\tau/K_A)$, was consequently calculated using DHPG as the reference agonist. To compare different pathways (e.g. $j1$ vs $j2$), $\Delta\log(\tau/K_A)$ values were evaluated between pathways by calculating the LogBias ($\Delta\Delta\log(\tau/K_A)$):

$$\Delta\Delta Log\left(\tau/K_A\right)_{j1-j2} = Log(bias) = \Delta Log\left(\tau/K_A\right)_{j1} - \Delta Log\left(\tau/K_A\right)_{j2} \quad (4)$$

Affinity, cooperativity and potency parameters were derived and represented as logarithmic mean ± SEM. Analysis of bias parameters was performed using one-way analysis of variance (ANOVA) with Tukey's post-hoc test. Comparison of operational parameters between iCa^{2+} mobilization and IP_1 accumulation in cortical neurons was determined using unpaired Student's t-test.

3. Results

Eight allosteric ligands previously classified as either PAMs or PAM-agonists based on glutamate stimulation of $mGlu_5$-mediated iCa^{2+} mobilization representing four distinct chemotypes were selected for this study to probe the potential for biased agonism and biased modulation of $mGlu_5$ (Supplementary Fig. 1). In preclinical studies, the structurally related VU0403602 and VU0424465 have known adverse effect liability (Bridges et al., 2013; Rook et al., 2013) and provide a reference for modulators with undesirable properties. We also included two other ligands from this scaffold, VU0360172 and VU0405398, both of which have lower cooperativity with glutamate in iCa^{2+} assays, and minimal agonism compared to VU0403602 or VU0424465 (Gregory et al., 2012). CDPPB and VU29 were included as structurally distinct allosteric modulators from the same chemotype class, where CDPPB has been reported to be a PAM-agonist and VU29 a 'pure' PAM (Chen et al., 2007; Lindsley et al., 2004). CDPPB has previously been tested *in vivo*, showing efficacy in models of Huntington's disease, fear extinction, psychosis and addiction (Cleva et al., 2011; Doria et al., 2015; Ganella et al., 2014; Gass et al., 2014; Uslaner et al., 2009). Recently, VU0409551 was described as a biased modulator on the basis that VU0409551 positively modulates $mGlu_5$ activity *in vitro* but does not enhance $mGlu_5$ modulation of NMDA receptor currents or NMDA receptor dependent plasticity in the hippocampus (Rook et al., 2015). Importantly, VU0409551 has efficacy in preclinical models of antipsychotic-like activity, cognition-enhancement and a genetic model of schizophrenia (Balu et al., 2016; Conde-Ceide et al., 2015; Rook et al., 2015). DPFE, a structurally distinct ligand relative to the three previous classes, was also included to offer further insight into the relationship between chemical scaffold and pharmacological outcome. As with CDPPB & VU0409551 behavioral studies have been conducted with DPFE (Gregory et al., 2013a; Peters et al., 2015), thereby allowing the potential to link *in vivo* efficacies with *in vitro* pharmacological fingerprints.

We first confirmed the pharmacological phenotypes for each of the eight allosteric modulators as potentiators of glutamate stimulation of $mGlu_5$-mediated iCa^{2+} mobilization in HEK293A-$mGlu_5$-low cells. In agreement with previous studies, compared to the orthosteric agonists glutamate and DHPG, VU0424465, VU0403602, and DPFE were efficacious partial allosteric agonists, achieving maximal responses 50–80% of the glutamate response. VU0360172, VU0409551 and CDPPB were also partial allosteric agonists. VU29 and VU0405398 had no appreciable allosteric agonist activity (Fig. 1A and B). The rank order of agonist efficacies was: glutamate = DHPG > VU0424465 > VU0403602 > DPFE ≥ VU0409551 > VU0360172 > CDPPB (see Supplementary Table 1 for E_{max} values). The rank order of agonist potencies (Supplementary table 1) was: VU0403602 > CDPPB ≥ VU0424465 > glutamate > VU0360172 > DHPG = VU0409551 > DPFE.

All eight compounds had different degrees of positive cooperativity (logβ) with glutamate for iCa^{2+} mobilization, causing concentration-dependent increases in glutamate potency that approached a limit (Supplementary Fig. 1). Modulator effects on glutamate concentration-response curves for iCa^{2+} mobilization

were fitted to an operational model of allosterism to quantify the functional affinity (pK_B) and efficacy modulation (logβ) for each of the ligands (Table 1). The resulting affinity and cooperativity estimates agree with those determined in previous studies (Bridges et al., 2013; Gregory et al., 2012, 2013a; Manka et al., 2010).

3.1. Select $mGlu_5$ PAMs show 'probe dependence' for potentiation of $mGlu_5$-iCa^{2+} mobilization

Although glutamate is the cognate agonist, it is a sub-optimal ligand to study the effects of $mGlu_5$ alone in primary neuronal

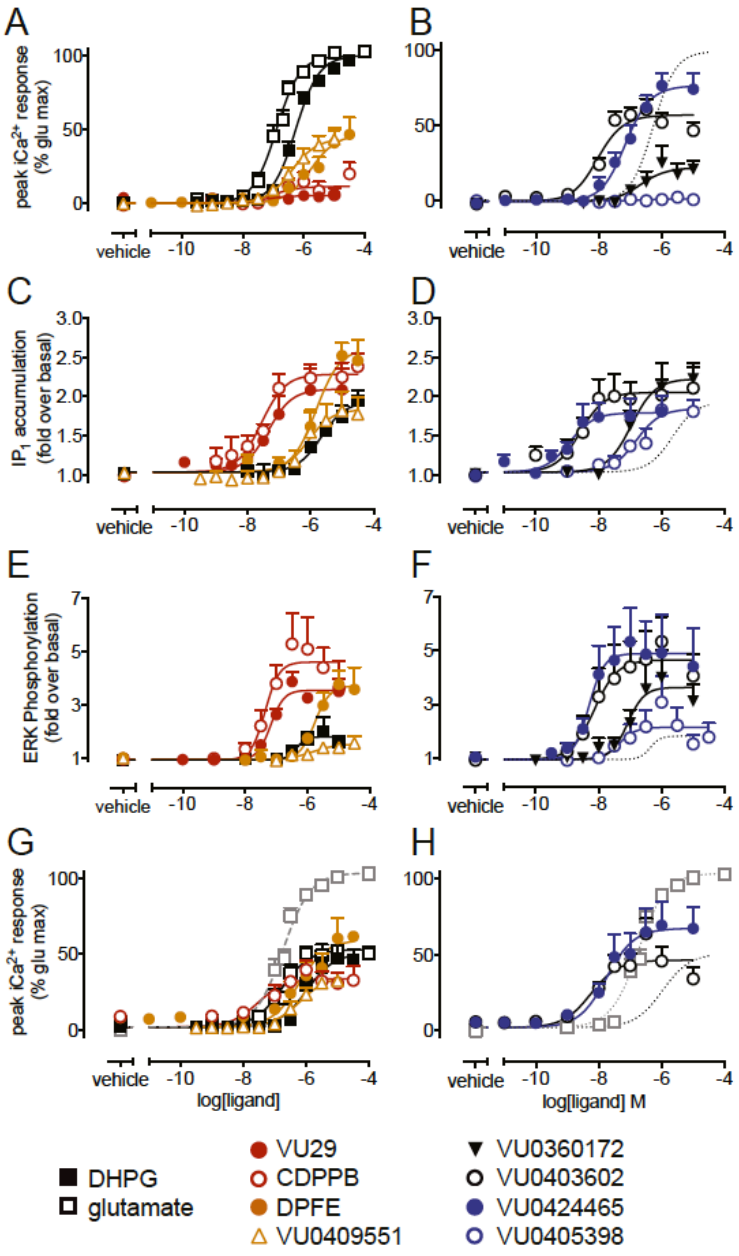

Fig. 1. $mGlu_5$ allosteric ligands have agonist activity for iCa^{2+} mobilization, IP_1 accumulation and ERK phosphorylation in HEK293A-$mGlu_5$-low. Concentration-response curves for indicated $mGlu_5$ orthosteric and allosteric ligands for iCa^{2+} mobilization (A & B), IP_1 accumulation (C & D), ERK1/2 phosphorylation (E & F) and iCa^{2+} mobilization in the absence of 1.2 mM $CaCl_2$ (G & H; % glu max represents maximal glutamate response in the presence of 1.2 mM $CaCl_2$, curve from panel A shown in grey). In panels B, D, F and H, the DHPG curve is plotted as dotted lines for ease of reference. Responses were normalized to either the glutamate maximal response (iCa^{2+} mobilization) or represented as fold over basal (IP_1 accumulation and ERK phosphorylation). IP_1 and ERK1/2 phosphorylation experiments were performed in the presence of 10 U/mL GPT to minimize contribution of ambient glutamate. Data are expressed as mean + SEM of 3–17 experiments performed in duplicate, error bars not shown lie within the dimensions of the symbols.

cultures due to the presence of multiple glutamate receptor subtypes and transporters in these native cells. Thus, we chose the more selective DHPG as the reference orthosteric agonist for assessing ligand pharmacology in primary neuronal cultures. We first confirmed that all eight allosteric ligands potentiated DHPG-mediated iCa^{2+} mobilization in HEK293A-$mGlu_5$-low cells. DHPG concentration-response curves for iCa^{2+} mobilization in the absence or presence of different concentrations of each allosteric ligand (Fig. 2) were analyzed using the operational model of allosterism. As expected, affinity estimates were similar, irrespective of which orthosteric agonist was used (Table 1). Cooperativity estimates (logβ) for the interaction with DHPG were also similar to those determined with glutamate for VU0403602, VU0360172, VU0409551 and CDPPB. In contrast, the cooperativity between VU0424465, DPFE or VU0405398 with DHPG was ~2-fold higher than with glutamate. VU29 had ~5-fold higher positive cooperativity with DHPG compared to glutamate.

3.2. All allosteric ligands have direct agonist activity for $mGlu_5$-mediated IP_1 accumulation and ERK1/2 phosphorylation in HEK293A-$mGlu_5$-low cells

We next assessed IP_1 accumulation and ERK1/2 phosphorylation in response to the $mGlu_5$ allosteric ligands, as alterations in these two pathways have been linked to diverse physiological outcomes (Bezprozvanny and Hayden, 2004; Ribeiro et al., 2010b; Tang et al., 2005). IP_1 accumulation was assessed over a 1 h period. Glutamic pyruvic transaminase (GPT) 10 U/mL was added to reduce the effect of any ambient extracellular glutamate, which may confound observations of allosteric agonism (Supplementary Fig. 2). Inclusion of GPT reduced baseline levels of IP_1 accumulation and phosphorylated ERK1/2 (pERK1/2) (Supplementary Fig. 2).

Relative to the reference orthosteric agonist, DHPG, all eight allosteric modulators were agonists for $mGlu_5$-IP_1 accumulation, achieving a similar maximal response to DHPG (Fig. 1C–D). All eight allosteric ligands stimulated pERK1/2, characterized by a transient peak (5–7 min post-addition) that returned to baseline levels within 30 min (Supplementary Fig. 2). Concentration-response curves for $mGlu_5$-pERK1/2 constructed at the peak time point revealed VU0409551 and VU0405398 to be equally as efficacious agonists as DHPG (Fig. 1E–F). Consistent with a previous report (Gregory et al., 2012), VU29, CDPPB, DPFE, VU0360172, VU0424465 and VU0403602 elicited higher maximal responses for pERK1/2 than the orthosteric agonist. DHPG had significantly lower potency (7-fold) for IP_1 accumulation relative to pERK1/2 and iCa^{2+} mobilization (Supplementary Table 1). Conversely, VU0424465 was 10–30 fold more potent in pERK1/2 and IP_1 relative to iCa^{2+} assays, and VU0403602 had similar potencies for IP_1 and iCa^{2+}, but was ~5-fold more potent for pERK1/2. The potencies for VU0360172, CDPPB, VU0409551 and DPFE were similar across all three measures of receptor activation, as were VU29 and VU0405398 between pERK1/2 and IP_1 accumulation. These differences in the rank orders of ligand potency for between different signaling pathways are suggestive of biased agonism.

3.3. $mGlu_5$-mediated calcium mobilization is a composite of intracellular and extracellular calcium sources

Upon activation of G_q-coupled receptors, inositol phosphate hydrolysis is widely known to result in mobilization of intracellular calcium. Therefore it was unexpected that ligands that were agonists for IP_1 had lower potency or efficacy in iCa^{2+} assays. However, it is also well-known that $mGlu_5$ couples to various calcium ion channels (Sengmany and Gregory, 2015). Hence, iCa^{2+} mobilization detected upon receptor activation may be the combination of both extracellular calcium entering the cell via ion channels, and the calcium released from internal stores. To differentiate the sources of calcium, extracellular calcium was excluded from the buffer, thereby allowing measurement of calcium arising from intracellular stores. The maximal responses to both glutamate and DHPG were significantly reduced in the absence of 1.2 mM extracellular calcium, although potencies were unaffected (Fig. 1G). With the exception of CDPPB, which had increased efficacy in the absence of extracellular Ca^{2+}, there was no significant change in the potency or maximal responses to DPFE, VU0409551, VU0403602 or VU0424465 between the differing calcium conditions with the $mGlu_5$ allosteric ligands studied (Fig. 1G–H, Supplementary Table 1).

3.4. Assessment of agonist activity of $mGlu_5$ allosteric ligands in cortical neurons

The same four measures of $mGlu_5$ activity that we investigated in recombinant cells were next examined in cortical neurons to assess the potential of biased allosteric agonist activity in a native system (Fig. 3). Cortical neurons represent a physiologically relevant system to assess $mGlu_5$ allosteric ligand activity, and can serve as a vital translational link for validating allosteric modulator pharmacology prior to preclinical assessments. To eliminate the influence of $mGlu_1$, which is also expressed in the cortex, the $mGlu_1$ selective negative allosteric modulator CPCCOEt 30 μM, was used in conjunction with DHPG for all experiments in cortical neurons. GPT had no effect on basal IP_1 levels or allosteric agonism (Supplementary Fig. 3) and was not included in these experiments.

Table 1
Affinity and cooperativity estimates for allosteric modulation of orthosteric agonist-mediated iCa^{2+} mobilization and IP_1 accumulation in HEK293A-$mGlu_5$-low and cortical neurons. Data are mean ± SEM of 3–9 independent experiments performed in duplicate.

	HEK293A: Glu-iCa^{2+}		HEK293A: DHPG-iCa^{2+}		Cortical: DHPG-iCa^{2+}		Cortical: DHPG-IP_1	
	pK_B[a]	logβ[b]	pK_B	Logβ	pK_B	Logβ	pK_B	Logβ
VU0424465	6.94 ± 0.19	0.37 ± 0.11	7.00 ± 0.11	0.84 ± 0.13[c]	n/a	n/a	n/a	n/a
VU0403602	7.62 ± 0.17	0.97 ± 0.15	7.23 ± 0.34	1.06 ± 0.12	n/a	n/a	n/a	n/a
VU0360172	6.67 ± 0.18	0.53 ± 0.13	7.24 ± 0.36	0.52 ± 0.07	7.11 ± 0.29	0.75 ± 0.10	6.55 ± 0.15	0.20 ± 0.09[d]
VU29	6.87 ± 0.22	0.13 ± 0.09	6.67 ± 0.28	0.81 ± 0.08[c]	5.70 ± 0.45	1.07 ± 0.24	6.51 ± 0.19	0.29 ± 0.04
CDPPB	6.58 ± 0.25	0.69 ± 0.16	6.87 ± 0.17	0.72 ± 0.08	6.61 ± 0.25	0.66 ± 0.15	6.81 ± 0.41	0.25 ± 0.12
DPFE	6.04 ± 0.27	0.60 ± 0.13	5.35 ± 0.25	1.07 ± 0.11[c]	5.45 ± 0.22	0.84 ± 0.05	5.50 ± 0.23	0.26 ± 0.14[d]
VU0405398	7.00 ± 0.12	0.31 ± 0.06	6.97 ± 0.24	0.57 ± 0.06[c]	5.37 ± 0.29	0.56 ± 0.08	6.46 ± 0.13[d]	0.11 ± 0.03[d]
VU0409551	5.96 ± 0.43	1.00 ± 0.27	5.88 ± 0.20	1.06 ± 0.09	6.04 ± 0.24	1.16 ± 0.27	6.14 ± 0.16	0.35 ± 0.13[d]

[a] pK_B, negative logarithm of the equilibrium dissociation constant determined using an operational model of allosterism.
[b] logβ, logarithm of the efficacy modulation factor. n/a denotes operational parameters not determined due to confounding agonism.
[c] Denotes $p < 0.05$, comparing logβ values between glutamate and DHPG-stimulated iCa^{2+} mobilization.
[d] Denotes $p < 0.05$, comparing respective operational parameters between iCa^{2+} mobilization and IP_1 accumulation for cortical neurons, using an unpaired Student's *t*-test.

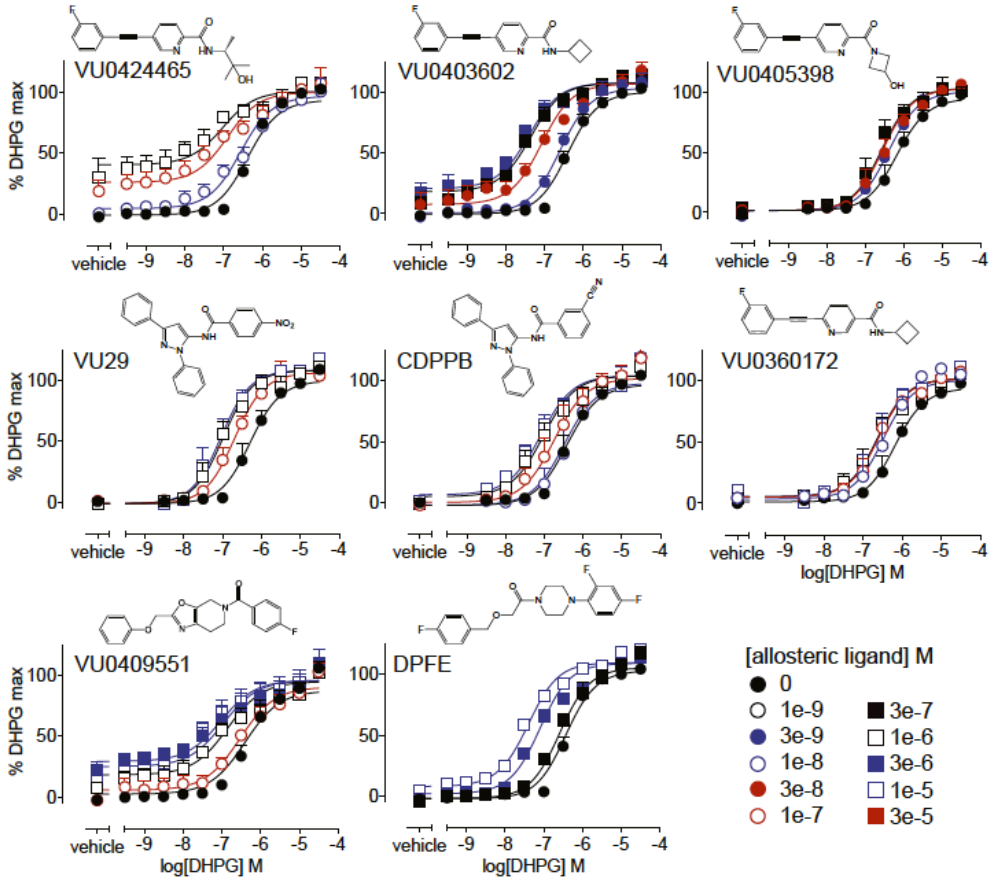

Fig. 2. Allosteric modulation of DHPG-stimulated iCa^{2+} mobilization in HEK293A-$mGlu_5$-low cells. DHPG concentration-response curves for iCa^{2+} mobilization in the absence and presence of indicated concentrations of allosteric ligands. Interaction studies for DPFE, VU0409551, VU0424465, and VU0403602 were performed using simultaneous addition of both ligands, to minimize allosteric ligand-induced acute desensitization due to intrinsic agonist activity. VU29, VU0405398, CDPPB and VU0360172 were added 1 min prior to addition of glutamate. Data sets were globally fitted to an operational model of allosterism to estimate affinity and cooperativity. Curves represent the best fit of the data. Data are mean + SEM of n = 3–10 experiments performed in duplicate. Error bars not shown lie within the dimensions of the symbol.

DHPG was ~10 fold less potent for IP_1 accumulation relative to iCa^{2+} (in absence and presence of 1.2 mM extracellular Ca^{2+}) and ERK1/2 phosphorylation (Supplementary Table 3). In iCa^{2+} mobilization assays relative to DHPG, VU0424465 and VU0403602 were nearly full agonists, whereas VU0360172, DPFE, VU29 and CDPPB were all partial agonists (Fig. 3A, B, Supplementary Table 2). VU0405398 also showed agonist activity, however, the maximal response was highly variable and restricted to concentrations above 3 μM. VU0409551 had no appreciable agonist activity for iCa^{2+} mobilization. The rank order of agonist efficacy: DHPG > VU0424465 = VU0403602 > CDPPB = VU29 = VU0360172 > VU0405398 ≫ VU0409551, was different to that observed in HEK293A cells.

For IP_1 accumulation the relative efficacies of the allosteric ligands were similar to that observed for iCa^{2+} assays, with the exception of VU0409551 which had appreciable agonist activity for IP_1 accumulation (Fig. 3C–D). The time course for $mGlu_5$-mediated ERK1/2 phosphorylation by both orthosteric and allosteric ligands was characterized by sustained elevations or inhibition in cortical neurons, a markedly different profile to the transient response observed in HEK293A cells (Supplementary Fig. 4). VU0424465, VU0403602, VU0360172, VU29, CDPPB and VU0409551 were all agonists for pERK1/2 in cortical neurons eliciting maximal responses to similar to DHPG (Fig. 3E–F). Allosteric agonism (iCa^{2+}, pERK1/2 and IP_1) in cortical neurons was inhibited by pre-exposure to the $mGlu_5$ selective neutral allosteric ligand 5MPEP confirming that agonism was mediated via interaction with $mGlu_5$ (Supplementary Fig. 5). Interestingly, while DPFE and VU0405398 were partial agonists for IP_1 accumulation, they exhibited a bell-shaped concentration-response relationship for pERK1/2, elevating pERK1/2 at 1 μM and dropping below basal at concentrations above 1 μM (Fig. 3E–F). Similar to observations in HEK293A-$mGlu_5$-low cells, the DHPG maximal response was significantly reduced in the absence of extracellular calcium (Fig. 3G). There were no significant differences in potency or maximal response of VU0424465, VU0403602, VU0360172, or CDPPB between differing calcium conditions (Fig. 3G–H). However, agonist activity by VU29, DPFE and VU0405398 was lost.

3.5. $mGlu_5$ allosteric ligands are biased agonists

In order to rigorously and quantitatively assess the apparent bias of $mGlu_5$ allosteric agonists in HEK293A-$mGlu_5$-low cells and cortical neurons, observational bias between assays, and systems bias of the cell background should be minimized – thereby resulting

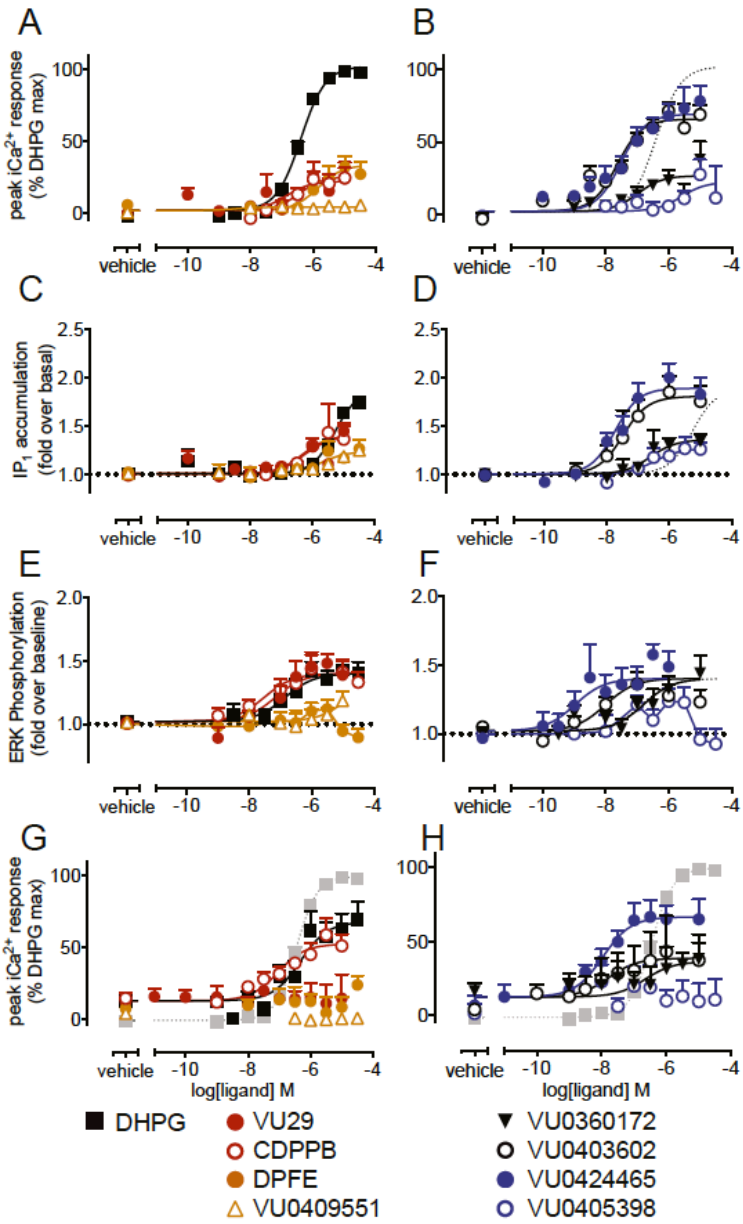

Fig. 3. $mGlu_5$ allosteric ligands have agonist activity for iCa^{2+} mobilization, IP_1 accumulation and ERK phosphorylation in cultured cortical neurons. Concentration-response curves for indicated $mGlu_5$ orthosteric and allosteric ligands for iCa^{2+} mobilization (A&B), IP_1 accumulation (C & D), ERK1/2 phosphorylation (E&F) and iCa^{2+} mobilization in the absence of 1.2 mM $CaCl_2$ (G & H; % DHPG max represents maximal DHPG response in the presence of 1.2 mM $CaCl_2$, curve from panel A is shown in grey). In panels B, D, F and H, the DHPG curve is plotted as a dotted line for ease of reference. Responses were normalized to either the glutamate maximal response (iCa^{2+} mobilization) or represented as fold over basal (IP_1 accumulation and ERK phosphorylation). All assays were performed in the presence of 30 μM CPCCOEt to eliminate the contribution of $mGlu_1$. Data are expressed as mean + SEM of 3–22 experiments performed in duplicate, error bars not shown lie within the dimensions of the symbols.

in a more faithful estimate of true (conformationally-driven) biased agonism (Kenakin et al., 2012). From each assay, a transduction coefficient $\log(\tau/K_A)$ (Supplementary Table 4), that is, the composite of ligand efficacy and affinity, was derived as previously described (Kenakin et al., 2012) and normalized to the reference ligand DHPG ($\Delta\log(\tau/K_A)$). Subsequent normalization of $\Delta\log(\tau/K_A)$ between pathways, $\Delta\Delta\log(\tau/K_A)$, allows for quantification of the degree of bias between pathways (Fig. 4). Each allosteric ligand displayed a unique signaling bias fingerprint in HEK293A-$mGlu_5$-low cells and neurons, although there were some notable trends. Relative to DHPG, VU0424465 showed significant bias away from iCa^{2+} mobilization and toward IP_1 accumulation (110-fold) and ERK1/2 phosphorylation (9-fold) in HEK293A-$mGlu_5$-low cells, a profile that was largely retained in neurons. VU0403602 was biased toward IP_1 over

pERK1/2 (11-fold) and iCa^{2+} mobilization (14-fold) in HEK293A-$mGlu_5$-low cells, however this wasn't reflected in the neurons. VU29 and CDPPB were biased (3–25 fold) toward IP_1 over pERK1/2 and/or iCa^{2+} mobilization in both HEK293A cells and neurons. DPFE, VU0409551 and VU0405398 showed no discernible bias in HEK293A cells, but had distinct bias fingerprints in cortical neurons. VU0405398 and DPFE were biased toward IP_1 over iCa^{2+} (12 and 26-fold respectively) coupled with biphasic pERK1/2 responses that could not be analyzed using the operational model. VU0409551 was the only ligand to show significant bias (24-fold) between IP_1 and pERK1/2 in cortical neurons.

3.6. CDPPB, DPFE, VU0405398 are biased allosteric modulators of DHPG in cortical neurons

We were unable to perform interaction studies between the modulators with DHPG to quantify affinity and cooperativity in HEK293A-$mGlu_5$-low cells, because of the robust agonism for IP_1 accumulation and ERK1/2 phosphorylation displayed by each allosteric ligand in their own right. However, in cortical neurons, a number of allosteric ligands had minimal or partial agonist effects, such that a sufficient response window remained to allow for allosteric interaction experiments with DHPG in this physiologically relevant system. Thus, the resulting DHPG concentration-response curves for IP_1 and iCa^{2+} in the absence and presence of increasing concentrations of VU0360172, VU29, CDPPB, DPFE, VU0409551 or VU0405398 were constructed and analyzed using an operational model of allosterism (Fig. 5, Supplementary Fig. 6). Affinity estimates were similar for each allosteric ligand across the two pathways, with the exception of VU0405398, which had higher affinity in the IP_1 assay (Table 1). For all six allosteric modulators, the magnitude of logβ was lower for IP_1 versus iCa^{2+} (Fig. 5D); this reached significance for DPFE (3.8-fold), VU0360172 (3.6-fold), VU0409551 (6.5-fold) and VU0405398 (2.8-fold). Given that VU0360172, VU0405398 and DPFE were also partial agonists for ERK1/2 phosphorylation, we assessed modulation of the DHPG concentration-response curve by these three modulators. In cortical neurons, VU0360172 was a PAM-agonist for DHPG-stimulated ERK1/2 phosphorylation with similar affinity and cooperativity estimates (pK_B: 6.49 ± 0.20 and logβ: 0.69 ± 0.18) to those determined in iCa^{2+} assays (Fig. 5D). In contrast, DPFE and VU0405398 showed a unique bell-shaped modulatory response in ERK1/2 phosphorylation. While 1 μM of each ligand potentiated DHPG responses, 10 μM of each ligand resulted in decreased DHPG maximal responses for ERK1/2 phosphorylation (Fig. 5).

4. Discussion

Allosteric modulators of $mGlu_5$ offer considerable therapeutic potential for the treatment of numerous psychiatric and

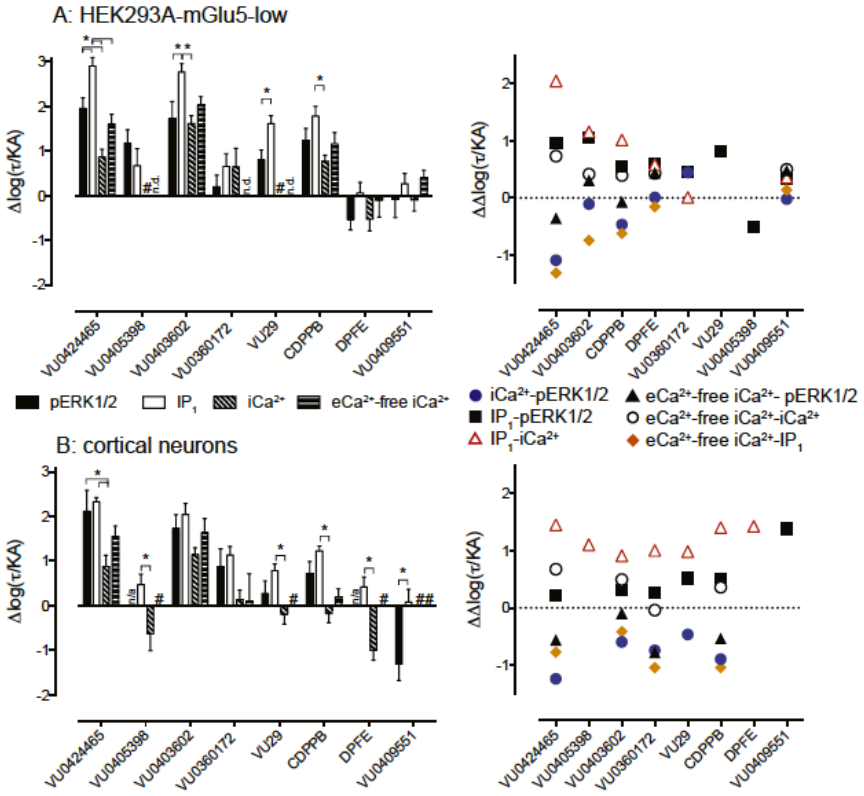

Fig. 4. $mGlu_5$ allosteric ligands are biased agonists relative to DHPG in HEK293A-$mGlu_5$-low and cortical neurons. The transduction coefficient ($\log(\tau/K_A)$) was derived by applying equation (3) to agonist concentration-response curves in HEK293A-$mGlu_5$-low (A, curves in Fig. 1) and cortical neurons (B, curves in Fig. 2) and normalized to DHPG ($\Delta\log(\tau/K_A)$). To calculate the degree of bias evident for different ligands between different pathways, $\Delta\log(\tau/K_A)$ values were subtracted from one another ($\Delta\Delta\log(\tau/K_A)$) to determine Log bias factors. Data for $\Delta\log(\tau/K_A)$ represent the mean ± SEM, whereas Log bias estimates are mean only. * denotes significantly different comparisons, $p < 0.05$, one-way ANOVA with Tukey's post-test.

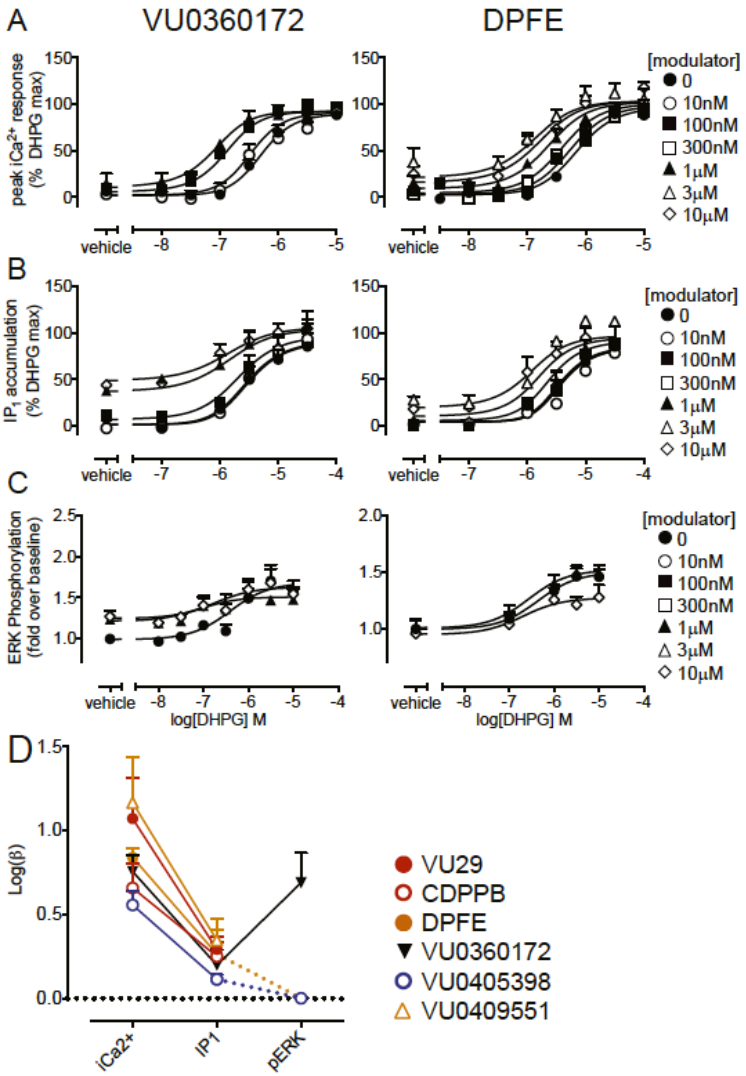

Fig. 5. $mGlu_5$ allosteric ligands are biased modulators of DHPG responses in native cortical neurons. DHPG concentration response curves for iCa^{2+} mobilization (A), IP_1 accumulation (B) and ERK1/2 phosphorylation (C) in the absence and presence of VU0360172 and DPFE. Both VU0360172 and DPFE produced leftward shifts in DHPG potency for iCa^{2+} and IP_1 assays. Data sets were globally fitted to an operational model of allosterism to estimate affinity and cooperativity. Curves represent the best fit of the data. In ERK1/2 phosphorylation assays, DPFE produced a leftward shift with 1 μM however reduced the maximal response of DHPG at 10 μM. D) Cooperativity estimates (Logβ) of allosteric ligands were plotted to enable comparison of modulation across pathways. For DPFE and VU0405398, which showed mixed modulatory activity, Log β values were plotted as zero to highlight the implicit bias; the absolute numerical value in this instance has no meaning. Data are mean ± SEM of n = 3–9 experiments performed in duplicate. Error bars not shown lie within the dimensions of the symbol.

neurological disorders. In particular, $mGlu_5$ PAMs have demonstrated efficacy in preclinical models of psychosis, cognition-enhancement and NMDA receptor hypofunction (Ayala et al., 2009; Gregory et al., 2013a; Horio et al., 2013; Rook et al., 2015; Uslaner et al., 2009). However, a number of recent studies have reported adverse effects with select $mGlu_5$ allosteric modulators (Rook et al., 2013; Parmentier-Batteur et al., 2014). Therefore in order to realize the therapeutic potential of $mGlu_5$ allosteric modulators, there is a need to better understand the full scope of allosteric drug action. We tested the hypothesis that structurally diverse PAMs had unappreciated biased pharmacology. We found that $mGlu_5$ allosteric ligands had diverse biased signaling fingerprints in both recombinant and native systems. Furthermore, this bias extended to modulation of orthosteric agonist activity, where the magnitude of cooperativity between allosteric and orthosteric ligands differed depending upon the measure of receptor activation. The prevalence of biased agonism and modulation for diverse $mGlu_5$ PAM chemotypes highlights the paucity in our understanding of the functional consequences of $mGlu_5$ allosteric modulation, and raises new avenues for therapeutic discovery. Armed with a better appreciation of the full scope of $mGlu_5$ allosteric modulator action, it may be possible to link activation (and/or enhancement) of specific pathways to different physiological outcomes to promote therapeutic effects and avoid adverse effects.

In particular, many of the studied $mGlu_5$ allosteric ligands, which previously were largely classified based on modulation of glutamate-stimulated iCa^{2+} mobilization, showed significant differences in coupling efficiency to iCa^{2+} mobilization, IP_1 accumulation and ERK1/2 phosphorylation. Most strikingly, each allosteric ligand tested had greater efficacy for IP_1 accumulation relative to iCa^{2+} mobilization. Therefore the ligands tested cannot be considered as pure $mGlu_5$ PAMs, and do not posses the safety advantages of pure allosteric modulators, i.e., the advantage of spatiotemporal fine-tuning of receptor responses and saturable effects. Classically, iCa^{2+} mobilization is considered to be downstream of inositol phosphate hydrolysis, however, our data show that IP_1 accumulation does not necessarily result in iCa^{2+} mobilization via $mGlu_5$. It is possible that these differences between IP_1 and iCa^{2+} are related to the different kinetics of response coupling measurements for these two assays. A lack of equilibrium being achieved by allosteric ligands relative to orthosteric agonists in the transient iCa^{2+} assay may also be a contributing factor. Indeed, underlying temporal differences between assays and ligands influences bias at the dopamine D2 receptor, such that kinetic context may also play a crucial role in understanding biased agonism (Klein Herenbrink et al., 2016). However, it is widely accepted that the $mGlu_5$ receptor is coupled to various calcium channels (Gao et al., 2013; Kammermeier et al., 2000; Lu et al., 1999; McCool et al., 1998; Ribeiro et al., 2010a; Tu et al., 1999), thereby resulting in Ca^{2+} mobilization from both intracellular and extracellular stores. In order to differentiate the sources of Ca^{2+}, we compared iCa^{2+} mobilization in the presence and absence of 1.2 mM Ca^{2+} in HEK293A-$mGlu_5$-low cells. Interestingly, while glutamate and DHPG had reduced maximal responses in the absence of extracellular Ca^{2+}, all studied $mGlu_5$ allosteric ligands were unaffected. By applying a rigorous analytical approach to quantify bias, we found that VU0424465 showed significant bias between IP_1 and extracellular Ca^{2+}-free iCa^{2+} assays (20-fold) and between IP_1 and iCa^{2+} assays (110-fold). These data suggest that allosteric agonists couple to a different complement of effectors than orthosteric agonists to influence intracellular Ca^{2+} levels.

Our data clearly demonstrate that allosteric modulator activity in an $mGlu_5$-iCa^{2+} mobilization assay is not necessarily predictive of activity for other $mGlu_5$-mediated effects. Our data contribute to a growing body of evidence for biased agonism at metabotropic glutamate receptors including for $mGlu_1$ (Emery et al., 2012; Hathaway et al., 2015) and group III mGlu receptors (Jalan-Sakrikar et al., 2014). Further, we observed probe-dependence for potentiation of $mGlu_5$-iCa^{2+} mobilization in HEK293A cells, where the magnitude of cooperativity for select allosteric ligands was dependent upon the orthosteric agonist present. Probe dependence has not previously been observed for $mGlu_5$, however, is known to be prevalent for other mGlu subtypes (Jalan-Sakrikar et al., 2014). The phenomenon of probe dependence is a crucial consideration, particularly when translating findings from *in vitro* assays to native preparations, such as slice electrophysiology, where surrogate agonists are often used. Interestingly, while VU29 had higher positive cooperativity with DHPG compared to glutamate, CDPPB potentiated both agonists to a similar extent. Similarly, for the three picolinamide acetylenes studied, VU0424465 and VU0405398 had differential cooperativities with DHPG and glutamate whereas VU0403602 did not. These data demonstrate that the probe dependence observed is not linked to a particular chemotype, or consistent between ligands from the same scaffold.

While probe dependence is an important consideration when moving from recombinant to physiologically relevant systems, the change in cell background in itself may be a confounding factor in understanding drug pharmacology. Indeed, in this study, we observed clear differences in the temporal profile for $mGlu_5$-ERK1/2 phosphorylation between HEK293A-$mGlu_5$-low and cortical neurons. While ERK1/2 phosphorylation was transient in HEK293A-$mGlu_5$-low cells, in cortical neurons pERK1/2 levels remained elevated over 30 min. These data suggest that distinct intracellular effectors are mediating pERK1/2 in response to $mGlu_5$ activation in cortical neurons versus HEK293A cells. Moreover, sustained ligand-induced responses suggest that the consequences of receptor activation will continue after a ligand has vacated the receptor. It is also possible that cellular context is driving differential compartmentalization and/or internalization of $mGlu_5$ in these two cell types. Of note, 50–80% of $mGlu_5$ receptors are thought to be located on intracellular membranes (Hubert et al., 2001; Kumar et al., 2008), and subcellular localisation of $mGlu_5$ can dictate the overall cellular response (Jong et al., 2009; Kumar et al., 2012). It remains to be determined whether or not the $mGlu_5$ allosteric ligands tested cross the plasma membrane, induce receptor internalization or are internalized with the receptor. DHPG is not actively transported across the plasma membrane, only activating receptors at the cell surface (Jong et al., 2009), this suggests that the sustained pERK1/2 response in cortical neurons originates from cell surface receptors, however, it is possible that the continued signaling may be driven by internalised cell surface receptors within endosomes.

Comparison of the biased agonism signaling fingerprints for all eight allosteric ligands revealed that VU0424465 had the most divergent profile in both HEK cells and neuronal cultures. Our earlier study linked VU0424465 intrinsic efficacy (for $mGlu_5$-iCa^{2+} in HEK cells) to seizure activity and behavioral convulsions (Rook et al., 2013). However, comparison of the bias signaling fingerprint of VU0424465 with that of DPFE, VU0409551 and CDPPB, three ligands that have efficacy in models of cognition and psychosis but no reported adverse effects (Gregory et al., 2013a; Uslaner et al., 2009; Balu et al., 2016; Rook et al., 2015), suggests that the pronounced bias (10–100 fold) of VU0424465 toward IP_1 and ERK1/2 relative to iCa^{2+} in HEK293A-$mGlu_5$-low cells may be a better prediction of adverse effect liability. It is worth noting that all experiments in cortical neurons were performed in the presence of CPCCOEt (an $mGlu_1$ negative allosteric modulator) to eliminate DHPG activation of $mGlu_1$. However, $mGlu_1$ and $mGlu_5$ are known to heteromerize (Sevastyanova and Kammermeier, 2014). Heteromerization of metabotropic glutamate receptors ($mGlu_2$ and $mGlu_4$) can influence allosteric modulator pharmacology (Yin et al., 2014). In the future it would be of interest to determine if $mGlu_1$/$mGlu_5$ heteromers influence the biased agonism observed for $mGlu_5$ selective PAM-agonists. Understanding the bias profile of different ligands, and linking this to known preclinical profiles, offers the opportunity to design therapeutics that avoid signaling pathways associated with adverse effects.

We found that allosteric ligand bias profiles differed between HEK293A-$mGlu_5$-low cells and cortical neuronal cultures. Of note, VU0409551 was the only ligand to show significant bias away from pERK1/2 (relative to IP_1) and a lack of agonist efficacy for iCa^{2+} mobilization in cortical neurons. These data are consistent with the previous report that VU0409551 acting at $mGlu_5$ does not potentiate NMDA channel currents (Rook et al., 2015) or stimulate pERK1/2 levels in the hippocampus or prefrontal cortex when dosed chronically (Balu et al., 2016). Interestingly, DPFE and VU0405398 had distinctly different concentration-response relationships for ERK1/2 phosphorylation in cortical neurons, eliciting a bi-phasic response. While VU0405398 has not yet been tested *in vivo*, DPFE has a unique preclinical efficacy profile. Considerably lower doses of DPFE (0.56 mg/kg) are required for cognition enhancement, whereas >10 mg/kg is needed for efficacy in reversing amphetamine-induced hyperlocomotion (Gregory et al., 2013a,b,c). In contrast, cognition studies with CDPPB (Horio et al.,

2013; Stefani and Moghaddam, 2010) have demonstrated efficacy at doses similar those required for efficacy in reversing amphetamine-induced hyperlocomotion (Kinney et al., 2005). It is tempting to speculate that the distinct coupling profiles for DPFE and VU0409551 with respect to pERK1/2 may be predictive of *in vivo* efficacy that is biased toward cognition enhancement.

In addition to biased agonism, biased modulation was also demonstrated for different $mGlu_5$ allosteric ligands in cortical neurons. Biased modulation may be more favorable for CNS drugs, rather than direct activation of receptors, as it allows for greater control over basal glutamatergic tone. Multiple studies have demonstrated that different $mGlu_5$ effectors and second messengers can be perturbed in different CNS disorders. For example, disrupted mTOR and Akt signaling is associated with major depressive disorder and suicide (Dwivedi et al., 2010; Jernigan et al., 2011) whereas increases in basal pERK1/2, Akt and altered IP_3/iCa^{2+} signaling are observed in a mouse model of Huntington's disease (Bezprozvanny and Hayden, 2004; Ribeiro et al., 2010b; Tang et al., 2005). Therefore, biased modulation may provide the means to tailor enhancement or inhibition of $mGlu_5$ activity to effectors associated with different disease states.

In summary, we have determined the signaling fingerprint of several $mGlu_5$ allosteric ligands at iCa^{2+} mobilization, IP_1 accumulation and ERK1/2 phosphorylation in both recombinant and native systems. Probe dependence, biased agonism and biased modulation were operative at this receptor. Importantly, the most divergent bias profiles were associated with ligands previously shown to possess distinct *in vivo* efficacy profiles. Drug discovery for neuroscience-related disorders continues to suffer from high attrition rates, in large part due to an inability to translate promising preclinical pharmacological profiles to clinically effective therapeutics. Our findings suggest that unappreciated biased agonism and/or modulation may contribute to these failures and highlight the need to examine multiple measures of receptor activity to best classify the pharmacology of ligands. In the future, these biased signaling fingerprints may provide a framework that can be used to rationally develop $mGlu_5$ allosteric ligands with optimal *in vitro* profiles that translate to desirable activity in preclinical models and avoid on-target adverse effects.

Acknowledgements

This work was supported by the National Health & Medical Research Council of Australia (NHMRC): CJ Martin Overseas Biomedical postdoctoral training Fellowship (KJG: APP1013709), Project Grant APP1084775 (KJG), Program Grant APP1055134 (AC) and Senior Principal Research Fellowship APP1102950 (AC). Work within the Vanderbilt Center for Neuroscience Drug Discovery on $mGlu_5$ PAMs was supported by the NIH/NIMH R01MH062646. PJC is an inventor on patents that protect multiple classes of $mGlu_5$ PAMs and receives research support from AstraZeneca. ERK SureFire kits were a kind gift from Dr. Michael Crouch and TGR Biosciences (Thebarton, Australia). We thank Ms. Sabine Albold for expert technical assistance.

Appendix A. Supplementary data

Supplementary data related to this article can be found at http://dx.doi.org/10.1016/j.neuropharm.2016.07.001.

References

Ayala, J.E., Chen, Y., Banko, J.L., Sheffler, D.J., Williams, R., Telk, A.N., Watson, N.L., Xiang, Z., Zhang, Y., Jones, P.J., Lindsley, C.W., Olive, M.F., Conn, P.J., 2009. mGluR5 positive allosteric modulators facilitate both hippocampal LTP and LTD and enhance spatial learning. Neuropsychopharmacol 34, 2057–2071.

Balu, D.T., Li, Y., Takagi, S., Presti, K.T., Ramikie, T.S., Rook, J.M., Jones, C.K., Lindsley, C.W., Conn, P.J., Bolshakov, V.Y., Coyle, J.T., 2016. An mGlu5-positive allosteric modulator rescues the neuroplasticity deficits in a genetic model of NMDA receptor hypofunction in schizophrenia. Neuropsychopharmacol 41, 2052–2061.

Bezprozvanny, I., Hayden, M.R., 2004. Deranged neuronal calcium signaling and Huntington disease. Biochem. Biophys. Res. Commun. 322, 1310–1317.

Bridges, T.M., Rook, J.M., Noetzel, M.J., Morrison, R.D., Zhou, Y., Gogliotti, R.D., Vinson, P.N., Xiang, Z., Jones, C.K., Niswender, C.M., Lindsley, C.W., Stauffer, S.R., Conn, P.J., Daniels, J.S., 2013. Biotransformation of a novel positive allosteric modulator of metabotropic glutamate receptor subtype 5 contributes to seizure-like adverse events in rats involving a receptor agonism-dependent mechanism. Drug Metab. Dispos. 41, 1703–1714.

Chen, Y., Nong, Y., Goudet, C., Hemstapat, K., de Paulis, T., Pin, J.P., Conn, P.J., 2007. Interaction of novel positive allosteric modulators of metabotropic glutamate receptor 5 with the negative allosteric antagonist site is required for potentiation of receptor responses. Mol. Pharmacol. 71, 1389–1398.

Christopoulos, A., Kenakin, T., 2002. G protein-coupled receptor allosterism and complexing. Pharmacol. Rev. 54, 323–374.

Cleva, R.M., Hicks, M.P., Gass, J.T., Wischerath, K.C., Plasters, E.T., Widholm, J.J., Olive, M.F., 2011. mGluR5 positive allosteric modulation enhances extinction learning following cocaine self-administration. Behav. Neurosci. 125, 10–19.

Conde-Ceide, S., Martinez-Viturro, C.M., Alcazar, J., Garcia-Barrantes, P.M., Lavreysen, H., Mackie, C., Vinson, P.N., Rook, J.M., Bridges, T.M., Daniels, J.S., Megens, A., Langlois, X., Drinkenburg, W.H., Ahnaou, A., Niswender, C.M., Jones, C.K., Macdonald, G.J., Steckler, T., Conn, P.J., Stauffer, S.R., Bartolome-Nebreda, J.M., Lindsley, C.W., 2015. Discovery of VU0409551/JNJ-46778212: an mGlu5 positive allosteric modulator clinical candidate targeting schizophrenia. ACS Med. Chem. Lett. 6, 716–720.

Dore, A.S., Okrasa, K., Patel, J.C., Serrano-Vega, M., Bennett, K., Cooke, R.M., Errey, J.C., Jazayeri, A., Khan, S., Tehan, B., Weir, M., Wiggin, G.R., Marshall, F.H., 2014. Structure of class C GPCR metabotropic glutamate receptor 5 transmembrane domain. Nature 511, 557–562.

Doria, J.G., de Souza, J.M., Andrade, J.N., Rodrigues, H.A., Guimaraes, I.M., Carvalho, T.G., Guatimosim, C., Dobransky, T., Ribeiro, F.M., 2015. The mGluR5 positive allosteric modulator, CDPPB, ameliorates pathology and phenotypic signs of a mouse model of huntington's disease. Neurobiol. Dis. 73, 163–173.

Dwivedi, Y., Rizavi, H.S., Zhang, H., Roberts, R.C., Conley, R.R., Pandey, G.N., 2010. Modulation in activation and expression of phosphatase and tensin homolog on chromosome ten, Akt1, and 3-phosphoinositide-dependent kinase 1: further evidence demonstrating altered phosphoinositide 3-kinase signaling in postmortem brain of suicide subjects. Biol. Psychiat 67, 1017–1025.

Emery, A.C., Pshenichkin, S., Takoudjou, G.R., Grajkowska, E., Wolfe, B.B., Wroblewski, J.T., 2010. The protective signaling of metabotropic glutamate receptor 1 Is mediated by sustained, beta-arrestin-1-dependent ERK phosphorylation. J. Biol. Chem. 285, 26041–26048.

Emery, A.C., DiRaddo, J.O., Miller, E., Hathaway, H.A., Pshenichkin, S., Takoudjou, G.R., Grajkowska, E., Yasuda, R.P., Wolfe, B.B., Wroblewski, J.T., 2012. Ligand bias at metabotropic glutamate 1a receptors: molecular determinants that distinguish beta-arrestin-mediated from G protein-mediated signaling. Mol. Pharmacol. 82, 291–301.

Ganella, D.E., Thangaraju, P., Lawrence, A.J., Kim, J.H., 2014. Fear extinction in 17 day old rats is dependent on metabotropic glutamate receptor 5 signaling. Behav. Brain. Res. 298, 32–36.

Gao, C., Tronson, N.C., Radulovic, J., 2013. Modulation of behavior by scaffolding proteins of the post-synaptic density. Neurobiol. Learn. Mem. 105, 3–12.

Gass, J.T., Trantham-Davidson, H., Kassab, A.S., Glen Jr., W.B., Olive, M.F., Chandler, L.J., 2014. Enhancement of extinction learning attenuates ethanol-seeking behavior and alters plasticity in the prefrontal cortex. J. Neurosce 34, 7562–7574.

Gentry, P.R., Sexton, P.M., Christopoulos, A., 2015. Novel allosteric modulators of G protein-coupled receptors. J. Biol. Chem. 290, 19478–19488.

Gregory, K.J., Herman, E.J., Ramsey, A.J., Hammond, A.S., Byun, N.E., Stauffer, S.R., Manka, J.T., Jadhav, S., Bridges, T.M., Weaver, C.D., Niswender, C.M., Steckler, T., Drinkenburg, W.H., Ahnaou, A., Lavreysen, H., Macdonald, G.J., Bartolome, J.M., Mackie, C., Hrupka, B.J., Caron, M.G., Daigle, T.L., Lindsley, C.W., Conn, P.J., Jones, C.K., 2013a. N-aryl piperazine metabotropic glutamate receptor 5 positive allosteric modulators possess efficacy in preclinical models of NMDA hypofunction and cognitive enhancement. J. Pharmacol. Exp. Ther. 347, 438–457.

Gregory, K.J., Nguyen, E.D., Malosh, C., Mendenhall, J.L., Zic, J.Z., Bates, B.S., Noetzel, M.J., Squire, E.F., Turner, E.M., Rook, J.M., Emmitte, K.A., Stauffer, S.R., Lindsley, C.W., Meiler, J., Conn, P.J., 2014. Identification of specific ligand-receptor interactions that govern binding and cooperativity of diverse modulators to a common metabotropic glutamate receptor 5 allosteric site. ACS Chem. Neurosci. 5, 282–295.

Gregory, K.J., Nguyen, E.D., Reiff, S.D., Squire, E.F., Stauffer, S.R., Lindsley, C.W., Meiler, J., Conn, P.J., 2013b. Probing the metabotropic glutamate receptor 5 (mGlu5) positive allosteric modulator (PAM) binding pocket: discovery of point mutations that engender a "molecular switch" in PAM pharmacology. Mol. Pharmacol. 83, 991–1006.

Gregory, K.J., Noetzel, M.J., Niswender, C.M., 2013c. Pharmacology of metabotropic glutamate receptor allosteric modulators: structural basis and therapeutic potential for CNS disorders. Prog. Mol. Biol. Transl. Sci. 115, 61–121.

Gregory, K.J., Noetzel, M.J., Rook, J.M., Vinson, P.N., Stauffer, S.R., Rodriguez, A.L.,

Emmitte, K.A., Zhou, Y., Chun, A.C., Felts, A.S., Chauder, B.A., Lindsley, C.W., Niswender, C.M., Conn, P.J., 2012. Investigating metabotropic glutamate receptor 5 allosteric modulator cooperativity, affinity, and agonism: enriching structure-function studies and structure-activity relationships. Mol. Pharmacol. 82, 860–875.

Hathaway, H.A., Pshenichkin, S., Grajkowska, E., Gelb, T., Emery, A.C., Wolfe, B.B., Wroblewski, J.T., 2015. Pharmacological characterization of mGlu1 receptors in cerebellar granule cells reveals biased agonism. Neuropharmacol 93, 199–208.

Horio, M., Fujita, Y., Hashimoto, K., 2013. Therapeutic effects of metabotropic glutamate receptor 5 positive allosteric modulator CDPPB on phencyclidine-induced cognitive deficits in mice. Fundam. Clin. Pharmacol. 27, 483–488.

Hubert, G.W., Paquet, M., Smith, Y., 2001. Differential subcellular localization of mGluR1a and mGluR5 in the rat and monkey Substantia nigra. J. Neurosci. 21, 1838–1847.

Jernigan, C.S., Goswami, D.B., Austin, M.C., Iyo, A.H., Chandran, A., Stockmeier, C.A., Karolewicz, B., 2011. The mTOR signaling pathway in the prefrontal cortex is compromised in major depressive disorder. Prog. Neuro-Psychoph 35, 1774–1779.

Jalan-Sakrikar, N., Field, J.R., Klar, R., Mattmann, M.E., Gregory, K.J., Zamorano, R., Engers, D.W., Bollinger, S.R., Weaver, C.D., Days, E.L., Lewis, L.M., Utley, T.J., Hurtado, M., Rigault, D., Acher, F., Walker, A.G., Melancon, B.J., Wood, M.R., Lindsley, C.W., Conn, P.J., Xiang, Z., Hopkins, C.R., Niswender, C.M., 2014. Identification of positive allosteric modulators VU0155094 (ML397) and VU0422288 (ML396) reveals new insights into the biology of metabotropic glutamate receptor 7. ACS Chem. Neurosci. 5, 1221–1237.

Jong, Y.J., Kumar, V., O'Malley, K.L., 2009. Intracellular metabotropic glutamate receptor 5 (mGluR5) activates signaling cascades distinct from cell surface counterparts. J. Biol. Chem. 284, 35827–35838.

Kammermeier, P.J., Xiao, B., Tu, J.C., Worley, P.F., Ikeda, S.R., 2000. Homer proteins regulate coupling of group I metabotropic glutamate receptors to N-type calcium and M-type potassium channels. J. Neurosci. 20, 7238–7245.

Kenakin, T., Christopoulos, A., 2013. Signalling bias in new drug discovery: detection, quantification and therapeutic impact. Nat. Rev. Drug. Discov. 12, 205–216.

Kenakin, T., Watson, C., Muniz-Medina, V., Christopoulos, A., Novick, S., 2012. A simple method for quantifying functional selectivity and agonist bias. ACS Chem. Neurosci. 3, 193–203.

Kinney, G.G., O'Brien, J.A., Lemaire, W., Burno, M., Bickel, D.J., Clements, M.K., Chen, T.B., Wisnoski, D.D., Lindsley, C.W., Tiller, P.R., Smith, S., Jacobson, M.A., Sur, C., Duggan, M.E., Pettibone, D.J., Conn, P.J., Williams Jr., D.L., 2005. A novel selective positive allosteric modulator of metabotropic glutamate receptor subtype 5 has in vivo activity and antipsychotic-like effects in rat behavioral models. J. Pharmacol. Exp. Ther. 313, 199–206.

Klein Herenbrink, C., Sykes, D.A., Donthamsetti, P., Canals, M., Coudrat, T., Shonberg, J., Scammells, P.J., Capuano, B., Sexton, P.M., Charlton, S.J., Javitch, J.A., Christopoulos, A., Lane, J.R., 2016. The role of kinetic context in apparent biased agonism at GPCRs. Nat. Commun. 7, 10842.

Kumar, V., Fahey, P.G., Jong, Y.J., Ramanan, N., O'Malley, K.L., 2012. Activation of intracellular metabotropic glutamate receptor 5 in striatal neurons leads to up-regulation of genes associated with sustained synaptic transmission including Arc/Arg3.1 protein. J. Biol. Chem. 287, 5412–5425.

Kumar, V., Jong, Y.J., O'Malley, K.L., 2008. Activated nuclear metabotropic glutamate receptor mGlu5 couples to nuclear Gq/11 proteins to generate inositol 1,4,5-trisphosphate-mediated nuclear Ca2+ release. J. Biol. Chem. 283, 14072–14083.

Leach, K., Sexton, P.M., Christopoulos, A., 2007. Allosteric GPCR modulators: taking advantage of permissive receptor pharmacology. Trends Pharmacol. Sci. 28, 382–389.

Lindsley, C.W., Wisnoski, D.D., Leister, W.H., O'Brien, J.A., Lemaire, W., Williams Jr., D.L., Burno, M., Sur, C., Kinney, G.G., Pettibone, D.J., Tiller, P.R., Smith, S., Duggan, M.E., Hartman, G.D., Conn, P.J., Huff, J.R., 2004. Discovery of positive allosteric modulators for the metabotropic glutamate receptor subtype 5 from a series of N-(1,3-diphenyl-1H- pyrazol-5-yl)benzamides that potentiate receptor function in vivo. J. Med. Chem. 47, 5825–5828.

Lu, W.Y., Xiong, Z.G., Lei, S., Orser, B.A., Dudek, E., Browning, M.D., MacDonald, J.F., 1999. G-protein-coupled receptors act via protein kinase C and Src to regulate NMDA receptors. Nat. Neurosci. 2, 331–338.

Manka, J., Zhou, Y., Chun, A., Dawson, E.S., Vinson, P.N., Niswender, C.M., Noetzel, M.J., Rook, J.M., Bridges, T.M., Daniels, J.S., Jones, C., Conn, P.J., Lindsley, C.W., Stauffer, S.R., 2010. Identification of a selective allosteric agonist of mGlu5. Probe reports from the NIH molecular libraries Program. Natl. Cent. Biotechnol. Inf. (US), Bethesda (MD).

McCool, B.A., Pin, J.P., Harpold, M.M., Brust, P.F., Stauderman, K.A., Lovinger, D.M., 1998. Rat group I metabotropic glutamate receptors inhibit neuronal Ca2+ channels via multiple signal transduction pathways in HEK 293 cells. J. Neurophysiol. 79, 379–391.

Melancon, B.J., Hopkins, C.R., Wood, M.R., Emmitte, K.A., Niswender, C.M., Christopoulos, A., Conn, P.J., Lindsley, C.W., 2012. Allosteric modulation of seven transmembrane spanning receptors: theory, practice, and opportunities for central nervous system drug discovery. J. Med. Chem. 55, 1445–1464.

Niswender, C.M., Conn, P.J., 2010. Metabotropic glutamate receptors: physiology, pharmacology, and disease. Annu. Rev. Pharmacol. Toxicol. 50, 295–322.

Noetzel, M.J., Gregory, K.J., Vinson, P.N., Manka, J.T., Stauffer, S.R., Lindsley, C.W., Niswender, C.M., Xiang, Z., Conn, P.J., 2013. A novel metabotropic glutamate receptor 5 positive allosteric modulator acts at a unique site and confers stimulus bias to mGlu5 signaling. Mol. Pharmacol. 83, 835–847.

Noetzel, M.J., Rook, J.M., Vinson, P.N., Cho, H.P., Days, E., Zhou, Y., Rodriguez, A.L., Lavreysen, H., Stauffer, S.R., Niswender, C.M., Xiang, Z., Daniels, J.S., Jones, C.K., Lindsley, C.W., Weaver, C.D., Conn, P.J., 2012. Functional impact of allosteric agonist activity of selective positive allosteric modulators of metabotropic glutamate receptor subtype 5 in regulating central nervous system function. Mol. Pharmacol. 81, 120–133.

Parmentier-Batteur, S., Hutson, P.H., Menzel, K., Uslaner, J.M., Mattson, B.A., O'Brien, J.A., Magliaro, B.C., Forest, T., Stump, C.A., Tynebor, R.M., Anthony, N.J., Tucker, T.J., Zhang, X.F., Gomez, R., Huszar, S.L., Lambeng, N., Faure, H., Le Poul, E., Poli, S., Rosahl, T.W., Rocher, J.P., Hargreaves, R., Williams, T.M., 2014. Mechanism based neurotoxicity of mGlu5 positive allosteric modulators-development challenges for a promising novel antipsychotic target. Neuropharmacol 82, 161–173.

Peters, J., Scofield, M.D., Ghee, S.M., Heinsbroek, J.A., Reichel, C.M., 2015. Perirhinal cortex mGlu5 receptor activation reduces relapse to methamphetamine seeking by restoring novelty salience. Neuropsychopharmacol 41, 1477–1485.

Ribeiro, F.M., Paquet, M., Cregan, S.P., Ferguson, S.S., 2010a. Group I metabotropic glutamate receptor signalling and its implication in neurological disease. CNS Neurol. Disord. Drug Targets 9, 574–595.

Ribeiro, F.M., Paquet, M., Ferreira, L.T., Cregan, T., Swan, P., Cregan, S.P., Ferguson, S.S., 2010b. Metabotropic glutamate receptor-mediated cell signaling pathways are altered in a mouse model of Huntington's disease. J. Neurosci. 30, 316–324.

Rodriguez, A.L., Grier, M.D., Jones, C.K., Herman, E.J., Kane, A.S., Smith, R.L., Williams, R., Zhou, Y., Marlo, J.E., Days, E.L., Blatt, T.N., Jadhav, S., Menon, U.N., Vinson, P.N., Rook, J.M., Stauffer, S.R., Niswender, C.M., Lindsley, C.W., Weaver, C.D., Conn, P.J., 2010. Discovery of novel allosteric modulators of metabotropic glutamate receptor subtype 5 reveals chemical and functional diversity and in vivo activity in rat behavioral models of anxiolytic and antipsychotic activity. Mol. Pharmacol. 78, 1105–1123.

Rook, J.M., Noetzel, M.J., Pouliot, W.A., Bridges, T.M., Vinson, P.N., Cho, H.P., Zhou, Y., Gogliotti, R.D., Manka, J.T., Gregory, K.J., Stauffer, S.R., Dudek, F.E., Xiang, Z., Niswender, C.M., Daniels, J.S., Jones, C.K., Lindsley, C.W., Conn, P.J., 2013. Unique signaling profiles of positive allosteric modulators of metabotropic glutamate receptor subtype 5 determine differences in in vivo activity. Biol. Psychiatry 73, 501–509.

Rook, J.M., Xiang, Z., Lv, X., Ghoshal, A., Dickerson, J.W., Bridges, T.M., Johnson, K.A., Foster, D.J., Gregory, K.J., Vinson, P.N., Thompson, A.D., Byun, N., Collier, R.L., Bubser, M., Nedelcovych, M.T., Gould, R.W., Stauffer, S.R., Daniels, J.S., Niswender, C.M., Lavreysen, H., Mackie, C., Conde-Ceide, S., Alcazar, J., Bartolome-Nebreda, J.M., Macdonald, G.J., Talpos, J.C., Steckler, T., Jones, C.K., Lindsley, C.W., Conn, P.J., 2015. Biased mGlu5-positive allosteric modulators provide in vivo efficacy without potentiating mGlu5 modulation of NMDAR currents. Neuron 86, 1029–1040.

Sengmany, K., Gregory, K.J., 2015. Metabotropic glutamate receptor subtype 5: molecular pharmacology, allosteric modulation and stimulus bias. Br. J. Pharmacol. http://dx.doi.org/10.1111/bph.13281.

Sevastyanova, T.N., Kammermeier, P.J., 2014. Cooperative signaling between homodimers of metabotropic glutamate receptors 1 and 5. Mol. Pharmacol. 86, 492–504.

Stefani, M.R., Moghaddam, B., 2010. Activation of type 5 metabotropic glutamate receptors attenuates deficits in cognitive flexibility induced by NMDA receptor blockade. Eur. J. Pharmacol. 639, 26–32.

Tang, T.S., Slow, E., Lupu, V., Stavrovskaya, I.G., Sugimori, M., Llinas, R., Kristal, B.S., Hayden, M.R., Bezprozvanny, I., 2005. Disturbed Ca2+ signaling and apoptosis of medium spiny neurons in Huntington's disease. Proc. Natl. Acad. Sci. U. S. A. 102, 2602–2607.

Tu, J.C., Xiao, B., Naisbitt, S., Yuan, J.P., Petralia, R.S., Brakeman, P., Doan, A., Aakalu, V.K., Lanahan, A.A., Sheng, M., Worley, P.F., 1999. Coupling of mGluR/Homer and PSD-95 complexes by the Shank family of postsynaptic density proteins. Neuron 23, 583–592.

Uslaner, J.M., Parmentier-Batteur, S., Flick, R.B., Surles, N.O., Lam, J.S., McNaughton, C.H., Jacobson, M.A., Hutson, P.H., 2009. Dose-dependent effect of CDPPB, the mGluR5 positive allosteric modulator, on recognition memory is associated with GluR1 and CREB phosphorylation in the prefrontal cortex and hippocampus. Neuropharmacol 57, 531–538.

Wu, H., Wang, C., Gregory, K.J., Han, G.W., Cho, H.P., Xia, Y., Niswender, C.M., Katritch, V., Meiler, J., Cherezov, V., Conn, P.J., Stevens, R.C., 2014. Structure of a class C GPCR metabotropic glutamate receptor 1 bound to an allosteric modulator. Science 344, 58–64.

Yin, S., Noetzel, M.J., Johnson, K.A., Zamorano, R., Jalan-Sakrikar, N., Gregory, K.J., Conn, P.J., Niswender, C.M., 2014. Selective actions of novel allosteric modulators reveal functional heteromers of metabotropic glutamate receptors in the CNS. J. Neurosci. 34, 79–94.

Zhang, Y., Rodriguez, A.L., Conn, P.J., 2005. Allosteric potentiators of metabotropic glutamate receptor subtype 5 have differential effects on different signaling pathways in cortical astrocytes. J. Pharmacol. Exp. Ther. 315, 1212–1219.

Supplementary Information

Biased allosteric agonism and modulation of metabotropic glutamate receptor 5: implications for optimizing preclinical neuroscience drug discovery

Kathy Sengmany[a], Junaid Singh[a], Gregory D. Stewart[a], P. Jeffrey Conn[b], Arthur Christopoulos[a*], and Karen J. Gregory[a*]

[a]Drug Discovery Biology, Monash Institute of Pharmaceutical Sciences and Department of Pharmacology, Monash University, Parkville, VIC, Australia.
[b] Vanderbilt Center for Neuroscience Drug Discovery, Vanderbilt University Medical Center, Nashville, TN, USA.
* To whom correspondence should be addressed:

Prof. Arthur Christopoulos and Dr. Karen J Gregory

381 Royal Parade

Parkville, VIC, Australia

3052

[redacted]

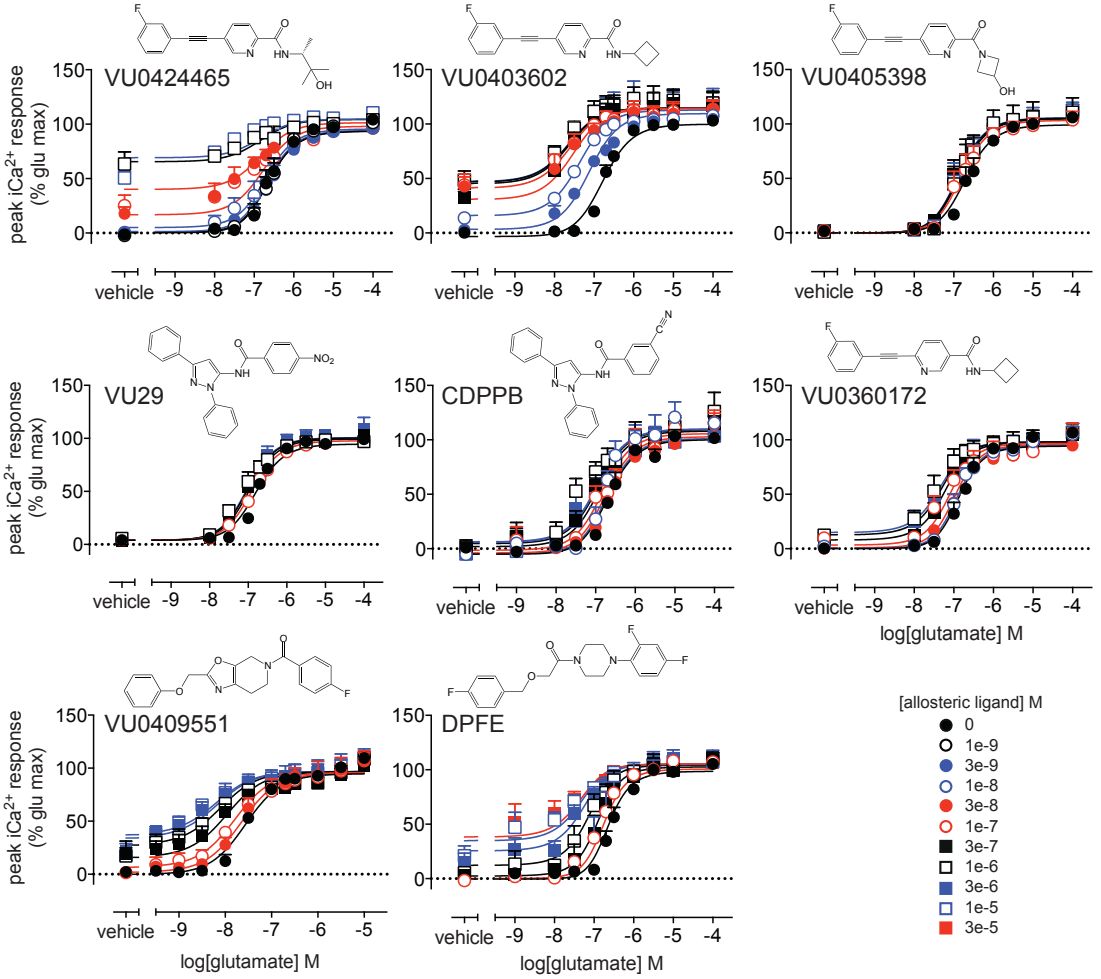

Supplementary Figure 1: Allosteric modulation of glutamate-stimulated iCa^{2+} mobilization in HEK293A-mGlu$_5$-low cells. Glutamate concentration-response curves for iCa^{2+} mobilization in the absence and presence of indicated concentrations of allosteric ligands. Interaction studies for DPFE, VU0424465, VU0403602, VU0409551 and CDPPB were performed using simultaneous addition of both ligands, to eliminate allosteric ligand-induced acute desensitization due to intrinsic agonist activity. VU29, VU0405398 and VU0360172 were added 1 min prior to addition of glutamate. Data sets were globally fitted to an operational model of allosterism to estimate affinity and cooperativity. Curves represent the best fit of the data. Data are mean + SEM of n=3-10 experiments performed in duplicate. Error bars not shown lie within the dimensions of the symbol.

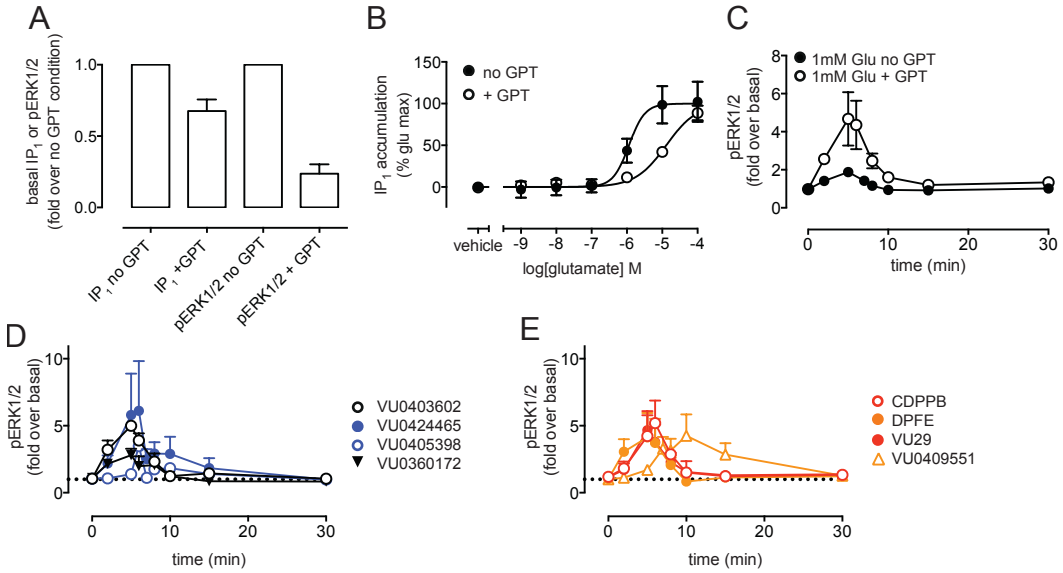

Supplementary Figure 2: Establishing the temporal profile of ERK1/2 phosphorylation and the effect of glutamic pyruvic transaminase on ERK1/2 phosphorylation and IP$_1$ accumulation in HEK293A-mGlu5-low cells. A) Incubation with 10U/mL glutamic pyruvic transaminase (GPT) reduces the basal levels of IP$_1$ and phosphorylated ERK1/2. Data are normalised to the basal level in the absence of GPT. Mean + 95% confidence intervals for GPT treatments are shown from n=3-6 independent experiments, demonstrating a marked decrease in basal levels in the presence of GPT. B) In IP$_1$ assays, 10U/mL GPT completely degrades up to 1μM exogenously applied glutamate. Data are mean ±SEM from n=7-10. C) In ERK1/2 phosphorylation assays, inclusion of GPT increases the signal window. Data are mean ±SEM from n=4-5. D&E) ERK1/2 phosphorylation levels peak at 5-7min in response to stimulation by allosteric agonists (10μM). Data are mean + SEM from n=3-5.

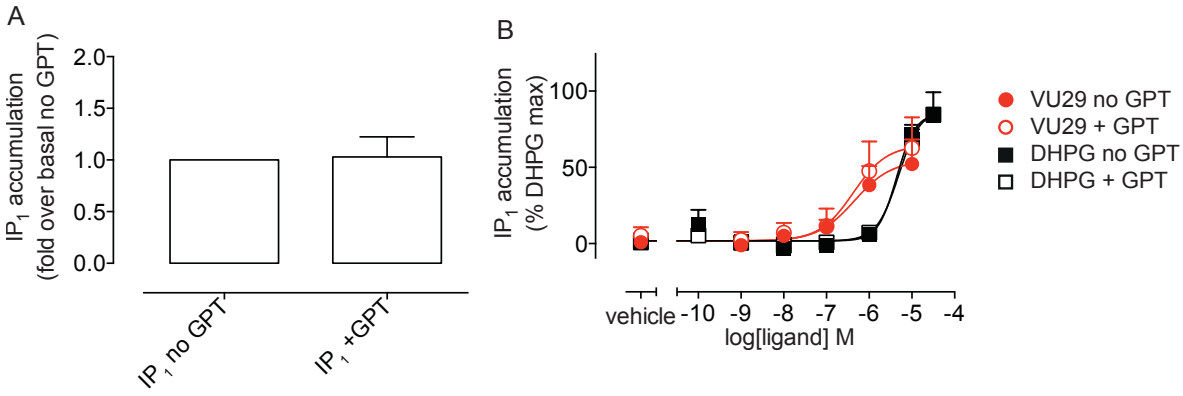

Supplementary Figure 3: In cortical neurons GPT has no effect on basal IP$_1$ levels or agonism by VU29. A) Basal levels of IP1 accumulation were similar in the absence and presence of GPT. Data for GPT treatment group are mean + 95% confidence interval from n=4. B) Incubation with GPT had no effect on DHPG or VU29 agonism in the IP$_1$ accumulation assay. Data are mean + SEM from n=3-4 performed in duplicate. Error bars not shown lie within the dimensions of the symbols.

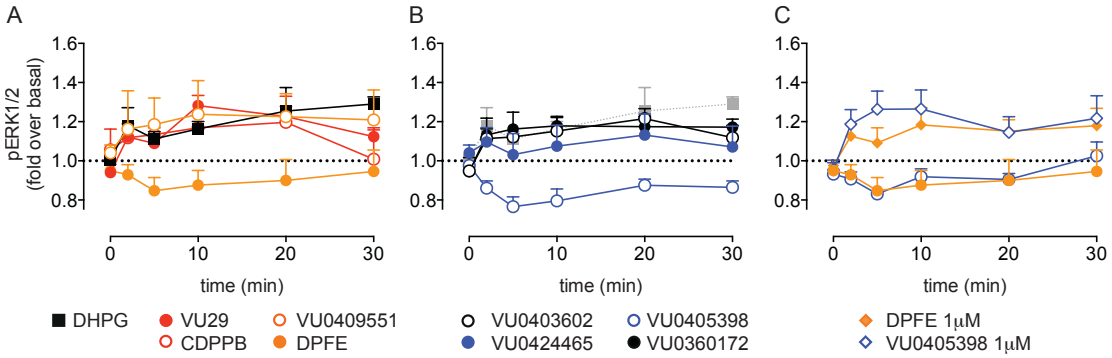

Supplementary Figure 4: The time course for ERK1/2 phosphorylation in cultured cortical neurons is characterised by a sustained response over 30 minutes. A-C) Exposure to 10μM of indicated ligands (30 μM for DPFE in panel A; 1 μM for VU0424465 in panel B) caused a sustained change in the levels of phosphorylated ERK1/2. Data are mean + SEM from n=3-9 performed in duplicate. Error bars not shown lie within the dimensions of the symbol.

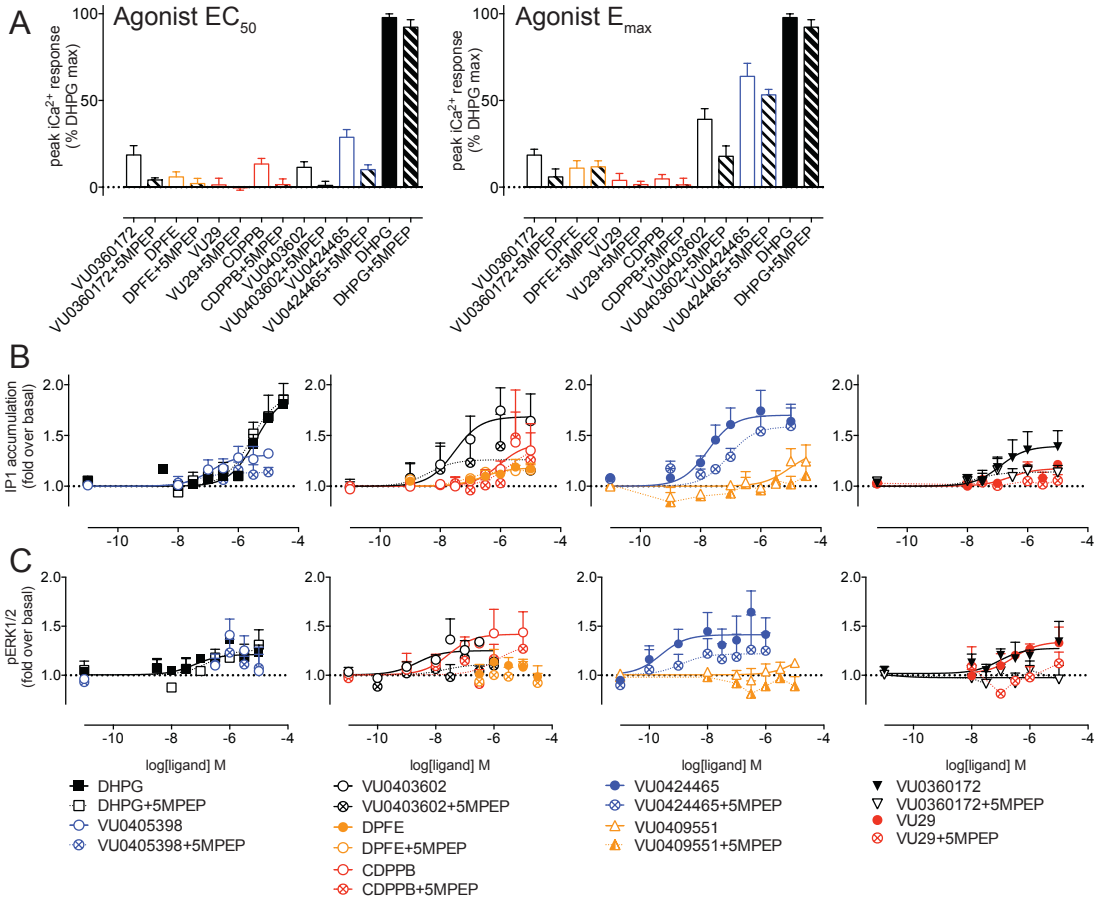

Supplementary Figure 5: Agonist activity of allosteric ligands is mGlu$_5$ dependent in cortical neurons. Cortical neurons were pre-incubated with 10μM 5MPEP, an mGlu$_5$ neutral allosteric ligand as well as the mGlu$_1$ negative allosteric modulator CPCCOEt (30 μM) for 30min. A) The peak iCa^{2+} mobilization in response to either an EC$_{50}$ or E$_{max}$ concentration (all 10 μM) of indicated allosteric ligand was inhibited by 5MPEP. Agonist concentrations for ~EC$_{50}$ were: 1μM for DPFE, VU29, CDPPB; 30nM for VU0403602 & VU0424465; 300nM for VU0360172. The response to maximal DHPG (10μM) is shown in both panels for reference. B) With the exception of DPFE, agonist activity of allosteric ligands for IP$_1$ accumulation (B) and ERK1/2 phosphorylation (C) was inhibited by 10μM 5MPEP. The DHPG response was unaffected by 5MPEP. Data represent the mean + s.e.m of n=4-8 experiments performed in duplicate.

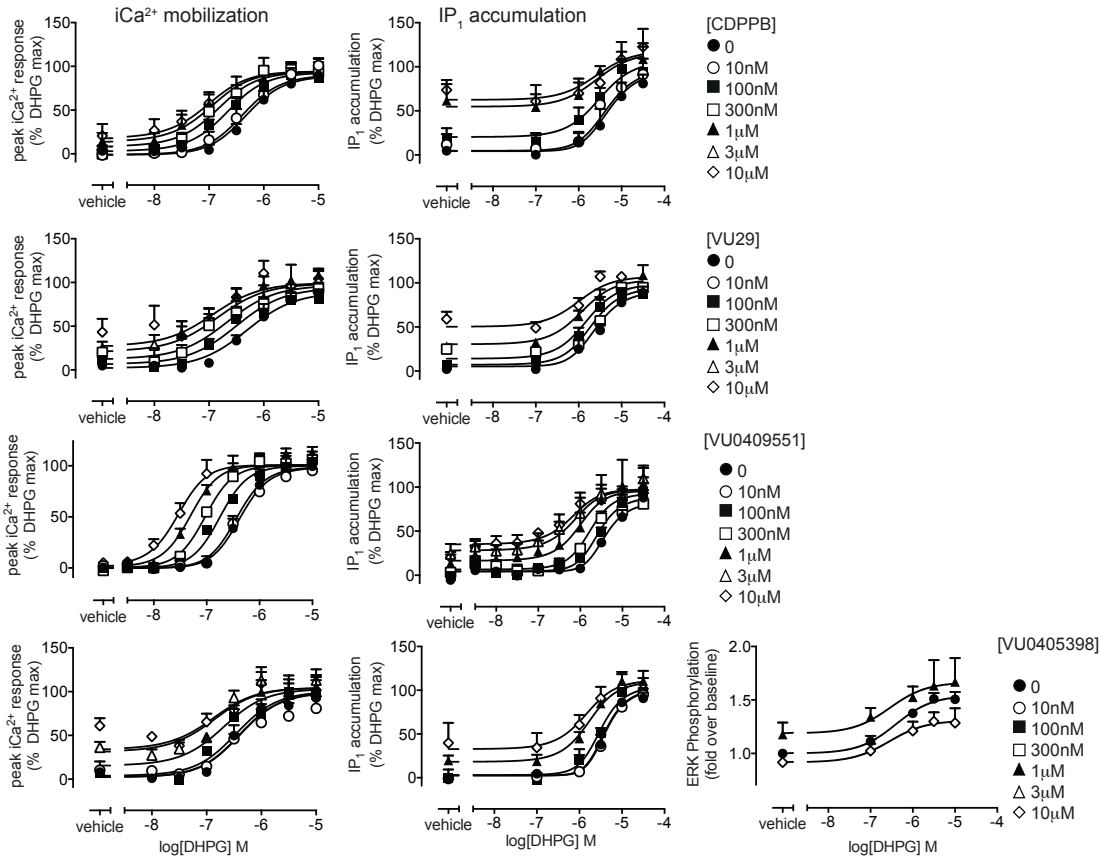

Supplementary Figure 6: Allosteric modulation of DHPG-stimulated iCa^{2+} mobilization, IP$_1$ accumulation and ERK1/2 phosphorylation. CDPPB, VU29 and VU0409551 enhanced the potency of DHPG for both iCa^{2+} and IP$_1$ in a concentration-dependent manner. The leftward shifts in the DHPG concentration-response curves approached a limit as expected for an allosteric interaction. Interaction experiments were not undertaken for pERK1/2 due to the confound of allosteric agonism. VU0405398 potentiated DHPG mediated iCa^{2+} mobilization and IP$_1$ accumulation, and had a mixed modulatory effect on DHPG-mediated ERK1/2 phosphorylation. Data are mean ± SEM from n=3-5 performed in duplicate.

Supplementary Table 1. Potency (pEC_{50}) and efficacy (E_{max}) estimates of $mGlu_5$ ligands for iCa^{2+} mobilization (in the absence and presence of 1.2 mM extracellular Ca^{2+}), IP_1 accumulation and ERK phosphorylation in HEK293A-$mGlu_5$-low cells. Data are mean ± SEM of 3-26 independent experiments performed in duplicate.

	iCa^{2+}		**eCa^{2+} free[a]-iCa^{2+}**		**IP_1**		**pERK1/2**	
HEK293A	*pEC_{50}*	*E_{max} (% glu)*	*pEC_{50}*	*E_{max} (% glu)*	*pEC_{50}*	*E_{max} (fold over basal)*	*pEC_{50}*	*E_{max} (fold over basal)*
Glutamate	6.87±0.06	100.3±0.2	6.89±0.09	50.5±4.1[d]	n.d.	n.d.	n.d.	n.d.
DHPG	6.31±0.10	92.9±2.6	6.06±0.07	46.41±19.8[d]	5.68±0.17	1.9±0.2	6.19±0.27	2.1±0.6
VU0424465	7.12±0.14	74.8±8.4	7.61±0.19	66.7±14.4	8.70±0.13[b]	1.9±0.2	8.24±0.14[c]	4.7±1.0
VU0403602	8.01±0.06	56.2±3.1	8.19±0.12	44.0±6.9	8.76±0.21[c]	2.1±0.3	8.10±0.28	5.2±0.9
VU0360172	6.55±0.16	29.1±9.0	n/a	n/a	6.64±0.37	2.3±0.2	7.04±0.12	3.3±0.7
VU29	n.r.	n.r.	n/a	n/a	7.37±0.15	2.1±0.4	7.06±0.12	2.9±0.6
CDPPB	7.35±0.21	18.9±4.9	7.13±0.19	36.1±4.7[d]	7.60±0.18	2.3±0.1	7.65±0.26	4.6±0.9
DPFE	5.72±0.17	49.7±8.7	6.29±0.35	67.1±9.0	5.95±0.12	2.7±0.2	6.25±0.53	4.0±1.1
VU0405398	n.r.	n.r.	n/a	n/a	6.64±0.34	1.9±0.2	7.18[e]	3.4[e]
VU0409551	6.23±0.15	55.3±5.8	6.33±0.17	32.0±1.3[d]	6.16±0.13	1.7±0.2	6.05±0.39	1.5±0.2

n.r. denotes allosteric ligands did not display intrinsic efficacy

n/a due to little or no intrinsic agonist activity under standard conditions these ligands were not assessed in the absence of 1.2mM $CaCl_2$

n.d. denotes not determined, in these assays glutamic pyruvic transaminase was included to breakdown ambient glutamate

[a] denotes assay in the absence of extracellular Ca^{2+} and presence of 1mM EDTA.

[b] significantly different to pEC_{50} estimate in standard iCa^{2+} and eCa^{2+}-free assays ($p<0.05$, one-way ANOVA, Tukey's post-test).

[c] significantly different to pEC_{50} estimate in standard iCa^{2+} assay ($p<0.05$, one-way ANOVA, Tukey's post-test).

[d] significantly different to the maximal response in the presence of 1.2mM extracellular Ca^{2+} ($p<0.05$, student's t-test).

[e] in one of the three data sets a concentration-response curve could not be fit, the mean value from n=2 non-linear fits is shown.

Supplementary Table 2. Potency (pEC_{50}) and efficacy (E_{max}) estimates of $mGlu_5$ ligands for iCa^{2+} mobilization (in the absence and presence of 1.2 mM extracellular Ca^{2+}), IP_1 accumulation and ERK1/2 phosphorylation in cortical neurons. Data are mean ± SEM of 3-20 independent experiments performed in duplicate.

	iCa^{2+}		eCa^{2+} free[a]-iCa^{2+}		IP_1		pERK1/2	
Cortical neurons	*pEC_{50}*	*E_{max} (% DHPG)*	*pEC_{50}*	*E_{max} (% DHPG)*	*pEC_{50}*	*E_{max} (fold over basal)*	*pEC_{50}*	*E_{max} (fold over basal)*
DHPG	6.44±0.06	100.6±0.5	6.17±0.15	60.2±11.5*	5.48±0.12[b,d]	1.9±0.1	6.78±0.15[c,d]	1.4±0.0
VU0424465	7.14±0.34	81.1±7.0	7.88±0.07	66.2±10.3	7.60±0.09[b]	1.9±0.2	9.39±0.20[b,c,d]	1.5±0.1
VU0403602	7.75±0.17	57.3±8.3	8.21±0.35	37.9±19.6	7.43±0.18[b]	1.9±0.2	8.62±0.20[c]	1.3±0.1
VU0360172	6.63±0.44	43.5±10.0	6.69±0.48	43.2±11.0	6.65±0.18	1.3±0.1	7.68±0.36	1.3±0.0
VU29	6.43±0.36	37.0±12.1	n.r.	n.r.	6.28±0.13	1.5±0.1	7.06±0.19[c]	1.4±0.1
CDPPB	6.94±0.35	33.5±4.8	6.82±0.13	52.6±9.5	6.55±0.16	1.4±0.2	7.47±0.19[c]	1.4±0.1
DPFE	5.66±0.23	43.6±5.8	n.r.	n.r.	5.46±0.24	1.3±0.1	n.d.	n.d.
VU0405398	6.35±0.48	43.7±16.4	n.r.	n.r.	6.66±0.39	1.3±0.1	n.d.	n.d.
VU0409551	n.r.	n.r.	n.r	n.r	6.00±0.46	1.5±0.2	5.90±0.56	1.2±0.1

n.r. denotes allosteric ligands did not display intrinsic efficacy

n.d. due to an apparent biphasic concentration-response relationship potency and E_{max} values were not determined.

* denotes significantly different ($p<0.05$) to E_{max} value derived under standard assay conditions (iCa^{2+}, 1.2mM $CaCl_2$), student's t-test.

[a] denotes assay in the absence of extracellular Ca^{2+} and presence of 1mM EDTA.

[b] significantly different to pEC_{50} estimate in iCa^{2+} assays ($p<0.05$, one-way ANOVA, Tukey's post-test).

[c] significantly different to pEC_{50} estimate in IP_1 assays ($p<0.05$, one-way ANOVA, Tukey's post-test).

[d] significantly different to pEC_{50} estimate in eCa^{2+}-free-iCa^{2+} assays ($p<0.05$, one-way ANOVA, Tukey's post-test).

Supplementary Table 3: Operational parameter estimates for allosteric modulation of orthosteric agonist-mediated iCa^{2+} mobilization and IP_1 accumulation in HEK293A-$mGlu_5$-low and cortical neurons. Data are mean ± SEM of 3-9 independent experiments performed in duplicate.

HEK293A	**iCa^{2+} mobilization: Glutamate**					**iCa^{2+} mobilization: DHPG**				
	E_m	$Log\tau_B$	n	Basal	$Log\tau_A$	E_m	$Log\tau_B$	n	Basal	$Log\tau_A$
VU0424465	119.2±14.1	0.11±0.04	1.5±0.1	-0.2±2.3	0.49±0.17	104.1±4.1	-0.12±0.08	1.2±0.0	-0.9±1.0	0.91±0.03
VU0403602	120.4±7.7	-0.13±0.14	1.7±0.6	-2.5±1.4	0.58±0.06	108.7±4.6	-0.53±0.19	1.2±0.0	-0.7±0.7	0.99±0.07
VU0360172	104.4±5.7	-0.29±0.12	2.2±0.3	-0.9±1.2	0.72±0.06	102.0±1.3	-0.80±0.07	1.4±0.2	0.1±1.0	0.93±0.23
VU29	103.2±2.3	n.r.	1.8±0.1	1.5±1.6	0.69±0.02	108.8±1.5	n.r.	1.3±0.3	-1.5±0.1	0.88±0.11
CDPPB	129.5±8.6	-0.71±0.10	1.7±0.3	-6.7±1.6	0.48±0.04	106.9±4.1	-0.78±0.32	1.2±0.2	-2.9±2.0	0.97±0.09
DPFE	106.9±2.3	-0.16±0.12	2.6±0.7	-2.1±2.1	0.55±0.05	110.6±3.4	-0.62±0.10	1.3±0.2	-2.7±0.3	0.97±0.07
VU0405398	109.0±6.4	n.r.	2.2±0.5	-0.4±0.6	0.56±0.12	107.4±4.9	n.r.	1.4±0.2	1.2±0.4	0.83±0.26
VU0409551	102.5±3.4	-0.25±0.03	1.0±0.0	-2.7±0.6	1.37±0.09	101.7±5.5	-0.26±0.06	1.2±0.1	-1.0±0.7	0.92±0.12
Cortical	**iCa^{2+} mobilization: DHPG**					**IP_1 accumulation: DHPG**				
VU0360172	103.9±2.1	-0.74±0.29	1.4±0.1	1.0±2.1	0.84±0.07	129.9±15.6	-0.10±0.06	1.9±0.1	0.3±0.2	0.22±0.10
VU29	107.5±3.8	-0.15±0.28	1.1±0.0	3.4±2.2	0.78±0.07	128.1±1.2	-0.07±0.04	2.2±0.4	0.8±4.4	0.29±0.04
CDPPB	103.0±1.8	-0.64±0.27	1.1±0.1	-2.1±3.2	0.88±0.05	124.3±14.0	0.06±0.12	3.3±0.6	3.0±2.9	0.24±0.15
DPFE	107.3±4.2	-0.56±0.27	1.4±0.1	2.4±1.9	0.77±0.09	115.4±8.6	-0.05±0.10	3.2±0.7	2.1±4.1	0.26±0.08
VU0405398	109.5±7.1	0.03±0.12	1.3±0.1	2.3±3.0	1.05±0.11	135.3±10.9	-0.22±0.17	3.0±0.6	0.3±0.4	0.28±0.10
VU0409551	100.8±1.6	-0.94±0.43	1.7±0.2	-0.1±1.7	0.99±0.04	119.0±11.0	-0.17±0.05	2.4±0.1	3.9±2.2	0.19±0.07

n.r. indicates value not determined due to little/no appreciable agonism.

Supplementary Table 4: Log R values for $mGlu_5$ ligands for iCa^{2+} mobilization (in the absence and presence of 1.2 mM extracellular Ca^{2+}), IP_1 accumulation and ERK phosphorylation (pERK1/2) in HEK293A-$mGlu_5$-low cells and cortical neurons. Data are mean ± SEM of 3-26 independent experiments performed in duplicate.

	HEK293A-$mGlu_5$-low				**Cortical neurons**			
	iCa^{2+}	*IP_1*	*pERK1/2*	*eCa^{2+}-free iCa_{2+}*	*iCa^{2+}*	*IP_1*	*pERK1/2*	*eCa^{2+}-free iCa_{2+}*
glutamate	6.91±0.07	n.m.	n.m	6.89±0.09	n.m.	n.m	n.m	n.m
DHPG	6.32±0.08	5.80±0.14[a,b]	6.37±0.22	6.04±0.07	6.43±0.05	5.34±0.05[a,b,c]	6.69±0.19	6.34±0.13
VU0424465	7.18±0.16	8.70±0.12[a,c]	8.32±0.10[a,c]	7.64±0.22	7.31±0.24	7.67±0.08	8.81±0.43 [a,d]	7.89±0.19
VU0403602	7.93±0.16	8.57±0.12	8.09±0.32	8.07±0.18	7.57±0.15	7.39±0.24	8.42±0.24[a,d]	7.97±0.29
VU0360172	6.52±0.25	6.44±0.39	7.02±0.18	n/a	6.56±0.22	6.47±0.19	7.45±0.35[d]	6.42±0.61
VU29	n.r.	7.41±0.11	7.17±0.05	n/a	6.24±0.21	6.13±0.14	6.96±0.21[a,d]	n.r.
CDPPB	7.09±0.11	7.58±0.17	7.60±0.16	7.20±0.24	6.26±0.20	6.57±0.10	7.41±0.18[a,c,d]	6.52±0.14
DPFE	5.79±0.25	5.86±0.19	5.83±0.08	5.95±0.38	5.43±0.21	5.76±0.21	n.d.	n.r.
VU0405398	n.r.	6.47±0.35	7.54±0.21	n/a	5.80±0.37	5.81±0.23	n.d.	n.r.
VU0409551	6.23±0.24	6.06±0.18	6.30±0.36	6.45±0.15	n.r.	5.55±0.26	5.38±0.31	n.r.

n.r. denotes allosteric ligands did not display intrinsic efficacy

n.d. due to an apparent biphasic concentration-response relationship logR values were not determined.

n.m. not measured due to either the presence of GPT, or cortical neuronal background.

n/a due to little or low agonist activity in the standard paradigm, these ligands were not assessed in the absence of extracellular Ca^{2+}.

[a] significantly different to logR estimate in iCa^{2+} assay ($p<0.05$, one-way ANOVA, Tukey's post-test).

[b] significantly different to logR estimate in pERK1/2 assay ($p<0.05$, one-way ANOVA, Tukey's post-test).

[c] significantly different to logR estimate in eCa^{2+}-free assay ($p<0.05$, one-way ANOVA, Tukey's post-test).

[d] significantly different to logR estimate in IP_1 assay ($p<0.05$, one-way ANOVA, Tukey's post-test).

Chapter 3

Kinetic and system bias as drivers of biased metabotropic glutamate receptor 5 allosteric modulation

For submission to Neuropharmacology

Title: Kinetic and system bias as drivers of biased metabotropic glutamate receptor 5 allosteric modulation

Running title: Biased modulation of mGlu$_5$ NAMs

Kathy Sengmany[a], Sabine Albold[a], Shane D. Hellyer[a], Taide Wang[a], P. Jeffrey Conn[b], Lauren T. May[a], Arthur Christopoulos[a], Katie Leach[a] and Karen J. Gregory[a*]

[a]Drug Discovery Biology, Monash Institute of Pharmaceutical Sciences and Department of Pharmacology, Monash University, Parkville, VIC, Australia.

[b] Vanderbilt Center for Neuroscience Drug Discovery, Vanderbilt University Medical Center, Nashville, TN, USA.

* To whom correspondence should be addressed:

Dr. Karen J Gregory

381 Royal Parade

Parkville, VIC, Australia

3052

[redacted]

[redacted]

[redacted]

Abstract

Allosteric modulators of the metabotropic glutamate receptor subtype 5 ($mGlu_5$) are potential therapies for a range of CNS disorders ranging from anxiety and depression to autism and pain. These ligands bind to sites distinct from the orthosteric (or endogenous) ligand, often with improved subtype selectivity, and spatial and temporal control over receptor responses. We recently revealed that $mGlu_5$ allosteric agonists and positive allosteric modulators exhibit biased agonism and/or modulation, enhancing some receptor signaling pathways to the relative exclusion of others. To establish whether negative allosteric modulators (NAMs) engender similar bias, we herein rigorously characterize the pharmacology of eight diverse $mGlu_5$ NAMs. Radioligand inhibition binding studies revealed novel modes of interaction with $mGlu_5$ for select NAMs, with biphasic or incomplete inhibition of [^{3}H]methoxy-PEPy. We assessed $mGlu_5$-mediated intracellular Ca^{2+} (iCa^{2+}) mobilization and inositol phosphate (IP_1) accumulation in HEK293A cells stably expressing low levels of $mGlu_5$ (HEK293A-$mGlu_5$-low) and mouse embryonic cortical neurons. The apparent affinity of select acetylenic NAMs (MPEP, MTEP and dipraglurant) was dependent on the signaling pathway measured, agonist used and cell type (HEK293A-$mGlu_5$-low versus cortical neurons). In contrast, the partial acetylenic NAM, M-5MPEP, and structurally distinct NAMs had similar affinity estimates irrespective of the assay or cellular background. Biased cooperativity was evident for VU0366248 in cortical neurons where it was a NAM for DHPG-iCa^{2+} mobilization, but neutral with DHPG in IP_1 accumulation assays. Co-application of CPCCOEt to block $mGlu_1$ activity in cortical neurons differentially influenced cooperativity with DHPG of certain NAMs. Overall, this study extends our understanding and appreciation of

biased modulation as a critical factor in drug design for neuropsychiatric and neurological disorders.

Keywords: biased modulation, kinetics, negative allosteric modulator, metabotropic glutamate receptor 5

Chemical compounds studied in this article:

Glutamate (L-glutamic acid; PubChem CID: 33032); DHPG (PubChem CID: 108001); MPEP (PubChem CID: 3025961), fenobam (PubChem CID: 162834), MTEP (PubChem CID: 9794218), M-5MPEP (PubChem CID: 16036762), dipraglurant (PubChem CID: 44557636), VU0366058 (PubChem CID: 57328392).

Abbreviations

cAMP, cyclic adenosine monophosphate; CNS, central nervous system; CPCCOEt, 7-(hydroxyimino)cyclopropa[*b*] chromen-1a-carboxylate ethyl ester; DHPG, (*S*)-3,5-dihydroxyphenylglycine; dipraglurant, 6-fluoro-2-[4-(2-pyridinyl)-3-butyn-1-yl]-Imidazo[1,2-a]pyridine; DMEM, Dulbecco's modified Eagle's medium; ERK1/2, extracellular signal-regulated kinases 1 and 2; FBS, fetal bovine serum; fenobam, 1-(3-chlorophenyl)-3-[(2e)-1-methyl-4-oxoimidazolidin-2-ylidene]urea; GPCR, G protein-coupled receptor; GPT, glutamic pyruvic transaminase; HBSS, Hank's Balanced Salt Solution; HEK293A, human embryonic kidney 293; iCa^{2+}, intracellular calcium, IP_1, inositol 1-phosphate; M-5MPEP, 2-[2-(3-methoxyphenyl)ethynyl]-5-methylpyridine; $mGlu_1$, metabotropic glutamate receptor subtype 1; $mGlu_5$, metabotropic glutamate receptor subtype 5; MPEP, 2-Methyl-6-(phenylethynyl)pyridine, MTEP, 2-methyl-4-(pyridin-3-ylethynyl)thiazole; 3-((2-Methyl-1,3-thiazol-4-yl)ethynyl)pyridine; NAL, neutral allosteric ligand; NAM,

negative allosteric modulator; Opti-MEM, Opti- modified Eagle's medium; PAM, positive allosteric modulator; VU0366058, 2-(1,3-benzoxazol-2-ylamino)-4-(4-fluorophenyl)pyrimidine-5-carbonitrile; VU0366248, N-(3-Chloro-2-fluorophenyl)-3-cyano-5-fluoro-benzamide; VU0409106, 3-Fluoro-*N*-(4-methyl-2-thiazolyl)-5-(5-pyrimidinyloxy)benzamide.

3.1. Introduction

The metabotropic glutamate receptor subtype 5 ($mGlu_5$) is a G protein-coupled receptor (GPCR) widely expressed throughout the brain, and implicated in various central nervous system (CNS) disorders, ranging from anxiety and depression to Parkinson's disease and autism (Gregory et al., 2013c). $mGlu_5$ is a well-established G_q-coupled receptor, with activation leading to production of inositol-1,2,3-trisphosphate (IP_3), and mobilization of intracellular calcium (iCa^{2+}) (Niswender and Conn, 2010). $mGlu_5$ is one of eight mGlu subtypes, subdivided into group I ($mGlu_{1/5}$), group II ($mGlu_{2/3}$) and group III ($mGlu_{4,6\text{-}8}$), which share a highly conserved glutamate binding site that is difficult to selectively target. Recent approaches in targeting $mGlu_5$ have therefore focused on ligands that bind to less conserved topographically distinct, or allosteric, binding sites (Sengmany and Gregory, 2016). Allosteric ligands may modulate activity of orthosteric ligands, by influencing the affinity and/or efficacy (a property termed cooperativity), to either enhance (positive allosteric modulator; PAM), or diminish (negative allosteric modulator; NAM) endogenous receptor responses (Changeux and Christopoulos, 2016). Some PAMs also activate the receptor in the absence of orthosteric ligand and are categorized as PAM-agonists, while neutral allosteric ligands (NALs) bind to allosteric sites without influencing orthosteric ligand activity or affinity (Changeux and Christopoulos, 2016). In the absence of endogenous agonist, pure PAMs and NAMs offer the advantage of spatial and temporal fine-tuning of receptor responses – a desirable clinical outcome within the delicate CNS network.

Fine-tuning neurotransmitter receptor activity can also be achieved through biased agonism and modulation (Kenakin and Christopoulos, 2013), whereby individual

ligands may differentially activate/modulate different receptor responses to the relative exclusion of others and as such have a unique "signaling fingerprint". Biased agonism and modulation is operative across a wide range of GPCRs, from opioid and endocannabinoid systems to adrenergic and adenosine receptors, to name a few (Baltos et al., 2017; da Silva Junior et al., 2017; Khajehali et al., 2015; Priestley et al., 2017; Violin et al., 2014). Thus, determining ligand signaling fingerprints for different effectors offers the invaluable opportunity to design ligands that bias receptor signaling towards desired pathways and subsequent clinical outcomes, while avoiding receptor responses that result in unwanted, or adverse, effects.

While the notion of bias is gaining traction, the continued use of high-throughput single-assay drug screening approaches is not capturing the full scope of ligand activity. Importantly, it is increasingly evident that $mGlu_5$ is pleiotropically coupled to multiple G proteins and signaling partners (Francesconi and Duvoisin, 1998; Joly et al., 1995; Mao et al., 2005; Peavy et al., 2001; Rush et al., 2002; Thandi et al., 2002). For allosteric modulators, bias may be evident in three distinct parameters that dictate allosteric modulator activity; namely affinity, cooperativity and intrinsic efficacy. Indeed, we have clearly shown biased agonism and modulation to be operative amongst several chemotypes of $mGlu_5$ ligands broadly classified as PAMs or PAM-agonists (Sengmany et al., 2017). Importantly, we revealed how previous classification of $mGlu_5$ allosteric ligands based solely on their activity in iCa^{2+} mobilization assays failed to recognize the robust agonism characteristic of most $mGlu_5$ allosteric ligands in IP_1 accumulation and ERK1/2 phosphorylation assays (Sengmany et al., 2017). Thus, simply categorizing an $mGlu_5$ allosteric ligand as a PAM or NAM based on a single functional assay precludes recognition of the rich

complexity each ligand may offer. Consequently, potential therapeutic compounds may be discarded, while unexplained adverse effects from clinical candidates may arise.

While $mGlu_5$ NAMs have been broadly classified as such based on their activity in iCa^{2+} mobilization assays, recent clinical failures are suggestive of an insufficient understanding of $mGlu_5$ modulator pharmacology. For instance, fenobam showed promise some 30 years ago in the treatment of generalized anxiety disorder (Pecknold et al., 1982), but also impairs learning at therapeutic doses in preclinical models (Jacob et al., 2009). Cognition impairment, as well as abuse and psychoactive potential remain common adverse effects amongst several $mGlu_5$ NAMs including prototypical compounds such as MPEP and MTEP (Abou Farha et al., 2014; Dekundy et al., 2011; Hughes et al., 2013; Swedberg et al., 2014; Swedberg and Raboisson, 2014). It has been proposed that "partial NAMs", i.e. NAMs with limited cooperativity, may offer the advantage of reduced adverse effect liability due to incomplete blockade of $mGlu_5$ responses (Nickols et al., 2016). However, there remains a need to better quantify and assess the interaction between chemically and pharmacologically diverse NAMs to truly appreciate the underlying mechanisms of action that contribute to therapeutically beneficial versus adverse effects.

Here we aimed to determine the signaling profiles of select $mGlu_5$ NAMs, through rigorous assessment of interactions between $mGlu_5$ orthosteric and negative allosteric ligands in iCa^{2+} mobilization and IP_1 accumulation assays in both recombinant and neuronal systems. We show that some $mGlu_5$ NAMs exhibit differential apparent affinities depending on cell background, pre-equilibration time, orthosteric agonist

used and in cortical neurons co-application of CPCCOEt. Cooperativity of select NAMs was also influenced by co-application of CPCCOEt, and biased cooperativity was evident for VU0366248. In all, this study highlights the importance of robust evaluation of allosteric modulatory activity to appreciate the inherent complexity when applying standard high-throughput assays, and potential pitfalls. Moreover, the distinct pharmacological fingerprints identified may be linked to differential therapeutic efficacy and adverse effect liability of select NAMs, and may provide a framework to develop biased mGlu5 NAMs in the future.

3.2. Methods

3.2.1. Materials

Dulbecco's modified Eagle's medium (DMEM), Neurobasal medium, Fluo-4-AM and antibiotics were purchased from Invitrogen (Carlsbad, CA). Fetal bovine serum (FBS) was sourced from Thermo Electron Corporation (Melbourne, Australia). IP-ONE HTRF® assay kit was purchased from Cisbio, Genesearch (Arundel, Australia) and AlphaScreen detection beads from PerkinElmer Life and Analytical Sciences (Melbourne, Australia). Select mGlu$_5$ ligands: 2-(1,3-benzoxazol-2-ylamino)-4-(4-fluorophenyl)pyrimidine-5-carbonitrile (VU0366058), 2-[2-(3-methoxyphenyl)ethynyl]-5-methylpyridine (M-5MPEP), 3-Fluoro-*N*-(4-methyl-2-thiazolyl)-5-(5-pyrimidinyloxy)benzamide (VU0409106), and N-(3-chloro-2-fluorophenyl)-3-cyano-5-fluorobenzamide (VU0366248) were synthesized as previously described (Felts et al., 2013; Mueller et al., 2012; Rodriguez et al., 2005b; Sharma et al., 2008). (*S*)-3,5-dihydroxyphenylglycine (DHPG), 3-((2-methyl-1,3-thiazol-4-yl)ethynyl)pyridine hydrochloride (MTEP), and 7-(hydroxyimino)cyclopropa[b]chromen-1a-carboxylate ethyl ester (CPCCOEt) were purchased from Tocris Bioscience (Melbourne, Australia) and dipraglurant (ADX 48621) from ApexBio (Houston, TX). [^{3}H]methoxy-PEPy was custom synthesized by Quotient Bioresearch (Rushden, Northamptonshire, UK) using the previously reported synthetic route (Cosford et al., 2003). Unless otherwise stated, all other reagents were purchased from Sigma-Aldrich (St. Louis, MO) and were of analytical grade.

3.2.2. Cell culture

HEK293A cells stably transfected with wild-type rat $mGlu_5$ (HEK293A-$mGlu_5$-low) at low levels comparable to those observed in primary cortical astrocytes (Noetzel et al., 2013) were maintained at 37°C and 5% CO_2 in DMEM supplemented with 5% FBS, 16 mM HEPES and 500 μg/mL G418. One day prior to experimentation, cells were plated onto poly-D-lysine coated, clear-bottom 96 well plates in glutamine-free DMEM supplemented with 5% dialyzed FBS, 16 mM HEPES and 500 μg/mL G418 at 40,000 cells/well.

3.2.3. Primary cell culture

All animal experiments were approved by the Monash Institute of Pharmaceutical Sciences Animal Ethics Committee (Protocol no. MIPS.2014.37). 8-week old female Asmu:Swiss wild-type mice were provided by the Monash Animal Research Platform (Clayton, VIC, Australia). Pregnant female mice were humanely sacrificed and E16 embryos collected for primary cell culture. Cortices were dissected from E16 Asmu:Swiss wild type mice and mechanically dissociated in Hank's Balanced Salt Solution (HBSS: KCl 5.3 mM, KH_2PO_4 0.44 mM, $NaHCO_3$ 4.17 mM, NaCl 137.93 mM, Na_2HPO_4 0.34 mM, D-glucose 5.56 mM). Neurons were plated on poly-D-lysine, FBS-coated clear-bottom 96 well plates in Neurobasal media supplemented with 2 mM L-glutamine, 1 x B-27®, 50 U/mL penicillin, 50 U/mL streptomycin, 1.25 μg/mL Fungizone® antimycotic, at a density of 100,000 cells/well. Neurons were maintained at 37°C and 5% CO_2 for 5-7 days prior to experimentation.

3.2.4. Intracellular calcium mobilization

Intracellular calcium (iCa^{2+}) mobilization was measured as previously described (Gregory et al., 2012). Briefly, changes in fluorescence of the Ca^{2+} indicator dye Fluo-4-AM were measured using the Flexstation I or III, with $mGlu_5$ allosteric ligands added either 1 min or 30 min prior to orthosteric agonist. Experiments were conducted at room temperature (RT) for HEK293A-$mGlu_5$-low cells, and at 37°C for cortical neurons. A 5-point smoothing function was applied to raw fluorescence traces, with peak iCa^{2+} responses normalized to the maximal responses of either glutamate (HEK293A-$mGlu_5$-low) or DHPG (cortical neurons).

3.2.5. Inositol monophosphate (IP_1) accumulation assay

Recombinant cells or primary cortical neurons were washed with phosphate buffered saline (PBS; 1.1 mM KH_2PO_4, 155 mM NaCl, 3 mM Na_2HPO_4, pH 7.4) and incubated with stimulation buffer (HBSS, with 20 mM HEPES, 30 mM $LiCl_2$, 1.2 mM $CaCl_2$, pH 7.4) supplemented with 1-10U/mL glutamic pyruvic transaminase and 6 mM sodium pyruvate for 1 h at 37°C and 5% CO_2, followed by compound addition. After 1 h ligand incubation, cells were aspirated and lysed with Lysis buffer (HTRF® IP-one assay kit) and IP_1 levels detected as per kit instructions. Fluorescence was measured using the Envision plate reader (PerkinElmer), and expressed as fold over basal.

3.2.6. Whole cell radioligand binding

[^{3}H]methoxy-PEPy whole-cell inhibition binding assays on mouse embryonic cortical neurons were performed at RT for 1 h in 24-well plates in HEPES-based binding buffer (145 mM NaCl, 10 mM D-glucose, 5 mM KCl, 1 mM $MgSO_4$, 10 mM HEPES,

1.3 mM CaCl2, 15 mM $NaHCO_3$, pH 7.45). For binding studies in HEK293A-mGlu$_5$-low, cells were plated onto white-walled, clear bottom poly-D-lysine coated 96-well isoplates at a density of 40,000 cells/well. Inhibition of ~2 nM [^{3}H]methoxy-PEPy binding by increasing concentrations of the various allosteric ligands was assessed. The concentration of DMSO (0.3%) was kept constant throughout. Non-specific binding was determined using 10 μM MPEP. Assays were terminated by washing three times with ice-cold 0.9% NaCl. For cortical neurons, cells were lysed with 250 μl/well of 0.2 M NaOH, lysates transferred to scintillation vials, 4 mL UltimaGold scintillation cocktail added and incubated for >2 h. For HEK293A-mGlu$_5$-low cells, Microscint20 (40 μl/well) was added directly to isoplates, plate sealed and incubated for >2 h. Bound radioactivity was measured using either a MicroBeta2 plate counter or Tri-Carb 2900TR liquid scintillation counter (PerkinElmer, Waltham, MA).

3.2.7. Data analysis

Inhibition of [^{3}H]methoxy-PEPy binding were fitted to either a one-site or two-site inhibition binding model as previously described (Gregory et al., 2012; Lazareno and Birdsall, 1995) and estimates of dissociation constants (K_i) were derived using the Cheng-Prusoff equation (Cheng and Prusoff, 1973).

For ligands that did not fully displace radioligand, inhibition binding curves were fitted with a modified allosteric ternary complex model (Lazareno and Birdsall, 1993):

$$\frac{Y}{Y_{max}} = \frac{[D]}{[D] + \frac{K_D(1+\frac{[B]}{K_B})}{(1+\frac{\propto[B]}{K_B})}} \quad (1)$$

where Y/Y_{max} is the fraction specific binding, the molar concentration of radioligand

is [D] and K_D is the radioligand equilibrium dissociation constant, [B] is the molar concentration of unlabeled allosteric modulator, K_B is the equilibrium dissociation constant of the unlabeled allosteric ligand, and α is the affinity cooperativity factor are as defined above.

Allosteric modulation of glutamate or DHPG-mediated responses were fitted to the operational model of allosterism (Leach et al., 2007):

$$Effect = \frac{E_m(\tau_A[A](K_B+\alpha\beta[B])+\tau_B[B]K_A)^n}{([A]K_B+K_AK_B+K_A[B]+\alpha[A][B])^n+(\tau_A[A](K_B+\alpha\beta[B])+\tau_B[B]K_A)^n} \quad (2)$$

where [A] is the molar concentrations of orthosteric agonist (glutamate or DHPG). β is a scaling factor that denotes the magnitude of effect an allosteric modulator has on orthosteric agonist efficacy. [B], KB, and α are as defined above for equation 1. Affinity cooperativity (α) was assumed to be neutral as validated previously (Gregory et al., 2012) and thus constrained to a value of 1. K_A is the equilibrium dissociation constants of the orthosteric agonist. K_A values for orthosteric agonists were constrained to reported affinity estimates determined from inhibition binding assay as validated previously (Gregory et al., 2012; Mutel et al., 2000; Schoepp et al., 1994). τ_A and τ_B are the respective ligand's intrinsic efficacy, while E_m and n represent the maximal system response and the transducer slope respectively.

Affinity and cooperativity estimates were also derived by globally fitting an orthosteric agonist concentration response curve (equation 3) and an allosteric modulator titration curve in the presence of a single concentration of agonist (equation 4):

$$y = basal + \frac{E_m-basal}{1+\frac{K_A+[A]}{\tau_A+[A]}} \quad (3)$$

$$y = basal + \frac{(E_m-basal)[\tau_A[A](K_B+\alpha\beta[B])]^n}{[\tau_A[A](K_B+\alpha\beta[B])^n+([A]K_B+K_AK_B+K_A[B]+\alpha[A][B])^n} \quad (4)$$

Where K_A, τ_A, E_m and basal values were shared across analyses. For equation 4, [A] was held constant to the molar agonist concentration added, that is, ~EC_{80} response in the particular assay.

All operational parameters are presented as logarithms and expressed as mean ± SEM. Statistical analyses of binding data were performed as indicated using an extra sum-of-squares F test to determine the preferred model (one-site versus two-site binding) for each data set. Statistical analyses of functional assays were performed as indicated by using unpaired Student's t-test or one-way analysis of variance (ANOVA) with Tukey's or Sidak's post hoc test, to compare affinity and cooperativity estimates between signaling assays and cell backgrounds.

3.3. Results

Eight $mGlu_5$ allosteric ligands previously reported as NAMs of glutamate-mediated iCa^{2+} mobilization were chosen for this study. All of these ligands have been proposed to interact with a "common allosteric $mGlu_5$ site" located in the 7 transmembrane (7TM) spanning domain (Gregory et al., 2012; Porter et al., 2005a). MPEP, a disubstituted alkyne, is a prototypical $mGlu_5$ NAM (Gasparini et al., 1999a) from which MTEP, reported to have greater $mGlu_5$ selectivity and potency, was derived (Cosford et al., 2003b; Iso et al., 2006). M-5MPEP, also derived from MPEP, has limited negative cooperativity (also referred to as partial NAM activity) with glutamate (Nickols and Conn, 2014; Rodriguez et al., 2005b). VU0409106, VU0366058 and VU0366248 represent chemotypes distinct from MPEP – namely the aryl ether series (Felts et al., 2013), 5-cyanopyrimides (Mueller et al., 2012) and 3-cyano-5-fluoro-N-arylbenzamides (Felts et al., 2010) respectively. Previous reports indicate VU0409106 and VU0366058 are full NAMs of glutamate-mediated iCa^{2+} mobilization, while VU0366248 is a partial NAM (Felts et al., 2013; Gregory et al., 2012). Fenobam and dipraglurant were included to represent $mGlu_5$ NAMs that have progressed to clinical trials (Pecknold et al., 1982; Tison et al., 2016).

Radioligand binding studies were conducted on intact adherent HEK293A-$mGlu_5$-low cells and primary cortical neurons (Fig. 3.1). Interestingly, MPEP and MTEP inhibition binding curves were best fitted to a two-site model in both recombinant and native cells. Fenobam inhibition curves were also consistent with two-site binding in recombinant cells, but best fitted to a one-site non-competitive model in neurons. M-5MPEP, VU0366248, VU0409106 and dipraglurant inhibition curves were consistent with one-site binding in both cell types. VU0366058, VU0366248, VU0409106 and

dipraglurant did not completely displace [^{3}H]methoxy-PEPy binding in either cell type. Affinity (pK$_i$) estimates for recombinant and native cells are summarized in Table 3.1. With the exception of MTEP, allosteric ligands had similar pK$_i$ estimates between HEK293A-mGlu$_5$-low and cortical neurons (Table 3.1).

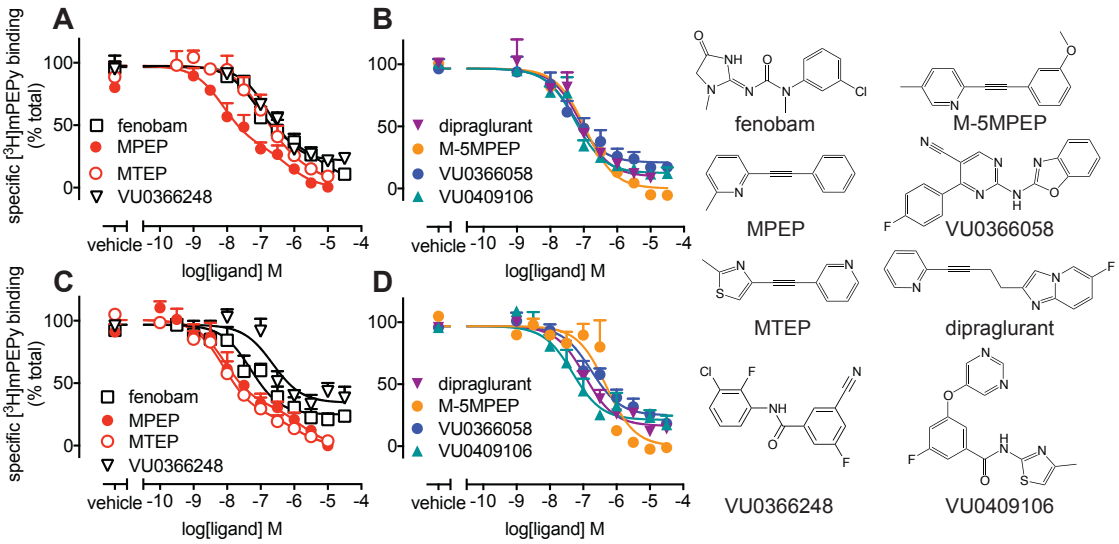

Figure 3.1. Inhibition of [^{3}H]methoxy-PEPy binding to HEK293A-mGlu$_5$-low cells and cortical neurons. Using intact adherent cells, inhibition of [^{3}H]methoxy-PEPy binding was determined in HEK293A-mGlu$_5$-low cells (**A** & **B**) and cortical neurons (**C** & **D**). Data were fitted to either a one-site or two-site inhibition-binding model as determined by an F-test on each individual experiments. Data are mean + S.E.M. from 3-5 independent experiments performed in duplicate.

Table 3.1. Binding affinities of $mGlu_5$ allosteric ligands derived from inhibition of [^{3}H]methoxy-PEPy binding in intact and adherent HEK293A-$mGlu_5$-low cells and cortical neurons. Data represent mean ± SEM of 3-6 independent experiments performed in duplicate.

	HEK293A-$mGlu_5$-low pK_i				Cortical neurons pK_i			
	High	Low	Fraction High	Logα	High	Low	Fraction High	Logα
MPEP	8.26 ±0.23	6.25 ±0.11	0.62 ±0.11	n.a.	8.38 ±0.30	5.92 ±0.20	0.73 ±0.11	n.a.
fenobam	7.15 ±0.28	4.66 ±0.22	0.71 ±0.09	n.a.	7.65 ±0.44[a]	n.a.	1[a]	-0.71 ±0.11
VU0409106	7.47 ±0.07	n.a.	1	-1.12 ±0.12	7.48 ±0.15	n.a.	1	-0.78 ±0.13
VU0366248	6.94 ±0.13	n.a.	1	-0.77 ±0.06	6.72 ±0.06	n.a.	1	-0.54 ±0.06
VU0366058	7.26 ±0.10	n.a.	1[b]	-0.82 ±0.07	6.76 ±0.23	n.a.	1[b]	-0.71 ±0.07
M-5MPEP	7.13 ±0.07	n.a.	1	n.a.	6.43 ±0.25	n.a.	1	n.a.
dipraglurant	7.31 ±0.11	n.a.	1	-1.24 ±0.17	6.98 ±0.14	n.a.	1	-0.89 ±0.08
MTEP	7.20 ±0.28	5.45 ±0.30	0.83 ±0.04	n.a.	8.16 ±0.14*	6.09 ±0.45	0.74 ±0.04	n.a.

[a] One individual experiment (from n=5) was best fitted to a two-site binding curve (F test p>0.05).
[b] Two individual experiments (from n=5-6) were best fitted to a two-site binding curve.
n.a. not applicable due to one-site or competitive binding curve fit
* Denotes *p<0.05*, One-way ANOVA, Sidak's multiple comparisons test, compared to HEK293A-$mGlu_5$-low

3.3.1. $mGlu_5$ allosteric ligands are NAMs of glutamate-mediated iCa^{2+} mobilization in HEK293A-$mGlu_5$-low cells.

In agreement with previous studies, all eight allosteric ligands were NAMs of glutamate-mediated iCa^{2+} mobilization in HEK293A-$mGlu_5$-low cells after 1 min pre-incubation (Fig. 3.2) (Felts et al., 2010; Felts et al., 2013; Gregory et al., 2012; Mueller et al., 2012; Porter et al., 2005a). In particular, MPEP, MTEP, fenobam, dipraglurant and VU0409106 were full NAMs, while M-5MPEP and VU0366248 displayed limited negative cooperativity. VU0366058 is fluorescent, which limited the testing of concentrations above 1 μM, however, inhibition of glutamate-mediated iCa^{2+} mobilization was consistent with high negative cooperativity. In order to quantify functional affinity and cooperativity estimates, NAM interactions with glutamate were fitted to the operational model of allosterism (Leach et al., 2007). With the exception of dipraglurant, functional affinity estimates (pK_B values) were in good agreement with pK_i estimates (for the high affinity site where applicable) determined from inhibition binding assays in HEK293A-$mGlu_5$-low cells (Tables 3.1 & 3.2). The affinity of dipraglurant was significantly higher in iCa^{2+} mobilization assays (6 fold) relative to the inhibition binding estimate. All NAMs had similar magnitudes of negative cooperativity with glutamate as previously reported (Table 3.2, Gregory et al., 2010).

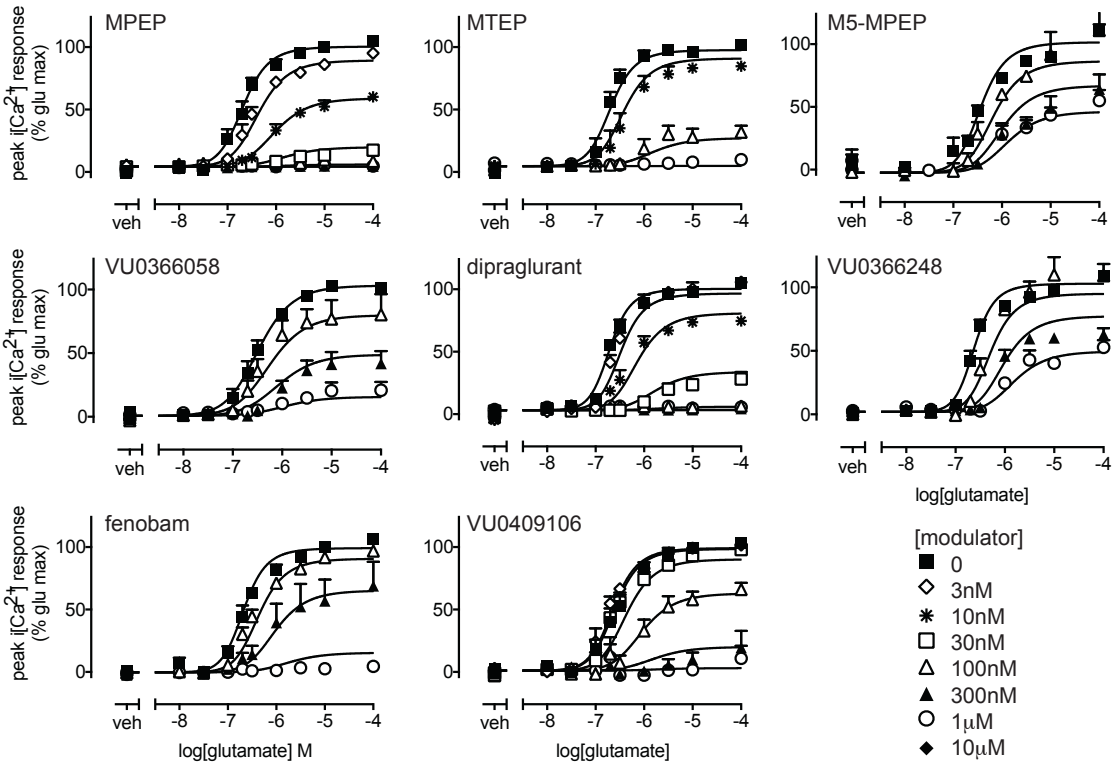

Figure 3.2. Negative allosteric modulation of glutamate-mediated iCa^{2+} mobilization in HEK293A-mGlu$_5$-low cells. Concentration response curves for glutamate mediated iCa^{2+} mobilization in the absence or presence of indicated allosteric ligands following 1 min pre-incubation. Data are expressed as mean + SEM of 3-5 experiments performed in duplicate. Error bars not shown lie within the dimensions of the symbols.

Table 3.2. Comparison of affinity and cooperativity estimates for allosteric modulation of glutamate-mediated iCa^{2+} mobilization following 1 min vs 30 min pre-incubation of mGlu$_5$ allosteric ligands in HEK293A-mGlu$_5$-low cells. Data represent mean ± SEM of 3-7 independent experiments performed in duplicate.

	1 min		30 min	
	pK$_B$[a]	log αβ[b]	pK$_B$	log αβ
MPEP	8.39±0.13	Full NAM[c]	7.90±0.08	Full NAM
fenobam	6.98±0.09	Full NAM	7.27±0.11	Full NAM
VU0409106	7.27±0.12	Full NAM	7.38±0.12	Full NAM
VU0366248	7.22±0.09	-0.90±0.12	6.57±0.18[e]	-0.58±0.08
VU0366058	6.98±0.11	Full NAM	7.11±0.28	Full NAM
M-5MPEP	7.00±0.07	-0.59±0.03	6.72±0.26	-0.52±0.06
dipraglurant	8.16±0.06[d]	Full NAM	7.47±0.07[e]	Full NAM
MTEP	7.83±0.09	Full NAM	6.97±0.15[e]	Full NAM

[a] pK$_B$, negative logarithm of the equilibrium dissociation constant determined using an operational model of allosterism
[b] log αβ, logarithm of the cooperativity factor determined using an operational model of allosterism where α was assumed to be equal to 1
[c] "full NAM" denotes complete inhibition of DHPG response, such that β approaches zero.
[d] Denotes $p<0.05$, One-way ANOVA, Tukey's multiple comparisons test, compared to binding pK$_i$ estimates
[e] Denotes $p<0.05$, One-way ANOVA, Tukey's multiple comparisons test, compared to pK$_B$ estimate derived from iCa^{2+} mobilization assays (1 min versus 30 min paradigm)

3.3.2. Ligand-receptor equilibrium influences $mGlu_5$ NAM apparent affinity with glutamate for iCa^{2+} mobilization in HEK293A-$mGlu_5$-low

Differing ligand incubation times between different assays may result in potential bias within a kinetic context (Klein Herenbrink et al., 2016; Lane et al., 2017), especially for non-equilibrium assays. Non-equilibrium conditions may also contribute to differences in affinity estimates. Therefore, we extended the NAM pre-incubation period to 30min prior to conducting glutamate-mediated iCa^{2+} mobilization assays in HEK293A-$mGlu_5$-low cells (Fig. 3.3). With an increased pre-incubation time for dipraglurant prior to iCa^{2+} mobilization assays, the pK_B value was in much closer agreement with the pK_i estimate (Table 3.2). Extended pre-incubation with MTEP resulted in a lower pK_B estimate (7-fold) when compared with the 1 min paradigm. VU0366248 also had lower negative cooperativity although this did not reach significance (Table 3.2).

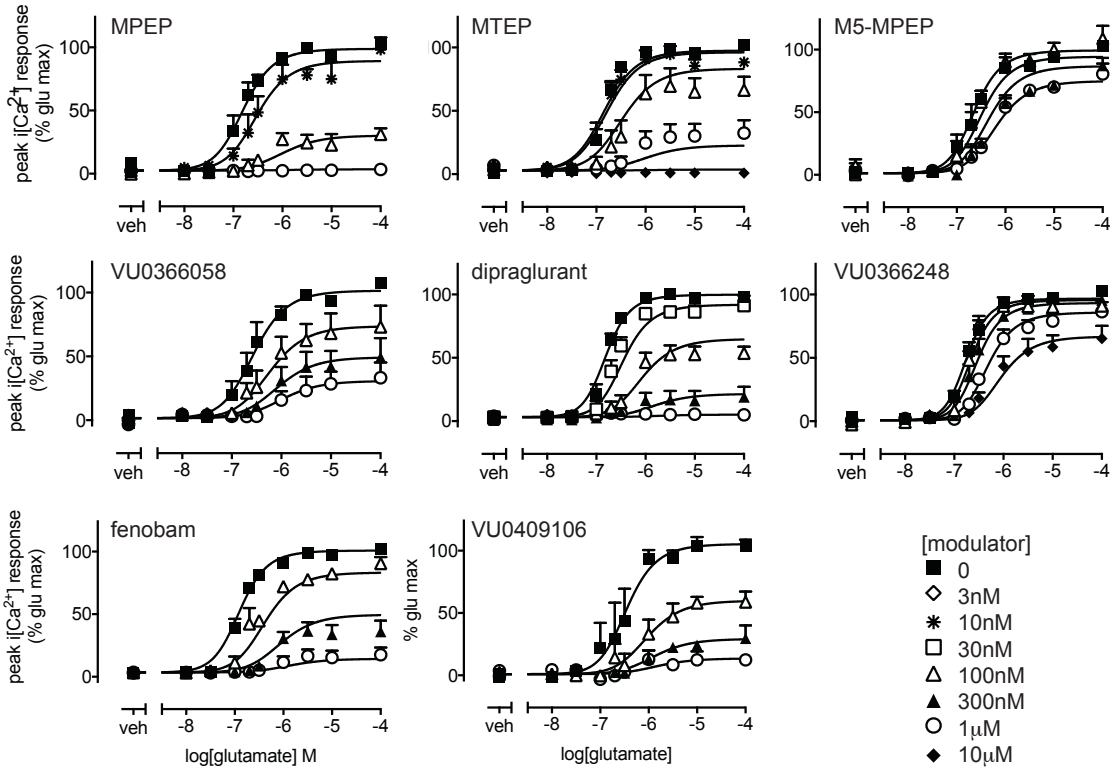

Figure 3.3. Negative allosteric modulation of glutamate-mediated iCa^{2+} mobilization in HEK293A-mGlu$_5$-low cells with extended pre-incubation. Concentration response curves for glutamate mediated iCa^{2+} mobilization in the absence or presence of indicated allosteric ligands following 30 min pre-incubation. Data are expressed as mean + SEM of 3-5 experiments performed in duplicate. Error bars not shown lie within the dimensions of the symbols.

3.3.3 $mGlu_5$ NAMs are inverse agonists for IP_1 accumulation in HEK293A-$mGlu_5$-low cells

IP_1 accumulation was assessed as an alternative signaling endpoint, given previous observations of biased agonism/modulation for $mGlu_5$ PAMs between iCa^{2+} mobilization and IP_1 accumulation (Sengmany et al., 2017). Measurement of IP_1 accumulation provides insight into receptor activity at ligand equilibrium relative to transient, non-equilibrium, iCa^{2+} mobilization responses. In the presence of GPT, which eliminates ambient glutamate, all eight $mGlu_5$ NAMs decreased baseline IP_1 accumulation in a concentration dependent manner in the absence of agonist (Fig. 3.4). These data are consistent with constitutive $mGlu_5$ activity and inverse agonism. The potencies of MTEP and dipraglurant as inverse agonists were similar to binding affinity estimates, whereas for the remaining six NAMs, potencies were 2-4 fold lower than pK_i values (Table 3.3). Due to appreciable constitutive activity/inverse agonism for all eight NAMs for IP_1 accumulation in HEK293A-$mGlu_5$-low cells, it was not feasible to assess interactions between NAMs and glutamate using the operational model of allosterism.

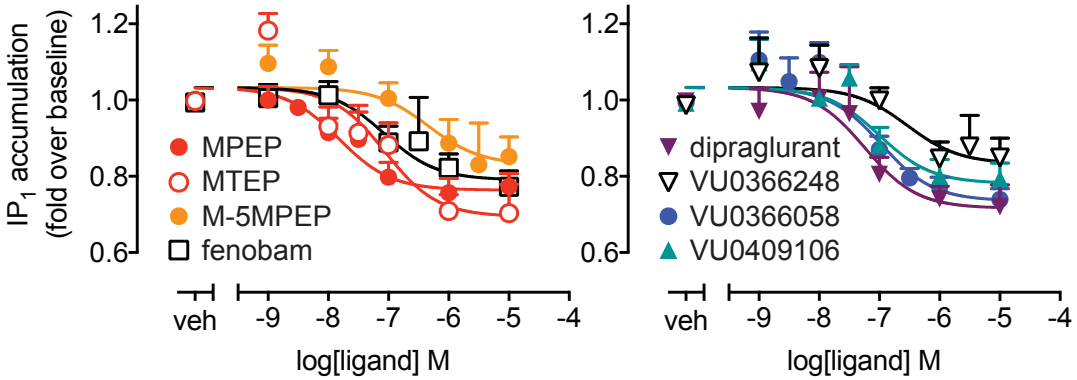

Figure 3.4. Inverse agonism of constitutive IP$_1$ accumulation in HEK293A-mGlu$_5$-low cells. Concentration response curves for inhibition of constitutive mGlu$_5$-mediated IP$_1$ accumulation by indicated allosteric ligands. Data are expressed as mean + SEM of 3-9 experiments performed in duplicate. Error bars not shown lie within the dimensions of the symbols.

Table 3.3. Potency and efficacy of mGlu$_5$ NAMs as inverse agonists of IP$_1$ accumulation in HEK293A-mGlu$_5$-low cells. Data represent mean ± SEM of 5-9 independent experiments performed in duplicate.

	pIC$_{50}$[a]	I$_{max}$[b]
MPEP	7.86 ±0.27	0.74 ±0.03
fenobam	6.83 ±0.26	0.76 ±0.03
VU0409106	6.89 ±0.26	0.74 ±0.05
VU0366248	6.48 ±0.16	0.81 ±0.05
VU0366058	6.98 ±0.17	0.73 ±0.03
M-5MPEP	6.53 ±0.17	0.81 ±0.05
dipraglurant	7.36 ±0.15	0.73 ±0.04
MTEP	7.36 ±0.16	0.70 ±0.05

[a] negative logarithm of the molar concentration required to give a half maximal inhibitory response
[b] maximal inhibitory response, expressed as fold over basal IP$_1$ accumulation levels.

3.3.4. $mGlu_5$ allosteric ligands are NAMs of DHPG-mediated iCa^{2+} mobilization in cultured cortical neurons.

We next sought to confirm the pharmacology of all eight ligands in primary mouse embryonic cortical neuron cultures. The complex cell background in neuronal cells limits the use of glutamate as an orthosteric agonist due to the presence of other glutamate receptors and transporters. Thus, we adopted a commonly used approach to measure mGlu signaling in response to the $mGlu_{1/5}$ orthosteric agonist, DHPG, co-added with the $mGlu_1$ NAM, CPCCOEt (to minimize $mGlu_1$ signaling) (Jong et al., 2009; Kettunen et al., 2002; Luccini et al., 2007; Sengmany et al., 2017; Viwatpinyo and Chongthammakun, 2009). Inclusion of 30 uM CPCCOEt had no effect on DHPG potency or E_{max} for iCa^{2+} mobilization or IP_1 accumulation at cortical neurons (Supplementary Figure 3.1). We first assessed affinity and cooperativity profiles of the NAMs with DHPG in HEK293A-$mGlu_5$-low cells. To do so, we analysed NAM inhibition of an EC_{80} DHPG iCa^{2+} mobilization response, in parallel with a control DHPG concentration-response curve, using both 1 min and 30 min pre-incubation paradigms (Supplementary Figure 3.2 and Supplementary Tables 3.1 & 3.2). NAM affinity and cooperativity estimates derived from DHPG Ca^{2+} mobilization inhibition curves were generally similar to those derived from glutamate inhibition curves, although there were a few exceptions (Table 3.2 and Supplementary Table 3.1 & 3.2). For instance, MPEP and MTEP had higher affinity estimates when DHPG was used as the agonist compared to glutamate, with significant differences observed for MTEP using the 1 min paradigm (3-fold) and for MPEP using the 30 min paradigm (10 fold). Differential apparent affinities for these two NAMs under the same assay conditions but derived from interaction studies with different agonists is suggestive of probe dependence.

Consistent with HEK293A-mGlu$_5$-low cells, in the absence of agonist none of the eight NAMs influenced basal iCa^{2+} mobilization in cortical neurons (data not shown). All compounds inhibited the response to an EC_{80} DHPG concentration in a concentration dependent manner following 1 min pre-incubation (Fig. 3.5A-B). Maximal concentrations of MPEP, fenobam, VU0409106, dipraglurant and MTEP resulted in complete inhibition of the DHPG EC_{80} for iCa^{2+} mobilization. VU0366248 and M-5MPEP showed limited negative cooperativity, as evidenced by incomplete inhibition of DHPG-mediated iCa^{2+} mobilization (Fig. 3.5A-B). VU0366058 also showed incomplete inhibition of DHPG but could not be definitively characterised as a limited or full NAM due to the restricted concentration range. Similar to observations in recombinant cells, quantification of these data with the operational model of allosterism revealed there were anomalies with respect to pK_i versus pK_B estimates for some ligands. For dipraglurant the pK_B estimate derived from iCa^{2+} mobilization assays was significantly greater than pK_i values (12-fold, Table 3.4). Extending the pre-incubation time in cortical neurons had no significant effect on NAM K_B estimates, although there was a trend for reduced affinity for MTEP and dipraglurant (Fig. 3.5C, D, Table 3.4). Increasing the pre-incubation time had no effect on negative cooperativity with DHPG for any of the NAMs (Table 3.5).

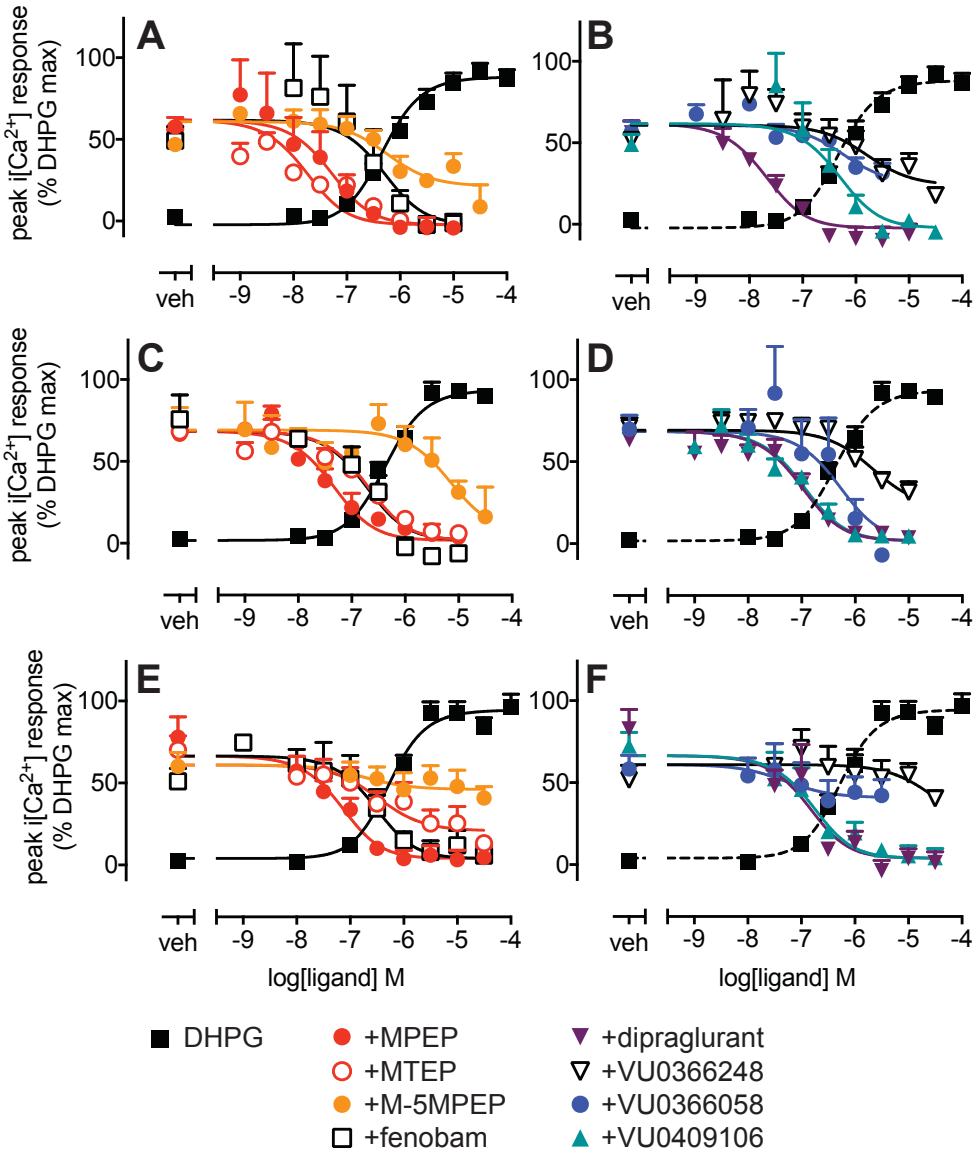

Figure 3.5. Negative allosteric modulator activity at iCa^{2+} mobilization in embryonic mouse cortical neurons. Concentration response curves for modulation of DHPG EC$_{80}$ (1 μM)-mediated iCa^{2+} mobilization with 1min (**A** & **B**) or 30 min (**C** & **D**) pre-incubation with mGlu$_5$ NAMs were performed in parallel with DHPG concentration-response curves. Modulation of DHPG-stimulated iCa^{2+} mobilization in the absence of CPCCOEt (**E** & **F**). Data are expressed as mean + SEM of 3-5 experiments performed in duplicate. Error bars not shown lie within the dimensions of the symbols.

Table 3.4. Comparison of mGlu$_5$ NAM functional affinity estimates across different measures of receptor activity in primary cortical neurons in the presence and absence of 30 μM CPCCOEt. Data represent mean ± SEM of 4-8 independent experiments performed in duplicate.

	iCa^{2+} mobilization		IP$_1$ accumulation	no CPCCOEt	
	pK$_B$ [a] (1min)	pK$_B$ (30min)	pK$_B$	pK$_B$ (iCa^{2+})	pK$_B$ (IP$_1$)
MPEP	7.90 ±0.32[b]	7.61 ±0.09	7.17 ±0.24	7.42±0.15	6.94±0.31[c]
fenobam	6.68 ±0.25	7.37 ±0.15	6.72 ±0.36	6.78±0.13	6.61±0.29
VU0409106	6.62 ±0.15	7.40 ±0.17[d]	6.44 ±0.22	6.97±0.24	6.66±0.22
VU0366248	6.03 ±0.39[b]	6.30 ±0.24	n.r.	5.77±0.45	n.r.
VU0366058	7.02 ±0.26	6.99 ±0.29	7.16 ±0.33	6.84 ±0.37	6.24±0.10
M-5MPEP	6.86 ±0.13	5.98±0.22	6.66 ±0.36	6.87 ±0.34	6.50±0.36
dipraglurant	8.06 ±0.22[c]	7.46 ±0.22	6.91 ±0.11[d]	7.16±0.22[e]	6.94±0.10
MTEP	7.97 ±0.32	7.09 ±0.18[f]	6.81 ±0.21[c,d]	6.51±0.41[c,e]	6.67±0.14[c]

[a] pK$_B$, negative logarithm of the equilibrium dissociation constant determined using an operational model of allosterism

[b] Denotes $p<0.05$, One-way ANOVA, Tukey's multiple comparisons test, compared to pK$_B$ estimate derived from iCa^{2+} mobilization assays in HEK293A-mGlu$_5$-low cells

[c] Denotes $p<0.05$, One-way ANOVA, Tukey's multiple comparisons test, compared to binding estimate

[d] Denotes $p<0.05$, One-way ANOVA, Tukey's multiple comparisons test, compared with pK$_B$ estimate derived from iCa^{2+} mobilization assays using a 1min paradigm

[e] Denotes *p<0.05*, One-way ANOVA, Tukey's multiple comparisons test, when compared with pK$_B$ estimate derived in the presence of 30 μM CPCCOEt in the equivalent experiment

[f] Denotes *p<0.05*, One-way ANOVA, Sidak's multiple comparisons test, when compared pK$_B$ estimate derived from iCa^{2+} mobilization assays in HEK293A-mGlu$_5$-low cells using a 30min paradigm

n.r. no modulatory response was evident.

Table 3.5. Comparison of $mGlu_5$ NAM cooperativity values with DHPG across different measures of receptor activity in primary cortical neurons in the presence and absence of 30 µM CPCCOEt. Data represent mean ± SEM of 3-8 independent experiments performed in duplicate.

	iCa^{2+} mobilization		IP_1 accumulation	no CPCCOEt	
	log αβ[a] (1min)	log αβ (30min)	log αβ	log αβ (iCa^{2+})	log αβ (IP_1)
MPEP	full NAM[b]	full NAM	full NAM	full NAM	full NAM
fenobam	full NAM	full NAM	full NAM	full NAM	full NAM
VU0409106	full NAM	full NAM	full NAM	full NAM	-0.54±0.14
VU0366248	-0.90 ±0.21	-1.00 ±0.29	n.r.	-0.38±0.10	n.r.
VU0366058	-0.60 ±0.15[c]	full NAM	-0.28 ±0.01	-0.62 ±0.11[c]	full NAM
M-5MPEP	-0.46 ±0.10	-1.06 ±0.29	-0.42 ±0.20	-0.48 ±0.06	-0.33±0.06
dipraglurant	full NAM	full NAM	full NAM	full NAM	full NAM
MTEP	full NAM	full NAM	full NAM	-0.85±0.17	-0.34±0.10

[a] log αβ, logarithm of the cooperativity factor determined using an operational model of allosterism where α was assumed to be equal to 1
[b] "full NAM" denotes complete inhibition of DHPG response, such that β values approach zero.
[c] limited concentration range was tested due to compound fluorescence therefore cannot definitively state that cooperativity is limited.
n.r. no modulatory response was evident.

3.3.5. Inhibition of $mGlu_1$ affects $mGlu_5$ NAM affinity and cooperativity with DHPG in cortical neuron iCa^{2+} mobilization assays

Given the observed differences between NAM pK_i estimates determined in neuronal radioligand binding assays versus functional assay pK_B estimates derived in the presence of CPCCOEt, we sought to ensure that CPCCOEt did not influence $mGlu_5$ NAM affinity and/or cooperativity. This was of particular concern for two reasons: (i) we recently showed that CPCCOEt binds to $mGlu_5$ (with comparable affinity for $mGlu_1$) albeit it exhibits neutral cooperativity with $mGlu_5$ agonists (Hellyer et al., 2018), (ii) $mGlu_1$ and $mGlu_5$ can heterodimerize to form higher order oligomers (Correa et al., 2017), thus CPCCOEt could influence $mGlu_5$ across an $mGlu_1/mGlu_5$ dimer. Thus, we re-evaluated the pharmacology of the eight studied $mGlu_5$ allosteric ligands in the absence of CPCCOEt in cortical neurons (Fig. 3.5, Table 3.4-3.5). In iCa^{2+} mobilization assays with 1 min pre-incubation and in the absence of CPCCOEt, dipraglurant and MTEP had significantly lower pK_B estimates versus in the presence of CPCCOEt (8 and 29-fold respectively), while MTEP transformed from a full to partial NAM. Thus, inclusion of CPCCOEt in the cortical neuron functional assays influenced $mGlu_5$ NAM pharmacology in a ligand-dependent manner. It is presently not clear whether this is due to unappreciated CPCCOEt activity at $mGlu_5$ alone, or mediated across an $mGlu_1/mGlu_5$ heteromer.

3.3.6. $mGlu_5$ allosteric ligands have differing degrees of cooperativity with DHPG when assessed in IP_1 accumulation in cultured cortical neurons.

In contrast to recombinant cells, there was no evidence for inverse agonist activity for all eight $mGlu_5$ NAMs for IP_1 accumulation in cortical neurons (Supplementary Figure 3.3). In the presence of CPCCOEt, with the exception of VU0366248, all of the allosteric modulators were NAMs of DHPG-mediated IP_1 accumulation in cortical neurons (Fig. 3.6A-B). VU0366248 showed negligible modulatory activity of DHPG-mediated IP_1 accumulation (Fig. 3.6B). Increasing concentrations of MPEP, fenobam, VU0409106, VU0366058, dipraglurant and MTEP resulted in complete inhibition of DHPG mediated IP_1 accumulation responses, while maximal M-5MPEP concentrations produced partial inhibition. Analysis of interactions with DHPG revealed that MTEP had a ~20-fold lower affinity estimate in IP_1 accumulation relative to inhibition binding, while all other ligand affinities were similar between assays (Table 3.4). Additionally, dipraglurant and MTEP had significantly lower (~10-fold) affinity estimates in IP_1 accumulation relative to 1 min pre-incubation iCa^{2+} mobilization assays. All NAMs showed similar degrees of negative cooperativity with DHPG between IP_1 accumulation and iCa^{2+} mobilization in the presence of CPCCOEt (Table 3.5). In the absence of CPCCOEt, there were no significant differences in DHPG potency or E_{max} in IP_1 accumulation (Supplementary Figure 3.1). Furthermore, there were no significant differences in functional affinity estimates for any of the eight NAMs between the presence and absence of CPCCOEt, based on modulation of DHPG-stimulated IP_1 accumulation (Fig. 3.6C-D; Table 3.4). In terms of cooperativity, however, MTEP and VU0409106 became partial NAMs in the absence of CPCCOEt (Table 3.5).

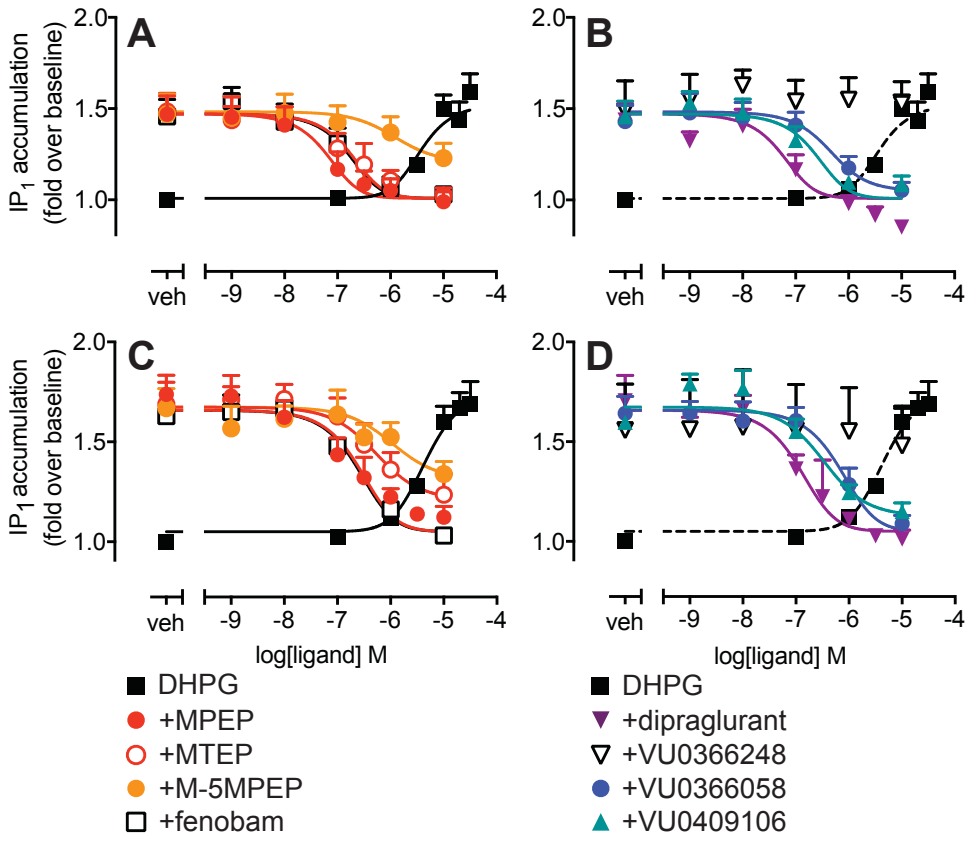

Figure 3.6. Inhibition of DHPG EC$_{80}$-mediated IP$_1$ accumulation by mGlu$_5$ NAMs in cortical neurons in the presence or absence of CPCCOEt 30 µM. Concentration response curves for modulation of DHPG EC$_{80}$(1 µM)-mediated IP$_1$ accumulation in the presence (**A** & **B**) or absence (**C** & **D**) of CPCCOEt. Data are expressed as mean + SEM of 3-8 experiments performed in duplicate. Error bars not shown lie within the dimensions of the symbols.

3.3.7. Comparison of signaling fingerprints between recombinant and native cells reveals differential apparent affinities.

To better visualize the differences and similarities in $mGlu_5$ NAM pharmacology in recombinant and native systems, we plotted the functional affinity estimates relative to binding estimates side by side (Fig. 3.7). Of note, when comparing affinity estimates between the different cell types in equivalent iCa^{2+} mobilization assays with the same orthosteric agonist, MPEP, MTEP, dipraglurant and VU0366248 had lower apparent affinities in cortical neurons compared to recombinant cells. Acetylenic full NAMs (MPEP, MTEP and dipraglurant) have similar profiles with respect to pK_B fingerprints, in which affinity estimates differ between binding and different measures of receptor activation. The switch of VU0366248 to neutral cooperativity in cortical neuron IP_1 accumulation assays precluded estimation of affinity. In contrast, the acetylenic partial NAM M-5MPEP and the structurally distinct NAMs, VU0366058, fenobam and VU0409106, have consistently similar pK_B values across all measures in both cell systems. Importantly, these data suggest that the differences in functional affinity estimates observed between IP_1 accumulation and iCa^{2+} mobilization assays are ligand dependent and not simply attributable to differences in assay conditions. For the most part, magnitudes of negative cooperativity between NAMs and DHPG were similar in neurons to HEK293A-$mGlu_5$-low cells (Table 3.5).

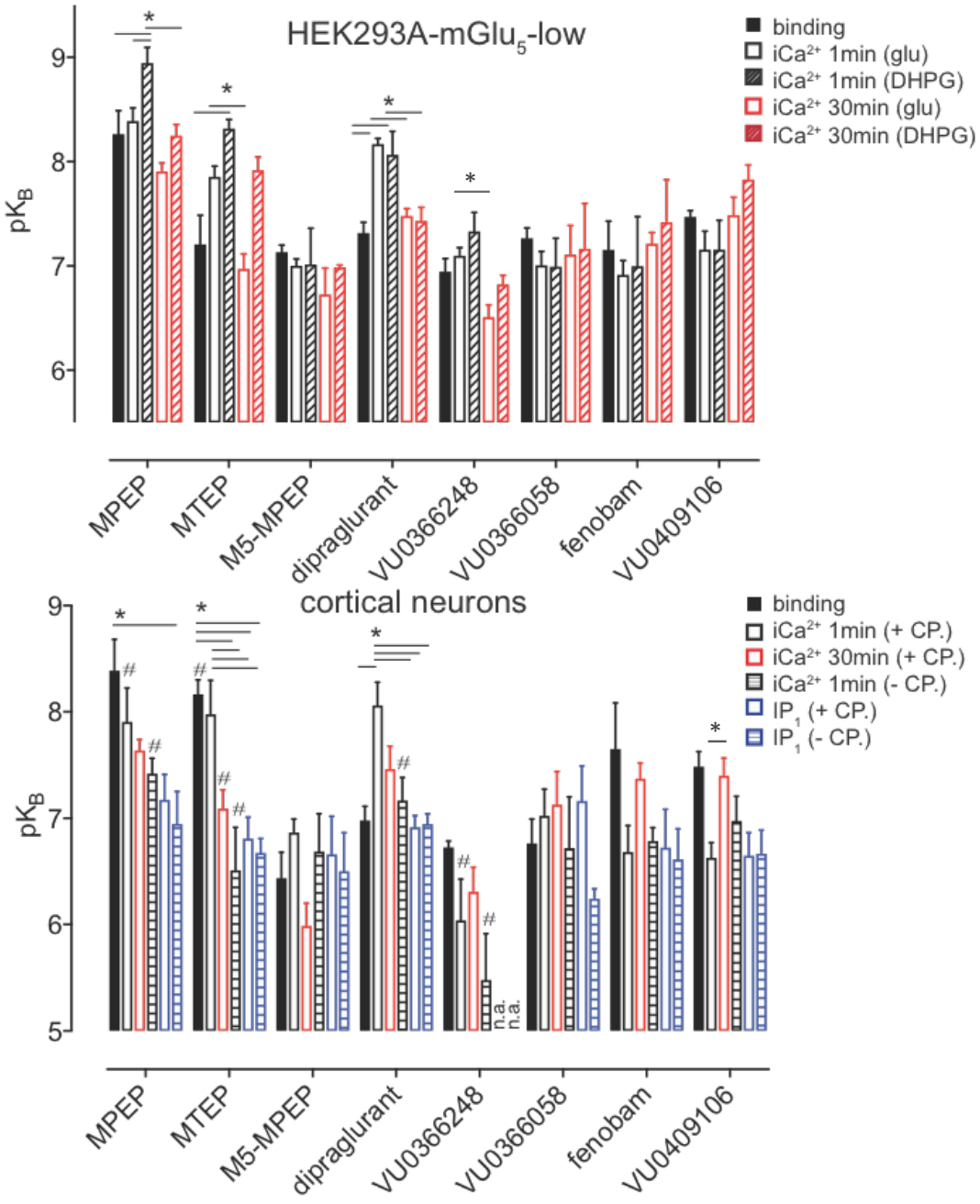

Figure 3.7. Comparison of affinity estimates in HEK293A-mGlu$_5$-low cells and cortical neurons. Affinity estimates from inhibition binding (pK_I) and functional assays (pK_B) in HEK293A-mGlu$_5$ low cells or cortical neurons. Comparisons within each cell type were performed using one-way ANOVA with Tukey's post test, from 3-10 experiments performed in duplicate, where significance (*) was considered $p<0.05$. Not determined (n.a.) due to lack of appreciable modulation. Comparisons between HEK293A-mGlu$_5$-low cells and cortical neurons were performed using Sidak's post-test, where # indicates significantly different ($p<0.05$) from equivalent estimate in HEK293A-mGlu$_5$-low cells.

3.4. Discussion

Inhibition of $mGlu_5$ offers therapeutic potential for CNS disorders, ranging from anxiety and depression to autism and addiction (Sengmany and Gregory, 2016). However, adverse effect liability in the form of cognitive impairments (Simonyi et al., 2010), abuse and psychotomimetic potential (Abou Farha et al., 2014; Swedberg et al., 2014; Swedberg and Raboisson, 2014), highlights the need to better understand the underlying pharmacology of $mGlu_5$ inhibitors. Our quantitative pharmacological profiling of eight ligands, previously classified as $mGlu_5$ NAMs of glutamate in iCa^{2+} mobilization assays, revealed differences in apparent affinities between binding and functional assays (iCa^{2+} mobilization and IP_1 accumulation) for acetylenic full NAMs (MPEP, MTEP and dipraglurant) in recombinant and/or neuronal systems, whereas, non-acetylenic NAMs or the prototypical acetylenic "partial NAM" M-5MPEP were similar across all measures. Biased NAM pharmacology was evident at the level of cooperativity with DHPG; most strikingly in cortical neurons where VU0366248 behaved as a neutral allosteric ligand in IP_1 accumulation assays but was a NAM of DHPG-mediated iCa^{2+} mobilization. In contrast, all other compounds were NAMs in both paradigms. Importantly, M-5MPEP had similar levels of cooperativity with DHPG and glutamate, independent of cell type or assay paradigm, demonstrating an absence of bias at the level of cooperativity as well as affinity. Collectively, our study highlights the importance of rigorous assessment of allosteric ligands to quantify affinity and cooperativity, thereby enriching our appreciation of how $mGlu_5$ NAM pharmacology contributes to efficacy.

Several orthosteric agonists of mGlu receptors are well-established biased agonists (Emery et al., 2012; Hathaway et al., 2015), while positive allosteric modulators

within Class C GPCRs also engender bias (Cook et al., 2015; Sengmany et al., 2017; Zhang et al., 2005). However, there has been less focus on biased modulation, and in particular bias engendered by negative allosteric modulators. In the family C calcium sensing receptor, the NAM NPS2143 demonstrated biased modulation toward iCa^{2+} mobilization relative to pERK1/2 (Davey et al., 2012; Leach et al., 2016; Leach et al., 2013). However, for many of the $mGlu_5$ NAMs studied herein, a single *in vitro* functional assay (iCa^{2+} mobilization) has been used to classify allosteric pharmacology. There are some exceptions, namely MPEP, M-5MPEP, VU0366248 and VU0366058, for which two different functional assays (iCa^{2+} mobilization and ERK1/2 phosphorylation) using glutamate as the orthosteric agonist in recombinant cell lines have been assessed (Gregory et al., 2012). No significant bias in functional affinity or cooperativity estimates between iCa^{2+} mobilization and ERK1/2 phosphorylation were observed (Gregory et al., 2012). In contrast, herein multiple NAMs showed differential magnitudes of cooperativity with DHPG in native cells depending on the measure (iCa^{2+} mobilization versus IP_1 accumulation) or the presence of CPCCOEt in IP_1 accumulation assays. Importantly, these differences were not observed for all NAMs, with M-5MPEP retaining similar cooperativity with DHPG across all measures and cell types. Thus, our results highlight the need to assess multiple receptor endpoints to probe the full scope of allosteric ligand pharmacology.

Another feature of our study that is distinct from previous work was the presence of two-site inhibition binding. MPEP, MTEP and fenobam displayed two-site inhibition binding, contrary to the one-site binding previously reported (Gregory et al., 2012; Lea and Faden, 2006; Porter et al., 2005a). Furthermore, dipraglurant, VU0366058,

VU0409106 and VU0366248 did not fully displace [^{3}H]methoxy-PEPy binding. There are multiple possible underlying explanations for these observations. An important difference in the current study was the use of intact and adherent cells as opposed to membrane preparations, which have typically been employed (Cosford et al., 2003a; Gregory et al., 2012; Lindemann et al., 2011; Porter et al., 2005a; Raboisson et al., 2012; Rodriguez et al., 2010a; Rodriguez et al., 2005b). Incomplete radioligand displacement is generally considered evidence for non-competitive binding interactions (Flanagan, 2016; Pagano et al., 2000). However, in light of the two-site binding observed for select ligands, incomplete displacement may be due to very low (pK_i <4.5) dipraglurant, VU0366058, VU0409106 and VU0366248 affinity for this apparent second site. The complex binding isotherms could also be attributable to allosteric ligands stabilizing distinct receptor conformations that are only evident within an intact cell preparation; high and low affinity states possibly aligning with discrete signaling profiles. Within intact cells, dynamic cellular processes such as G protein coupling, interactions with other effectors or scaffolding partners, receptor dimerization and subcellular localization could contribute to an apparent "second site". Indeed, each of the eight NAMs tested were also inverse agonists for IP_1 accumulation in recombinant cells and could conceivably be influenced by receptor-G protein coupling. Moreover, $mGlu_5$ is well-known to be expressed at the plasma membrane as well as on intracellular membranes (Jong et al., 2014). Differential membrane permeability or access to subcellular compartments may contribute to the complex binding isotherms observed in intact cells. In keeping with this idea, all ligands that fully displaced [^{3}H]methoxy-PEPy belong to a similar chemotype and have low molecular weights <250, thus have the potential to bind intracellular $mGlu_5$ receptors. Irrespective of mechanism, it is clear that $mGlu_5$

NAMs, both within and across chemotypes, can stabilize different receptor conformational states.

Assessment of ligand pharmacology within physiologically relevant systems aims to most closely predict a drug response within the body. However, complex native cell backgrounds and the need to use surrogate ligands raises additional issues: 1) the notion of probe dependence whereby ligand activity may be dependent on the chosen orthosteric ligand; and 2) the phenomenon of system bias, where different cell backgrounds result in different ligand pharmacology. While probe dependence between glutamate and DHPG was evident in cooperativity of select $mGlu_5$ PAMs (Sengmany et al., 2017), there was minimal evidence for this phenomenon with $mGlu_5$ NAMs. Although under certain conditions both MPEP and MTEP showed higher apparent affinity when DHPG was used as the agonist over glutamate. DHPG is a membrane impermeable agonist, and unlike glutamate is not actively transported into cells (Jong et al., 2005); therefore $mGlu_5$ modulator probe dependence may arise from differential access of ligands to subcellular compartments, which may also be linked to two-site binding curves observed herein. Further, differences in accessory proteins available in mouse embryonic cortical neurons and HEK293 cells may have also influenced the coupling mechanisms and hence system bias observed. The expression pattern of $mGlu_5$ may be another underlying factor in potential observed system bias. $mGlu_5$ expression is higher within the developing rodent brain relative to adult, while the $mGlu_{5a}$ splice variant is most abundant in young rodent brains, with $mGlu_{5b}$ predominating in adult brains (Romano et al., 1996). Interestingly, in young rodents, $mGlu_1$ expression levels remain relatively low compared to $mGlu_5$ (Casabona

et al., 1997) – yet another complicating facet in the use of embryonic cortical neurons to study drugs targeting an adult brain.

This context-dependent pharmacology, or system bias, has also previously been described for $mGlu_7$ receptors, where NAMs differentially inhibit coupling in differing cell backgrounds (Niswender et al., 2010). In our study, the influence of the system was evident for select $mGlu_5$ NAMs, with differential functional affinities in comparable conditions observed between HEK293A cells and neurons. However, despite these caveats, distinct NAM fingerprints were evident which may be linked to the known adverse effect and/or preclinical efficacy of these agents. Acetylenic full NAMs exhibit differential affinities in both cell types, whereas different NAM chemotypes and the partial acetylenic NAM do not. MPEP and MTEP have undergone extensive preclinical testing, and have anxiolytic and antidepressant efficacy along with adverse effect liability (cognitive and psychotomimetic) (Balschun and Wetzel, 2002; Belozertseva et al., 2007; Campbell et al., 2004; Chojnacka-Wojcik et al., 2001; Kumar et al., 2013; Lea and Faden, 2006; Li et al., 2006; Palucha-Poniewiera et al., 2014; Schulz et al., 2001; Spooren et al., 2000; Swedberg et al., 2014; Tatarczynska et al., 2001). In comparison the unbiased partial NAM, M-5MPEP, is both efficacious and devoid of adverse psychotomimetic effects (Gould et al., 2016). For the structurally diverse NAMs (VU0409106, VU0366058, VU0366248) fewer preclinical studies have been performed, therefore it remains to be established if the NAM pK_B fingerprints established here can be used to inform future discovery efforts for $mGlu_5$, which may seek to identify biased NAMs that more selectively target therapeutic signaling over adverse effects.

Another contributing factor to system bias in the more complex neuronal system is the co-expression of $mGlu_1$, which is known to influence $mGlu_5$ activity via heteromerization and/or signaling cross-talk (Bonsi et al., 2005; Lujan et al., 1996; Neyman and Manahan-Vaughan, 2008). In order to minimize the $mGlu_1$ contribution we initially included CPCCOEt in all experiments as described previously (Jong et al., 2009; Sengmany et al., 2017). However, we recently showed that CPCCOEt has similar affinity for $mGlu_1$ and $mGlu_5$, and displays a non-competitive negative interaction with MPEP (Hellyer et al., 2018). Interestingly, in the absence of CPCCOEt, dipraglurant had decreased functional affinity in cortical neurons when measured in iCa^{2+} mobilization but not IP_1 accumulation, whereas VU0409106 and MTEP had reduced cooperativity with DHPG in one or both assays. Therefore, these ligands appear to prefer interacting with $mGlu_5$ when $mGlu_1$ is also inhibited, which may be mediated by co-localization or heteromerization of the two receptors (Pandya et al., 2016; Sevastyanova and Kammermeier, 2014b). These effects may also be mediated via positive allosteric interactions at two different allosteric sites within a single receptor. Indeed, Class C GPCRs are known to have multiple allosteric sites (Jensen and Brauner-Osborne, 2007; Noetzel et al., 2013; Pin and Prézeau, 2007; Rodriguez et al., 2010b). Collectively, the differences observed between recombinant and native cells, demonstrate that while assessment in recombinant cells may be convenient and have greater reproducibility, it is important to recognise the potential for disconnect between differing cell backgrounds.

Another key consideration is the influence of the kinetic context on biased pharmacology (Klein Herenbrink et al., 2016; Lane et al., 2017), where ligand-receptor and receptor-effector interactions require time to achieve equilibrium.

Previously, we showed that the majority of $mGlu_5$ PAMs had strong biased agonism toward IP_1 accumulation over iCa^{2+} mobilization, which may have been associated with differences in ligand-receptor equilibrium between the two measures (Sengmany, et al., 2017). Intriguingly, we found experiments performed at equilibrium (radioligand binding and IP_1 accumulation) for multiple, but not all, $mGlu_5$ NAMs yielded lower affinity estimates relative to the transient non-equilibrium iCa^{2+} mobilization assay. Additionally, this phenomenon was not evident with prolonged ligand pre-incubation prior to iCa^{2+} mobilization assays. Higher affinity in shorter timed assay was unexpected and somewhat counterintuitive. However, if we appreciate that the impact of kinetics involves multiple arms – ligand binding, effector coupling and downstream cell signaling processes (Lane et al., 2017), the paradoxical results observed for $mGlu_5$ NAM affinity may well be explained. While iCa^{2+} mobilization and IP_1 accumulation are endpoints traditionally linked through the G_q activation pathway, it is well established that $mGlu_5$ couples to ion channels (Kammermeier et al., 2000; Latif-Hernandez et al., 2016; Lu et al., 1999; McCool et al., 1998; Tu et al., 1999), resulting in a rapid influx of extracellular Ca^{2+}. Therefore, the iCa^{2+} mobilization measured is a composite of both intracellular and extracellular calcium influx (Sengmany et al., 2017). Due to the rapid opening of ion channels relative to GPCR signaling cascades, it is possible that initial responses may be via extracellular calcium influx through ion channels. Therefore, select $mGlu_5$ NAMs (MTEP, dipraglurant, MPEP) may have higher affinity for $mGlu_5$ states that couple to plasma membrane channels, as opposed to the canonical $G_{q/11}$-PLC-IP_3-pathway. Thus, this study highlights the importance of recognizing different influencers of allosteric pharmacology (orthosteric agonist, receptor, system) and how

these can be dissected to reveal new insights into negative allosteric modulator activity.

Overall, this study provides a rigorous characterization of $mGlu_5$ NAMs, highlighting the stabilization of unique receptor conformations in both recombinant and native cells. In particular, ligand-dependent disparities in cooperativity, between iCa^{2+} mobilization and IP_1 accumulation, highlight differential modulation of DHPG responses by select $mGlu_5$ NAMs. Differing kinetic and cellular contexts also underscore the pharmacological fingerprints observed, underlining the necessity to assess multiple signaling pathways, within multiple cellular backgrounds. Acetylenic full $mGlu_5$ NAMs showed the most divergent pharmacological fingerprints, which may be linked to the capacity of these ligands to engender adverse effects in the form of psychotomimetic and cognitive impairments, whereas a partial and unbiased NAM from the same scaffold does not. Discovery efforts targeting GPCRs for CNS disorders continue to suffer high attrition rates, attributable to the difficulties in translating agents with promising in vitro pharmacology to efficacy in preclinical models and extending this to the clinic. Our findings highlight the inherent complexity in allosteric modulator pharmacology and the potential contribution of unappreciated bias at the level of affinity and/or cooperativity to translational failures.

Supplementary Information

Title: Kinetic and system bias as drivers of biased metabotropic glutamate receptor 5 allosteric modulation

Kathy Sengmany[a], Sabine Albold[a], Shane D. Hellyer[a], Taide Wang[a], P. Jeffrey Conn[b], Lauren T. May[a], Arthur Christopoulos[a], Katie Leach[a], and Karen J. Gregory[a*]

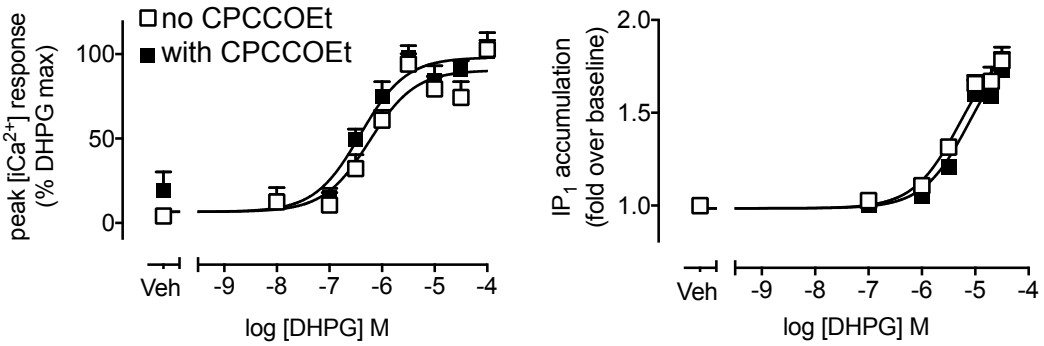

Supplementary Figure 3.1. DHPG concentration-response curves for iCa^{2+} mobilization or IP$_1$ accumulation in the absence or presence of CPCCOet (30 μM) in primary cortical neurons. Data are mean + s.e.m from 3-7 independent experiments performed in parallel. Error bars not shown lie within the dimensions of the symbols.

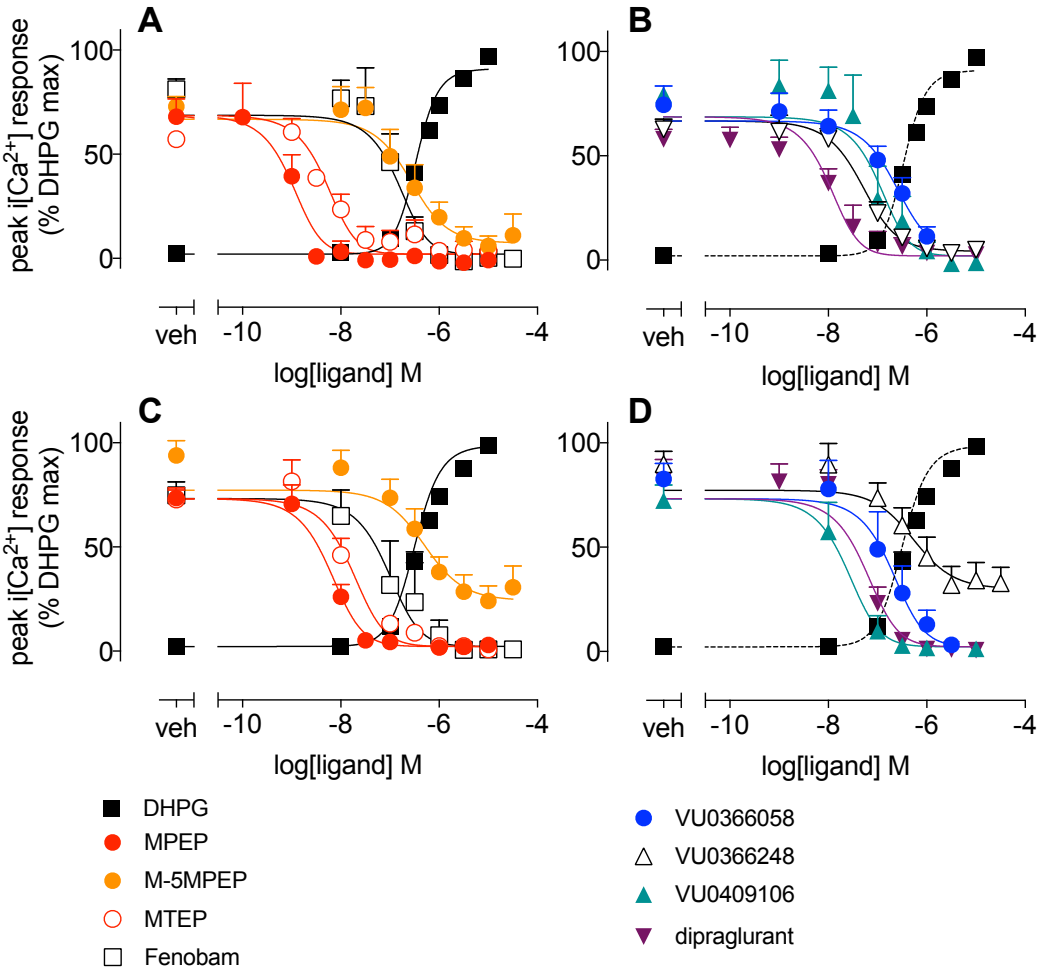

Supplementary Figure 3.2. Negative allosteric modulation of DHPG-mediated iCa^{2+} mobilization in HEK293A-mGlu$_5$-low cells. Concentration response curves for inhibition of DHPG EC$_{80}$-mediated iCa^{2+} mobilization by indicated allosteric ligands were performed in parallel with a concentration-response curve to DHPG (**A** - **D**). Mobilization of iCa^{2+} assays were performed with 1 min (**A** & **B**) or 30 min (**C** & **D**) pre-incubation of allosteric ligand followed by addition DHPG EC$_{80}$ (600nM). Data are expressed as mean + SEM of 3-8 experiments performed in duplicate. Error bars not shown lie within the dimensions of the symbols.

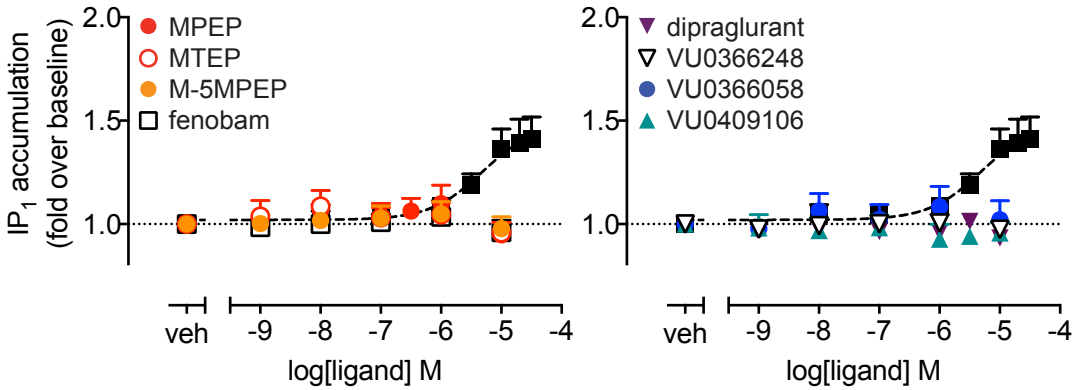

Supplementary Figure 3.3: No evidence for inverse agonism of mGlu$_5$ NAMs for IP$_1$ accumulation in primary cortical neurons. No change in IP$_1$ accumulation basal levels were observed following 60 min exposure to NAMs. Glutamic pyruvic transaminase (1U/mL) was included to eliminate ambient glutamate. DHPG control curve from parallel experiments is shown for reference (closed black squares). Data are mean + s.e.m from 3-4 independent experiments performed in parallel. Error bars not shown lie within the dimensions of the symbols.

Supplementary Table 3.1: Comparison of affinity estimates for modulation of DHPG-mediated iCa^{2+} mobilization following 1 min vs 30 min pre-incubation of $mGlu_5$ allosteric ligands in HEK293A-$mGlu_5$-low cells.

Data represent mean ± SEM of 3-8 independent experiments performed in duplicate.

	iCa^{2+} mobilization	
	pK_B [a] (1min)	pK_B [a] (30min)
MPEP	8.94 ±0.16[b,c]	8.24 ±0.11[d]
fenobam	6.99 ±0.21	7.11 ±0.44
VU0409106	7.15 ±0.28	7.82 ±0.14
VU0366248	7.33 ±0.18	6.82 ±0.09
VU0366058	6.71 ±0.18	7.36 ±0.38
M-5MPEP	7.01 ±0.35	6.98 ±0.03
dipraglurant	8.06 ±0.23[b]	7.43 ±0.14[d]
MTEP	8.31 ±0.09[b]	7.91 ±0.13[c]

[a] pK_B, negative logarithm of the equilibrium dissociation constant determined using an operational model of allosterism

[b] Denotes $p<0.05$, One-way ANOVA, Tukey's multiple comparisons test, compared to binding estimate

[c] Denotes $p<0.05$, One-way ANOVA, Tukey's multiple comparisons test, compared to pK_B estimate derived from glutamate iCa^{2+} mobilization assays (equivalent incubation paradigm)

[d] Denotes $p<0.05$, One-way ANOVA, Tukey's multiple comparisons test, compared to pK_B estimate derived from DHPG iCa^{2+} mobilization assays (1min paradigm)

Supplementary Table 3.2: Comparison of cooperativity estimates for modulation of DHPG-mediated iCa^{2+} mobilization following 1 min vs 30 min pre-incubation of $mGlu_5$ allosteric ligands in HEK293A-$mGlu_5$-low cells.
Data represent mean ± SEM of 3-8 independent experiments performed in duplicate.

	iCa^{2+} mobilization	
	log αβ[a] (1min)	log αβ[a] (30min)
MPEP	full NAM[b]	full NAM
fenobam	full NAM	full NAM
VU0409106	full NAM	full NAM
VU0366248	-0.96 ±0.10	-0.46 ±0.15
VU0366058	full NAM	full NAM
M-5MPEP	-0.98 ±0.36	-0.56 ±0.19
dipraglurant	full NAM	full NAM
MTEP	full NAM	full NAM

[a] log αβ, logarithm of the efficacy scaling factor determined using an operational model of allosterism
[b] "full NAM" denotes complete inhibition of DHPG response, such that αβ approaches zero.

Chapter 4

Probing the structural basis of $mGlu_5$ biased agonism and modulation

Abstract

The metabotropic glutamate receptor subtype 5 ($mGlu_5$) has been implicated in a wide range of neuronal disorders, and thus provides an attractive target for potential CNS therapeutics. We recently showed that select $mGlu_5$ PAMs displayed distinct bias relative to DHPG at IP_1 accumulation and pERK1/2 receptor endpoints in addition to iCa^{2+} mobilisation (Sengmany et al., 2017). Following this, we aimed to assess key residues influencing the biased profiles. Four $mGlu_5$ PAMs/PAM-agonists, VU0424465, DPFE, VU29 and VU0409551, were evaluated – with biased agonism, functional affinity and cooperativity with DHPG-mediated iCa^{2+} mobilisation determined. Seven mutations lining the $mGlu_5$ allosteric binding site were studied, based on previous significant changes in allosteric ligand affinity and/or cooperativity (Gregory et al., 2013b). None of the mutations affected DHPG-mediated iCa^{2+} mobilisation, IP_1 accumulation and pERK1/2 agonism, with the exception of Y658V. DPFE-mediated iCa^{2+} mobilisation was abolished in all studied mutants, while VU0424465 agonism was largely reduced across all studied pathways. VU29 agonism was mostly unaffected in IP_1 accumulation and pERK1/2 relative to wild type (WT), while VU0409551 agonism in pERK1/2 and iCa^{2+} mobilisation was abolished at four of the seven studied mutants. VU0424465 functional affinity was reduced, while DPFE was increased at three of the seven mutants, and VU29 had reduced cooperativity at the majority of mutants. Biased signalling profiles were lost at the majority of mutants, with the exception of A809V and A809G for VU0424465. Gain of iCa^{2+}-IP_1 bias was observed for DPFE at S808A, while T780A led to gain of VU29 agonism of iCa^{2+} mobilisation. Overall, our study highlights key residues involved in iCa^{2+} mobilisation, IP_1 accumulation and pERK1/2 $mGlu_5$ allosteric agonism and provides a more complete scope of $mGlu_5$ structure-function relationships.

4.1. Introduction

Mutagenesis, molecular modelling and structure-activity studies have offered insight into the interactions of $mGlu_5$ allosteric ligands within the "common", or MPEP, allosteric binding pocket (Bennett et al., 2015). Recent crystallisation of the NAM-bound $mGlu_5$ transmembrane region has also provided greater understanding of residues that influence allosteric ligand binding (Christopher et al., 2015; Dore et al., 2014). Distinct from the Venus Fly-Trap orthosteric site, the $mGlu_5$ common allosteric binding site lies between TMs 2, 3, 5, 6 and 7, and extends deeper into the TM domain relative to its related group I $mGlu_1$ receptor (Christopher et al., 2015; Dore et al., 2014). This $mGlu_5$ allosteric pocket comprises two large and separate cavities connected by a narrow channel, through which the common $mGlu_5$ allosteric ligand chemotype, the alkyne triple-bond, transverses (Christopher et al., 2015; Dore et al., 2014). Despite recent knowledge of the structure of $mGlu_5$, in conjunction with numerous mutagenesis studies, there remains a lack of understanding of residues involved in biased agonism, functional affinity and cooperativity – in particular at signalling pathways other than iCa^{2+} mobilisation.

Thus, following on from Chapter 2, that showed biased agonism in the actions of chemically and pharmacologically diverse $mGlu_5$ PAMs, we aimed to probe the structural determinants of $mGlu_5$ allosteric ligand bias. We conducted a robust evaluation of $mGlu_5$ biased ligands at the three previously studied receptor endpoints: iCa^{2+} mobilisation, IP_1 accumulation and ERK1/2 phosphorylation (pERK1/2) at $mGlu_5$ receptors containing single-point mutations within the allosteric binding pocket. As an extension of Gregory *et al*., 2013, mutations were selected that resulted in significant changes in either affinity and/or cooperativity of certain PAMs –

namely T780A, S808A, Y658V, W784A, P654F, A809V and A809G – to assess the ligands that showed distinct bias profiles in our previous study (Chapter 2) (Sengmany et al., 2017). Of note, pharmacological "switches" – i.e. PAM to NAM or vice versa, or PAM/NAM to NAL activity – were observed with alanine substitutions of S808 (TM7) and T780 (TM6), two key residues involved in hydrogen bonding with a water molecule within the base of the allosteric binding pocket (Gregory et al., 2013b). Valine substitution of Y658 (TM3) also resulted in the PAM, VU0405398, displaying negative cooperativity of glutamate-stimulated iCa^{2+} mobilisation, while the mutations P654F (TM3), W784A (TM6), A809V (TM7) and A809G (TM7) resulted in significant changes in affinity and/or cooperativity of select $mGlu_5$ PAMs (Gregory et al., 2013b). While these studies have probed the impact of these mutations on allosteric ligand affinity and cooperativity in modulation of glutamate-stimulated calcium responses, little has been done in assessing other receptor signalling endpoints, and evaluating the influence of these mutations on the biased signalling profiles of $mGlu_5$ allosteric ligands.

Accordingly, we hypothesise that these mutations will not only affect agonism for iCa^{2+} mobilisation, but also IP_1 accumulation and pERK1/2, thus affecting the ligand's biased signalling profile. We further hypothesise alterations of functional affinity and cooperativity for DHPG-mediated iCa^{2+} mobilisation at mutant receptors relative to WT responses. Ultimately, these mutations offer potential insight into activation of diverse receptor endpoints, rather than simply the canonical calcium mobilisation, and will add to the plethora of data available on the structure-function relationship of $mGlu_5$ allosteric ligands and its binding site.

4.2. Methods

4. 2.1. Materials

Dulbecco's modified Eagle's medium (DMEM), Neurobasal medium, Fluo-4-AM and antibiotics were purchased from Invitrogen (Carlsbad, CA). Foetal bovine serum (FBS) was purchased from Thermo Electron Corporation (Melbourne, Australia). IP-ONE HTRF® assay kit was purchased from Cisbio, Genesearch (Arundel, Australia) and AlphaScreen detection beads were purchased from PerkinElmer Life and Analytical Sciences. Select $mGlu_5$ ligands *(R)*-5-((3-fluorophenyl)ethynyl)-*N*-(3-hydroxy-3-methylbutan-2-yl)picolinamide (VU0424465), 1-(4-(2,4-difluorophenyl)piperazin-1-yl)-2-((4-fluorobenzyl)oxy)ethanone (DPFE), (4-fluorophenyl)(2-(phenoxymethyl)-6,7-dihydrooxazolo[5,4-*c*]pyridin-5(4*H*)-yl)methanone (VU0409551) were synthesised at Vanderbilt Centre for Neuroscience Drug Discovery as described previously (Gregory et al., 2013a; Gregory et al., 2012; Rodriguez et al., 2010b; Rook et al., 2013). *N*-(1,3-Diphenyl-1*H*-pyrazolo-5-yl)-4-nitrobenzamide (VU29) was purchased from Tocris Bioscience (Melbourne, Australia). HEK293A cells stably transfected with mutant rat $mGlu_5$ constructs (A809V, A809G, F787A, P654F, S808A, T780A, W784A, Y658V) were kindly gifted by Vanderbilt Centre for Neuroscience Drug Discovery. Unless otherwise stated, all other reagents were purchased from Sigma-Aldrich (St. Louis, MO) and were of analytical grade.

4.2.2. Cell culture

HEK293A cells stably transfected with low levels of wild-type rat $mGlu_5$ (HEK293A-$mGlu_5$-low) or mutants thereof were maintained at 37°C and 5% CO_2 in DMEM supplemented with 5% FBS, 16 mM HEPES and 500 μg/mL G418. One day prior to experimentation, cells were plated onto poly-D-lysine coated, clear-bottom 96 well

plates in glutamine-free DMEM supplemented with 5% dialysed FBS, 16 mM HEPES and 500 μg/mL G418 at 40,000 cells/well.

4.2.3. Intracellular calcium mobilisation

On the day of experimentation, cells were loaded with calcium-sensitive Fluo-4-AM dye (1μM, Invitrogen) to assay receptor-mediated iCa^{2+} mobilisation using Flexstation I or III (Molecular Devices, Sunnyvale, CA). Ligands or vehicle (0.3% DMSO) were diluted in calcium assay buffer comprising Hank's Balanced Salt Solution (HBSS; 1.2 mM $CaCl_2$, KCl 5.33 mM, KH_2PO_4 0.44 mM, $NaHCO_3$ 4.17 mM, NaCl 137.93 mM, Na_2HPO_4 0.34 mM, D-glucose 5.56 mM) with 2.5 mM probenecid and 16 mM HEPES, pH 7.4, and either co-added (VU0424465) or added 1 min prior (DPFE, VU29, VU0409551) to DHPG. A 5-point smoothing function was applied to the raw fluorescence traces and peak fluorescence values were expressed as either fold over basal (DHPG) or normalised to the maximal DHPG response.

4.2.4. Inositol monophosphate (IP_1) accumulation assay

HEK293A-$mGlu_5$ WT and mutant cells were washed and incubated for 1 h with stimulation buffer (HBSS as above, with 16 mM HEPES, 30 mM $LiCl_2$, 1.2 mM $CaCl_2$, pH 7.4) before ligand addition. Cells were incubated for a further 1 h at 37°C and 5% CO_2 before addition of Lysis Buffer (HTRF® IP-one assay kit). IP_1 levels were determined using the HTRF® IP-one assay kit as per manufacturer's instructions and fluorescence measured using the Envision. Data were expressed as fold over basal response.

4.2.5. ERK1/2 phosphorylation

Receptor-mediated ERK1/2 phosphorylation was determined using an AlphaScreen-based ERK SureFire kit. Cells were serum-starved, with glutamine-free DMEM supplemented with 16mM HEPES, 4 – 6 h prior to experimentation. Time course experiments were performed to determine the peak response by each ligand (10 μM). 10% FBS was added at 7 min as a positive control. Compounds resulted in peak pERK1/2 responses between 5-7 min across all mutants, largely in line with WT responses (Sengmany et al., 2017) (Fig 4.1). Agonist concentration response curves were obtained by adding increasing concentrations of ligand and terminating the assay at the time in which maximal pERK1/2 was determined via the time course assays. Following addition of lysis buffer and 5 min shaking, 4 μL of lysate was transferred to a white 384 well ProxiPlate (PerkinElmer). Under low-light conditions, 7 μL AlphaScreen detection mixture (1:7 (v/v) activation buffer: reaction buffer; with 1:240 (v/v) acceptor and donor beads) was added to each well and incubated 1 h at 37°C. AlphaScreen signal was measured using an Envision with standard AlphaScreen settings. Data were expressed as fold over basal level of pERK1/2.

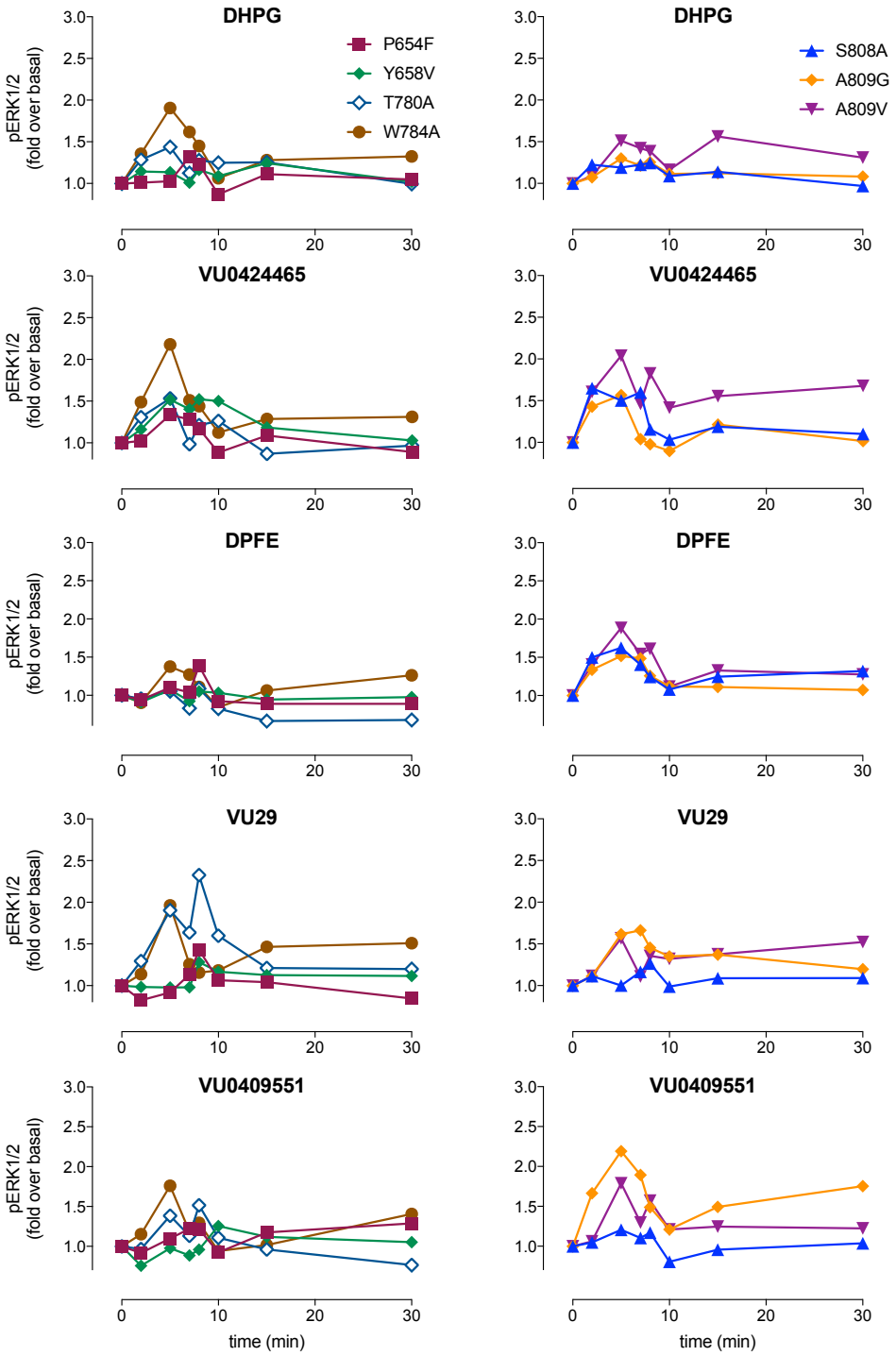

Fig 4.1. ERK1/2 phosphorylation time courses of DHPG, VU0424465, DPFE VU29 and VU0409551 in HEK293A-mGlu$_5$ WT or mutant receptors. 10 μM of allosteric ligand was applied to cells at various time points over a 30 min period, in the presence of 1 U/mL GPT. Data are expressed as fold over basal, normalised to vehicle (0.3% DMSO) responses. Time at which peak responses were achieved was then chosen as stimulation time for consequent concentration response curves. Data are expressed as mean of 2-4 experiments performed in duplicate.

4.2.6. Data analysis

Agonist-concentration response curves were fitted to a variable four-parameter logistic equation:

$$y = \frac{bottom+(top-bottom)}{(1+10^{(logEC_{50}-Log[A])n}} \quad (1)$$

where bottom and top are lower and upper plateau levels of the concentration response curve respectively, *n* is the Hill coefficient, [A] is the molar concentration of agonist, and EC_{50} is the agonist concentration required to produce a half maximal response between top and bottom values (potency).

Biased agonism was quantified using an operational model of agonism (Kenakin et al., 2012):

$$Y = basal + \frac{(Em - basal)\left(\frac{\tau}{K_A}\right)^n [A]^n}{[A]^n(\frac{\tau}{K_A})^n+\left(1+\frac{[A]}{K_A}\right)^n} \quad (2)$$

where E_m is the maximal response of the system, *n* is the transducer slope, K_A is the equilibrium dissociation constant of the agonist and τ is the coupling efficiency of the agonist as defined by R_T/K_E, where R_T is the receptor number and K_E if the coupling efficiency of the system. From this equation the transduction coefficient log(τ/K_A) a composite of both affinity and efficacy can be derived, which describes agonism for a given pathway.

The transduction coefficient was then normalised to the reference ligand DHPG to give Δlog(τ/K_A). Comparisons between studied pathways (e.g. *j1* vs *j2*) was completed through subtraction of Δlog(τ/K_A) values between pathways to derive ΔΔlog(τ/K_A), or LogBias:

$$LogBias = \Delta\log(\tau/K_A)_{j1} - \Delta\log(\tau/K_A)_{j2} \quad (3)$$

Allosteric modulation of DHPG-mediated responses were fitted to the operational model of allosterism (Leach et al., 2007):

$$Effect = \frac{E_m(\tau_A[A](K_B+\alpha\beta[B])+\tau_B[B]K_A)^n}{([A]K_B+K_AK_B+K_A[B]+\alpha[A][B])^n+(\tau_A[A](K_B+\alpha\beta[B])+\tau_B[B]K_A)^n} \quad (4)$$

where [A] and [B] are the molar concentrations of orthosteric agonist DHPG and allosteric modulator respectively. α represents affinity cooperativity and β is a scaling factor that denotes the magnitude of effect an allosteric modulator has on orthosteric agonist efficacy. Affinity cooperativity (α) was constrained to 1 as previously described (Gregory et al., 2012). K_A and K_B are the equilibrium dissociation constants of the orthosteric agonist and allosteric modulator respectively. K_A for DHPG was constrained to -5.409 as per previous binding studies (Gregory et al., 2012; Wisniewski and Car, 2002). τ_A and τ_B are the respective ligand's intrinsic efficacy. E_m and n represent the maximal system response and the transducer slope respectively.

Transduction coefficients, potency, efficacy, affinity and cooperativity parameters were derived and represented as logarithmic mean ± SEM. Analysis of bias parameters was performed using one-way analysis of variance (ANOVA) with Dunnett's post-test to compare receptor responses in mutants to wild-type mGlu$_5$, and one-way ANOVA with Tukey's post-test to compare $\Delta\log(\tau/K_A)$ between pathways.

4.3. Results

Seven single amino acid mutations within the $mGlu_5$ allosteric binding site were selected based on significant changes to affinity and cooperativity of select $mGlu_5$ allosteric ligands (Gregory et al., 2013b) (Fig 4.2). Y658V, S808A and T780A resulted in cooperativity switches, while select mutations also significantly affected ligand affinities in glutamate-stimulated iCa^{2+} mobilisation. The mutants Y658V, T780A, S808A, W784A, P654F, A809G and A809V either abolished or significantly reduced functional affinity estimates of several nicotinamide and picolinamide $mGlu_5$ PAM chemotypes (Gregory et al., 2013b). Wild type (WT) responses of the studied ligands were derived from experiments performed as part of Sengmany *et al*. (2017), in Chapter 2.

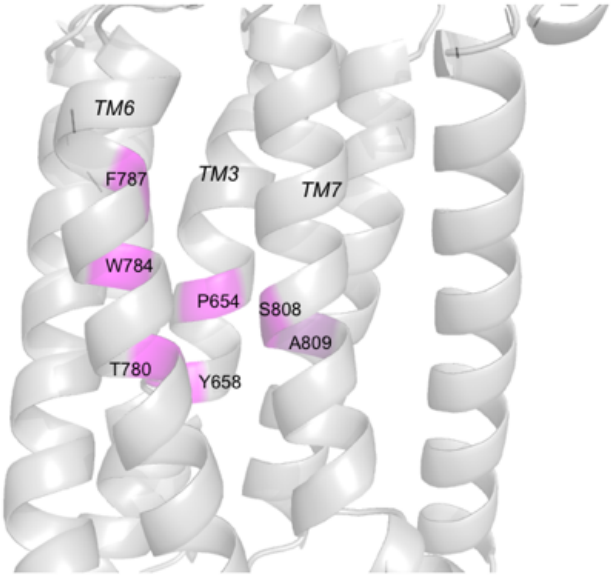

Fig 4.2. Location of mutations studied within rat $mGlu_5$. Mutations within this study line the allosteric binding pocket across TMs 3, 6 and 7 (magenta). In particular, P654 and Y658 lie within TM3, T780, W784, F787 within TM6 and S808 and A809 within TM7.

4.3.1. Effects of mutations of DHPG potency (pEC_{50}) and efficacy (E_{max}) in iCa^{2+} mobilisation, IP_1 accumulation and ERK1/2 phosphorylation

First, we wanted to determine whether these mutations affected global activation of the receptor. To do this, we assessed DHPG agonism in iCa^{2+} mobilisation in wild-type and mutant $mGlu_5$ receptors. As DHPG binds to the orthosteric binding site within the Venus Fly Trap domain, we hypothesised that there would be limited impact of mutations (situated within the 7TM) on DHPG affinity, and any observed changes in ligand activity would likely be attributed to the mutations affecting receptor conformations that are sampled by the assay. We also extended our study to include IP_1 accumulation and ERK1/2 phosphorylation, to provide a broader insight into the effect of the studied mutations on receptor activity.

In iCa^{2+} mobilisation assays, all mutations resulted in reduced DHPG potency, however, only A809V resulted in a significant 3-fold change relative to WT (Fig 4.3A-B). Comparisons of maximal DHPG responses (E_{max}), however, showed significant reductions with all mutations. In particular, the mutations A809V and T780A resulted in approximately a 50% decrease in DHPG maximal response relative to WT, while A809G produced the least change, with DHPG reaching 80% E_{max} compared to WT (table 4.1).

For IP_1 accumulation, there were no significant differences when comparing DHPG potencies, however, Y658V significantly decreased DHPG maximal response relative to WT, with E_{max} at approximately 70% of WT responses (table 4.1, Fig 4.3C-D). DHPG-mediated pERK1/2 was observed with all mutants, although with reduced

maximal responses relative to WT; except Y658V, which abolished DHPG agonism (Figure 4.3E-F).

However, while there were differences in absolute pEC_{50} and E_{max} values of DHPG at select mutations, these parameters offer a "qualitative" measure of ligand agonism, highly dependent on the biological system used, receptor density, and stimulus-response coupling for the studied assay (Kenakin, 2004; Kenakin et al., 2012; Stephenson, 1956). A more robust analytical method involves integration of ligand affinity and intrinsic efficacy, while normalising for receptor density and "intensity" of the coupling reaction (Kenakin, 2004; Kenakin et al., 2012). This is achieved through application of Black-Leff operational model of agonism (Black and Leff, 1983), in which the equilibrium dissociation constant (K_A) and intrinsic efficacy at a specific pathway (τ) is derived. The ratio of these two parameters is known as the transduction coefficient ($\log(\tau/K_A)$), and describes the ligand's overall activity at the studied pathway (Kenakin et al., 2012). Thus, we applied this model to assess DHPG agonism at the three studied receptor endpoints for mGlu$_5$ mutant receptors.

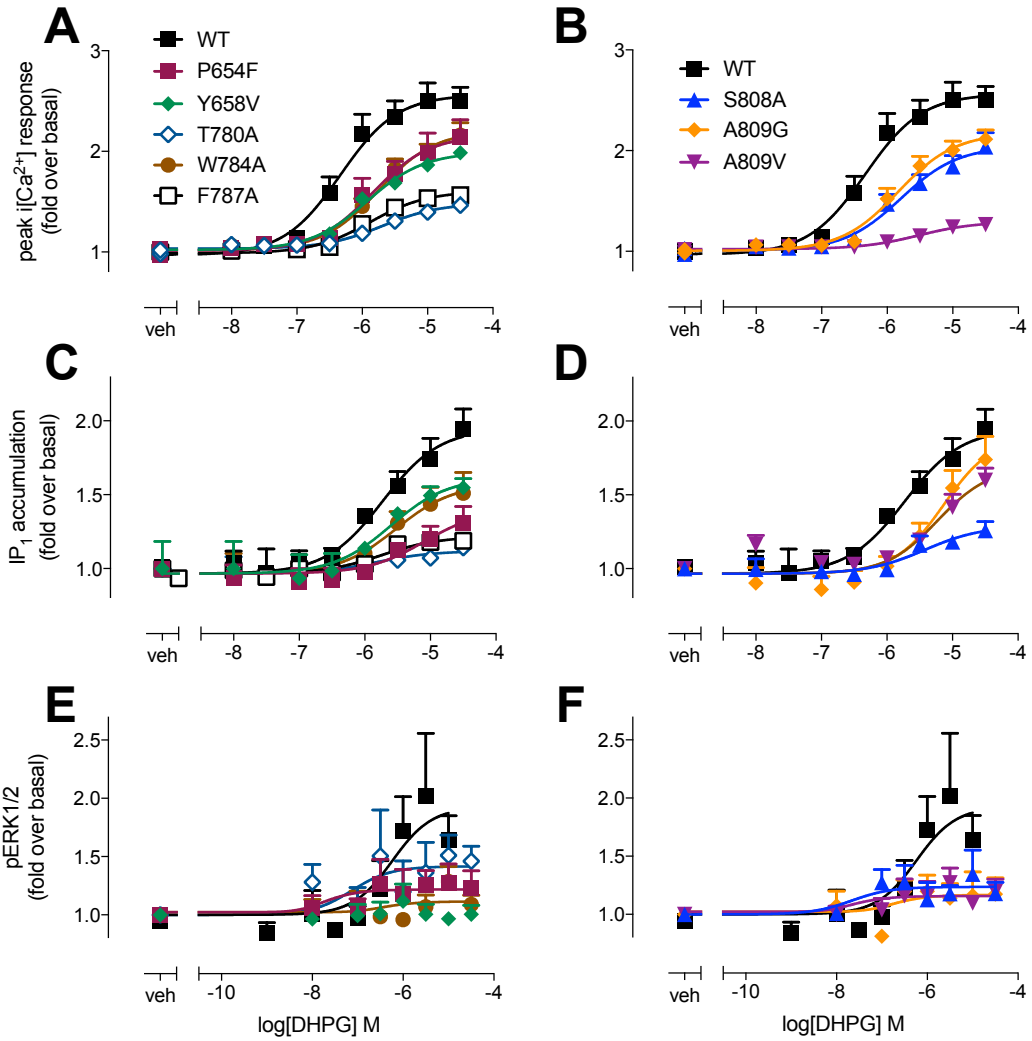

Fig 4.3. Concentration-response curves for DHPG for iCa^{2+} mobilisation (A-B), IP$_1$ accumulation (C-D), and ERK1/2 phosphorylation (E-F) in WT or mutant mGlu$_5$ HEK293A cells. Responses are represented as fold over basal response. IP$_1$ accumulation and ERK1/2 phosphorylation experiments were performed in the presence of 1 U/mL GPT to minimise contribution of ambient glutamate. Data are expressed as mean ± SEM of 3-9 experiments performed in duplicate, error bars not shown lie within the dimensions of the symbols.

4.3.2. Mutations within the allosteric binding site did not affect DHPG transduction coefficients in iCa^{2+} mobilisation, IP$_1$ accumulation and ERK1/2 phosphorylation.

While differences were observed with DHPG potency and E_{max} values in select mGlu$_5$ mutations, there were no significant differences in transduction ratios across the studied mutants at iCa^{2+} mobilisation, IP$_1$ accumulation and pERK1/2 receptor endpoints relative to WT responses (table 4.1, Fig 4.4). Y658V was the exception – with abolishment of DHPG-mediated pERK1/2 agonism. However, because transduction ratios are a composite of K_A and τ values, we next aimed to derive these parameters individually.

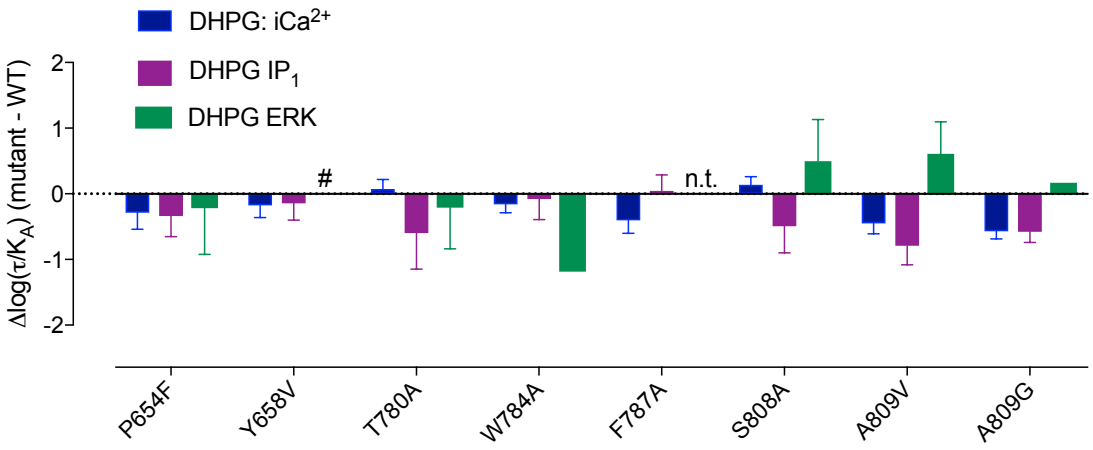

Fig 4.4. The effect of various mutations in the allosteric binding pocket of the mGlu$_5$ receptor on the transduction ratio (log(τ/K$_A$)) of DHPG obtained in iCa^{2+} mobilisation, IP$_1$ accumulation and pERK1/2 assays. The data are normalised to the wild-type receptor and values below zero indicate a decrease in transduction ratio at the mutant receptor, whereas a value above zero indicates an increase. Note, there were no significant differences between transduction ratios relative to WT (one-way ANOVA, Dunnett's post-test). N.t. not tested, # no observed agonism.

Table 4.1. Potency (pEC_{50}), maximal response (E_{max}) and transduction coefficient ($\log(\tau/K_A)$) estimates of DHPG for iCa^{2+} mobilisation, IP_1 accumulation and pERK1/2 in HEK293A-$mGlu_5$-low and mutant cells. Data are mean ± SEM of 3-9 independent experiments performed in duplicate.

	iCa^{2+} mobilisation			**IP_1 accumulation**			**pERK1/2**		
	pEC_{50}	E_{max} (fold over basal)	$\log(\tau/K_A)$	pEC_{50}	E_{max} (fold over basal)	$\log(\tau/K_A)$	pEC_{50}	E_{max} (fold over basal)	$\log(\tau/K_A)$
WT	6.34±0.12	2.6±0.1	6.31±0.11	5.73±0.13	1.9±0.2	5.80±0.14	6.19±0.27	1.9±0.2	6.37±0.22
P654F	5.98±0.14	1.9±0.1 [a]	6.02±0.23	5.26±0.39	1.4±0.1	5.46±0.28	6.06±0.45 [b]	1.4±0.1 [b]	6.57±0.66
Y658V	6.08±0.18	1.9±0.02 [a]	6.14±0.15	5.38±0.20	1.3±0.03 [a]	5.65±0.21	n.r.	n.r.	n.r.
T780A	5.97±0.18	1.4±0.1 [a]	6.38±0.10	5.69±0.64	1.8±0.6	5.20±0.53	5.94±0.67	1.4±0.1 [a]	5.93±0.51
W784A	6.03±0.12	2.0±0.1 [a]	6.15±0.06	5.38±0.35	1.7±0.2	5.72±0.28	5.52±0.82 [b]	1.2±0.1 [a,b]	5.07±0.28
F787A	5.88±0.09	1.6±0.03 [a]	5.74±0.05	5.70±0.21	1.2±0.03	5.70±0.72	n.t.	n.t.	n.t.
S808A	6.05±0.16	1.9±0.1 [a]	6.45±0.06	5.36±0.24	1.4±0.04	5.31±0.38	5.88±0.72 [b]	1.2±0.1 [a,b]	6.86±0.44
A809G	6.02±0.08	2.0±0.1 [a]	5.91±0.17	5.11±0.09	2.0±0.2	5.22±0.08	6.37±0.66 [b]	1.3±0.1 [a,b]	6.37±0.86
A809V	5.80±0.12 [a]	1.3±0.1 [a]	5.86±0.13	5.08±0.25	1.8±0.1	5.01±0.25	6.89±0.64	1.2±0.1 [a]	8.13±0.78

n.r. no response

[a] significantly different from $mGlu_5$ WT response ($p<0.05$, one-way ANOVA, Dunnett's post-test)

[b] concentration response curve and/or operational model was globally fitted to 3 or more independent experiments

n.t. not tested due to time constraints

Note, wild type (WT) parameters were derived from experiments performed in Chapter 2 (Sengmany *et al.* (2017))

4.3.3. DHPG affinity and efficacy are unaltered following depletion of mutant $mGlu_5$ receptors.

The potency (EC_{50}) of a compound comprises both affinity and efficacy parameters. To delineate affinity and efficacy, a dose-response curve of a full agonist and a second-dose response curve, determined after depletion of receptor numbers, are globally fitted to an operational model of receptor depletion (GraphPad Prism 7.0). This operational model assumes the affinity of the compound for the receptor is unchanged by the alteration in receptor numbers. Thus, affinity can be estimated from functional concentration-response curves for a full agonist.

Using the clickable $mGlu_5$ photoprobe RVDU-3-185 to irreversibly bind $mGlu_5$ receptors and hence deplete the number of functional $mGlu_5$ receptors, DHPG affinity and efficacy were able to be determined at the studied mutants (Fig 4.5). RVDU-3-185 (1 μM) was used in WT receptors, as this concentration allowed sufficient depletion of receptor levels, while RVDU-3-185 (10 μM) was chosen for the mutant receptors to allow sufficient depletion. P654F, S808A and A809V, however, showed minimal inhibition by the irreversible NAM, thus limiting assessment of DHPG affinity/efficacy in a reduced receptor expression state. This is perhaps not surprising, as this clickable ligand binds within the common allosteric site in which these mutations lie, thus the mutations may have impacted ligand binding (Gregory et al., 2016). Nonetheless, no significant change in DHPG affinity (pK_A) and efficacy ($\Delta\log \tau$) was observed in Y658V, W784A, F787A and A809G relative to WT, and thus DHPG was used as a reference ligand for bias calculations, with the supposition that DHPG activity was unchanged in the studied mutations (table 4.2).

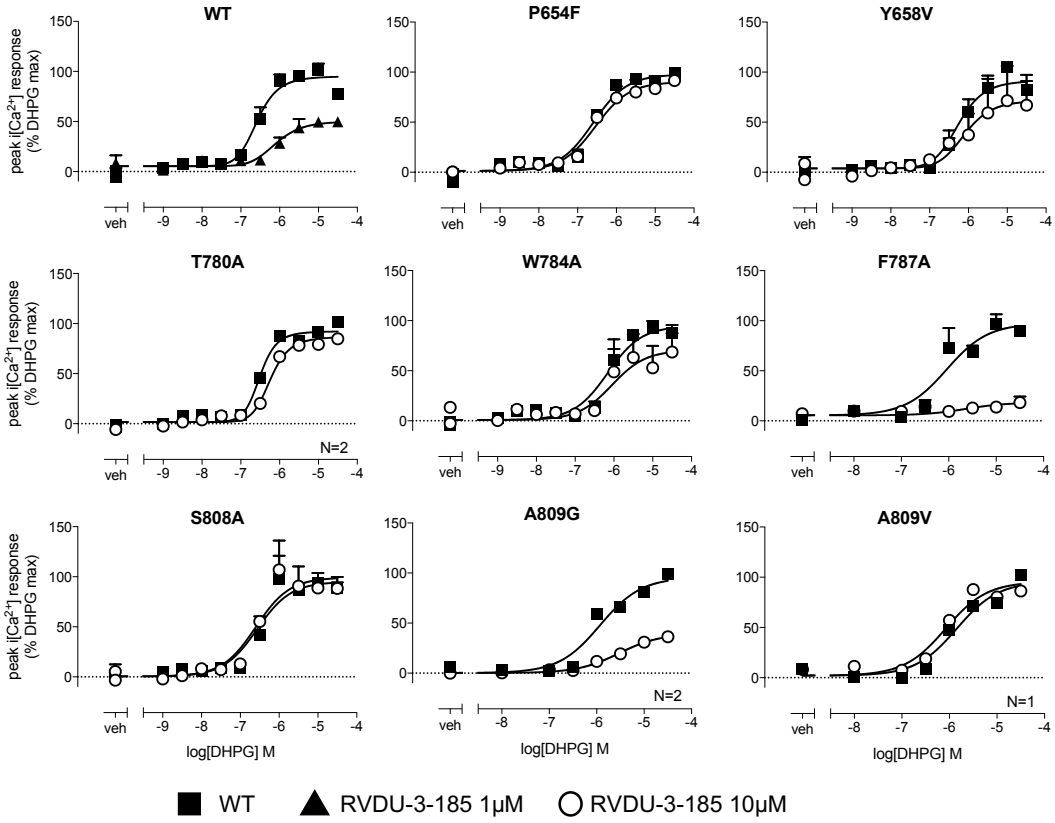

Figure 4.5. Effect of irreversible binding of the mGlu$_5$ NAM photoprobe RVDU-3-185 on DHPG-mediated iCa^{2+} mobilisation in HEK293A-mGlu$_5$-low (WT) or mutant mGlu$_5$ receptors. Cells were pre-treated with indicated mGlu$_5$ NAM (1 or 10 μM) then washed (five 45 min washes) before determining DHPG-mediated iCa^{2+} mobilisation. Data represent mean ± SEM of 3-4 experiments performed in duplicate unless otherwise specified. Vehicle responses were recorded twice in duplicates.

Table 4.2. Impact of irreversible binding of RVDU-3-185 1 μM (wild type) or 10 μM (mutant) on DHPG mediated iCa^{2+} mobilisation in wild type and mutant HEK293A-$mGlu_5$ cells. Data represent mean ± SEM from 3-4 independent experiments unless otherwise stated

	pEC_{50} (untreated)[a]	pEC_{50} (treated)	ΔE_{max}[b]	$\Delta \log \tau$[c]	pK_A[d]
Wild type	6.57±0.11	5.93±0.17	-42.59±7.10	-0.38±0.22	6.36±0.33
P654F	6.56±0.09	6.57±0.13	-10.66±6.63	-0.09±0.06	6.14±0.07
Y658V	6.13±0.13	6.13±0.45	-27.92±16.33	-0.17±0.51	6.14±0.69
T780A[#] n=2	6.43	6.28	-12.08	-0.21	6.03
W784A	6.07±0.15	6.14±0.34	-30.51±12.45	-0.24±1.19	5.84±0.48
F787A	6.11±0.18	4.84±1.34	-89.06±17.25	-0.16±0.25	5.60±0.17
S808A	6.49±0.18	6.64±0.22	0.02±11.05	0.05±0.10	6.13±0.13
A809G[#] n=2	5.94	5.51	-55.79	-0.78	5.38
A809V[#] n=1	5.82	6.09	-7.46	n.d.	n.d.

[a] The negative logarithm of the molar concentration of agonist required to yield a half maximal response

[b] The change in maximal response (E_{max}) expressed as a percentage of the maximum response to DHPG

[c] The change in the coupling efficiency of DHPG, determined by globally fitting treated and untreated datasets to an operational model of agonism

[d] The negative logarithm of the equilibrium dissociation constant of DHPG

n.d. not determined.

[#] n=1 or 2 independent experiments – not completed due to time constraints

4.3.4. Effect of mutations on $mGlu_5$ allosteric ligand VU0424465 agonism for iCa^{2+} mobilisation, IP_1 accumulation and pERK1/2.

As the studied mutations had no discernable effects on DHPG agonism, we next assessed the impact of these mutations on four $mGlu_5$ allosteric ligands. These ligands, from differing chemotype scaffolds, display agonism at iCa^{2+} mobilisation, IP_1 accumulation and ERK1/2 phosphorylation, however to differing degrees and are thus biased ligands (Sengmany et al., 2017). VU0424465 was the first allosteric ligand selected due to its robust PAM-agonism at the three aforementioned pathways in WT $mGlu_5$ (Fig 4.6), with E_{max} at IP_1 comparable to that of DHPG, and surpassing DHPG in ERK1/2 phosphorylation. All mutants, with the exception of S808A, T780A, Y658V produced VU0424465-mediated iCa^{2+} mobilisation maximal responses greater than that seen in $mGlu_5$ WT (Fig 4.6A-B). Three of the studied mutants also significantly altered VU0424465 potency at iCa^{2+} mobilisation, with P654F, and A809V decreasing and F787A increasing VU0424465 potency (table 4.3).

For IP_1 accumulation, all mutations significantly decreased VU0424465 potency relative to WT, with the exception of F787A, which had greater potency (Fig 4.6C-D). All mutants also decreased efficacy, except A809V, which produced an E_{max} comparable to WT. All mutations also significantly reduced VU0424465 pERK1/2 agonism, with maximal responses reaching approximately 1.5 fold over basal levels,

compared to 5-fold values seen in WT receptors (Fig 4.6E-G). T780A produced variable responses resulting in the inability to fit a concentration-response curve.

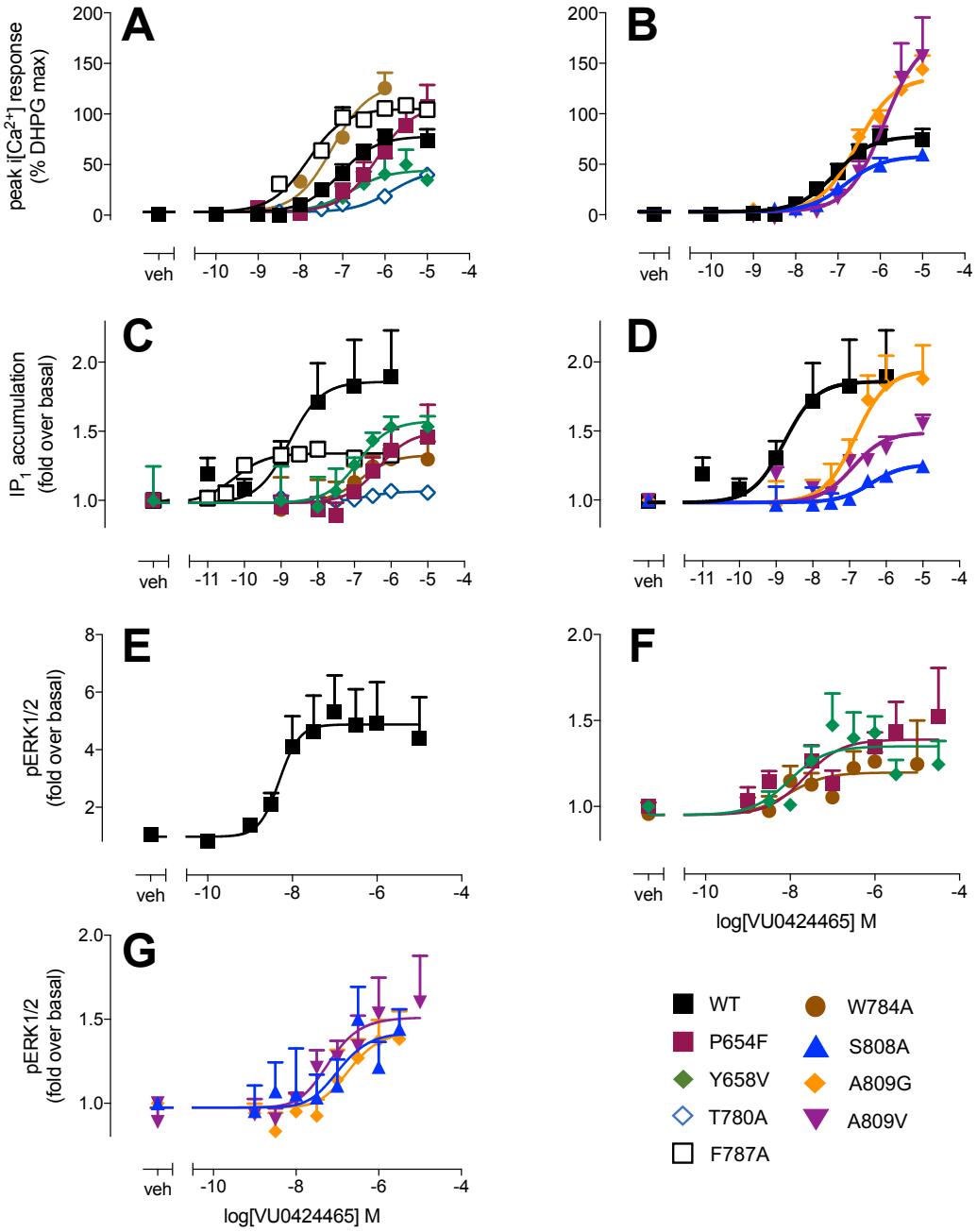

Fig 4.6. Concentration-response curves for VU0424465 for iCa^{2+} mobilisation (A & B), IP$_1$ accumulation (C & D), and ERK1/2 phosphorylation (E-G) in WT or mutant mGlu$_5$ HEK293A cells. Responses were represented as % DHPG maximal response (iCa^{2+} mobilisation) or fold over basal responses (IP$_1$ accumulation and pERK1/2). IP$_1$ accumulation and pERK1/2 phosphorylation experiments were performed in the presence of 1 U/mL GPT to minimise contribution of ambient

glutamate. Data are expressed as mean ± SEM of 3-9 experiments performed in duplicate, error bars not shown lie within the dimensions of the symbols.

4.3.5. Effect of mutations on $mGlu_5$ allosteric ligand DPFE agonism for iCa^{2+} mobilisation, IP_1 accumulation and pERK1/2.

DPFE was next selected for this study, as it represented a different chemotype from the common acetylene scaffold, and has previously been studied *in vivo* (Gregory et al., 2013a; Peters et al., 2016), thereby being a potential lead compound in $mGlu_5$ therapeutics. In WT, DPFE is an agonist of iCa^{2+} mobilisation, IP_1 accumulation and pERK1/2, however, showed no significant bias toward any of the three studied signalling endpoints (Fig 4.7).

All mutations abolished DPFE agonism in iCa^{2+} mobilisation, with the exception of S808A – although the response was minimal at 17% DHPG response (Fig 4.7A-B, table 4.3). All mutants also significantly reduced maximal responses of DPFE-mediated IP_1 accumulation relative to WT, however, only W784A significantly changed DPFE potency (Fig 4.7C-D, table 4.3). Again, all mutants decreased DPFE-stimulated pERK1/2 maximal response, with valine substitution at Y658 resulting in abolishment of agonism, similar to that seen with DHPG. Again, T780A resulted in variable pERK1/2 agonism, and may benefit from assessment of lower concentrations - thus a curve was not fitted to this dataset.

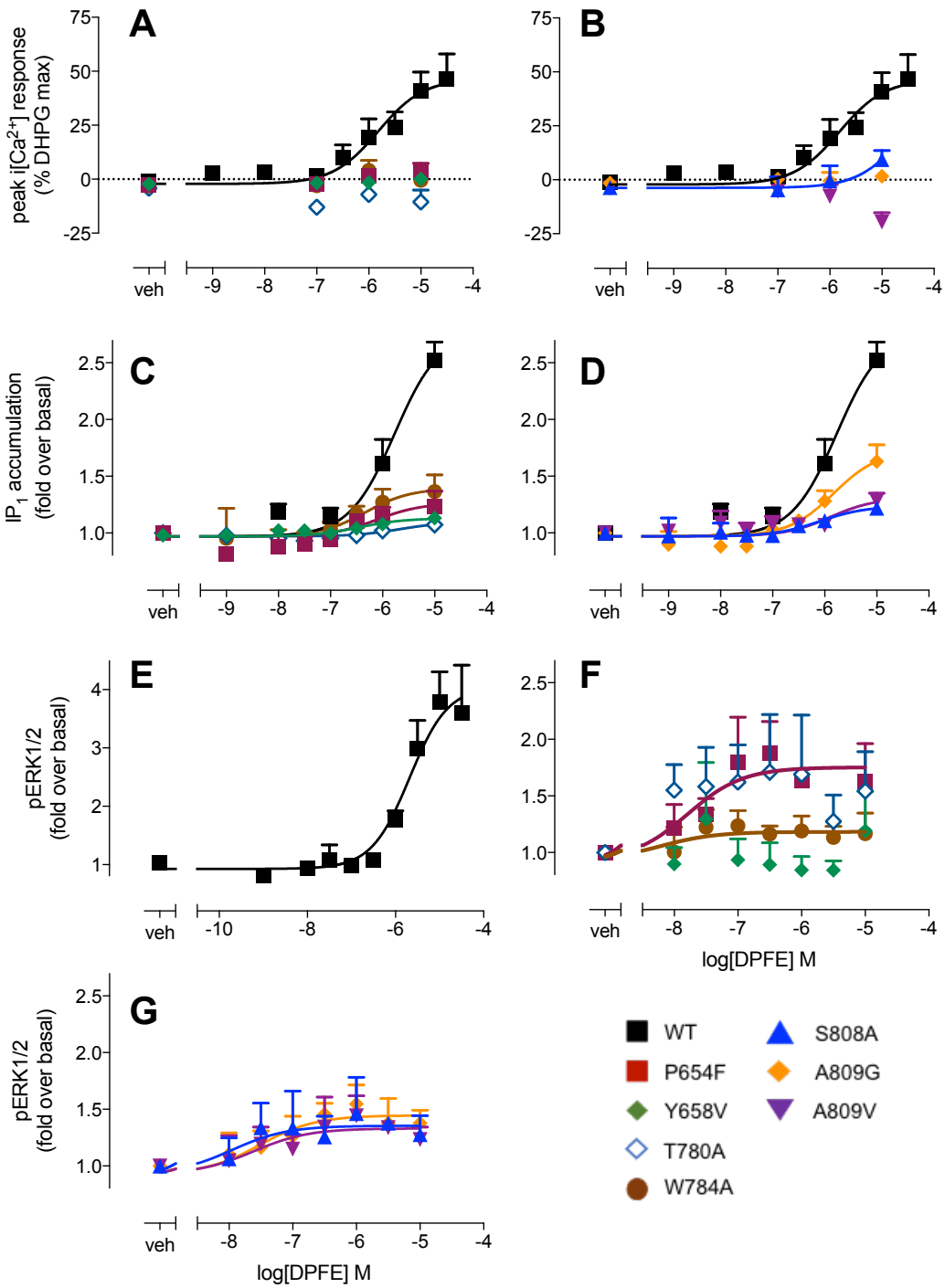

Fig 4.7. Concentration-response curves for DPFE for iCa^{2+} mobilisation (A & B), IP$_1$ accumulation (C & D), and ERK1/2 phosphorylation (E-G) in WT or mutant mGlu$_5$ HEK293A cells. Responses were represented as % DHPG maximal response (iCa^{2+} mobilisation) or fold over basal responses (IP$_1$ accumulation and pERK1/2). IP$_1$ accumulation and ERK1/2 phosphorylation experiments were performed in the presence of 1 U/mL GPT to minimise contribution of ambient glutamate. Data are expressed as mean ± SEM of 3-9 experiments performed in duplicate, error bars not shown lie within the dimensions of the symbols.

4.3.6. Effect of mutations on $mGlu_5$ allosteric ligand VU29 agonism for iCa^{2+} mobilisation, IP_1 accumulation and pERK1/2.

VU29 represented yet another structurally distinct $mGlu_5$ PAM chemotype, and had previously been described as a "pure" PAM, with no intrinsic agonist activity at iCa^{2+} mobilisation (Chen et al., 2007; Lindsley et al., 2004). However, we have recently shown robust agonism of this compound at IP_1 and ERK1/2 receptor endpoints in both $mGlu_5$ recombinant and cortical neuronal systems (Sengmany et al., 2017), thus behaving as a biased allosteric agonist. The selected mutations did not affect VU29 activity at iCa^{2+} mobilisation - that is, VU29 displayed no agonism at all mutants, with the exception of T780A, where minimal agonism was detected (12% DHPG response, Fig 4.8A-B, table 4.3). As with the previous two allosteric ligands, all the mutations decreased IP_1 accumulation and pERK1/2 agonism by VU29, with significant reductions in E_{max} within the majority of mutant cell lines (table 4.3, Fig 4.8C-G). Only P654F and A809V resulted in significant decreases in VU29 potency at IP_1 accumulation, with 30- and 60-fold reductions respectively.

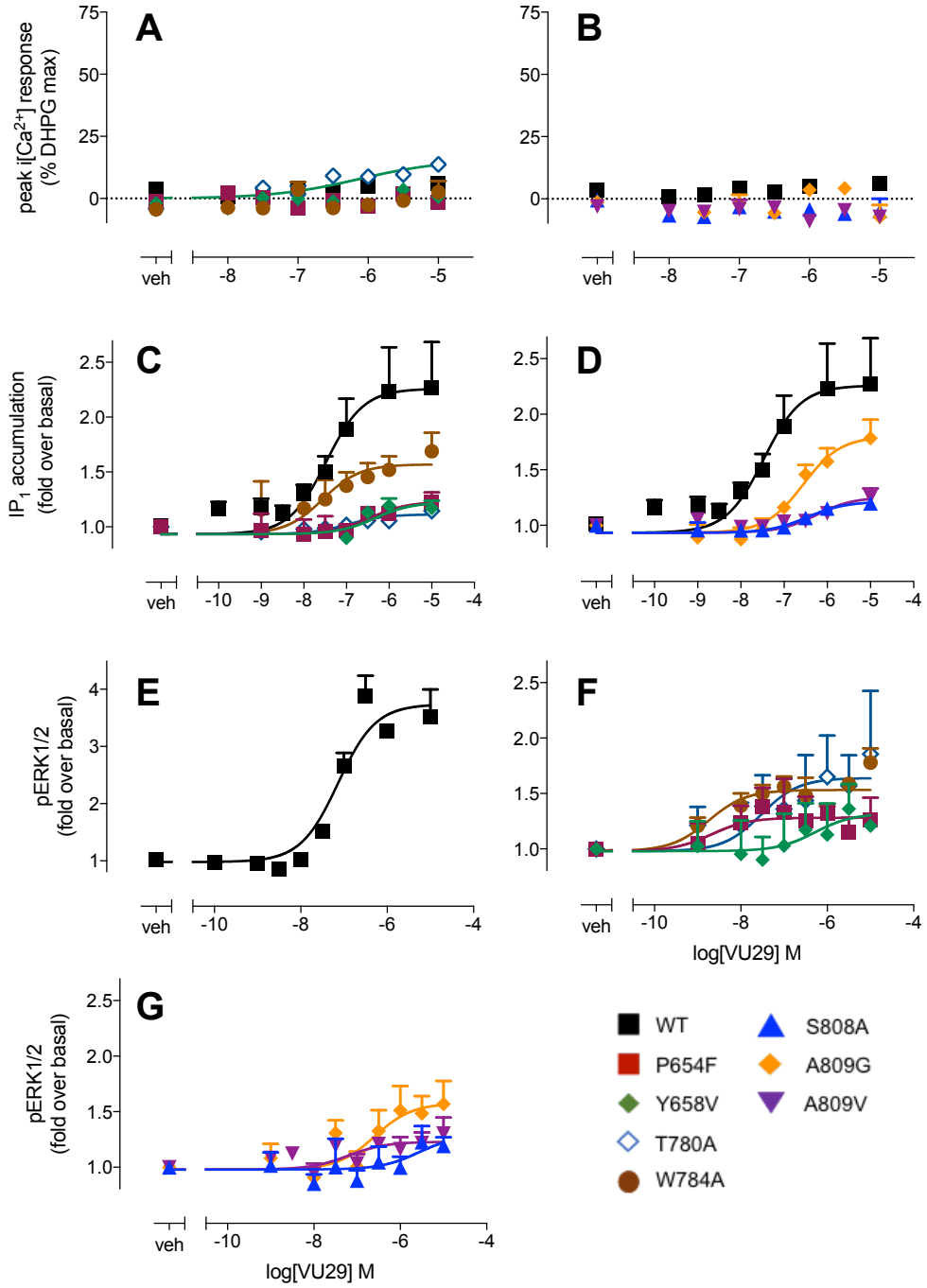

Fig 4.8. Concentration-response curves for VU29 for iCa^{2+} mobilisation (A & B), IP$_1$ accumulation (C & D), and ERK1/2 phosphorylation (E-G) in WT or mutant mGlu$_5$ HEK293A cells. Responses were represented as % DHPG maximal response (iCa^{2+} mobilisation) or fold over basal responses (IP$_1$ accumulation and pERK1/2). IP$_1$ accumulation and ERK1/2 phosphorylation experiments were performed in the presence of 1 U/mL GPT to minimise contribution of ambient glutamate. Data are expressed as mean ± SEM of 3-9 experiments performed in duplicate, error bars not shown lie within the dimensions of the symbols.

4.3.7. Effect of mutations on $mGlu_5$ allosteric ligand VU0409551 agonism for iCa^{2+} mobilisation, IP_1 accumulation and pERK1/2.

VU0409551 was the final allosteric agonist chosen for this study, as it has efficacy in preclinical models of psychosis (Balu et al., 2016; Rook et al., 2015), while also displaying biased agonism and modulation in recombinant and neuronal cells (Rook et al., 2015; Sengmany et al., 2017). In WT recombinant cells however, VU0409551 showed no distinct bias between the three studied pathways – although biased agonism toward IP_1 relative to pERK1/2 was observed in cortical neurons (Sengmany et al., 2017).

Here, only the mutants W784A, S808A and A809G retained VU0409551-mediated iCa^{2+} mobilisation, although to a minimal extent (Fig 4.9A-B). As for IP_1 accumulation, all mutants retained agonism, although again with reduced potencies and/or efficacies (table 4.3), while for pERK1/2, P654F, W784A and T780A lost agonism, while A809V and S808A had reduced potencies, hence a full concentration response curve could not be defined (Fig 4.9E-F). Only Y658V and A809G produced discernable VU0409551 pERK1/2 agonism, with potencies and E_{max} values comparable to that of WT responses (table 4.3).

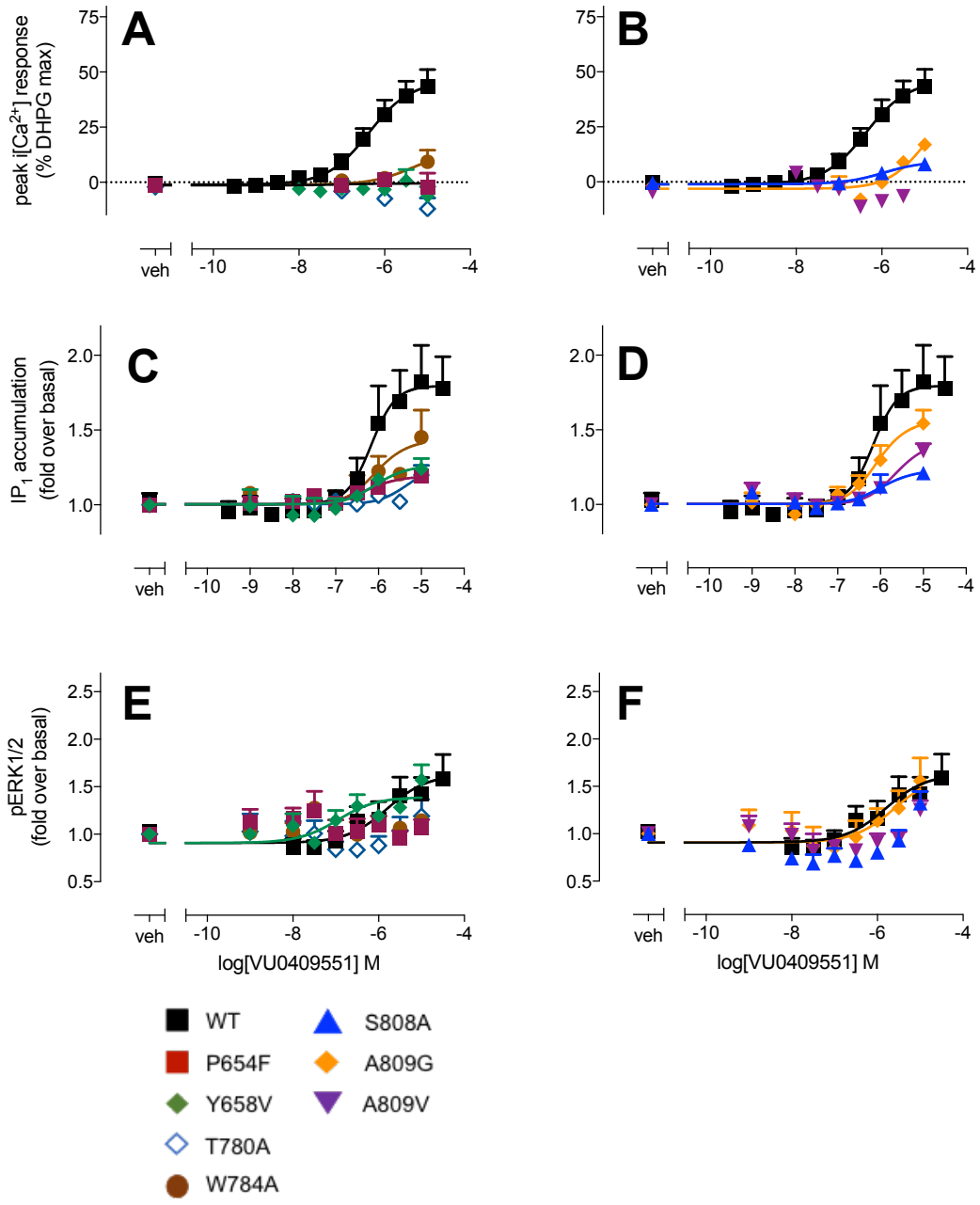

Fig 4.9. Concentration-response curves for VU0409551 for iCa^{2+} mobilisation (A & B), IP$_1$ accumulation (C & D), and ERK1/2 phosphorylation (E & F) in WT or mutant mGlu$_5$ HEK293A cells. Responses were represented as % DHPG maximal response (iCa^{2+} mobilisation) or fold over basal responses (IP$_1$ accumulation and pERK1/2). IP$_1$ accumulation and ERK1/2 phosphorylation experiments were performed in the presence of 1 U/mL GPT to minimise contribution of ambient glutamate. Data are expressed as mean ± SEM of 3-9 experiments performed in duplicate, error bars not shown lie within the dimensions of the symbols.

Table 4.3. Potency (pEC_{50}), maximal response (E_{max}) and transduction coefficient ($\log(\tau/K_A)$) estimates of VU0424465, DPFE, VU29 and VU0409551 for iCa^{2+} mobilisation, IP_1 accumulation and pERK1/2 in HEK293A-mGlu5-low and mutant cells. Data are mean ± SEM of 3-9 independent experiments performed in duplicate, unless otherwise specified.

	iCa^{2+} mobilisation			**IP_1 accumulation**			**pERK1/2**		
	pEC_{50}	E_{max} (%DHPG)	$\log(\tau/K_A)$	pEC_{50}	E_{max} (fold over basal)	$\log(\tau/K_A)$	pEC_{50}	E_{max} (fold over basal)	$\log(\tau/K_A)$
VU0424465									
WT	7.13±0.14	77.7±5.8	7.18±0.16	8.78±0.29	1.9±0.2	8.70±0.12	8.24±0.14	5.0±0.2	8.32±0.10
P654F	6.12±0.30 [a]	109.6±10.2[a]	6.25±0.19 [a]	6.55±0.05 [a]	1.5±0.2	6.66±0.06 [a]	7.00±0.37 [c]	1.3±0.2 [a]	7.30±0.67
Y658V	6.69±0.28	37.1±14.2	6.26±0.48 [a]	6.51±0.20 [a]	1.2±0.1	6.51±0.43 [a]	8.02±0.54	1.4±0.3 [a]	7.95±0.64
T780A	6.74±0.36	44.1±6.9 [a]	5.88±0.32 [a]	7.27±0.33 [a]	1.7±0.6	6.30±0.82 [a]	n.r.	n.r.	n.r.
W784A	7.42±0.16	132.3±17.9	7.33±0.17	7.30±0.65	1.5±0.2	7.25±0.91	8.26±0.84 [c]	1.2±0.1 [a,c]	7.87±0.51
F787A	8.13±0.02 [a]	106.2±4.7	8.27±0.05[a]	10.28±0.52	1.3±0.1	10.32±0.65	n.t.	n.t.	n.t.
S808A	6.80±0.32	72.8±4.2	6.70±0.26	6.82±0.21 [a]	1.2±0.1	6.35±0.39 [a]	7.56±0.46	1.4±0.3 [a]	8.08±0.45
A809G	6.66±0.07	128.2±10.1	6.70±0.06	7.04±0.17 [a]	2.0±0.3	7.14±0.18	7.73±0.43	1.4±0.4 [a]	7.12±0.23
A809V	6.19±0.13 [a]	149.1±23.5	6.30±0.09[a]	6.49±0.16 [a]	1.5±0.1	6.40±0.30 [a]	7.32±0.23	1.5±0.3 [a]	7.56±0.19
DPFE									
WT	5.65±0.28	48.8±7.5	5.79±0.25	5.95±0.12	2.7±0.2	5.86±0.19	6.25±0.53	4.1±0.3	5.83±0.08
P654F	n.r.	n.r.	n.r.	5.81±0.83	1.4±0.1 [a]	5.94±0.67	7.79±0.56 [c]	1.8±0.2 [a]	8.44 [b]
Y658V	n.r.	n.r.	n.r.	6.07±0.46	1.2±0.03 [a]	6.77±0.92	n.r.	n.r.	n.r.
T780A	n.r.	n.r.	n.r.	6.08±0.62	1.3±0.2 [a]	5.96±0.71	n.d.	n.d.	n.d.
W784A	n.r.	n.r.	n.r.	6.49±0.05	1.6±0.2	5.89±0.71	8.22±1.55 [c]	1.2±0.1 [a]	5.36 [b]
S808A	6.84 [b]	16.7 [b]	4.81±0.52 [c]	6.42±0.47	1.2±0.1 [a]	6.60±0.92	7.63±0.39	1.4±0.1 [a]	7.25 [b]
A809G	n.r.	n.r.	n.r.	5.81±0.21	1.8±0.2 [a]	5.83±0.23	6.77±0.18	1.5±0.1 [a]	6.38±0.18
A809V	n.r.	n.r.	n.r.	4.64±0.31	2.2±0.5	4.80±0.31	7.61±0.74 [c]	1.3±0.1 [a]	6.96±0.42

	iCa^{2+} mobilisation			**IP$_1$ accumulation**			**pERK1/2**		
	pEC$_{50}$	E$_{max}$ (%DHPG)	log(τ/K$_A$)	pEC$_{50}$	E$_{max}$ (fold over basal)	log(τ/K$_A$)	pEC$_{50}$	E$_{max}$ (fold over basal)	log(τ/K$_A$)
VU29									
WT	n.r.	n.r.	n.r.	7.47±0.14	2.3±0.1	7.41±0.11	7.06±0.12	3.7±0.2	7.17±0.04
P654F	n.r.	n.r.	n.r.	5.99±0.68 [a]	1.4±0.2 [a]	7.21±0.88	7.78 [b]	1.51 [b]	8.34±0.87
Y658V	n.r.	n.r.	n.r.	6.65±0.13	1.3±0.04 [a]	6.82±0.13	6.64 [b]	1.22 [b]	6.49 [b]
T780A	6.69±0.33	12.82±2.01	7.07±0.28	6.62±0.33	1.4±0.2 [a]	6.28±0.63	7.53±0.36 [c]	1.6±0.1 [a]	6.17±0.32
W784A	n.r.	n.r.	n.r.	7.32±0.42	1.7±0.2	8.78±0.46	8.00±0.16	1.5±0.1 [a]	8.05±0.29
S808A	n.r.	n.r.	n.r.	6.26±0.14	1.3±0.1 [a]	5.97±0.27	6.08±0.44	1.3±0.4 [a]	6.51±0.95
A809G	n.r.	n.r.	n.r.	6.62±0.09	1.8±0.2	6.65±0.09	6.52±0.30	1.6±0.1 [a]	6.91±0.32
A809V	n.r.	n.r.	n.r.	5.67±0.35 [a]	1.4±0.2 [a]	5.11±0.45 [a]	7.20±0.98 [c]	1.2±0.1 [a]	7.79±1.18
VU0409551									
WT	6.38±0.17	44.6±3.9	6.23±0.24	6.16±0.13	1.7±0.2	6.06±0.18	6.05±0.39	1.6±0.5	6.30±0.36
P654F	n.r.	n.r.	n.r.	6.12±0.14	1.2±0.03 [a]	5.73±0.36	n.r.	n.r.	n.r.
Y658V	n.r.	n.r.	n.r.	6.22 [b]	1.27 [b]	6.48 [b]	6.32 [b]	1.75 [b]	6.67±0.75
T780A	n.r.	n.r.	n.r.	5.66±0.45	1.2±0.1 [a]	5.15±0.40	n.r.	n.r.	n.r.
W784A	5.12±1.63	16.3±26.8	7.23 [b]	5.62±0.28	1.6±0.2	5.94±0.08	n.r.	n.r.	n.r.
S808A	5.94±0.52	9.2±2.9	6.52±0.60	6.08 [b]	1.3 [b]	5.61 [b]	n.r.	n.r.	n.r.
A809G	4.98±0.71	38.1±35.6	6.11±0.20	5.96±0.23	1.6±0.1	6.06±0.11	6.74±0.30	1.8±0.8	6.04±0.26
A809V	n.r.	n.r.	n.r.	5.27±0.42	1.7±0.3	4.94±0.13	n.r.	n.r.	n.r.

n.r. no response; n.d. not determined due to poor concentration-response curve fit; n.t. not tested due to time constraints

[a] significantly different from mGlu$_5$ WT response (*p<0.05,* one-way ANOVA, Dunnett's post-test)

[b] concentration response curve and/or operational model could only be fit to n=2 (from 3 or more) independent experiments

[c] concentration response curve and/or operational model was globally fitted to 3 or more independent experiments

Note, wild type (WT) parameters were derived from experiments performed in Chapter 2 (Sengmany *et al.* (2017))

4.3.8. Comparisons of transduction coefficients derived from iCa^{2+} mobilisation, IP_1, accumulation and pERK1/2 agonism by $mGlu_5$ allosteric ligands at WT and mutant receptors

As mentioned above, potency and E_{max} values represent qualitative measures of agonism, thus the operational model of agonism was fitted to the studied ligands at each receptor endpoint to derive transduction coefficients ($\log(\tau/K_A)$). The transduction coefficient at different mutant receptors was then normalised to WT responses and compared using one-way ANOVA with Dunnett's post-hoc test (Fig 4.10).

For VU0424465, all mutants decreased the transduction coefficient in iCa^{2+} mobilisation, with the exception of F787A, which was significantly increased by 12-fold relative to WT (table 4.3, Fig 4.10A). All mutants also decreased transduction ratios in agonism for IP_1 accumulation, with significance reached in the mutations T780A, Y658V, S808A, P654F and A809V. For ERK1/2 phosphorylation, VU0424465 had reduced transduction coefficients at all studied mutations, although this did not reach significant differences relative to WT responses, likely due to the greater variability observed between experiments (table 4.3, Fig 4.10A).

For mutants that retained DPFE agonism in iCa^{2+} mobilisation, IP_1 accumulation and ERK1/2 phosphorylation did not significantly influence transduction ratios relative to WT responses. The only exception was P654F, which increased transduction coefficient relative to WT by 400-fold. For VU29, no differences in transduction ratios were observed in all receptor endpoints, except A809V and IP_1 (Fig 4.10C), while mutations had no significant effects VU0409551, barring those that abolished agonism completely (Fig 4.10D).

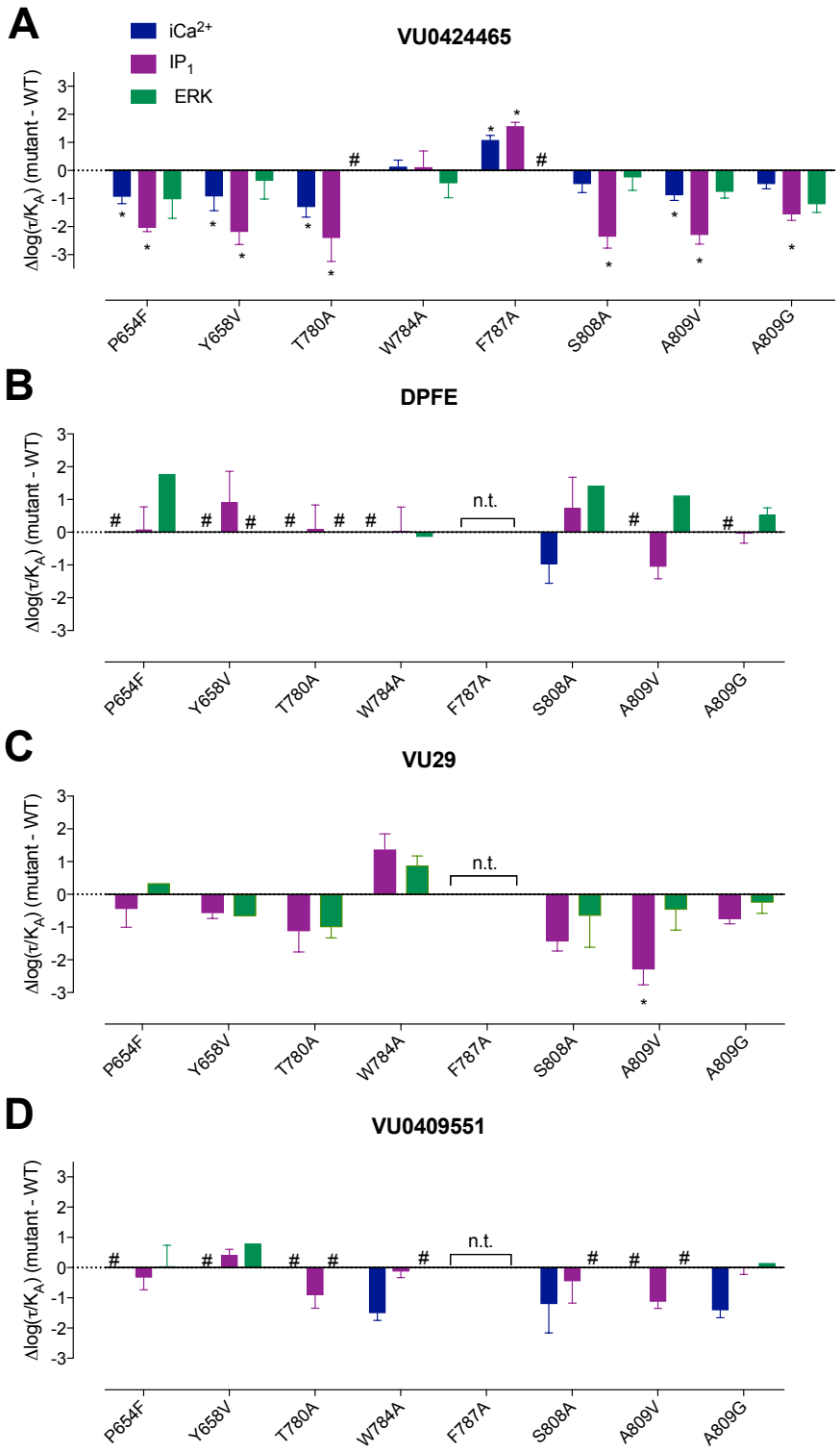

Fig 4.10. The effect of various mutations on the transduction ratio (log(τ/K$_A$)) of mGlu$_5$ allosteric ligands obtained in iCa^{2+} mobilisation, IP$_1$ accumulation and pERK1/2 assays. The data are normalised to the wild-type receptor and values below zero indicate a decrease in transduction ratio at the mutant receptor, whereas a value above zero indicates an increase. *p<0.05, significantly different from the wild-type receptor determined by a one-way ANOVA, Dunnett's post-hoc test. N.t. not tested, # no observed agonism.

4.3.9. Effect of mutations on biased agonism

While comparing agonism in mutants to WT responses at each individual receptor endpoint allows assessment of mutant effects at each pathway, we next aimed to assess whether these mutations affected the biased signalling profile of each ligand. To do this, we normalised transduction coefficients, derived from each assay at each mutant, to the reference ligand DHPG to give $\Delta\log(\tau/K_A)$ (Fig 4.11A, C, E, G). Comparisons between receptor pathways were quantified by subtracting $\Delta\log(\tau/K_A)$ between two receptor pathways to derive $\Delta\Delta\log(\tau/K_A)$ or LogBias (Fig 4.11B, D, F, G).

For VU0424465, only the WT receptor showed significant differences in $\Delta\log(\tau/K_A)$ between pathways (Fig 4.11A), with distinct bias toward IP_1 accumulation and pERK1/2 relative to iCa^{2+} mobilisation (Fig 4.11B). All mutants retained a trend toward greater IP_1 agonism relative to iCa^{2+} mobilisation, except W784A, which had comparable agonism between the two pathways (Fig 4.11B, blue circle). In WT, VU0424465 had significant biased agonism toward pERK1/2 relative to iCa^{2+} mobilisation, and this was retained (despite loss of significance) at P654F, W784A, and S808A, and reversed at Y658V and T780A. The bias toward IP_1 accumulation relative to pERK1/2 was also largely retained in A809G and A809V however was reversed with W784A and lost with S808A and P654F.

With DPFE, calculations were limited due to the lack of iCa^{2+} agonism in the majority of mutants, however, comparisons of IP_1 accumulation and pERK1/2 saw biased agonism toward IP_1 accumulation in S808A, A809V, and A809G, and bias toward pERK1/2 in P654F (Fig 4.11D). For VU29, the significant bias between IP_1

accumulation and pERK1/2 is lost with all mutations (Fig 4.11E). However, the lack of VU29-mediated iCa^{2+} mobilisation is largely retained (Fig 4.11E-F), thus, this ligand retains bias towards IP_1 accumulation and pERK1/2 relative to iCa^{2+} mobilisation, with the exception of T780A, which produced VU29 mediated iCa^{2+} mobilisation. Finally, for VU0409551, P654F, Y658V, T780A and A809V abolished both iCa^{2+} mobilisation and ERK1/2 phosphorylation relative to DHPG (Fig 4.11G), with A809G being the only ligand to retain the biased profile observed with $mGlu_5$ WT receptors (Fig 4.11H). W784A also resulted in a reversal of VU0409551 bias trend toward IP_1 accumulation compared to WT responses, with a trend toward agonism of iCa^{2+} mobilisation relative to IP_1 accumulation (Fig 4.11H).

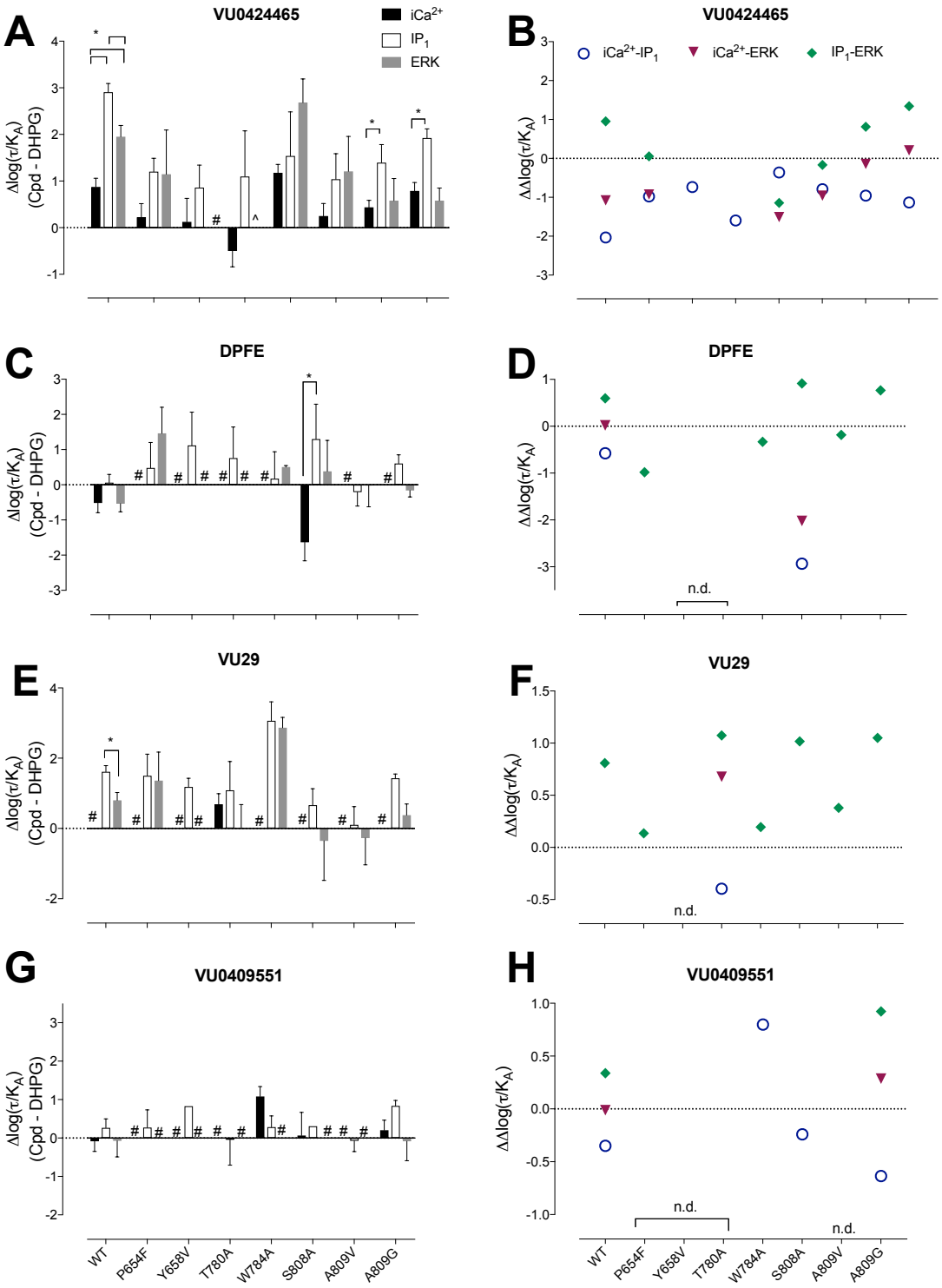

Fig 4.11. Quantification of biased agonism of mGlu$_5$ allosteric ligands at WT or mutant mGlu$_5$ receptors using the operational model of agonism. Log(τ/K$_A$) values for each allosteric agonist (A,C,E,G) were normalised to DHPG (Δlog(τ/K$_A$)) within each mutant. The degree of bias between different pathways (ΔΔlog(τ/K$_A$)), represents the bias factors for each agonist (B,D,F,H). Data for Δlog(τ/K$_A$) represent the mean ± SEM, whereas ΔΔlog(τ/K$_A$) values are mean only. * denotes significantly different comparisons, p<0.05, one-way ANOVA with Tukey's post-test. Cpd, compound, n.d. not determined, # no observed agonism, ^ unable to fit curve.

4.3.10. Determination of affinity, efficacy and cooperativity parameters through allosteric modulation of DHPG-mediated iCa^{2+} mobilisation

In order to determine whether changes in ligand activity were affinity or efficacy driven, we next conducted interaction studies with DHPG at iCa^{2+} mobilisation, to allow the derivation of affinity, cooperativity and intrinsic efficacy parameters from the operational model of allosterism (Leach et al., 2007). Previous mutagenesis studies were performed with glutamate as the orthosteric ligand, however, here we used our reference ligand DHPG to determine modulatory activity of the studied compounds. VU0424465 is shown as an example of the full interaction studies performed on each mutant receptor (Fig 4.12; see Appendix 1). Interaction studies with ligands with intrinsic agonist activity were performed as a simultaneous addition with DHPG to minimise acute desensitisation. All other interaction studies were performed with 1 min pre-incubation of allosteric ligand followed by DHPG addition. For ligands that showed robust agonism (e.g. VU0424465 and A809G, A809V (Fig 4.12F-G)), the operational model could not be accurately fit, thus curves only represent an empirical fit to Equation 1. Operational parameters of affinity (pK_B), cooperativity ($\log\beta$) and efficacy ($\log \tau_B$) were derived and are summarised in table 4.4.

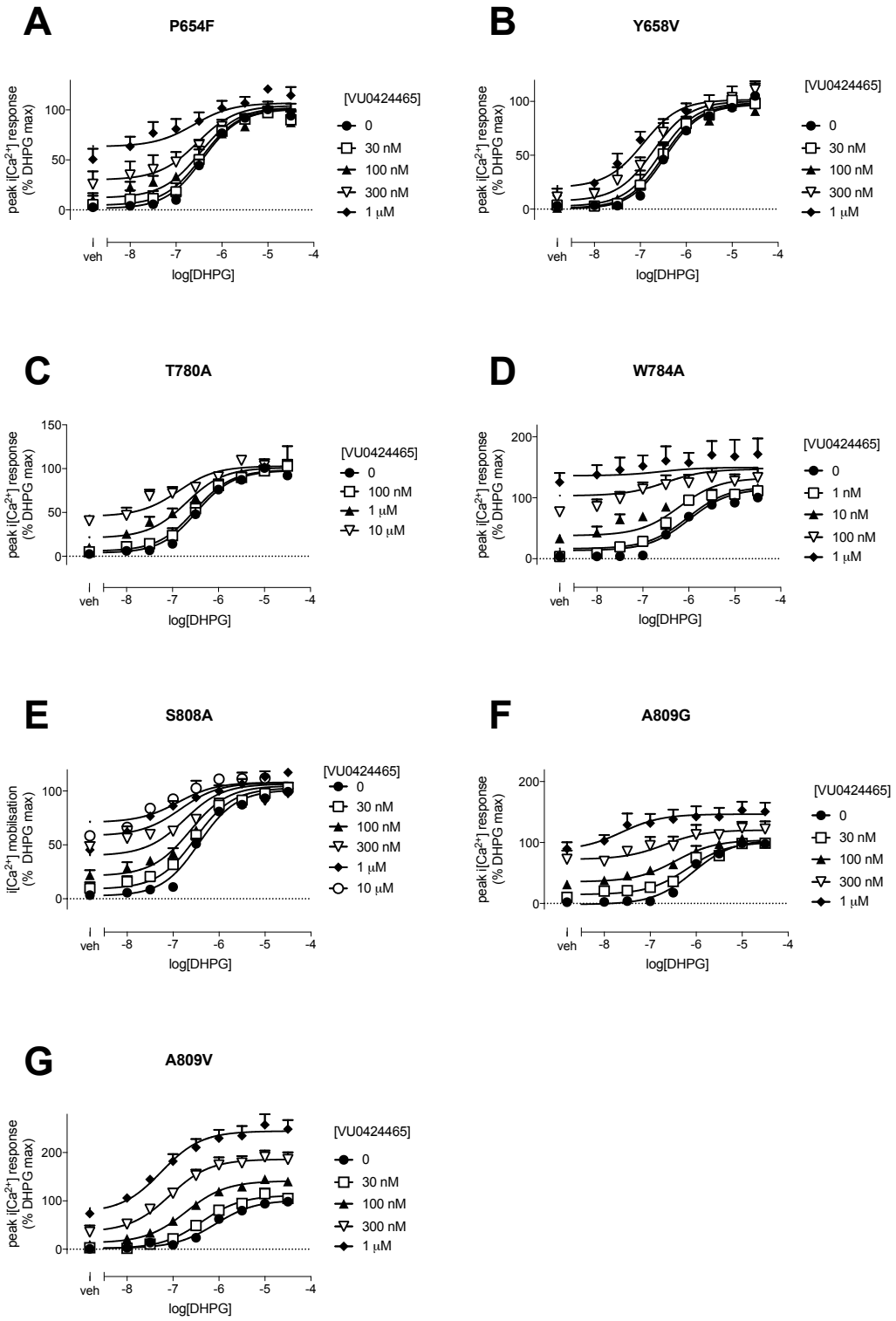

Fig 4.12. Allosteric modulation of DHPG-mediated iCa^{2+} mobilisation by VU0424465 at mutant mGlu$_5$ receptors (A-G). The operational model of allosterism could not be fit to data in A809G and A809V (F-G) due to the large agonist response masking any modulatory behaviour. Data are expressed as mean ± SEM of n=3-5 independent experiments performed in duplicate.

The mutants Y658V, T780A and S808A significantly reduced functional affinity of VU0424465 by 32-, 13- and 12-fold respectively (table 4.4), while the functional affinity of DPFE was increased in the following mutants: P654F and W784A (both 51-fold), and S808A (20-fold). No significant changes in affinity estimates were observed with VU0409551. VU29 however lost all ligand activity at P654F and S808A, with maximal concentrations unable to shift the DHPG concentration response curve. VU29 was also the only ligand to result in significant changes in cooperativity in the mutant Y658V (4-fold decrease). No significant changes in cooperativity were observed with the three other ligands at the seven mutant receptors. In alignment with the aforementioned agonism data (table 4.3, Fig 4.7A-B for DPFE, Fig 4.9A-B for VU0409551), DPFE agonism was abolished at all mutants, while VU0409551 agonism was abolished in P654F, Y658V, T780A, W784A and A809V. However, despite lack of agonism, both ligands retained positive cooperativity, as denoted by logβ>0 (table 4.4).

Table 4.4. Affinity and cooperativity estimates for allosteric modulation of DHPG-mediated iCa^{2+} mobilisation in mutant $mGlu_5$ cells.
Data are mean ±SEM of 3-5 independent experiments performed in duplicate unless otherwise stated.

	pK_B	$log\beta$	$log\tau_B$	pK_B	$log\beta$	$log\tau_B$
	VU0424465			**DPFE**		
WT	7.00±0.11	0.84±0.13	-0.12±0.08	5.35±0.25	1.07±0.11	-0.62±0.10
P654F	5.85 [c]	0.48 [c]	0.48 [c]	7.06±0.30 [a,b]	0.33±0.07 [b]	no agonism
Y658V	5.49 [c]	1.29 [c]	-0.04 [c]	5.15±0.13	0.99±0.07	no agonism
T780A	5.89±0.21 [a]	0.49±0.18	-0.20±0.15	5.28±0.49 [b]	0.47±0.14 [b]	no agonism
W784A	6.21±0.61 [b]	1.92±0.70 [b]	1.14±0.55 [b]	7.06 [c]	0.65	no agonism
S808A	5.92±0.30 [a]	1.01±0.34	0.45±0.22	6.64±0.18 [a]	0.60±0.14	no agonism
A809G	n.d.	n.d.	n.d.	5.39±0.37	1.03±0.16	no agonism
A809V	n.d.	n.d.	n.d.	6.03±0.31	0.85±0.19	no agonism
	VU29			**VU0409551**		
WT	6.67±0.28	0.81±0.08	no agonism	5.88±0.20	1.06±0.09	-0.26±0.06
P654F	no modulation	no modulation	no agonism	7.36±0.68	0.49±0.15	no agonism
Y658V	6.63±0.46	0.21±0.07 [a]	no agonism	6.74±0.44	0.55±0.09	no agonism
T780A	6.45±0.25	0.32±0.15	-1.05±0.10	5.93±0.38	0.76±0.12	no agonism
W784A	7.54±0.27	1.00±0.23	no agonism	6.14±0.22	0.92±0.06	no agonism
S808A	no modulation	no modulation	no agonism	6.37±0.42	0.60±0.13	-0.67±0.19 [b]
A809G	6.74±0.25	0.44±0.15	no agonism	5.65±0.12	1.01±0.18	-0.48±0.06
A809V	6.92±0.39	0.33±0.02	no agonism	5.94±0.35	0.86±0.22	no agonism

[a] $p<0.05$, significantly different from WT, One-way ANOVA, Dunnett's post test

[b] operational model of allosterism was globally fitted to 3 or more independent experiments

[c] operational model could only be fit to n=2 (from 3 or more) independent experiments

n.d. not determined, unable to fit data due to agonism; no agonism: $log(\tau_B)$ no different from -100 (F test)

Table 4.5. Summary of key findings relative to $mGlu_5$ WT receptors

Ligand	Agonism ($\Delta\log(\tau/K_A)$) relative to WT	Modulation (iCa^{2+} mobilisation) relative to WT	Biased agonism ($\Delta\Delta\log(\tau/K_A)$) relative to DHPG
VU0424465	• ↓ iCa^{2+}: P654F, Y658V, T780A, A809V • ↓ IP_1: all mutants except W784A • No effect on pERK1/2	• ↓pK_B: Y658V, T780A, S808A • No effect on cooperativity	• WT: significant bias between three studied pathways • Loss of all bias: P654F, Y658V, T780A, W784A, S808A • A809G, A809V retained bias between iCa^{2+}-IP_1, lost pERK1/2 bias
DPFE	• iCa^{2+}: all mutants – loss of agonism • No change in IP_1 or pERK1/2	• ↑pK_B: P654F, W784A, S808A • No effect on cooperativity	• WT: no significant bias between three studied pathways • S808A: Gain of bias between iCa^{2+} and IP_1
VU29	• ↓ IP_1: A809V • Gain in iCa^{2+} agonism: T780A • No change in pERK1/2	• ↓logβ: Y658V • P654F, S808A abolished cooperativity	• WT: no iCa^{2+} agonism, significant IP_1-pERK1/2 bias • Loss of IP_1-pERK1/2 bias with all mutants • Gain in iCa^{2+} agonism in T780A
VU0409551	• iCa^{2+}: P654F, Y658V, T780A, A809V abolished agonism • pERK1/2: P654F, T780A, W784A, S808A, A809V abolished agonism	• No changes in affinity or cooperativity	• WT: no significant bias between three studied pathways • No gain in bias between three studied pathways

4.4. Discussion

We recently showed biased agonism to be operative for select $mGlu_5$ PAMs (Sengmany et al., 2017), and here, extended this study to probe the residues involved in allosteric activation of discrete signalling endpoints. Seven point mutations were studied using four $mGlu_5$ allosteric ligands with distinct signalling profiles, and activity was quantified using the operational model of agonism (Black and Leff, 1983). Transduction coefficients were compared using the analytical methods previously described (Kenakin et al., 2012) to derive a biased signalling profile for each ligand at each mutant receptor. Estimates of functional affinity (pK_B), cooperativity ($log\beta$) were also derived to delineate residues driving either ligand affinity or cooperativity. The mutations Y658V, T780A and S808A significantly affected agonism, affinity and/or cooperativity with DHPG in iCa^{2+} mobilisation for all four studied ligands, and resulted in loss of VU0424465 bias between the three studied pathways, and a loss of VU29 bias toward IP_1 accumulation relative to pERK1/2. S808A, however, produced a gain in DPFE bias between iCa^{2+} mobilisation and IP_1 accumulation, while T780A resulted in a gain of VU29 iCa^{2+} mobilisation. VU0409551 iCa^{2+} mobilisation and pERK1/2 agonism was particularly sensitive to the selected receptor mutations, with abolishment of activity at most mutants, with only A809G retaining VU0409551 agonism at the three studied pathways. Changes in ligand agonism and bias between receptor signalling endpoints highlight the distinct changes in signalling profiles with each mutation – thereby providing further insight into the structural basis of $mGlu_5$ biased agonism.

First, we determined whether the introduced mutations affected the global receptor activation network, rather than influencing individual allosteric ligand efficacy. None

of the studied mutations affected DHPG agonism at the three studied endpoints, with the exception of Y658V and pERK1/2 agonism – thus confirming the mutations had limited effect on global receptor activation (pending repeated pERK1/2 experiments with Y658V). The majority of mutations, however, significantly affected VU0424465 agonism of iCa^{2+} mobilisation and IP_1 accumulation, with little changes in pERK1/2 relative to WT. Interestingly, all mutants abolished DPFE agonism of iCa^{2+} mobilisation, while the majority of mutations abolished VU0409551 both iCa^{2+} mobilisation and pERK1/2 agonism. This abolishment of agonism points to two possible scenarios – either the individual mutation negatively impacted ligand affinity, such that the ligand no longer binds to induce a receptor response, or rather, the ligand was able to bind but not "activate" the receptor. Since DHPG retained activity at all mutations except Y658V, this suggests allosteric ligands may activate either the calcium or pERK1/2 signalling pathways via receptor conformations distinct from that imposed by DHPG. This is further supported by the iCa^{2+} mobilisation seen with VU0424465 – the majority of mutants produced iCa^{2+} mobilisation responses greatly exceeding DHPG responses (i.e. >100% DHPG maximal calcium response), suggesting stabilisation of different active receptor conformations relative to orthosteric ligands.

Three mutations – Y658V (TM3), S808A (TM7) and T780A (TM6) – resulted in significant changes in agonism across the four studied ligands, with greatest reductions in iCa^{2+} mobilisation and pERK1/2 agonism but not IP_1 accumulation. Mutations of these three conserved residues also resulted in a significant reduction of VU0424465 functional affinity for DHPG-iCa^{2+} mobilisation, while Y658V and S808A significantly reduced, if not abolished VU29 positive cooperativity. Further,

VU29, a "pure" PAM of iCa^{2+} mobilisation, with no apparent agonism in WT, gained agonism of iCa^{2+} mobilisation in the mutant T780A. These results largely parallel previous studies, with reductions in affinity and/or cooperativity, as well as pharmacological switches, observed in various $mGlu_5$ chemotypes with alterations in any of these three residues (Gregory et al., 2014; Gregory et al., 2013b; Mølck et al., 2012; Turlington et al., 2013). These three residues, Y658, S808 and T780, reside toward the base of the $mGlu_5$ allosteric binding pocket and form critical hydrogen-bond links with a residing water molecule – suggested to be a receptor "activation switch" (Christopher et al., 2015; Dore et al., 2014). Perturbations in this hydrogen bond network, through incorporation of large phenyl substitutions in allosteric ligand chemotypes, has been noted to switch ligand pharmacology (O'Brien et al., 2003; Wood et al., 2011). Conversely, perturbations, or rather mutations, of the residues within this hydrogen-water network also affected allosteric ligand affinity and cooperativity (Gregory et al., 2014; Gregory et al., 2013b; Mølck et al., 2012; Turlington et al., 2013). Y658 and S808 also potentially form critical ligand-receptor binding interactions with each of the studied ligands – forming π-stacking interactions between the tyrosine and phenyl rings and hydrogen bonds between the serine hydroxyl group and nitrogen/amide constituent within each ligand (Christopher et al., 2015; Dore et al., 2014). Thus, alterations in either of these residues would result in altered ligand positioning – explaining the altered affinity and/or cooperativity observed with our data.

The residue W784, analogous to the Trp found in the Class A "rotamer toggle switch" CWxP (Holst et al., 2010; Shi et al., 2002), represents another potential key activator of receptor responses. Increases in affinity of certain $mGlu_5$ PAMs were observed

following mutation of this residue (Chen et al., 2007; Gregory et al., 2014; Gregory et al., 2013b; Muhlemann et al., 2006; Turlington et al., 2013), while the prototypical $mGlu_5$ NAM MPEP had reduced affinity and potency in this mutant (Gregory et al., 2013b; Malherbe et al., 2006; Malherbe et al., 2003; Mølck et al., 2012; Pagano et al., 2000). Congruent with the previous PAM studies (Chen et al., 2007; Gregory et al., 2014; Gregory et al., 2013b; Muhlemann et al., 2006; Turlington et al., 2013), DPFE affinity for iCa^{2+} mobilisation in W784A was increased in our study, however, DPFE agonism was abolished. The increase in affinity may potentially be explained through reduced steric hindrance following a smaller alanine substitution relative to the bulky tryptophan group, thereby allowing a larger receptor pocket for DPFE binding. However, as this residue is a key mediator of receptor activation, substitutions may sway the receptor toward distinct conformations, and potentially negatively impact activation of iCa^{2+} mobilisation – thus resulting in increases in DPFE affinity but abolishment of agonism.

The $mGlu_5$ allosteric binding site comprises two large hydrophobic regions, connected by a narrow channel (Christopher et al., 2015; Dore et al., 2014). As such, several $mGlu_5$ allosteric ligand chemotypes contain a "narrow" acetylene/alkyne moiety, or small flexible linker substituent, within the centre of the compound, connecting two larger hydrophobic ring structures (e.g. phenyl rings, pyrmidines and pyrazoles), one of which transverses the channel toward the base of the allosteric pocket (Christopher et al., 2015; Dore et al., 2014). Two residues chosen for this study, A809 and P654, form part of the narrow bridge between the two hydrophobic pockets, and thus were hypothesised to influence ligand positioning within the $mGlu_5$ binding site. Indeed, A809V significantly reduced transduction ratios of VU0424465

iCa^{2+} mobilisation and IP_1 accumulation, and VU29-mediated IP_1 accumulation – while glycine substitution at the same residue diminished VU0424465 IP_1 accumulation and abolished DPFE iCa^{2+} mobilisation. Biased signalling profiles, however, were largely retained between iCa^{2+} mobilisation and IP_1 accumulation by VU0424465 at both A809 mutants, however, bias toward pERK1/2 relative to iCa^{2+} mobilisation was lost. While the size of the aliphatic glycine and valine relative to alanine are perhaps comparable, movement or extension of the residue would potentially increase steric hindrance within the narrow channel, hindering the binding of allosteric ligands. Further, as A809 neighbours S808, the residue that forms part of the critical hydrogen-water network, any substitution would increase bulk within the region, consequently stressing helix stability, and potentially affecting the critical S808 position within the protein backbone (Lopez-Llano et al., 2006; Serrano et al., 1992). Thus, this residue remains a constraint in drug design, with the requirement of a narrow linker moiety within the compound to accommodate the narrow bridge within the allosteric site.

Modification of the second studied residue lining the narrow binding channel, P654, also significantly affected ligand activity. Phenylalanine substitution resulted in a reduction in VU0424465 agonism across the three studied pathways, however, increased DPFE-mediated pERK1/2 agonism. In contrast with previous studies that show unchanged DPFE functional affinity at glutamate-mediated iCa^{2+} mobilisation (Gregory et al., 2014), P654F also resulted in a significant increase in DPFE affinity for iCa^{2+} mobilisation – although it should be noted that DHPG in lieu of glutamate was used as the orthosteric agonist in our study, and probe dependence, whereby the nature of allosteric modulation may alter depending on the orthosteric ligand used,

may be operative (Sengmany et al., 2017). This mutation also abolished VU29 positive cooperativity in DHPG-mediated iCa^{2+} mobilisation. As this mutation did not significantly affect the cooperativity of VU0424465, DPFE and VU0409551, it suggests the loss of VU29 activity for iCa^{2+} mobilisation is largely affinity driven. Indeed, a bulky phenylalanine substitution would unsurprisingly hinder the ability of VU29, as well as other $mGlu_5$ allosteric ligands, to reach into the base of the allosteric binding pocket. This is further emphasised in the reduction of agonism of VU0424465 across the three pathways, as well as the loss of iCa^{2+} mobilisation with DPFE and VU0409551. Thus, these two residues, P654 and A809, linking the two hydrophobic binding pockets within the $mGlu_5$ allosteric site, are a critical factor in the design of allosteric ligands, with chemotypes required to successfully transverse the narrow channel for optimal ligand activity.

While our study provides unique insight into individual residues involved in iCa^{2+} mobilisation, IP_1 accumulation and ERK1/2 phosphorylation, several key experiments will allow a fuller understanding of the structural basis of signalling bias. First, receptor expression numbers in each mutant cell line should be determined, as receptor overexpression may alter coupling to discrete signalling pathways (Rohrer and Kobilka, 1998; Sarramegna et al., 2003; Wise et al., 2002). Due to time constraints, this was not completed. However, an enzyme-linked immunosorbent assay (ELISA) to quantify receptor protein would allow comparisons of receptor numbers and normalisation against WT expression levels. Second, assessment of allosteric interactions with DHPG at IP_1 accumulation and ERK1/2 phosphorylation is also required to allow comparisons of biased modulation between mutants. Again this was not completed due to time constraints, however, these experiments would provide

insight into residues driving functional affinity and/or cooperativity at alternate signalling pathways. Third, molecular dynamic stimulations via ligand docking to crystal structures would increase understanding of key residues implicated in ligand-receptor binding and activation. Current literature shows the residues chosen for this study cluster toward the base of the allosteric binding pocket – distinct from the overlapping $mGlu_1$ binding site – and form discrete hydrogen-water networks associated with receptor stability and activation (Christopher et al., 2015; Dore et al., 2014; Wu et al., 2014). These $mGlu_5$ crystal structures, however, represent an inactive and essentially static receptor, without N- and C-termini – thus limitations arise when assessing the movement of TM domains following receptor activation, as well as the interaction with G protein – itself an allosteric modulator (Christopher et al., 2015; Dore et al., 2014; Gregory et al., 2014). Nonetheless, solved receptor crystal structures provide an invaluable platform in understanding ligand-receptor pharmacology and would be an intuitive next step to understand ligand binding and receptor activation.

Overall, our study highlights key residues involved in $mGlu_5$ allosteric ligand binding, agonism and modulation, extending the literature to include the evaluation of IP_1 accumulation and pERK1/2 agonism. As biased agonism is operative in WT receptors, it is logical for mutagenesis studies to also assess ligand activity across multiple receptor endpoints, rather than simply the canonical signalling pathway. In doing so, we have delineated the residues involved in $mGlu_5$ iCa^{2+} mobilisation, IP_1 accumulation and pERK1/2 agonism, as well as residues influencing affinity, cooperativity and bias. Three key regions implicated in ligand agonism, affinity and cooperativity arose from our study – the hydrogen-water network, the analogous

"rotamer toggle switch", as well as the narrow bridge connecting the two hydrophobic binding pockets. Modifications of either of these regions resulted in significant changes in ligand activity – namely via changes in agonism and subsequent loss or gain of bias. Thus, our findings provide the foundations for optimised structure-activity relationships in the design of allosteric ligands with desirable pharmacological outcomes.

Chapter 5

$mGlu_5$ modulation of TRPV1 calcium responses in rat dorsal root ganglion neurons

5.1. Introduction

Tissue inflammation and injury cause glutamate release from sensory neurons, leading to an influx of inflammatory mediators and resultant increased sensitivity to noxious stimuli (deGroot et al., 2000; Jin et al., 2006; Lawand et al., 2000). Within the glutamatergic system, the group I metabotropic glutamate receptors (mGlu) are implicated in hyperalgesic effects (Karim et al., 2001; Walker et al., 2001). $mGlu_1$ and $mGlu_5$ are expressed on dorsal root ganglion (DRG) and trigeminal ganglion neurons, as well as unmyelinated nerve fibres (Bhave et al., 2001; Lee and Ro, 2007). Systemic injection of group I mGlu agonists results in increased thermal hyperalgesia, antagonists attenuate inflammatory pain (Bhave et al., 2001; Chung et al., 2015; Honda et al., 2017; Ren et al., 2012; Soliman et al., 2005), while peripheral injection of $mGlu_5$ antagonists ameliorates post-operative pain responses in rodents (Zhu et al., 2005). This thermal and mechanical hypersensitivity is linked to $mGlu_5$-mediated protein kinase C (PKC) protein phosphorylation (Chung et al., 2015; Honda et al., 2017; Lee and Ro, 2007). Thus, group I mGlus within primary afferent neurons provide an attractive drug target in the modulation of pain responses.

Co-expressed within DRG neurons and highly enriched in unmyelinated C-fibres, the transient receptor potential (TRP) vanilloid 1 (TRPV1) channel is a non-selective cation channel sensitive to temperatures greater than 43°C, low pH < 6.5 and irritants such as capsaicin and various lipids (Kobayashi et al., 2005; Nozadze et al., 2016; Schepers and Ringkamp, 2009). A global integrator of pain sensation within primary afferents (Caterina and Park, 2006), activation of TRPV1 channels initiates the influx of Ca^{2+} and Na^{+}, resulting in the release of tachykinin neuropeptides, including substance P and calcitonin-gene-related-peptide (CGRP) (Rosenbaum and Simon,

2007). These neuropeptides subsequently interact with resident immune and peripheral target cells, such as macrophages and endothelia, to induce the characteristic inflammatory response (Richardson and Vasko, 2002). TRPV1 phosphorylation via PKC, PKA and CaMKII sensitises the receptor to activation by capsaicin (Bhave et al., 2003; Jung et al., 2004; Rathee et al., 2002; Wang et al., 2015), while dephosphorylation of TRPV1 by calcineurin leads to a desensitised receptor state (Jung et al., 2004).

Previous studies have proposed direct activation of TRPV1 by $mGlu_5$ in presynaptic terminals within the rodent dorsal horn, with diacylglycerol produced from $mGlu_5$ stimulation mediating the coupling of $mGlu_5$ and TRPV1 receptors (Kim et al., 2009). Masuoka and colleagues further showed a biphasic modulatory effect of $mGlu_5$ activation on TRPV1-mediated calcium response, leading to transient thermal hyperalgesia followed by hypoalgesia in mice (Masuoka et al., 2015). Further, prolonged stimulation of DRG neurons with group I mGlu agonists increased the number of capsaicin-sensitive DRG neurons, thereby increasing sensitivity to noxious stimuli (Masuoka et al., 2016).

While studies involving $mGlu_5$ and TRPV1 have largely focused on prototypical orthosteric agonists and antagonists – namely the group I mGlu agonists glutamate, DHPG and quisqualate, the prototypical $mGlu_5$ negative allosteric modulator (NAM) MPEP, and the TRPV1 agonist capsaicin – little has been done involving other $mGlu_{1/5}$ allosteric modulators. As there is a clear relationship between group I mGlu and TRPV1 receptors, we aimed to probe the effects of various $mGlu_5$ allosteric ligands on TRPV1-mediated calcium responses. Furthermore, we extended the

TRPV1 agonist repertoire in this study to include endogenously expressing agonists (endovanilloids), as modulation of these ligands provides another layer of complexity, albeit opportunity, in targeting the multifaceted pain cascade. Overall, our study highlights the amenable nature of TRPV1 responses following incubation with $mGlu_5$ allosteric ligands within rat DRG neurons, with $mGlu_5$ activation offering a potential avenue in targeting TRPV1-mediated pain responses within the peripheral nervous system.

5.2. Materials and Methods

(*S*)-3,5-Dihydroxyphenylglycine (DHPG), 3-Cyano-*N*-(1,3-diphenyl-1*H*-pyrazol-5-yl)benzamide (CDPPB) and 7-(hydroxyimino)cyclopropa[b]chromen-1a-carboxylate ethyl ester (CPCCOEt) were purchased from Tocris Bioscience (Melbourne, Australia). All other reagents were purchased from Sigma-Aldrich (St. Louis, MO) and were of analytical grade, unless otherwise stated.

5.2.1. Animals

Adult male Wistar rats (approximately 200g, Charles River, UK) were group housed and maintained on a 12 hour light/dark cycle, with access to food and water *ad libitum*. All experiments were carried out in accordance with UK Home Office regulations (Scientific Procedures Act, 1986).

5.2.2. DRG preparation

5.2.2.1. Preparation of glass coverslips

Glass coverslips (19 mm diameter) were washed in 10% Decon (Decon Sciences) for a minimum of 2 h, before being rinsed twice in distilled water. Coverslips were then

soaked in 4 M HCl for 30 min and rinsed twice in distilled water, before air-drying overnight.

On the day of experimentation, coverslips were incubated with 100 μL sterile 0.1 mg/mL poly-D-lysine for 90 min at room temperature. Coverslips were washed once in distilled water and allowed to air dry. Laminin (1 mg/mL, 10 μL) was added to the centre of the coverslip and allowed to dry for 60 min, before being washed in distilled water and vacuum-dried before use.

5.2.2.2. Dorsal root ganglion (DRG) neuron preparation and culture

Adult male Wistar rats (weighing approximately 200 g) were sacrificed using cervical dislocation and decapitation. The dorsal surface of the rat was swabbed with industrial methylated spirits (IMS), and the fur and skin dissected to expose the underlying vertebral column. Cuts on either side of the vertebral column allowed removal of the spinal column onto a Petri dish containing Dulbecco's Ca^{2+} and Mg^{2+}-free phosphate buffered saline (PBS) (Sigma) at 37°C. Excess tissue and muscle was trimmed before an incision down the midline of the ventral plate revealed the spinal cord. The excised spinal cord allowed access to the DRGs, which were removed by incising peripheral and central trunks. Approximately 35 – 40 DRGs were collected per rat. Isolated DRGs were trimmed of excess spinal tissue and placed in a 15 mL falcon tubed filled with PBS. The DRGs were washed once under gravity and incubated in 5 mL Neurobasal media (Gibco) containing collagenase (2.5 mg/mL) supplemented with horse serum (10%), for 90 min at 37°C and 5% CO_2.

DRGs were then washed for a minimum of three times in PBS to allow the removal of the dorsal capsule and unwanted tissue debris. DRGs were then incubated in 2 mL trypsin (0.5x) at 37°C, 5% CO_2. After 30 min incubation, without disturbing the DRGs that settled to the base of the falcon tube, 1 mL trypsin solution was carefully removed, and 1 mL bovine serum albumin (BSA) solution (16% BSA in Hanks Balanced Saline Solution (HBSS) at pH 7.4) added to the DRG and trypsin mixture. This mixture was then triturated approximately 20 times, using a 1000 μL pipette, to form a cell suspension. The cell suspension was then carefully layered on top of 4 mL bovine serum albumin solution (16% BSA in HBSS, pH 7.4) and centrifuged (500 *g*, room temperature) for 6 min. The supernatant layer was aspirated and the remaining cell pellet was resuspended in 170 μL neurobasal media containing 50 mg/mL glial cell line-derived neurotropic factor (GDNF), 2 mM L-glutamine, 1 mg/mL nerve growth factor (NGF), 200 units/mL penicillin and 200 ng/mL streptomycin (complete media). 20 μL of the cell suspension was pipetted onto the centre of sterilised glass coverslips and incubated at 37°C, 5% CO_2 for a minimum 30 min to allow DRGs to adhere to the laminin and poly-D-lysine coating. Placing the DRGs on the centre of the coverslip ensured a dense population of cells within a small region, and increased the number of cells available for imaging within the chosen region of interest. 130 μL of complete media was then carefully pipetted around the DRG population and coverslips incubated overnight at 37°C, 5% CO_2 before experimentation the following day.

5.2.3. $mGlu_{1/5}$ ligand incubation

Drugs were dissolved in Ca^{2+} assay buffer (Hank's Balanced Salt Solution (HBSS; KCl 5.33 mM, KH_2PO_4 0.44 mM, $NaHCO_3$ 4.17 mM, NaCl 137.93 mM, Na_2HPO_4

0.34 mM, D-glucose 5.56 mM) with 16 mM HEPES, pH 7.4) in 0.3% DMSO. Capsaicin and NADA stocks were dissolved in 100% ethanol. Coverslips were washed in Ca^{2+} buffer and incubated with 2 mL of $mGlu_5$ drug solution at 37°C, 5% CO_2 for 30 min prior to washing, dye loading and calcium imaging (see below). MPEP, CDPPB and CPCCOEt (10 μM), DHPG (30 μM) and glutamate (30 μM) were studied. These concentrations were selected based on previous literature (Masuoka et al., 2016), as well as allowing for >90% receptor occupancy (approximately 10 x K_B estimates) (Sengmany et al., 2017). Capsaicin (100 nM), anandamide (AEA, 10 μM), oleoylethanolamide (OEA, 10 μM), and *N*-arachidonoyl-dopamine (NADA, 1 μM) were chosen as the endovanilloids studied, due to their commercial availability – allowing for robust replication of the experiments. The concentrations of endovanilloid studied were chosen based on an literature values of approximate EC_{50} response, allowing potentiation or inhibition of TRPV1 responses by $mGlu_5$ to be clearly observed (Ahern, 2003; Huang et al., 2002; Ross, 2003).

5.2.4. Fura-2AM cell loading

Intracellular calcium was visualised using the calcium sensitive dye Fura-2AM (L-[2-(carboxyoxazol-2-yl)-6-amino-benxofuran-5-oxy]-2-(2'-amino-5'-methylphenoxy)ethane-N,N,N,N-tetraacetic acid pentaacetoxymethylester). Cells were washed with Ca^{2+} assay buffer (HBSS as above, with 2.5 mM probenecid, pH 7.4) before incubation with 5 μL Fura-2-AM (1mg/mL) at 37°C for 30 min in reduced light conditions. Cells were then washed with Ca^{2+} assay buffer to remove extracellular dye, and coverslips kept in Ca^{2+} assay buffer for 15 min prior to experimentation to allow for cleavage by cellular esterases resulting in the active Fura-2 form.

5.2.5. Calcium imaging studies of DRG neurons

Intracellular calcium concentrations of individual DRG neurons were estimated as ratios of peak fluorescence emission intensities (measured at 500 nm) at excitation wavelengths of 340 and 380 nm using an Improvision imaging system. In the unbound form, Fura-2 has high excitation efficiency at 380 nm and low excitation efficiency at 340 nm. Upon calcium binding, Fura-2 fluoresces with high excitation efficiency at 340 nm and low excitation efficiency at 380 nm. The ratio between the two fluorescence intensities measured at both excitation wavelengths is quantified to give a ratiometric readout of calcium mobilisation. This ratiometric approach has the advantage of removing fluorophore uptake variability between cells, as well as intrinsic variability in primary cell culturing, such as uneven cell thickness. Diameters of DRG neurons chosen for the study were less than 35 μm, as estimated by Andor iQ Live Cell Imaging Software (Oxford Instruments), as these represented the smaller C-fibre neurons enriched with TRPV1 receptors.

Coverslips were fixed to a Perspex chamber using vacuum grease and DRGs were suprafused with Ca^{2+} buffer at 2 mL/min with TRPV1 receptor agonists capsaicin (100 nM), AEA (10 μM), OEA (10 μM) and NADA (1 μM) for 1 min followed by 45 min washout with Ca^{2+} buffer to allow DRG calcium responses to return to baseline. Following return to baseline levels, DRGs were suprafused with KCl 60 mM, to allow for maximal calcium influx as a positive control. Ratiometric responses were measured at 5 sec per frame.

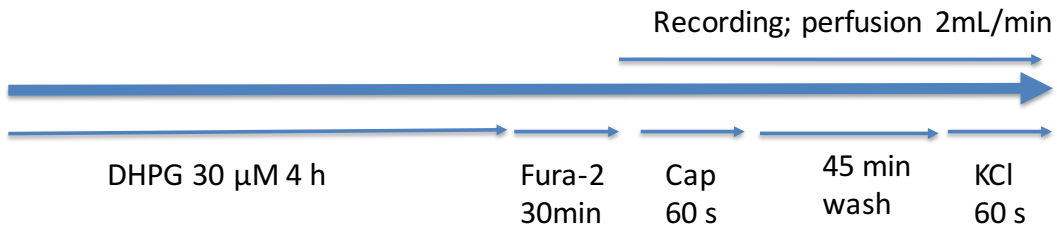

Fig 5.1. Summary of sample protocol used. DHPG is preincubated for 4 h on coverslips, followed by addition of Fura-2 dye then stimulation with capsaicin (Cap).

5.2.6. Data analysis

Calcium responses were measured as peak stimulated ratio (taken from 2 min post ligand addition) minus mean basal ratio (taken from 1 min prior to ligand addition). DRGs which showed less than 0.1 unit increase in ratio response following KCl addition were deemed unresponsive and hence excluded from analysis.

Changes in intracellular calcium mobilisation within each DRG neuron were expressed as a percentage of KCl response, and the number of responding cells were represented as a percentage of cells responding to KCl. Data are expressed as mean ± SEM. Statistical analysis was completed using one-way analysis of variance (ANOVA) with Dunnett's post-test to compare effects of $mGlu_5$ ligand incubation vs vehicle control on capsaicin or endovanilloid-mediated TRPV1 response in DRGs and number of DRG neurons responsive to capsaicin or endovanilloid stimulation.

For comparisons of peak calcium responses, each cell was defined as an individual 'n number', with experiments replicated with multiple rodents to give an overall experimental 'n number' (n=3 or more independent experiments). Statistical analyses were conducted comparing responses of individual cells collated across three or more independent experiments (i.e. 3 or more rats).

5.3. Results

While numerous studies have investigated DRG responses to capsaicin, little is known of endovanilloid modulation. Thus, for this study, we included several endogenously expressing TRPV1 agonists – anandamide (AEA), oleoylethanolamide (OEA) and *N*-arachidonoyl-dopamine (NADA) (Fig 5.2). Because these ligands are endogenously available within a (patho)physiological context, modulation of these compounds provides a favourable opportunity in targeting pain responses.

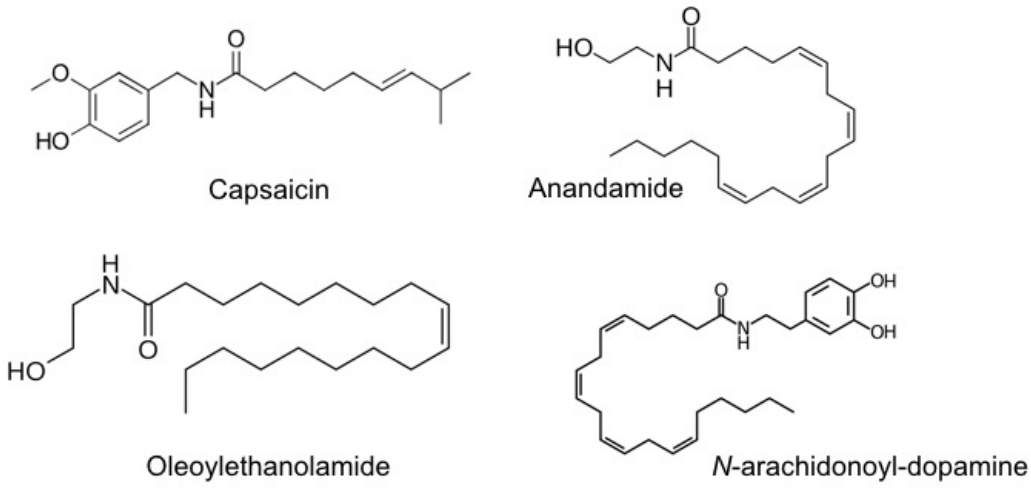

Fig 5.2. Structures of TRPV1 agonists used in this study. Capsaicin is the prototypical TRPV1 agonist. Anandamide, oleoylethanolamide and *N*-arachidonoyl-dopamine are endogenous agonists of TRPV1 (endovanilloids).

The endogenous mGlu receptor agonist glutamate, and the mGlu$_{1/5}$ orthosteric agonist DHPG were selected to evaluate effects of prolonged mGlu$_{1/5}$ activation on TRPV1 iCa^{2+} responses. An mGlu$_1$ NAM, CPCCOEt, mGlu$_5$ NAM, MPEP and mGlu$_5$ PAM-agonist, CDPPB were also assessed to provide a greater picture of mGlu modulatory activity of TRPV1 responses. The protocol of prolonged incubation, i.e. incubation of mGlu ligands for 4 h prior to stimulation with TRPV1 agonist, was chosen as

glutamate levels are known to remain elevated for over 3 h during inflammation (Omote et al., 1998).

5.3.1. Effects of capsaicin, AEA, OEA and NADA on intracellular calcium responses in adult rat dorsal root ganglion neurons.

Representative calcium traces of four individual DRG neurons on the same coverslip are shown in figure 5.3, whereby ligands were perfused for 1 min, followed by a minimum 45 min washout to allow calcium responses to return to basal levels. It should be noted that individual DRG neurons showed large variability in peak iCa^{2+} responses following ligand addition - for instance, the cell represented by the red trace was the only one that responded to the first OEA addition; three other cells showed minimal responses, while addition of AEA resulted in iCa^{2+} mobilisation in only two of the four cells shown – despite the four DRG neurons being derived from the same animal. This observation highlights the often variable nature of using primary cells.

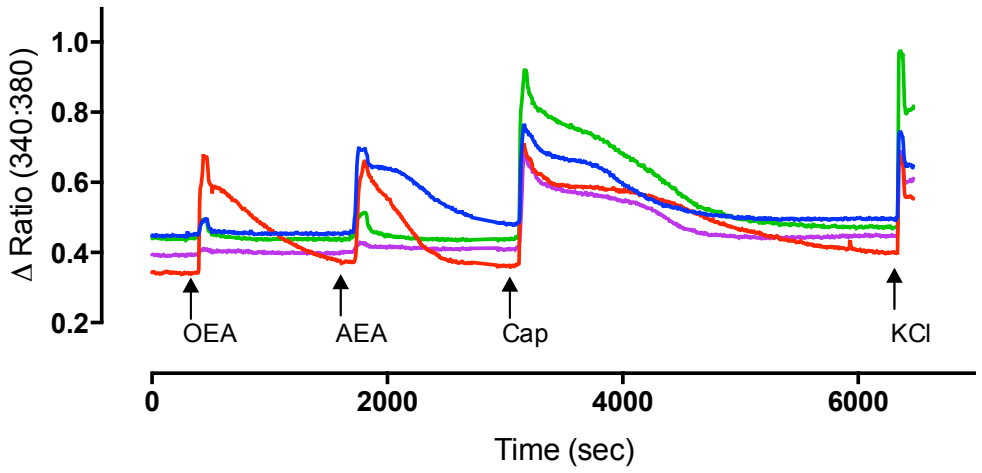

Fig 5.3. Representative traces showing changes in 340:380 ratios of four individual DRG neurons in response to addition of OEA (10 μM), AEA (10 μM), capsaicin (100 nM) and KCl (60 mM), within the same individual coverslip. Ligands were perfused for 1 min, followed by a washout with calcium assay buffer for a minimum of 45 min to allow iCa^{2+} responses to return to basal levels.

In untreated DRG neurons, the 340/380 nm ratio (reflecting basal intracellular calcium concentration [iCa^{2+}]) was 2% KCl (60 mM) response (n=308 cells from 6 independent experiments). Capsaicin was used as a positive control for TRPV1 expressing DRG neurons, with a concentration of 100 nM producing 108% KCl response (Fig 5.4A, table 1).

Of the studied endovanilloids, an approximately EC_{50} concentration was chosen from literature values to allow for either positive or negative modulation by the studied mGlu ligands (Ahern, 2003; Huang et al., 2002; Ross, 2003). AEA and OEA at 10 μM produced 66% and 56% KCl response respectively, while 1 μM NADA reached a maximum of 89% KCl response (Figure 5.4B-D, table 5.1).

5.3.2. Long-term activation of $mGlu_{1/5}$ by the orthosteric agonists glutamate and DHPG increased OEA-mediated iCa^{2+} responses but not those to capsaicin or AEA.

The effect of extended stimulation of $mGlu_{1/5}$ ligands on TRPV1 evoked iCa^{2+} responses was evaluated in DRG neurons following 4 h incubation in calcium assay buffer containing glutamate or DHPG (30 μM) (Masuoka et al., 2016). Glutamate pre-incubation resulted in a significant increase in OEA-mediated iCa^{2+} responses, to reach responses similar to KCl (Fig 5.4C, table 5.1), while having no significant effect on capsaicin or AEA responses (Fig 5.4A-B).

The $mGlu_{1/5}$ orthosteric agonist DHPG also had no significant effects on responses to capsaicin, AEA and OEA following 4 h pre-incubation, although calcium responses were perhaps saturated with capsaicin 100 nM (~100% KCl response), and thus resulting in minimal observable increases following $mGlu_{1/5}$ agonism.

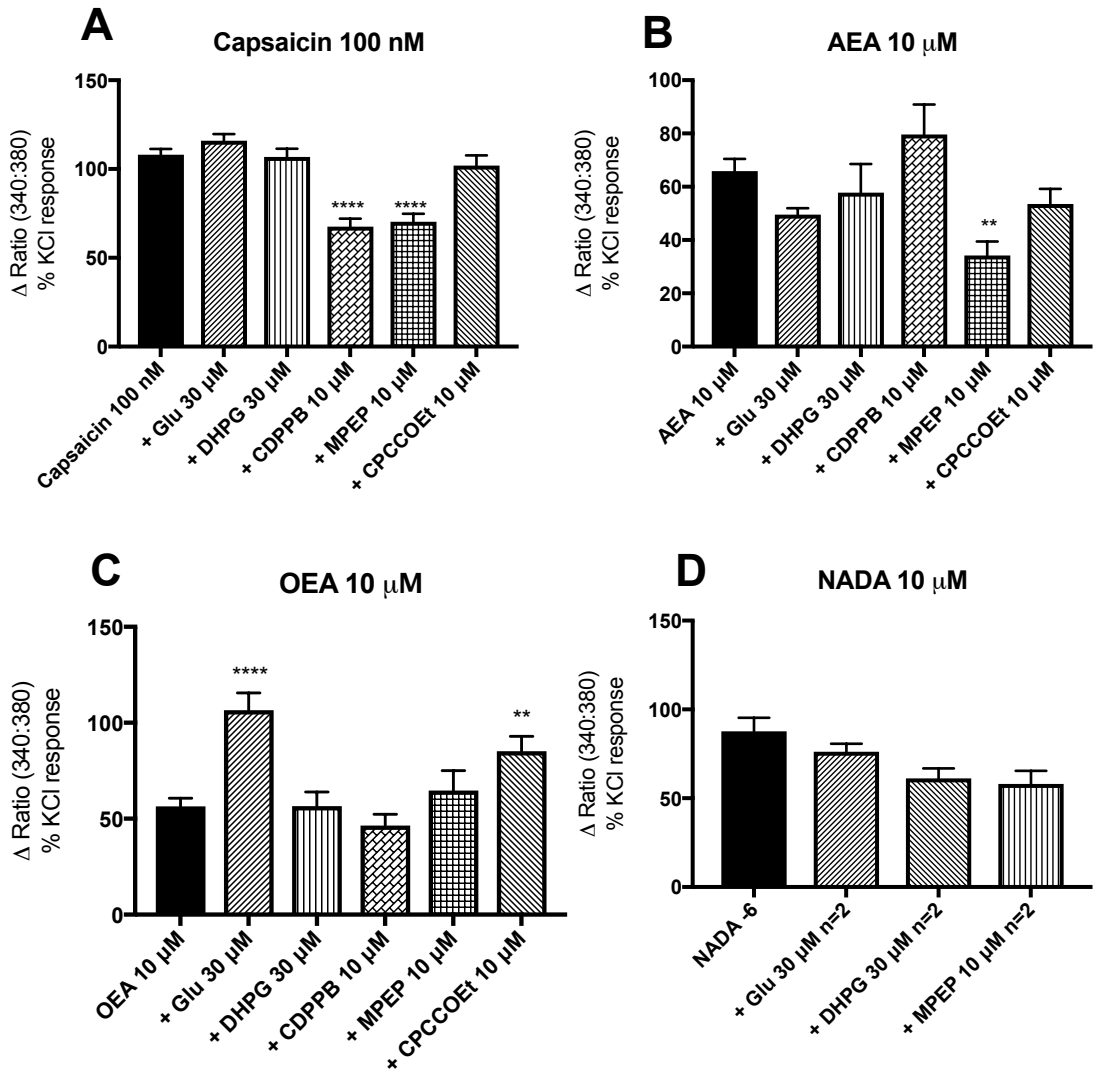

Fig 5.4. Effect of 4 h pre-incubation of mGlu$_{1/5}$ ligands on capsaicin and endovanilloid-mediated iCa^{2+} mobilisation in rat DRG neurons, normalised to KCl response. DRG neurons were pre-incubated with glutamate 30 μM, DHPG 30 μM, CDPPB 10 μM, MPEP 10 μM or CPCCOEt 10 μM before stimulation with 100 nM capsaicin (A), 10 μM AEA (B), 10 μM OEA (C) or 10 μM NADA (D). Peak iCa^{2+} responses were measured as fluorescent ratio of 340:380, normalised to KCl 60 mM responses. Data shown represent mean ± SEM of 30-200 cells from 3-10 independent experiments unless stated otherwise. Comparisons to responses evoked by endovanilloid alone were analysed using one-way ANOVA, Dunnett's post-test; **** p<0.0001, ** p<0.005 (see 5.2.6. for details of analysis).

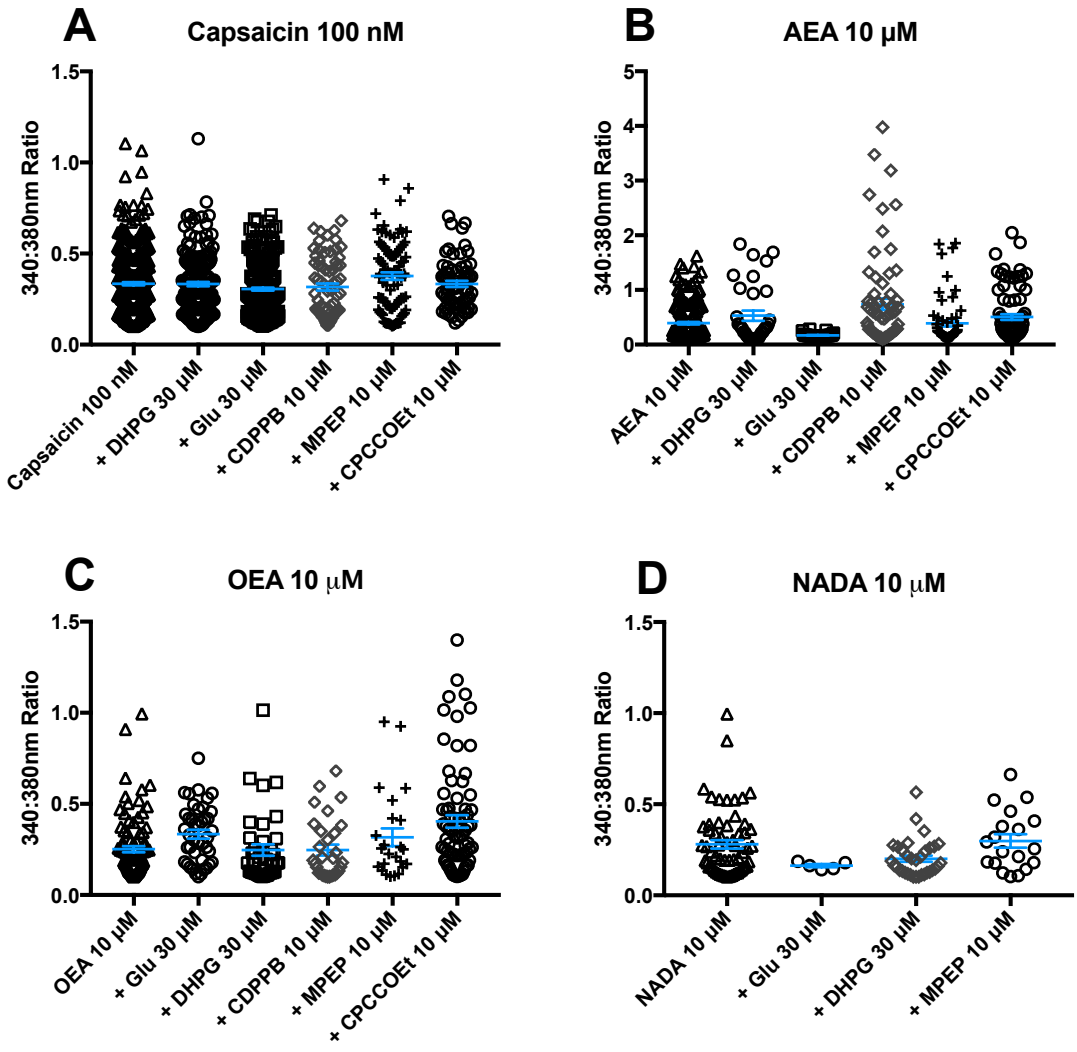

Fig 5.5. Effect of 4 h pre-incubation of $mGlu_{1/5}$ ligands on capsaicin and endovanilloid-mediated iCa^{2+} mobilisation in rat DRG neurons, expressed as 340:380 fluorescence ratio. DRG neurons were pre-incubated with glutamate 30 µM, DHPG 30 µM, CDPPB 10 µM, MPEP 10 µM or CPCCOEt 10 µM before stimulation with 100 nM capsaicin (A), 10 µM AEA (B), 10 µM OEA (C) or 10 µM NADA (D). Peak iCa^{2+} responses were measured as fluorescent ratio of 340:380. Data shown represent mean ± SEM (represented in blue) of 30-200 cells (represented by each point) from 3-10 independent experiments unless stated otherwise.

5.3.3. Prolonged incubation with the prototypical $mGlu_5$ NAM, MPEP, decreased capsaicin and AEA-mediated iCa^{2+} responses but had no effect on OEA.

MPEP was chosen for this study as it is the prototypical $mGlu_5$ NAM, and has previously been shown to ameliorate rodent pain responses mediated by capsaicin, as well as to reduce capsaicin-induced iCa^{2+} mobilisation in DRG neurons (Kim et al., 2009; Masuoka et al., 2016; Picker et al., 2011; Soliman et al., 2005). This effect was confirmed in our study, with a significant reduction in peak capsaicin-induced iCa^{2+} influx relative to vehicle control (108% to 70% KCl response; Fig 5.4A, table 5.1).

Prolonged MPEP stimulation also resulted in a decrease in AEA (10 μM) responses, from 66% to 34% KCl response (Fig 5.4B, table 5.1). A similar trend was observed with NADA (1 μM), with MPEP pre-incubation leading to an approximate 30% decrease in peak iCa^{2+} mobilisation, although statistical analyses were not performed due to insufficient independent experiments. There was no significant change in OEA-mediated iCa^{2+} response in the absence and presence of MPEP stimulation, with comparable peak iCa^{2+} responses at 56% and 64% KCl response, respectively (table 5.1). It should be noted however, that comparison of baseline corrected 340:380 ratios, not normalised to KCl responses, did not produce any significant changes in calcium responses mediated by endovanilloids, following mGlu ligand incubation (Fig 5.5).

5.3.4. Prolonged stimulation with the $mGlu_5$ PAM-agonist CDPPB reduced capsaicin responses, while the $mGlu_1$ NAM CPCCOEt increased OEA-mediated iCa^{2+} mobilisation.

Pre-incubation with the $mGlu_5$ PAM-agonist CDPPB produced a 40% decrease in capsaicin-evoked iCa^{2+} responses (Fig 5.4A, table 5.1), while having no significant effect on OEA-mediated responses. There was however a 13% increase in peak iCa^{2+} following AEA stimulation relative to vehicle control, although this failed to reach statistical significance.

The $mGlu_1$ NAM CPCCOEt, while having no effect on capsaicin and AEA-mediated iCa^{2+} activity, resulted in a significant increase in OEA evoked responses following 4h pre-incubation. Peak OEA iCa^{2+} responses increased from 56% to 85% KCl response following prolonged stimulation with 10 μM CPCCOEt (Fig 5.4C, table 5.1).

Table 5.1. Summary of peak iCa^{2+} responses (Ratio 340:380 normalised to % KCl peak response) following endovanilloid stimulation with 4 h preincubation of mGlu ligands or vehicle control. Data are expressed as mean ± SEM of 5 – 406 cells from 3 -11 independent experiments, unless otherwise specified.

	Vehicle		**+ Glu 30 μM**		**+ DHPG 30 μM**		**+ CDPPB 10 μM**		**+ MPEP 10 μM**		**+ CPCCOEt 10μM**	
	Peak iCa^{2+} (%KCl)	**n (exps)[#]**	**Peak iCa^{2+} (%KCl)**	**n (exps)[#]**	**Peak iCa^{2+} (%KCl)**	**n (exps)[#]**	**Peak iCa^{2+} (%KCl)**	**n (exps)[#]**	**Peak iCa^{2+} (%KCl)**	**n (exps)[#]**	**Peak iCa^{2+} (%KCl)**	**n (exps)[#]**
Capsaicin 100 nM	108.1±3.3	406 (11)	115.9±3.8	264 (8)	106.8±4.6	186 (7)	67.5±4.5 [a]	70 (3)	70.3±4.5 [a]	88 (3)	102.0±5.7	67 (3)
AEA 10 μM	65.9±4.6	195 (9)	49.5±2.4	37 (3)	57.8±10.8	34 (3)	79.7±11.2	71 (3)	34.2±5.3 [a]	63 (4)	53.5±5.6	85 (4)
OEA 10 μM	56.4±4.3	93 (6)	106.6±9.0 [a]	42 (5)	56.5±7.5	38 (3)	46.5±5.7	31 (3)	64.7±10.3	24 (4)	85.1±7.8 [a]	73 (5)
NADA 1 μM	87.7±7.6	62 (4)	76.2±4.5	5 (2)	61.2±5.7	34 (2)	n.d.	n.d.	58.1±7.4	19 (2)	n.d.	n.d.

n.d. not determined due to time constraints

[a] *p<0.05* comparing iCa^{2+} responses to vehicle control (one-way ANOVA, Dunnett's post-test)

n is the total number of responding cells, 'exps' is the number of independent experiments from individual donor animals

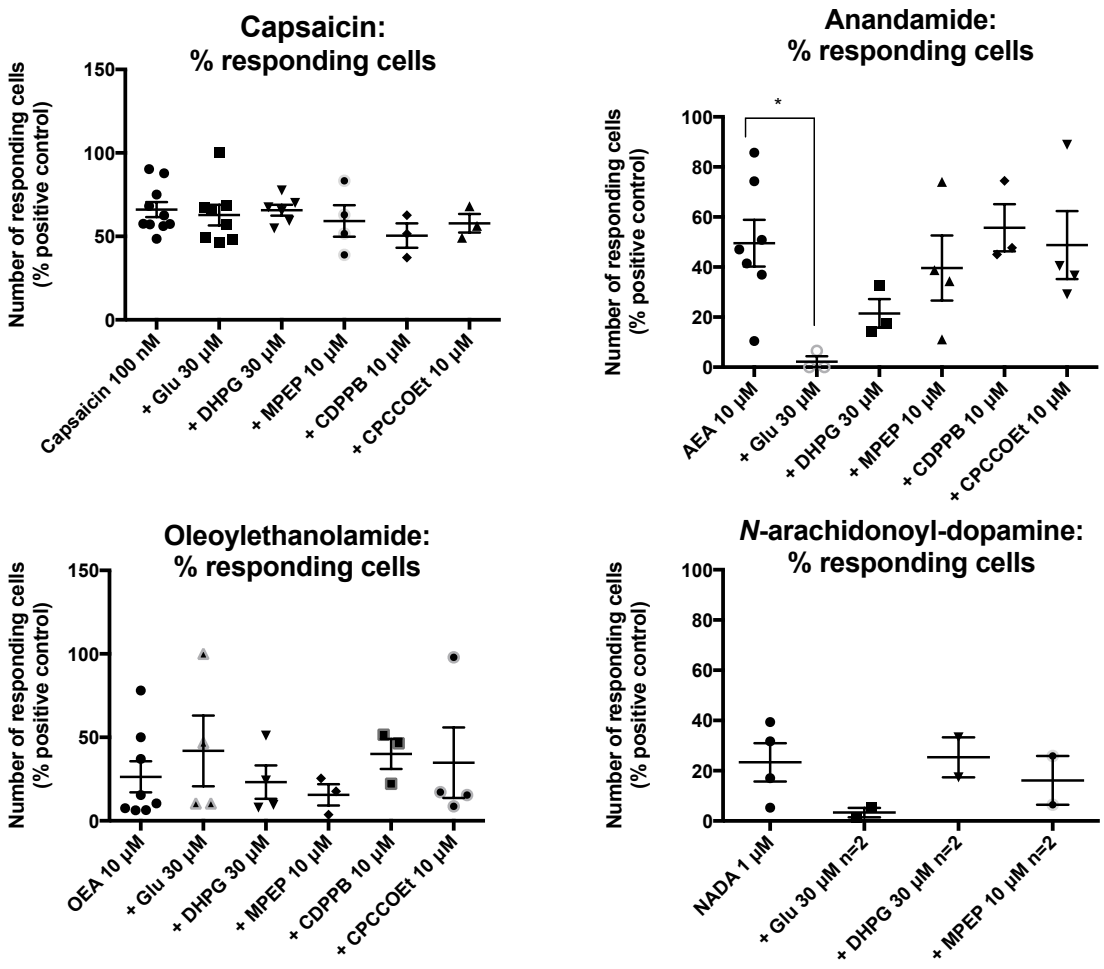

Fig 5.6. Number of cells responding to capsaicin or endovanilloid stimulation following pre-incubation with mGlu$_{1/5}$ ligands. Each symbol represents the results from a single donor animal, with the y-axis depicting the number of cells per coverslip responding to ligand stimulation, expressed as a percentage of the number of cells responding to the positive control 60 mM KCl. Data are expressed as mean ± SEM of 3-11 independent experiments unless otherwise specified. Comparisons to number of cells responding to endovanilloid alone were analysed using one-way ANOVA, Dunnett's post-test; * p<0.05 (see 5.2.6. for details of analysis).

Table 5.2. Number of responding cells (% cells responding to KCl) following endovanilloid stimulation with 4 h preincubation of mGlu ligands or vehicle control. Data are expressed as mean ± SEM of 5 – 406 cells from 3 -11 independent experiments, unless otherwise specified.

	Vehicle	**+ Glu 30 μM**	**+ DHPG 30 μM**	**+ CDPPB 10 μM**	**+ MPEP 10 μM**	**+ CPCCOEt 10μM**
Capsaicin 100 nM	66.1±4.5	62.8±6.2	65.7±3.3	50.5±7.4	59.2±9.4	57.9±5.5
AEA 10 μM	49.5±9.4	2.2±2.2	21.5±5.7	55.7±9.4	39.6±13.0	48.8±13.6
OEA 10 μM	26.4±9.3	41.9±21.2	23.2±9.9	40.1±9.0	15.6±6.4	34.8±21.1
NADA 1 μM	23.4±7.6	3.3±1.9^	25.4±8.0[#]	n.d.	16.2±9.7[$]	n.d.

^ n=5 individual cells from two independent experiments from two individual donor animals
# n=34 individual cells from two independent experiments from two individual donor animals
[$] n=19 individual cells from two independent experiments from two individual donor animal

5.3.5. Prolonged incubation with glutamate significantly decreased the population of AEA-sensitive DRG neurons, while all $mGlu_{1/5}$ ligands studied had no effect on other TRPV1 agonists.

Previous studies highlighted that prolonged $mGlu_5$ stimulation with 30 μM glutamate significantly increased the proportion of capsaicin-sensitive DRG neurons (Masuoka et al., 2016). We were unable to replicate these findings, and found no significant changes in the number of capsaicin-sensitive DRG neurons following pre-incubation with the $mGlu_5$ agonists DHPG and CDPPB, as well as the $mGlu_{1/5}$ NAMs MPEP and CPCCOEt (Fig 5.6A, table 5.2).

Moreover, we observed no significant differences in the number of cells responding to OEA and NADA following $mGlu_{1/5}$ ligand incubation (Fig 5.6C-D). Prolonged glutamate incubation, however, resulted in a significant reduction in the number of cells responding to AEA, with only 4 out of 95 cells responding across 3 independent experiments. No significant changes in the number of cells responding to AEA were observed with pre-incubation of the other studied ligands (Fig 5.6B, table 5.2).

5.4. Discussion

In this study, we evaluated the effects of prolonged $mGlu_{1/5}$ stimulation by various orthosteric and allosteric $mGlu_{1/5}$ ligands on capsaicin or endovanilloid-mediated intracellular calcium mobilisation in rat DRG neurons. We found that 4 h incubation with the $mGlu_5$ NAM MPEP significantly decreased capsaicin and AEA evoked iCa^{2+} fluorescence, while having no discernable effects on OEA. Prolonged stimulation with the $mGlu_1$ PAM agonist CDPPB also decreased capsaicin responses, while glutamate and the $mGlu_1$ NAM CPCCOEt increased OEA-mediated iCa^{2+} responses. Furthermore, the population of AEA-sensitive DRG neurons following prolonged glutamate stimulation significantly decreased. No other changes were observed with other endovanilloids or capsaicin in combination with other mGlu ligands. Thus, we show here that endogenous TRPV1 agonists, not only capsaicin, are responsive to modulation by mGlu ligands – thereby offering a potential therapeutic opportunity for modulation of TRPV1-mediated pain responses.

While TRPV1 studies have largely focused on capsaicin-induced responses, we expanded our study to include modulation of putative endogenous TRPV1 agonists – the fatty acid derivatives anandamide (AEA) and *N*-arachidonyl dopamine (NADA) (Devane et al., 1992; Di Marzo and De Petrocellis, 2010; Marinelli et al., 2007), and the satiety factor oleoylethanolamide (OEA) (Ahern, 2003). While anandamide has many reported antinociceptive effects mediated through the central cannabinoid system (Clapper et al., 2010), within DRG neurons, TRPV1 and not CB_1 receptors have been suggested to be involved in anandamide-induced calcium responses (Jerman et al., 2002). NADA, an endogenous capsaicin-like compound also possessing cannabinoid activity, was shown to act via TRPV1 receptors within DRG

neurons, with antagonism of TRPV1 responses abolishing NADA-evoked depolarization and calcium responses (Sagar et al., 2004). Thus, since cannabinoid receptors are expressed on DRG neurons (Ahluwalia et al., 2000), these two endovanilloids are able to act on both cannabinoid CB_1 and TRPV1 to provide a balance in pain pathology (Hong et al., 2009; Malek et al., 2015; Starowicz et al., 2012). OEA, on the other hand, is reported to be an agonist of the peroxisome proliferator-activated receptor-alpha (PPAR-α); its synthesis within the gastrointestinal tract associated with feeding behaviours provides evidence for a biological role in satiety to balance the orexigenic effects of AEA (Petersen et al., 2006; Thabuis et al., 2008). In terms of pain pathology, however, the effects of OEA remain ambiguous. In sensory neurons, OEA was shown to activate TRPV1 in a PKC-dependent manner, as well as cause visceral pain upon administration in mice (Ahern, 2003; Wang et al., 2005). However, other studies have reported analgesic effects in visceral and inflammatory pain models (Almási et al., 2008; Suardíaz et al., 2007). Interestingly, Almasi and colleagues reported OEA to be an antagonist of TRPV1, with concentration-dependent inhibition of capsaicin-evoked calcium influx in HT5-1 cells expressing TRPV1 (Almási et al., 2008). In our study, however, 10 μM OEA resulted in robust iCa^{2+} mobilisation. Thus, overall, the inclusion of these endovanilloids in this study also provides insight into the complex relationship between TRPV1, cannabinoid and mGlu receptors. Due to the amalgamation of several receptors indirectly modulating TRPV1, it is often referred to as an integrator molecule of polymodal nociceptors (Caterina and Park, 2006).

As mentioned above, glutamate is known to sensitise TRPV1 channels, thereby causing hyperalgesia (deGroot et al., 2000; Jin et al., 2006; Lawand et al., 2000). In

contrast to these studies, we found no significant differences in capsaicin-evoked calcium mobilisation following glutamate stimulation. This, however, is likely due to the studied concentration of capsaicin having a maximal system response (Millns et al., 2001), resulting in the inability to potentiate TRPV1 calcium mobilisation further. Glutamate pre-incubation, however, significantly increased the OEA-mediated calcium response, while having no significant effect on anandamide responses. This negative result may not tell the whole story, as when comparing the number of neurons sensitive to anandamide post-glutamate stimulation, there was a significant decrease of AEA-sensitive neurons – suggestive of potential desensitisation mechanisms, rather than diminishing functional calcium responses. Waning calcium responses over time e.g. comparing the first capsaicin-evoked maximal calcium response with the final KCl response, may further be indicative of receptor desensitisation. Indeed, the initial addition of 100 nM capsaicin produced a supramaximal calcium response – however this may simply be due to normalisation against the desensitised and hence lower KCl response. Without normalising to KCl, however, no significant changes in endovanilloid response were observed. The small proportion of neurons that retained AEA sensitivity following glutamate stimulation, however, still had calcium activity levels similar to that of AEA in the absence of glutamate incubation. Hence, downregulation or desensitisation of receptor numbers, rather than individual receptor responses, may provide an interesting therapeutic avenue in the treatment of pain – in particular following prolonged administration of therapeutics. Future studies may also include excitotoxicity experiments to assess the effect of prolonged glutamate stimulation on AEA-sensitive DRG neurons.

Unexpectedly, CDPPB, an $mGlu_5$ allosteric agonist of iCa^{2+} mobilisation, IP_1 and pERK1/2 (Lindsley et al., 2004; Sengmany et al., 2017), produced diminished capsaicin-evoked iCa^{2+} influx – a result contradictory to the TRPV1 sensitisation seen with the agonist glutamate. A potential explanation of this response may be the biphasic modulation of TRPV1 calcium responses by $mGlu_5$ – with activation resulting in transient hyperalgesia followed by hypoalgesia (Masuoka et al., 2015). This is in line with the desensitisation mechanism of TRPV1 following prolonged activation – a mechanism manipulated in commercial topical capsaicin pain therapies (Vyklicky et al., 2008).

$mGlu_5$ inhibition, on the other hand, ameliorates capsaicin-mediated responses both *in vivo* and in native cells (Bhave et al., 2001; Masuoka et al., 2015; Osikowicz et al., 2008; Walker et al., 2001; Zhu et al., 2005). Our results confirm the anti-nociceptive effects of the $mGlu_5$ NAM MPEP, as seen through diminished capsaicin and anandamide-evoked calcium responses in DRG. However, MPEP had no significant impact on OEA-mediated responses. Rather, the $mGlu_1$ NAM CPCCOEt was seen to increase OEA-mediated responses. While $mGlu_1$ receptors are expressed within DRGs, albeit at low levels (Carlton and Hargett, 2007), $mGlu_1$ inhibition would presumably inhibit its canonical G_q pathway – and consequently diminish PKC and desensitise TRPV1. Our contrasting result of enhancement of OEA-evoked calcium response following $mGlu_1$ inhibition highlights the ambiguous pharmacology of this endovanilloid, and ultimately the complex nature of the pain cascade.

For future studies, to better define the effects of TRPV1 alone, CB_1 antagonists may be applied to minimise not only effects of AEA on CB_1, but also the effects of CB_1 on

TRPV1 responses. Furthermore, adjunct addition of PKC inhibitors with endovanilloids will allow mechanistic evaluation of $mGlu_5$ effects on TRPV1 responses. Indeed, PKC appears an important mediator in sensitising TRPV1 responses, not only to capsaicin, but also to OEA and AEA (Ahern, 2003; Bhave et al., 2003; Jung et al., 2004; Rathee et al., 2002; Ross, 2003; Wang et al., 2015).

Further, while our approach of long term pre-incubation with mGlu ligands is due to the notion of elevated glutamate levels within the site of injury (Omote et al., 1998), co-incubation assays e.g. applying mGlu ligand and endovanilloid concurrently, would also be invaluable in assessing acute effects of mGlu activation on TRPV1 calcium response. The biphasic hyper- and hypoalgesic responses induced by TRPV1 (Masuoka et al., 2015), as well as altered neuronal sensitivity to capsaicin following glutamatergic stimulation (Masuoka et al., 2016) suggests pharmacological changes over time – thus comparisons of acute and chronic assays may provide insight into the discrete pain physiology, as well as potential therapeutics.

Overall, this study reiterates the potential role of mGlu receptors in pain therapies, via modulation of TRPV1-mediated calcium influx. Moreover, this study also highlights the complex nature of pain pathology. Current equivocal evidence of the role of endovanilloids in regulating pain responses must first be delineated before we are able to design drugs to modulate either cannabinoid or vanilloid receptor systems (or both). Nonetheless, preclinical studies demonstrating analgesia with $mGlu_5$ inhibition illustrates the promise of $mGlu_5$ pain therapies, and prompts further study of the role of $mGlu_5$ in pain pathology.

Chapter 6

General discussion

6. General discussion

G protein-coupled receptors (GPCRs), the largest family of cell surface proteins, remain one of the most tractable target classes in drug design and discovery. Classical pharmacological strategies in targeting orthosteric binding sites have produced agonists, competitive antagonists and inverse agonists, several of which have successfully progressed into clinic (Bridges and Lindsley, 2008; Lagerstrom and Schioth, 2008; Overington et al., 2006). However, as understanding of GPCR pharmacology expands, newer paradigms in drug discovery have emerged and subsequently influenced the direction of drug development (Christopoulos, 2014; Jacobson, 2015; Wootten et al., 2013). This thesis focuses on two main paradigms in GPCR pharmacology – allosterism and biased signalling – at the metabotropic glutamate receptor subtype 5 ($mGlu_5$). These two paradigms arise from the increased appreciation of the structure and fluidity of GPCRs, and the perhaps almost infinite potential receptor conformations – such that binding of an allosteric compound may modulate endogenous ligand-receptor responses (Changeux and Christopoulos, 2016; Christopoulos and Kenakin, 2002; Gregory et al., 2010). Further, as pleotropic G protein-coupling becomes widely observed, biased signalling, whereby ligands are able to stabilise distinct receptor conformations to provide a discrete subset of cellular responses (Kenakin and Christopoulos, 2013), will become either a challenge, or rather, a valuable opportunity to design therapeutics that target not only the desired receptor subtype, but also the desired signalling pathway at the target receptor.

The design of drugs that target allosteric sites overcomes several disadvantages of orthosteric ligands. First, due to the less conserved nature of allosteric sites, off-target adverse effects are limited – although perhaps not eliminated, due to interactions with

other proteins within the complex physiological system. Second, allosteric ligands are able to modulate endogenous ligand responses, such that receptor outcomes may be "fine-tuned" to desired levels – again minimising adverse effects, in particular within the delicate CNS environment. Third, allosteric ligands offer a better safety profile over orthosteric ligands due to a saturable "ceiling effect", as well as the requirement of an orthosteric ligand for activity in the case of "pure" modulators (Keov et al., 2011; Langmead and Christopoulos, 2014). Indeed, the concept of allosterism in GPCR drug design has been validated through two currently marketed allosteric drugs that target GPCRs – cinacalcet and maraviroc – a calcium sensing receptor PAM and a C-C chemokine receptor 5 NAM respectively (Dorr et al., 2005; Harrington and Fotsch, 2007).

Biased signalling adds further texture to drug development, through targeting desired receptor pathways, hence minimising 'on-target' adverse effects. Biased ligands may be agonists/partial agonists/inverse agonists, which activate a distinct subset of signalling pathways, or modulators, which influence the degree of orthosteric ligand activity to different extents at different pathways (Kenakin and Christopoulos, 2013; Langmead and Christopoulos, 2014; Lindsley et al., 2016). As further proof of feasibility in drug design, two currently marketed drugs, the antipsychotic, aripriprazole and the β-blocker carvedilol are proposed to be biased ligands (Klein Herenbrink et al., 2016; Urban et al., 2007; Wisler et al., 2007). However, while biased signalling provides exciting opportunities to create exquisitely targeted drugs, numerous challenges arise – from early stage drug discovery campaigns, to later translational *in vivo* stages.

A key element in early stage drug development is high throughput screening of potential "hit" compounds often determined from large chemical libraries. Here, hundreds of thousands of compounds are commonly screened at one canonical receptor signalling pathway, and based on derived potencies, are either discarded, or moved further along the drug discovery cascade. Additionally, compounds may be assessed in either PAM or NAM mode, that is, with an EC_{20} or EC_{80} concentration of orthosteric ligand, with potencies derived, and compounds retained or discarded (Lindsley et al., 2016). Several caveats arise from this protocol. First, while logistically, this method provides a quick snapshot into ligand activity, the assessment of only one signalling pathway results in immense loss of pharmacological information at other receptor signalling endpoints. Indeed, this was particularly highlighted in Chapter 2, whereby $mGlu_5$ allosteric ligands, largely classified as PAM or PAM-agonists of glutamate-mediated iCa^{2+} mobilisation, were shown to have exceptionally variable agonism at other signalling pathways. VU29 and VU0360172, for example, described as "pure" PAMs of glutamate/DHPG-mediated iCa^{2+} mobilisation, displayed robust IP_1 accumulation and pERK1/2 agonism, while the partial agonist VU0424465 of iCa^{2+} mobilisation, was a full agonist of both IP_1 accumulation and pERK1/2 phosphorylation. Thus, the absence of assessment along other signalling pathways excludes precious insight into true ligand pharmacology, and subsequent potential therapeutic avenues.

Second, allosteric modulator potencies derived from titration of a single orthosteric ligand concentration (EC_{20} or EC_{80}) are heavily dependent on the chosen orthosteric agonist concentration, as well as coupling efficiency between agonist and system; also, potency values represent a composite of affinity, efficacy, as well as

cooperativity (Kenakin, 2004; Kenakin and Christopoulos, 2011). Consequently, variation may be observed between potencies and ligand binding and intrinsic efficiency. Indeed, this was particularly highlighted with $mGlu_5$ PAMs, with up to 86% of studied PAMs showing potency estimates over three times binding affinity estimates (Lindsley et al., 2016). To overcome this issue, robust analysis of pharmacological responses must be determined. Rigorous quantitative assessment of agonism was performed throughout this thesis using the method proposed by Kenakin *et al*. (2012), to derive a composite value of ligand intrinsic efficacy and affinity – the transduction coefficient. Bias was determined through normalisation to a reference ligand – DHPG – and comparisons between different receptor signalling pathways. Allosteric modulation parameters were quantitatively determined using the operational model of allosterism (Leach et al., 2007), to derive functional affinity and cooperativity. Indeed, differences between potencies and transduction coefficients were particularly emphasised in Chapter 4, whereby mutations of residues resulted in reduced maximal responses, and altered potencies of DHPG relative to WT responses, however transduction coefficients remained unchanged. The same effect was observed with allosteric ligands, with smaller response windows (reduced E_{max}) relative to WT, despite no distinct changes in overall ligand agonism. Robust assessment of allosteric modulation has also allowed identification of biased allosteric modulation, whereby changes in affinity and/or cooperativity were observed with allosteric ligands across distinct receptor endpoints. This method was applied in both Chapter 2 and 3, through assessment of modulation bias between iCa^{2+} mobilisation, IP_1 accumulation and ERK1/2 phosphorylation of a suite of $mGlu_5$ chemotypes. Indeed, biased agonism as well as biased modulation was shown to be operative at the

$mGlu_5$ receptor, with numerous $mGlu_5$ PAMs, PAM-agonists and NAMs across both recombinant and neuronal cell backgrounds.

While assessment across the broadest range of receptor signalling outcomes is desirable to determine full ligand pharmacology – a balance is required between time, cost and pharmacological information derived. In this thesis, iCa^{2+} mobilisation, IP_1 accumulation and ERK1/2 phosphorylation were selected as $mGlu_5$ receptor outcomes, due to ease of reproducibility, as well as the importance of these endpoints in neuronal signalling, development and disease pathophysiology, ranging from cognitive deficits to addiction, autism and neuropathic pain (Berridge, 1998; Brini et al., 2014; Osterweil et al., 2010; Potter et al., 2013; Ribeiro et al., 2010b; Schroeder et al., 2008; Seese et al., 2014; Vincent et al., 2016). While there are undoubtedly numerous other receptor endpoints, such as G_q-mediated activation of PKA, or potential β-arrestin recruitment, it would be unfeasible to assess ligand pharmacology across all pathways. Thus, the relationship between receptor outcome and (patho)physiology must be determined for fruitful bias drug discovery campaigns. Indeed, at adenosine A_1 (Baltos et al., 2016) and μ-opioid receptors (Thompson et al., 2015), where receptor signalling endpoints have been closely aligned with pathophysiological and/or therapeutic outcome, clustering of ligands based on signalling fingerprints could fill the gap between ligand structure and receptor function – thereby aiding the design of biased ligands. However, in the absence of direct correlation between receptor signalling and *in vivo* efficacy, there is the risk of excluding potentially important receptor outcomes in the selection of chosen assays. One means of addressing this pitfall has been to assess global receptor activation following ligand stimulation. This approach was demonstrated with the β_2-adrenergic

receptor (Stallaert et al., 2012) as well as the dopamine D_2 receptor (Klein Herenbrink et al., 2016), using a label-free cellular impedance assay to provide an integrated readout of multiple signalling events. Clustering of signalling profiles obtained from these global readouts may consequently inform key signalling outcomes via comparisons with *in vivo* efficacy.

Nonetheless, several key themes arose from the assessment of ligand pharmacology through the three chosen signalling endpoints within this thesis. First, the notion of temporal bias was evident through differing assay kinetics influencing apparent signalling bias. Second, calcium signalling is a complex event comprising several components – leading to third, the influence of interacting receptors on $mGlu_5$ calcium responses. In Chapter 2, all studied ligands displayed clear biased agonism toward IP_1 accumulation relative to iCa^{2+} mobilisation. The stark differences were perhaps unexpected as, traditionally, at G_q-coupled receptors, calcium mobilisation is downstream from IP_1 accumulation. Two scenarios were assessed to elucidate the differences between calcium mobilisation and IP_1 accumulation assays observed: (1) the kinetic component following differing assay times and (2) the components of calcium mobilisation observed following receptor activation.

A possible explanation for the larger IP_1 accumulation response observed with the ligands studied in Chapter 2 was the prolonged ligand residence time in the IP_1 accumulation assay (1 h) relative to iCa^{2+} mobilisation (1 min). Thus, with a longer residence time during IP_1 accumulation, the ligands are able to reach equilibrium, and thus activate the receptor to the ligand's fullest extent. In Chapter 3, the concept of assay kinetics was further probed through comparisons of calcium mobilisation

following 1 min versus 30 min allosteric ligand incubation. Interestingly, unlike $mGlu_5$ PAMs, select $mGlu_5$ NAMs showed diminished affinity and/or cooperativity following longer residency time. A possible explanation again relies on kinetics, however, kinetics of cellular responses. $mGlu_5$ is known to couple to various ion channels (Kammermeier et al., 2000; Latif-Hernandez et al., 2016; Lu et al., 1999; McCool et al., 1998; Tu et al., 1999). Thus, calcium mobilisation, as determined through the Flexstation assays, represents a composite of intracellular and extracellular calcium. Indeed, in Chapter 2, extracellular calcium stores influenced orthosteric ligand (glutamate/DHPG)-mediated iCa^{2+} mobilisation, but had no effect on calcium responses following allosteric ligand (PAM-agonists) stimulation. Thus, the calcium mobilisation observed following PAM-agonist application was largely derived from intracellular calcium stores rather than coupling to calcium ion channels. With the studied $mGlu_5$ NAMs in Chapter 3, however, the prolonged incubation time resulted in reduced cooperativity and functional affinity, suggesting a kinetic bias towards coupling with fast-acting calcium ion channels, relative to the slower mobilisation of calcium from intracellular stores downstream of IP_1 accumulation. Indeed, there is growing appreciation of the importance of kinetics, not only in quantitatively determining signalling bias, but also fundamentally in physiological and therapeutic outcomes (Klein Herenbrink et al., 2016; Lane et al., 2017). For instance, extrapyramidal adverse effects of antipsychotics were linked to association kinetics, while elevated prolactin release was correlated to dissociation rates at dopamine D_2 receptors (Sykes et al., 2017). Thus, temporal bias remains a confounder of true ligand bias, however also an opportunity in optimising ligand binding kinetics, with further considerations of ligand residency time required in assay development, optimisation and validation.

Currently, there also remains a gap between receptor signalling outcome and physiological response following $mGlu_5$ stimulation. Indeed, the jump from the recombinant cell environment to prediction of *in vivo* response is large and often capricious. One method to increase the success of translation of ligand activity has been to bridge the gap between recombinant and *in vivo* with native tissue culture. Throughout this thesis, context-dependent receptor signalling of $mGlu_5$ allosteric ligands was determined through assessment in embryonic mouse cortical neurons. Indeed, context-dependent pharmacology has been demonstrated at $mGlu_7$ receptors between different recombinant and native cell lines (Niswender et al., 2010). $mGlu_5$ dysfunction is widely linked to various CNS disorders, many of which originate within the cortex (Niswender and Conn, 2010). Thus, assessment of $mGlu_5$ allosteric ligand activity within cortical neurons provides a logical and perhaps necessary step in determining the viability of potential therapeutic drugs. Again, with every stage of drug development, several caveats arise when moving into a more physiologically relevant cell background. First, the study of cortical neurons precludes the use of glutamate as an orthosteric agonist in assessing isolated $mGlu_5$ responses, due to the presence of numerous other glutamate ionic and metabotropic receptors, as well as glutamatergic transporters. Thus, DHPG, the group I mGlu agonist, was used as the surrogate orthosteric ligand throughout this thesis – which leads to the notion of probe dependence. Probe dependence is the paradigm in which allosteric ligand responses are dependent on the orthosteric ligand studied in conjunction (Valant et al., 2012). Probe dependence was indeed reported in Chapter 2 and 3, with differences in allosteric ligand responses observed between glutamate- and DHPG-mediated iCa^{2+} mobilisation. Thus, this remains an important consideration in assessment of ligand

pharmacology, as compounds move further through the drug design cascade toward *in vivo* settings.

Native tissues also contain a plethora of physiologically complex proteins, receptors, signalling partners, scaffolds etc., absent within a recombinant cell system. Within the CNS, $mGlu_5$ receptors interact with various proteins, receptors and ion channels (Borroto-Escuela et al., 2017; Lindsley et al., 2016; Niswender and Conn, 2010). Thus, while assessment of ligand pharmacology is necessary within a physiologically relevant context, the true targeted ligand response may be difficult to isolate. For instance, in our cortical neuronal studies in Chapters 2 and 3, DHPG was used as the orthosteric ligand, and the $mGlu_1$ antagonist, CPCCOEt was applied in conjunction to eliminate $mGlu_1$ agonism and isolate the $mGlu_5$ response, as previously described (Jong et al., 2009). However, within a therapeutic setting, glutamate would presumably act as the orthosteric ligand, and thus $mGlu_1$ and $mGlu_5$, as well as other glutamatergic responses, must be determined in combination with the allosteric ligand. We attempted to bridge this gap through application of DHPG, in the absence of CPCCOEt, to determine whether the additional $mGlu_1$ response affected allosteric ligand activity. Changes in affinity and/or cooperativity of select ligands, in particular dipraglurant, MTEP and VU0366248, in the absence of CPCCOEt, show potential loss of translation between isolated $mGlu_5$ responses and "global" ($mGlu_1$ and $mGlu_5$) response, despite both assessments within cortical neurons. Thus, while assessment of pharmacology in native cell tissues is necessary, restraints within the native context may influence ligand pharmacology, such that it remains divergent from the true physiological response.

Further, while increased complexity of cell background provides numerous challenges in optimising assay development, the $mGlu_5$ relationship with other receptors may be manipulated to form alternate avenues of therapeutics. For example, targeting $mGlu_5$ modulation of NMDA receptor (Balu et al., 2016; Benquet et al., 2002; Borroto-Escuela et al., 2017; Campbell et al., 2004; Collett and Collingridge, 2004; Tebano et al., 2005), adenosine (Borroto-Escuela et al., 2017; Cabello et al., 2009; Coccurello et al., 2004; Domenici et al., 2004; Nishi et al., 2003; Rodrigues et al., 2005), dopamine (Cabello et al., 2009; Ferre et al., 1999; Popoli et al., 2001), and opioid receptors (Brown et al., 2012b; Jin et al., 2006; Schroder et al., 2009; Zhou et al., 2013), to name a few, would expand the therapeutic indications of $mGlu_5$ ligands to target diseases ranging from the CNS to the periphery. This concept was probed in Chapter 5, through assessment of the relationship between $mGlu_5$ and TRPV1 receptors within rat dorsal root ganglion neurons. Previous studies have suggested a parallel relationship between inhibition of $mGlu_5$ responses and inhibition of TRPV1-mediated calcium influx (Chung et al., 2015; Honda et al., 2017; Masuoka et al., 2016; Masuoka et al., 2015), thereby providing potential analgesic therapy. Interestingly, our study highlighted the disconnect between recombinant and neuronal systems – that is, the presence of system bias. In particular, CDPPB, an $mGlu_5$ PAM agonist of iCa^{2+} mobilisation, IP_1 accumulation and pERK1/2 phosphorylation within HEK293A cells (in Chapter 2), produced an inverse response with TRPV1, with reduced capsaicin-mediated calcium influx within DRGs – thereby behaving as a NAM. Also, MPEP, the $mGlu_5$ NAM, significantly reduced capsaicin and anandamide responses, but not oleoylethanolamide and *N*-arachidonoyl-dopamine calcium influx – indicating the presence of "probe dependence" with the redundancy of endogenous TRPV1 agonists – albeit across the $mGlu_5$-TRPV1 system. Overall,

these results point to the complexity of the physiological context, with $mGlu_5$ and TRPV1 perhaps not having a directly correlated relationship. Thus, while targeting the $mGlu_5$ relationship between different receptors may be a viable therapeutic option, a greater understanding of the intricate interactions between the two receptors is required to allow design of targeted and predictable therapies.

Following on from assessment of biased agonism and modulation in recombinant and neuronal cells, this thesis aimed to determine the structural basis of bias. Recently solved receptor crystal structures have provided essential information into the allosteric binding pocket (Christopher et al., 2015; Dore et al., 2014; Wu et al., 2014), however a gap remains between ligand structure and subsequently receptor function. While numerous mutagenesis studies have provided insight into allosteric ligand induced iCa^{2+} mobilisation (Chen et al., 2007; Gregory et al., 2014; Gregory et al., 2013b; Gregory et al., 2012; Mølck et al., 2012; Muhlemann et al., 2006; Pagano et al., 2000), there are a lack of studies assessing other signalling endpoints. Indeed, as bias is operative in WT receptors, assessment of bias should extend to mutagenesis studies. Thus, in Chapter 4, a structure-function analysis was implemented with seven point mutations using four $mGlu_5$ allosteric ligands – assessing iCa^{2+} mobilisation, IP_1 accumulation and ERK1/2 phophorylation. As discussed in Chapter 4, three key areas were implicated in allosteric ligand affinity, cooperativity and intrinsic efficacy – the hydrogen-water network between Y658, T780 and S808A (Christopher et al., 2015; Dore et al., 2014), the W784 "rotamer toggle switch" analogous to the Class A CWxP motif (Holst et al., 2010; Shi et al., 2002) and the narrow channel, lined by P654 and A809, within the allosteric binding site, extending the pocket deep within the TM domain (Christopher et al., 2015; Dore et al., 2014). Another interesting finding was

that several allosteric ligands produced responses greater than the orthosteric ligand at various mutants. Thus, these mutants were determined to not affect global receptor activation, but perhaps affect distinct conformations required for activation of certain signalling pathways. That is, allosteric ligands are able to stabilise receptor conformations, distinct from that imposed by DHPG, to activate the same receptor signalling pathways. As receptors are able to exist in equilibrium between active and inactive states, binding of a foreign compound has the potential to stabilise a different distribution of active receptor states, to give a unique signalling fingerprint. Clustering of ligands with similar fingerprints will allow determination of structure-activity relationships, thereby refining drug design efforts to target desired receptor signalling outcomes.

From the findings within this thesis, key implications for future $mGlu_5$ drug discovery campaigns would include the need to assess biased signalling – both agonism and modulation – via adopting rigorous quantitative analysis using operational models of agonism and modulation (Kenakin and Christopoulos, 2013; Kenakin et al., 2012; Leach et al., 2007). Initial pharmacological experiments to assess global receptor activity via measurement of cell impedance and dynamic mass redistribution (e.g. xCELLigence, EPIC Systems (Halai et al., 2012; Limame et al., 2012; Owens et al., 2009)) would allow clustering of ligands based on similar global receptor effects, while parallel native studies provides insight into promising compounds to progress into *in vivo* studies. Linking of *in vivo* physiological outcomes to biased signalling profiles would further inform key receptor endpoints involved in therapeutic and adverse effects. Clustering of biased compounds with similar signalling profiles and physiological outcomes would allow determination of a potential structure-activity

relationship, thereby refining drug development to target receptor endpoints associated with disease pathophysiology and consequent therapeutic outcomes.

In conclusion, the studies presented within this thesis offer insight into the importance of assessment of biased agonism and modulation, as well as the caveats involved. From this, considerations of probe dependence, temporal/kinetic bias, systems or context-dependent bias, residues implicated in ligand affinity, cooperativity and efficacy and structure-activity relationships must also be addressed, and remain challenges for further drug design efforts. Nonetheless, increased appreciation for the presence of biased signalling, together with greater understanding of $mGlu_5$ disease physiology, ultimately lay the foundation for the next generation of $mGlu_5$ therapeutics with exceptionally targeted effects for a multitude of clinical disorders.

Chapter 7

References

Abe, T., Sugihara, H., Nawa, H., Shigemoto, R., Mizuno, N., Nakanishi, S., 1992. Molecular characterization of a novel metabotropic glutamate receptor mGluR5 coupled to inositol phosphate/Ca2+ signal transduction. J. Biol. Chem. 267, 13361-13368.

Abou Farha, K., Bruggeman, R., Balje-Volkers, C., 2014. Metabotropic glutamate receptor 5 negative modulation in phase I clinical trial: potential impact of circadian rhythm on the neuropsychiatric adverse reactions-do hallucinations matter? ISRN Psychiatry 2014, 652750.

Adler, C. M., Malhotra, A. K., Elman, I., Goldberg, T., Egan, M., Pickar, D., Breier, A., 1999. Comparison of ketamine-induced thought disorder in healthy volunteers and thought disorder in schizophrenia. Am. J. Psychiat. 156, 1646-1649.

Ahern, G. P., 2003. Activation of TRPV1 by the satiety factor oleoylethanolamide. J. Biol. Chem. 278, 30429-30434.

Ahluwalia, J., Urban, L., Capogna, M., Bevan, S., Nagy, I., 2000. Cannabinoid 1 receptors are expressed in nociceptive primary sensory neurons. Neuroscience 100, 685-688.

Almási, R., Szőke, É., Bölcskei, K., Varga, A., Riedl, Z., Sándor, Z., Szolcsányi, J., Pethő, G., 2008. Actions of 3-methyl-N-oleoyldopamine, 4-methyl-N-oleoyldopamine and N-oleoylethanolamide on the rat TRPV1 receptor in vitro and in vivo. Life Sci. 82, 644-651.

Amalric, M., 2015. Targeting metabotropic glutamate receptors (mGluRs) in Parkinson's disease. Curr. Opin. Pharmacol. 20, 29-34.

Ango, F., Robbe, D., Tu, J. C., Xiao, B., Worley, P. F., Pin, J. P., Bockaert, J., Fagni, L., 2002. Homer-dependent cell surface expression of metabotropic glutamate receptor type 5 in neurons. Mol. Cell Neurosci. 20, 323-329.

Auer, D. P., Putz, B., Kraft, E., Lipinski, B., Schill, J., Holsboer, F., 2000. Reduced glutamate in the anterior cingulate cortex in depression: an in vivo proton magnetic resonance spectroscopy study. Biol. Psychiat. 47, 305-313.

Auerbach, B. D., Osterweil, E. K., Bear, M. F., 2011. Mutations causing syndromic autism define an axis of synaptic pathophysiology. Nature 480, 63-68.

Austin, P. J., Betts, M. J., Broadstock, M., O'Neill, M. J., Mitchell, S. N., Duty, S., 2010. Symptomatic and neuroprotective effects following activation of nigral group III metabotropic glutamate receptors in rodent models of Parkinson's disease. Br. J. Pharmacol. 160, 1741-1753.

Bailey, D. B., Jr., Berry-Kravis, E., Wheeler, A., Raspa, M., Merrien, F., Ricart, J., Koumaras, B., Rosenkranz, G., Tomlinson, M., von Raison, F., Apostol, G., 2016. Mavoglurant in adolescents with fragile X syndrome: analysis of Clinical Global Impression-Improvement source data from a double-blind therapeutic study followed by an open-label, long-term extension study. J. Neurodev. Disord. 8, 1.

Balazs, R., Miller, S., Romano, C., de Vries, A., Chun, Y., Cotman, C. W., 1997. Metabotropic glutamate receptor mGluR5 in astrocytes: pharmacological properties and agonist regulation. J. Neurochem. 69, 151-163.

Ballester-Rosado, C. J., Albright, M. J., Wu, C. S., Liao, C. C., Zhu, J., Xu, J., Lee, L. J., Lu, H. C., 2010. mGluR5 in cortical excitatory neurons exerts both cell-autonomous and -nonautonomous influences on cortical somatosensory circuit formation. J. Neurosci. 30, 16896-16909.

Balschun, D., Wetzel, W., 2002. Inhibition of mGluR5 blocks hippocampal LTP in vivo and spatial learning in rats. Pharmacol. Biochem. Behav. 73, 375-380.

Baltos, J. A., Gregory, K. J., White, P. J., Sexton, P. M., Christopoulos, A., May, L. T., 2016. Quantification of adenosine A(1) receptor biased agonism: Implications for drug discovery. Biochem. Pharmacol. 99, 101-112.

Baltos, J. A., Vecchio, E. A., Harris, M. A., Qin, C. X., Ritchie, R. H., Christopoulos, A., White, P. J., May, L. T., 2017. Capadenoson, a clinically trialed partial adenosine A1 receptor agonist, can stimulate adenosine A2B receptor biased agonism. Biochem. Pharmacol. 135, 79-89.

Balu, D. T., Li, Y., Takagi, S., Presti, K. T., Ramikie, T. S., Rook, J. M., Jones, C. K., Lindsley, C. W., Conn, P. J., Bolshakov, V. Y., Coyle, J. T., 2016. An mGlu5-Positive Allosteric Modulator Rescues the Neuroplasticity Deficits in a Genetic Model of NMDA Receptor Hypofunction in Schizophrenia. Neuropsychopharmacol. 41, 2052-2061.

Bastide, M. F., Meissner, W. G., Picconi, B., Fasano, S., Fernagut, P. O., Feyder, M., Francardo, V., Alcacer, C., Ding, Y., Brambilla, R., Fisone, G., Jon Stoessl, A., Bourdenx, M., Engeln, M., Navailles, S., De Deurwaerdere, P., Ko, W. K., Simola, N., Morelli, M., Groc, L., Rodriguez, M. C., Gurevich, E. V., Quik, M., Morari, M., Mellone, M., Gardoni, F., Tronci, E., Guehl, D., Tison, F., Crossman, A. R., Kang, U. J., Steece-Collier, K., Fox, S., Carta, M., Angela Cenci, M., Bezard, E., 2015. Pathophysiology of L-dopa-induced motor and non-motor complications in Parkinson's disease. Prog. Neurobiol. 132, 96-168.

Battaglia, G., Busceti, C. L., Molinaro, G., Biagioni, F., Traficante, A., Nicoletti, F., Bruno, V., 2006. Pharmacological activation of mGlu4 metabotropic glutamate receptors reduces nigrostriatal degeneration in mice treated with 1-methyl-4-phenyl-1,2,3,6-tetrahydropyridine. J. Neurosci. 26, 7222-7229.

Bear, M. F., Huber, K. M., Warren, S. T., 2004. The mGluR theory of fragile X mental retardation. Trends Neurosci. 27, 370-377.

Belozertseva, I. V., Kos, T., Popik, P., Danysz, W., Bespalov, A. Y., 2007. Antidepressant-like effects of mGluR1 and mGluR5 antagonists in the rat forced swim and the mouse tail suspension tests. Eur. Neuropsychopharmacol. 17, 172-179.

Bennett, C. E., Burnett, D. A., Greenlee, W. J., Knutson, C. E., Korakas, P., Li, C., Tulshian, D., Wu, W. L., Bertorelli, R., Fredduzzi, S., Grilli, M., Lozza, G., Reggiani,

A., Veltri, A., 2012. Fused tricyclic mGluR1 antagonists for the treatment of neuropathic pain. Bioorg. Med. Chem. Lett. 22, 1575-1578.

Bennett, K. A., Dore, A. S., Christopher, J. A., Weiss, D. R., Marshall, F. H., 2015. Structures of mGluRs shed light on the challenges of drug development of allosteric modulators. Curr. Opin. Pharmacol. 20, 1-7.

Bennouar, K. E., Uberti, M. A., Melon, C., Bacolod, M. D., Jimenez, H. N., Cajina, M., Kerkerian-Le Goff, L., Doller, D., Gubellini, P., 2013. Synergy between L-DOPA and a novel positive allosteric modulator of metabotropic glutamate receptor 4: implications for Parkinson's disease treatment and dyskinesia. Neuropharmacology 66, 158-169.

Benquet, P., Gee, C., Gerber, U., 2002. Two distinct signaling pathways upregulate NMDA receptor responses via two distinct metabotropic glutamate receptor subtypes. J. Neurosci. 22, 9679 - 9686.

Berridge, M. J., 1998. Neuronal calcium signaling. Neuron 21, 13-26.

Berry-Kravis, E., Des Portes, V., Hagerman, R., Jacquemont, S., Charles, P., Visootsak, J., Brinkman, M., Rerat, K., Koumaras, B., Zhu, L., Barth, G. M., Jaecklin, T., Apostol, G., von Raison, F., 2016. Mavoglurant in fragile X syndrome: Results of two randomized, double-blind, placebo-controlled trials. Sci. Transl. Med. 8, 321ra325.

Berry-Kravis, E., Hessl, D., Coffey, S., Hervey, C., Schneider, A., Yuhas, J., Hutchison, J., Snape, M., Tranfaglia, M., Nguyen, D. V., Hagerman, R., 2009. A pilot open label, single dose trial of fenobam in adults with fragile X syndrome. J. Med. Genet. 46, 266-271.

Bhave, G., Hu, H. J., Glauner, K. S., Zhu, W., Wang, H., Brasier, D. J., Oxford, G. S., Gereau, R. W. t., 2003. Protein kinase C phosphorylation sensitizes but does not activate the capsaicin receptor transient receptor potential vanilloid 1 (TRPV1). Proc. Natl. Acad. Sci. U S A. 100, 12480-12485.

Bhave, G., Karim, F., Carlton, S. M., Gereau, R. W. t., 2001. Peripheral group I metabotropic glutamate receptors modulate nociception in mice. Nat. Neurosci. 4, 417-423.

Bird, M. K., Reid, C. A., Chen, F., Tan, H. O., Petrou, S., Lawrence, A. J., 2010. Cocaine-mediated synaptic potentiation is absent in VTA neurons from mGlu5-deficient mice. Int. J. Neuropsychopharmacol. 13, 133-141.

Black, J. W., Leff, P., 1983. Operational models of pharmacological agonism. Proc. R. Soc. Lond. B. Biol. Sci. 220, 141-162.

Black, Y. D., Xiao, D., Pellegrino, D., Kachroo, A., Brownell, A. L., Schwarzschild, M. A., 2010. Protective effect of metabotropic glutamate mGluR5 receptor elimination in a 6-hydroxydopamine model of Parkinson's disease. Neurosci. Lett. 486, 161-165.

Bonsi, P., Cuomo, D., De Persis, C., Centonze, D., Bernardi, G., Calabresi, P., Pisani, A., 2005. Modulatory action of metabotropic glutamate receptor (mGluR) 5 on mGluR1 function in striatal cholinergic interneurons. Neuropharmacology 49 Suppl 1, 104-113.

Borgdorff, A. J., Choquet, D., 2002. Regulation of AMPA receptor lateral movements. Nature 417, 649-653.

Borroto-Escuela, D. O., Carlsson, J., Ambrogini, P., Narvaez, M., Wydra, K., Tarakanov, A. O., Li, X., Millon, C., Ferraro, L., Cuppini, R., Tanganelli, S., Liu, F., Filip, M., Diaz-Cabiale, Z., Fuxe, K., 2017. Understanding the Role of GPCR Heteroreceptor Complexes in Modulating the Brain Networks in Health and Disease. Front. Cell. Neurosci. 11, 37.

Bortolotto, Z. A., Collett, V. J., Conquet, F., Jia, Z., van der Putten, H., Collingridge, G. L., 2005. The regulation of hippocampal LTP by the molecular switch, a form of metaplasticity, requires mGlu5 receptors. Neuropharmacology 49 Suppl 1, 13-25.
Bradbury, M. J., Campbell, U., Giracello, D., Chapman, D., King, C., Tehrani, L., Cosford, N. D., Anderson, J., Varney, M. A., Strack, A. M., 2005. Metabotropic glutamate receptor mGlu5 is a mediator of appetite and energy balance in rats and mice. J. Pharmacol. Exp. Ther. 313, 395-402.

Bradley, S. J., Challiss, R. A., 2011. Defining protein kinase/phosphatase isoenzymic regulation of mGlu(5) receptor-stimulated phospholipase C and Ca(2)(+) responses in astrocytes. Br. J. Pharmacol. 164, 755-771.

Bradley, S. J., Langmead, C. J., Watson, J. M., Challiss, R. A., 2011. Quantitative analysis reveals multiple mechanisms of allosteric modulation of the mGlu5 receptor in rat astroglia. Mol. Pharmacol. 79, 874-885.

Brakeman, P. R., Lanahan, A. A., O'Brien, R., Roche, K., Barnes, C. A., Huganir, R. L., Worley, P. F., 1997. Homer: a protein that selectively binds metabotropic glutamate receptors. Nature 386, 284-288.

Brauner-Osborne, H., Jensen, A. A., Krogsgaard-Larsen, P., 1999. Interaction of CPCCOEt with a chimeric mGlu1b and calcium sensing receptor. Neuroreport 10, 3923-3925.

Brauner-Osborne, H., Wellendorph, P., Jensen, A. A., 2007. Structure, pharmacology and therapeutic prospects of family C G-protein coupled receptors. Curr. Drug Targets 8, 169-184.

Bridges, T. M., Lindsley, C. W., 2008. G-protein-coupled receptors: from classical modes of modulation to allosteric mechanisms. ACS Chem. Biol. 3, 530-541.

Bridges, T. M., Rook, J. M., Noetzel, M. J., Morrison, R. D., Zhou, Y., Gogliotti, R. D., Vinson, P. N., Xiang, Z., Jones, C. K., Niswender, C. M., Lindsley, C. W., Stauffer, S. R., Conn, P. J., Daniels, J. S., 2013. Biotransformation of a novel positive allosteric modulator of metabotropic glutamate receptor subtype 5 contributes to

seizure-like adverse events in rats involving a receptor agonism-dependent mechanism. Drug Metab. Dispos. 41, 1703-1714.

Brini, M., Cali, T., Ottolini, D., Carafoli, E., 2014. Neuronal calcium signaling: function and dysfunction. Cell Mol. Life Sci. 71, 2787-2814.

Brody, S. A., Dulawa, S. C., Conquet, F., Geyer, M. A., 2004. Assessment of a prepulse inhibition deficit in a mutant mouse lacking mGlu5 receptors. Mol. Psychiatr. 9, 35-41.

Brown, R. M., Mustafa, S., Ayoub, M. A., Dodd, P. R., Pfleger, K. D., Lawrence, A. J., 2012a. mGlu5 Receptor Functional Interactions and Addiction. Front. Pharmacol. 3, 84.

Brown, R. M., Stagnitti, M. R., Duncan, J. R., Lawrence, A. J., 2012b. The mGlu5 receptor antagonist MTEP attenuates opiate self-administration and cue-induced opiate-seeking behaviour in mice. Drug Alcohol Depen. 123, 264-268.

Bruno, V., Battaglia, G., Copani, A., D'Onofrio, M., Di Iorio, P., De Blasi, A., Melchiorri, D., Flor, P. J., Nicoletti, F., 2001. Metabotropic glutamate receptor subtypes as targets for neuroprotective drugs. J. Cereb. Blood Flow Metab. 21, 1013-1033.

Cabello, N., Gandia, J., Bertarelli, D. C., Watanabe, M., Lluis, C., Franco, R., Ferre, S., Lujan, R., Ciruela, F., 2009. Metabotropic glutamate type 5, dopamine D2 and adenosine A2a receptors form higher-order oligomers in living cells. J. Neurochem. 109, 1497-1507.

Calabresi, P., Giacomini, P., Centonze, D., Bernardi, G., 2000. Levodopa-induced dyskinesia: a pathological form of striatal synaptic plasticity? Ann. Neurol. 47, S60-68; discussion S68-69.

Campbell, U. C., Lalwani, K., Hernandez, L., Kinney, G. G., Conn, P. J., Bristow, L. J., 2004. The mGluR5 antagonist 2-methyl-6-(phenylethynyl)-pyridine (MPEP) potentiates PCP-induced cognitive deficits in rats. Psychopharmacol. (Berl) 175, 310-318.

Caprioli, D., Venniro, M., Zeric, T., Li, X., Adhikary, S., Madangopal, R., Marchant, N. J., Lucantonio, F., Schoenbaum, G., Bossert, J. M., Shaham, Y., 2015. Effect of the Novel Positive Allosteric Modulator of Metabotropic Glutamate Receptor 2 AZD8529 on Incubation of Methamphetamine Craving After Prolonged Voluntary Abstinence in a Rat Model. Biol. Psychiat. 78, 463-473.

Carlton, S. M., Hargett, G. L., 2007. Colocalization of metabotropic glutamate receptors in rat dorsal root ganglion cells. J. Comp. Neurol. 501, 780-789.
Cartmell, J., Monn, J. A., Schoepp, D. D., 1999. The metabotropic glutamate 2/3 receptor agonists LY354740 and LY379268 selectively attenuate phencyclidine versus d-amphetamine motor behaviors in rats. J. Pharmacol. Exp. Ther. 291, 161-170.

Casabona, G., Knopfel, T., Kuhn, R., Gasparini, F., Baumann, P., Sortino, M. A., Copani, A., Nicoletti, F., 1997. Expression and Coupling to Polyphosphoinositide Hydrolysis of Group I Metabotropic Glutamate Receptors in Early Postnatal and Adult Rat Brain. Eur. J. Neurosci., 9, 12-17.

Caterina, M. J., Park, U., 2006. Chapter 4 TRPV1: A Polymodal Sensor in the Nociceptor Terminal. Curr. Top. Membr. Academic Press, pp. 113-150.

Chaki, S., Ago, Y., Palucha-Paniewiera, A., Matrisciano, F., Pilc, A., 2013. mGlu2/3 and mGlu5 receptors: potential targets for novel antidepressants. Neuropharmacology 66, 40-52.

Chan, T. O., Rittenhouse, S. E., Tsichlis, P. N., 1999. AKT/PKB and other D3 phosphoinositide-regulated kinases: kinase activation by phosphoinositide-dependent phosphorylation. Annu. Rev. Biochem. 68, 965-1014.

Changeux, J. P., Christopoulos, A., 2016. Allosteric Modulation as a Unifying Mechanism for Receptor Function and Regulation. Cell 166, 1084-1102.

Chen, C. C., Lu, H. C., Brumberg, J. C., 2012. mGluR5 knockout mice display increased dendritic spine densities. Neurosci. Lett. 524, 65-68.

Chen, H. H., Stoker, A., Markou, A., 2010. The glutamatergic compounds sarcosine and N-acetylcysteine ameliorate prepulse inhibition deficits in metabotropic glutamate 5 receptor knockout mice. Psychopharmacol. (Berl) 209, 343-350.

Chen, Y., Goudet, C., Pin, J. P., Conn, P. J., 2008. N-{4-Chloro-2-[(1,3-dioxo-1,3-dihydro-2H-isoindol-2-yl)methyl]phenyl}-2-hydroxybe nzamide (CPPHA) acts through a novel site as a positive allosteric modulator of group 1 metabotropic glutamate receptors. Mol. Pharmacol. 73, 909-918.

Chen, Y., Nong, Y., Goudet, C., Hemstapat, K., de Paulis, T., Pin, J. P., Conn, P. J., 2007. Interaction of novel positive allosteric modulators of metabotropic glutamate receptor 5 with the negative allosteric antagonist site is required for potentiation of receptor responses. Mol. Pharmacol. 71, 1389-1398.

Cheng, Y., Prusoff, W. H., 1973. Relationship between the inhibition constant (K1) and the concentration of inhibitor which causes 50 per cent inhibition (I50) of an enzymatic reaction. Biochem. Pharmacol. 22, 3099-3108.

Chesworth, R., Brown, R. M., Kim, J. H., Lawrence, A. J., 2013. The metabotropic glutamate 5 receptor modulates extinction and reinstatement of methamphetamine-seeking in mice. PLoS One 8, e68371.

Chevere-Torres, I., Kaphzan, H., Bhattacharya, A., Kang, A., Maki, J. M., Gambello, M. J., Arbiser, J. L., Santini, E., Klann, E., 2012. Metabotropic glutamate receptor-dependent long-term depression is impaired due to elevated ERK signaling in the DeltaRG mouse model of tuberous sclerosis complex. Neurobiol. Dis. 45, 1101-1110.

Chiamulera, C., Epping-Jordan, M. P., Zocchi, A., Marcon, C., Cottiny, C., Tacconi, S., Corsi, M., Orzi, F., Conquet, F., 2001. Reinforcing and locomotor stimulant effects of cocaine are absent in mGluR5 null mutant mice. Nat. Neurosci. 4, 873-874.

Choi, K. Y., Chung, S., Roche, K. W., 2011. Differential binding of calmodulin to group I metabotropic glutamate receptors regulates receptor trafficking and signaling. J. Neurosci. 31, 5921-5930.

Chojnacka-Wojcik, E., Klodzinska, A., Pilc, A., 2001. Glutamate receptor ligands as anxiolytics. Curr. Opin. Investig. Drugs 2, 1112-1119.

Christie, M. J., Summers, R. J., Stephenson, J. A., Cook, C. J., Beart, P. M., 1987. Excitatory amino acid projections to the nucleus accumbens septi in the rat: a retrograde transport study utilizing D[3H]aspartate and [3H]GABA. Neuroscience 22, 425-439.

Christopher, J. A., Aves, S. J., Bennett, K. A., Dore, A. S., Errey, J. C., Jazayeri, A., Marshall, F. H., Okrasa, K., Serrano-Vega, M. J., Tehan, B. G., Wiggin, G. R., Congreve, M., 2015. Fragment and Structure-Based Drug Discovery for a Class C GPCR: Discovery of the mGlu5 Negative Allosteric Modulator HTL14242 (3-Chloro-5-[6-(5-fluoropyridin-2-yl)pyrimidin-4-yl]benzonitrile). J. Med. Chem. 58, 6653-6664.

Christopoulos, A., 2014. Advances in G protein-coupled receptor allostery: from function to structure. Mol. Pharmacol. 86, 463-478.

Christopoulos, A., Changeux, J. P., Catterall, W. A., Fabbro, D., Burris, T. P., Cidlowski, J. A., Olsen, R. W., Peters, J. A., Neubig, R. R., Pin, J. P., Sexton, P. M., Kenakin, T. P., Ehlert, F. J., Spedding, M., Langmead, C. J., 2014. International union of basic and clinical pharmacology. XC. multisite pharmacology: recommendations for the nomenclature of receptor allosterism and allosteric ligands. Pharmacol. Rev. 66, 918-947.

Christopoulos, A., Kenakin, T., 2002. G protein-coupled receptor allosterism and complexing. Pharmacol. Rev. 54, 323-374.

Chung, M. K., Lee, J., Joseph, J., Saloman, J., Ro, J. Y., 2015. Peripheral group I metabotropic glutamate receptor activation leads to muscle mechanical hyperalgesia through TRPV1 phosphorylation in the rat. J. Pain 16, 67-76.

Clapper, J. R., Moreno-Sanz, G., Russo, R., Guijarro, A., Vacondio, F., Duranti, A., Tontini, A., Sanchini, S., Sciolino, N. R., Spradley, J. M., Hohmann, A. G., Calignano, A., Mor, M., Tarzia, G., Piomelli, D., 2010. Anandamide suppresses pain initiation through a peripheral endocannabinoid mechanism. Nat. Neurosci. 13, 1265-1270.

Coccurello, R., Breysse, N., Amalric, M., 2004. Simultaneous blockade of adenosine A2A and metabotropic glutamate mGlu5 receptors increase their efficacy in reversing Parkinsonian deficits in rats. Neuropsychopharmacol. 29, 1451-1461.

Collett, V. J., Collingridge, G. L., 2004. Interactions between NMDA receptors and mGlu5 receptors expressed in HEK293 cells. Br. J. Pharmacol. 142, 991-1001.
Conn, P. J., 2003. Physiological roles and therapeutic potential of metabotropic glutamate receptors. Ann. N. Y. Acad. Sci. 1003, 12-21.
Conn, P. J., Jones, C. K., 2009. Promise of mGluR2/3 activators in psychiatry. Neuropsychopharmacol. 34, 248-249.

Conn, P. J., Lindsley, C. W., Jones, C. K., 2008. Activation of metabotropic glutamate receptors as a novel approach for the treatment of schizophrenia. Trends Pharmacol. Sci. 30, 25-31.

Conn, P. J., Pin, J. P., 1997. Pharmacology and functions of metabotropic glutamate receptors. Annu. Rev. Pharmacol. Toxicol. 37, 205-237.

Cook, A. E., Mistry, S. N., Gregory, K. J., Furness, S. G., Sexton, P. M., Scammells, P. J., Conigrave, A. D., Christopoulos, A., Leach, K., 2015. Biased allosteric modulation at the CaS receptor engendered by structurally diverse calcimimetics. Br. J. Pharmacol. 172, 185-200.

Correa, A. M. B., Guimaraes, J. D. S., Dos Santos, E. A. E., Kushmerick, C., 2017. Control of neuronal excitability by Group I metabotropic glutamate receptors. Biophys. Rev. 9, 835-845.

Cosford, N. D., Roppe, J., Tehrani, L., Schweiger, E. J., Seiders, T. J., Chaudary, A., Rao, S., Varney, M. A., 2003a. [3H]-methoxymethyl-MTEP and [3H]-methoxy-PEPy: potent and selective radioligands for the metabotropic glutamate subtype 5 (mGlu5) receptor. Bioorg. Med. Chem. Lett. 13, 351-354.

Cosford, N. D., Tehrani, L., Roppe, J., Schweiger, E., Smith, N. D., Anderson, J., Bristow, L., Brodkin, J., Jiang, X., McDonald, I., Rao, S., Washburn, M., Varney, M. A., 2003b. 3-[(2-Methyl-1,3-thiazol-4-yl)ethynyl]-pyridine: a potent and highly selective metabotropic glutamate subtype 5 receptor antagonist with anxiolytic activity. J. Med. Chem. 46, 204-206.

Costantino, G., Pellicciari, R., 1996. Homology modeling of metabotropic glutamate receptors. (mGluRs) structural motifs affecting binding modes and pharmacological profile of mGluR1 agonists and competitive antagonists. J. Med. Chem. 39, 3998-4006.

Crawford, J. H., Wainwright, A., Heavens, R., Pollock, J., Martin, D. J., Scott, R. H., Seabrook, G. R., 2000. Mobilisation of intracellular Ca2+ by mGluR5 metabotropic glutamate receptor activation in neonatal rat cultured dorsal root ganglia neurones. Neuropharmacology 39, 621-630.

da Silva Junior, E. D., Sato, M., Merlin, J., Broxton, N., Hutchinson, D. S., Ventura, S., Evans, B. A., Summers, R. J., 2017. Factors influencing biased agonism in recombinant cells expressing the human alpha1A -adrenoceptor. Br. J. Pharmacol. 174, 2318-2333.

Davey, A. E., Leach, K., Valant, C., Conigrave, A. D., Sexton, P. M., Christopoulos, A., 2012. Positive and negative allosteric modulators promote biased signaling at the calcium-sensing receptor. Endocrinology 153, 1232-1241.
deGroot, J., Zhou, S., Carlton, S. M., 2000. Peripheral glutamate release in the hindpaw following low and high intensity sciatic stimulation. Neuroreport 11, 497-502.

Dekundy, A., Gravius, A., Hechenberger, M., Pietraszek, M., Nagel, J., Tober, C., van der Elst, M., Mela, F., Parsons, C. G., Danysz, W., 2011. Pharmacological characterization of MRZ-8676, a novel negative allosteric modulator of subtype 5 metabotropic glutamate receptors (mGluR5): focus on L: -DOPA-induced dyskinesia. J. Neural Transm. (Vienna) 118, 1703-1716.

Devane, W. A., Hanus, L., Breuer, A., Pertwee, R. G., Stevenson, L. A., Griffin, G., Gibson, D., Mandelbaum, A., Etinger, A., Mechoulam, R., 1992. Isolation and structure of a brain constituent that binds to the cannabinoid receptor. Science 258, 1946-1949.

Di Marzo, V., De Petrocellis, L., 2010. Endocannabinoids as regulators of transient receptor potential (TRP) channels: A further opportunity to develop new endocannabinoid-based therapeutic drugs. Curr. Med. Chem. 17, 1430-1449.

Dolen, G., Osterweil, E., Rao, B. S., Smith, G. B., Auerbach, B. D., Chattarji, S., Bear, M. F., 2007. Correction of fragile X syndrome in mice. Neuron 56, 955-962.

Domenici, M. R., Pepponi, R., Martire, A., Tebano, M. T., Potenza, R. L., Popoli, P., 2004. Permissive role of adenosine A2A receptors on metabotropic glutamate receptor 5 (mGluR5)-mediated effects in the striatum. J. Neurochem. 90, 1276-1279.

Domin, H., Jantas, D., Śmiałowska, M., 2015. Neuroprotective effects of the allosteric agonist of metabotropic glutamate receptor 7 AMN082 on oxygen-glucose deprivation- and kainate-induced neuronal cell death. Neurochem. Int. 88, 110-123.

Dore, A. S., Okrasa, K., Patel, J. C., Serrano-Vega, M., Bennett, K., Cooke, R. M., Errey, J. C., Jazayeri, A., Khan, S., Tehan, B., Weir, M., Wiggin, G. R., Marshall, F. H., 2014. Structure of class C GPCR metabotropic glutamate receptor 5 transmembrane domain. Nature 511, 557-562.

Dorr, P., Westby, M., Dobbs, S., Griffin, P., Irvine, B., Macartney, M., Mori, J., Rickett, G., Smith-Burchnell, C., Napier, C., Webster, R., Armour, D., Price, D., Stammen, B., Wood, A., Perros, M., 2005. Maraviroc (UK-427,857), a potent, orally bioavailable, and selective small-molecule inhibitor of chemokine receptor CCR5 with broad-spectrum anti-human immunodeficiency virus type 1 activity. Antimicrob. Agents Chemother. 49, 4721-4732.

Doumazane, E., Scholler, P., Zwier, J. M., Trinquet, E., Rondard, P., Pin, J. P., 2011. A new approach to analyze cell surface protein complexes reveals specific heterodimeric metabotropic glutamate receptors. Faseb J. 25, 66-77.

Duty, S., 2010. Therapeutic potential of targeting group III metabotropic glutamate receptors in the treatment of Parkinson's disease. Br. J. Pharmacol. 161, 271-287.

Ehlert, F. J., 1988. Estimation of the affinities of allosteric ligands using radioligand binding and pharmacological null methods. Mol. Pharmacol. 33, 187-194.
Eiler, W. J., 2nd, Baez, M., Yu, J., Witkin, J. M., 2011. mGlu5 receptor deletion reduces relapse to food-seeking and prevents the anti-relapse effects of mGlu5 receptor blockade in mice. Life Sci. 89, 862-867.

Emery, A. C., DiRaddo, J. O., Miller, E., Hathaway, H. A., Pshenichkin, S., Takoudjou, G. R., Grajkowska, E., Yasuda, R. P., Wolfe, B. B., Wroblewski, J. T., 2012. Ligand bias at metabotropic glutamate 1a receptors: molecular determinants that distinguish beta-arrestin-mediated from G protein-mediated signaling. Mol. Pharmacol. 82, 291-301.

Emmitte, K. A., 2013. mGlu5 negative allosteric modulators: a patent review (2010-2012). Expert Opin. Ther. Pat. 23, 393-408.

Felts, A. S., Lindsley, S. R., Lamb, J. P., Rodriguez, A. L., Menon, U. N., Jadhav, S., Jones, C. K., Conn, P. J., Lindsley, C. W., Emmitte, K. A., 2010. 3-Cyano-5-fluoro-N-arylbenzamides as negative allosteric modulators of mGlu(5): Identification of easily prepared tool compounds with CNS exposure in rats. Bioorg. Med. Chem. Lett. 20, 4390-4394.

Felts, A. S., Rodriguez, A. L., Morrison, R. D., Venable, D. F., Manka, J. T., Bates, B. S., Blobaum, A. L., Byers, F. W., Daniels, J. S., Niswender, C. M., Jones, C. K., Conn, P. J., Lindsley, C. W., Emmitte, K. A., 2013. Discovery of VU0409106: A negative allosteric modulator of mGlu5 with activity in a mouse model of anxiety. Bioorg. Med. Chem. Lett. 23, 5779-5785.

Fendt, M., Schmid, S., 2002. Metabotropic glutamate receptors are involved in amygdaloid plasticity. Eur. J. Neurosci. 15, 1535-1541.

Ferre, S., Karcz-Kubicha, M., Hope, B. T., Popoli, P., Burgueno, J., Gutierrez, M. A., Casado, V., Fuxe, K., Goldberg, S. R., Lluis, C., Franco, R., Ciruela, F., 2002. Synergistic interaction between adenosine A2A and glutamate mGlu5 receptors: implications for striatal neuronal function. Proc. Natl. Acad. Sci. U S A. 99, 11940-11945.

Ferre, S., Popoli, P., Rimondini, R., Reggio, R., Kehr, J., Fuxe, K., 1999. Adenosine A2A and group I metabotropic glutamate receptors synergistically modulate the binding characteristics of dopamine D2 receptors in the rat striatum. Neuropharmacology 38, 129-140.

Flanagan, C. A., 2016. GPCR-radioligand binding assays. Methods Cell Biol. 132, 191-215.

Fox, S. H., Katzenschlager, R., Lim, S.-Y., Ravina, B., Seppi, K., Coelho, M., Poewe, W., Rascol, O., Goetz, C. G., Sampaio, C., 2011. The Movement Disorder Society

Evidence-Based Medicine Review Update: Treatments for the motor symptoms of Parkinson's disease. Mov. Disord. 26, S2-S41.
Francesconi, A., Duvoisin, R. M., 1998. Role of the second and third intracellular loops of metabotropic glutamate receptors in mediating dual signal transduction activation. J. Biol. Chem. 273, 5615-5624.

Francesconi, A., Duvoisin, R. M., 2004. Divalent cations modulate the activity of metabotropic glutamate receptors. J. Neurosci. Res. 75, 472-479.

Galandrin, S., Onfroy, L., Poirot, M. C., Senard, J. M., Gales, C., 2016. Delineating biased ligand efficacy at 7TM receptors from an experimental perspective. Int. J. Biochem. Cell Biol. 77, 251-263.

Galici, R., Echemendia, N. G., Rodriguez, A. L., Conn, P. J., 2005. A selective allosteric potentiator of metabotropic glutamate (mGlu) 2 receptors has effects similar to an orthosteric mGlu2/3 receptor agonist in mouse models predictive of antipsychotic activity. J. Pharmacol. Exp. Ther. 315, 1181-1187.

Galici, R., Jones, C. K., Hemstapat, K., Nong, Y., Echemendia, N. G., Williams, L. C., de Paulis, T., Conn, P. J., 2006. Biphenyl-indanone A, a positive allosteric modulator of the metabotropic glutamate receptor subtype 2, has antipsychotic- and anxiolytic-like effects in mice. J. Pharmacol. Exp. Ther. 318, 173-185.

Galik, J., Youn, D. H., Kolaj, M., Randic, M., 2008. Involvement of group I metabotropic glutamate receptors and glutamate transporters in the slow excitatory synaptic transmission in the spinal cord dorsal horn. Neuroscience 154, 1372-1387.

Gallagher, S. M., Daly, C. A., Bear, M. F., Huber, K. M., 2004. Extracellular signal-regulated protein kinase activation is required for metabotropic glutamate receptor-dependent long-term depression in hippocampal area CA1. J. Neurosci. 24, 4859-4864.

Galling, B., Calsina Ferrer, A., Abi Zeid Daou, M., Sangroula, D., Hagi, K., Correll, C. U., 2015. Safety and tolerability of antidepressant co-treatment in acute major depressive disorder: results from a systematic review and exploratory meta-analysis. Expert Opin. Drug Saf. 14, 1587-1608.

Gama, L., Wilt, S. G., Breitwieser, G. E., 2001. Heterodimerization of calcium sensing receptors with metabotropic glutamate receptors in neurons. J. Biol. Chem. 276, 39053-39059.

Gao, C., Tronson, N. C., Radulovic, J., 2013. Modulation of behavior by scaffolding proteins of the post-synaptic density. Neurobiol. Learn. Mem. 105, 3-12.

Garber, K. B., Visootsak, J., Warren, S. T., 2008. Fragile X syndrome. Eur. J. Hum. Genet. 16, 666-672.

Gasparini, F., Andres, H., Flor, P. J., Heinrich, M., Inderbitzin, W., Lingenhohl, K., Muller, H., Munk, V. C., Omilusik, K., Stierlin, C., Stoehr, N., Vranesic, I., Kuhn, R.,

2002. [(3)H]-M-MPEP, a potent, subtype-selective radioligand for the metabotropic glutamate receptor subtype 5. Bioorg. Med. Chem. Lett. 12, 407-409.
Gasparini, F., Floersheim, P., Flor, P. J., Heinrich, M., Inderbitzin, W., Ott, D., Pagano, A., Stierlin, C., Stoehr, N., Vranesic, I., Kuhn, R., 2001. Discovery and characterization of non-competitive antagonists of group I metabotropic glutamate receptors. Farmaco 56, 95-99.

Gasparini, F., Lingenhohl, K., Stoehr, N., Flor, P., Heinrich, M., Vranesic, I., Biollaz, M., Allgeier, H., Heckendorn, R., Urwyler, S., Verney, M., Johnson, E., Hess, S., Rao, S., Sacaan, A., Santori, E., Velicelebi, G., Kuhn, R., 1999a. 2-Methyl-6-(phenylethynyl)-pyridine (MPEP), a potent, selective and systemically active mGlu5 receptor antagonist. Neuropharmacology 38, 1493 - 1503.

Gasparini, F., Lingenhohl, K., Stoehr, N., Flor, P. J., Heinrich, M., Vranesic, I., Biollaz, M., Allgeier, H., Heckendorn, R., Urwyler, S., Varney, M. A., Johnson, E. C., Hess, S. D., Rao, S. P., Sacaan, A. I., Santori, E. M., Velicelebi, G., Kuhn, R., 1999b. 2-Methyl-6-(phenylethynyl)-pyridine (MPEP), a potent, selective and systemically active mGlu5 receptor antagonist. Neuropharmacology 38, 1493-1503.

Gee, C. E., Peterlik, D., Neuhauser, C., Bouhelal, R., Kaupmann, K., Laue, G., Uschold-Schmidt, N., Feuerbach, D., Zimmermann, K., Ofner, S., Cryan, J. F., van der Putten, H., Fendt, M., Vranesic, I., Glatthar, R., Flor, P. J., 2014. Blocking metabotropic glutamate receptor subtype 7 (mGlu7) via the Venus flytrap domain (VFTD) inhibits amygdala plasticity, stress, and anxiety-related behavior. J. Biol. Chem. 289, 10975-10987.

Gerrow, K., Triller, A., 2010. Synaptic stability and plasticity in a floating world. Curr. Opin. Neurobiol. 20, 631-639.

Gorelova, N., Yang, C. R., 1997. The course of neural projection from the prefrontal cortex to the nucleus accumbens in the rat. Neuroscience 76, 689-706.

Goudet, C., Chapuy, E., Alloui, A., Acher, F., Pin, J. P., Eschalier, A., 2008. Group III metabotropic glutamate receptors inhibit hyperalgesia in animal models of inflammation and neuropathic pain. Pain 137, 112-124.

Goudet, C., Gaven, F., Kniazeff, J., Vol, C., Liu, J., Cohen-Gonsaud, M., Acher, F., Prezeau, L., Pin, J. P., 2004. Heptahelical domain of metabotropic glutamate receptor 5 behaves like rhodopsin-like receptors. Proc. Natl. Acad. Sci. U S A. 101, 378-383.

Goudet, C., Kniazeff, J., Hlavackova, V., Malhaire, F., Maurel, D., Acher, F., Blahos, J., Prezeau, L., Pin, J. P., 2005. Asymmetric functioning of dimeric metabotropic glutamate receptors disclosed by positive allosteric modulators. J. Biol. Chem. 280, 24380-24385.

Gould, R. W., Amato, R. J., Bubser, M., Joffe, M. E., Nedelcovych, M. T., Thompson, A. D., Nickols, H. H., Yuh, J. P., Zhan, X., Felts, A. S., Rodriguez, A. L., Morrison, R. D., Byers, F. W., Rook, J. M., Daniels, J. S., Niswender, C. M., Conn, P. J., Emmitte, K. A., Lindsley, C. W., Jones, C. K., 2016. Partial mGlu(5) Negative

Allosteric Modulators Attenuate Cocaine-Mediated Behaviors and Lack Psychotomimetic-Like Effects. Neuropsychopharmacol. 41, 1166-1178.
Gregory, K. J., Herman, E. J., Ramsey, A. J., Hammond, A. S., Byun, N. E., Stauffer, S. R., Manka, J. T., Jadhav, S., Bridges, T. M., Weaver, C. D., Niswender, C. M., Steckler, T., Drinkenburg, W. H., Ahnaou, A., Lavreysen, H., Macdonald, G. J., Bartolome, J. M., Mackie, C., Hrupka, B. J., Caron, M. G., Daigle, T. L., Lindsley, C. W., Conn, P. J., Jones, C. K., 2013a. N-aryl piperazine metabotropic glutamate receptor 5 positive allosteric modulators possess efficacy in preclinical models of NMDA hypofunction and cognitive enhancement. J. Pharmacol. Exp. Ther. 347, 438-457.

Gregory, K. J., Nguyen, E. D., Malosh, C., Mendenhall, J. L., Zic, J. Z., Bates, B. S., Noetzel, M. J., Squire, E. F., Turner, E. M., Rook, J. M., Emmitte, K. A., Stauffer, S. R., Lindsley, C. W., Meiler, J., Conn, P. J., 2014. Identification of specific ligand-receptor interactions that govern binding and cooperativity of diverse modulators to a common metabotropic glutamate receptor 5 allosteric site. ACS Chem. Neurosci. 5, 282-295.

Gregory, K. J., Nguyen, E. D., Reiff, S. D., Squire, E. F., Stauffer, S. R., Lindsley, C. W., Meiler, J., Conn, P. J., 2013b. Probing the metabotropic glutamate receptor 5 (mGlu5) positive allosteric modulator (PAM) binding pocket: discovery of point mutations that engender a "molecular switch" in PAM pharmacology. Mol. Pharmacol. 83, 991-1006.

Gregory, K. J., Noetzel, M. J., Niswender, C. M., 2013c. Pharmacology of metabotropic glutamate receptor allosteric modulators: structural basis and therapeutic potential for CNS disorders. Prog. Mol. Biol. Transl. 115, 61-121.
Gregory, K. J., Noetzel, M. J., Rook, J. M., Vinson, P. N., Stauffer, S. R., Rodriguez, A. L., Emmitte, K. A., Zhou, Y., Chun, A. C., Felts, A. S., Chauder, B. A., Lindsley, C. W., Niswender, C. M., Conn, P. J., 2012. Investigating metabotropic glutamate receptor 5 allosteric modulator cooperativity, affinity, and agonism: enriching structure-function studies and structure-activity relationships. Mol. Pharmacol. 82, 860-875.

Gregory, K. J., Sexton, P. M., Christopoulos, A., 2010. Overview of receptor allosterism. Curr. Protoc. Pharmacol. Chapter 1, Unit 1.21.

Gregory, K. J., Velagaleti, R., Thal, D. M., Brady, R. M., Christopoulos, A., Conn, P. J., Lapinsky, D. J., 2016. Clickable Photoaffinity Ligands for Metabotropic Glutamate Receptor 5 Based on Select Acetylenic Negative Allosteric Modulators. ACS Chem. Biol. 11, 1870-1879.

Halai, R., Croker, D. E., Suen, J. Y., Fairlie, D. P., Cooper, M. A., 2012. A Comparative Study of Impedance versus Optical Label-Free Systems Relative to Labelled Assays in a Predominantly Gi Coupled GPCR (C5aR) Signalling. Biosensors 2, 273-290.

Hall, D. A., 2000. Modeling the functional effects of allosteric modulators at pharmacological receptors: an extension of the two-state model of receptor activation. Mol. Pharmacol. 58, 1412-1423.

Hamilton, A., Esseltine, J. L., DeVries, R. A., Cregan, S. P., Ferguson, S. S., 2014. Metabotropic glutamate receptor 5 knockout reduces cognitive impairment and pathogenesis in a mouse model of Alzheimer's disease. Mol. Brain 7, 40.

Hammond, A. S., Rodriguez, A. L., Townsend, S. D., Niswender, C. M., Gregory, K. J., Lindsley, C. W., Conn, P. J., 2010. Discovery of a Novel Chemical Class of mGlu(5) Allosteric Ligands with Distinct Modes of Pharmacology. ACS Chem. Neurosci. 1, 702-716.

Harrington, P. E., Fotsch, C., 2007. Calcium sensing receptor activators: calcimimetics. Curr. Med. Chem. 14, 3027-3034.

Hashimoto, K., Sawa, A., Iyo, M., 2007. Increased levels of glutamate in brains from patients with mood disorders. Biol. Psychiat. 62, 1310-1316.

Hathaway, H. A., Pshenichkin, S., Grajkowska, E., Gelb, T., Emery, A. C., Wolfe, B. B., Wroblewski, J. T., 2015. Pharmacological characterization of mGlu1 receptors in cerebellar granule cells reveals biased agonism. Neuropharmacology 93, 199-208.

Hellyer, S. D., Albold, S., Wang, T., Chen, A. N., May, L. T., Leach, K., Gregory, K. J., 2018. "Selective" Class C G protein-coupled receptor modulators are neutral or biased mGlu5 allosteric ligands. Mol. Pharmacol. doi: 10.1124/mol.117.111518

Helton, D. R., Tizzano, J. P., Monn, J. A., Schoepp, D. D., Kallman, M. J., 1997. LY354740: a metabotropic glutamate receptor agonist which ameliorates symptoms of nicotine withdrawal in rats. Neuropharmacology 36, 1511-1516.

Hemstapat, K., de Paulis, T., Chen, Y., Brady, A. E., Grover, V. K., Alagille, D., Tamagnan, G. D., Conn, P. J., 2006. A novel class of positive allosteric modulators of metabotropic glutamate receptor subtype 1 interact with a site distinct from that of negative allosteric modulators. Mol. Pharmacol. 70, 616-626.

Hermans, E., Challiss, R. A., 2001. Structural, signalling and regulatory properties of the group I metabotropic glutamate receptors: prototypic family C G-protein-coupled receptors. Biochem. J. 359, 465-484.

Holst, B., Nygaard, R., Valentin-Hansen, L., Bach, A., Engelstoft, M. S., Petersen, P. S., Frimurer, T. M., Schwartz, T. W., 2010. A conserved aromatic lock for the tryptophan rotameric switch in TM-VI of seven-transmembrane receptors. J. Biol. Chem. 285, 3973-3985.

Homayoun, H., Stefani, M. R., Adams, B. W., Tamagan, G. D., Moghaddam, B., 2004. Functional Interaction Between NMDA and mGlu5 Receptors: Effects on Working Memory, Instrumental Learning, Motor Behaviors, and Dopamine Release. Neuropsychopharmacol. 29, 1259-1269.

Honda, K., Shinoda, M., Kondo, M., Shimizu, K., Yonemoto, H., Otsuki, K., Akasaka, R., Furukawa, A., Iwata, K., 2017. Sensitization of TRPV1 and TRPA1 via peripheral mGluR5 signaling contributes to thermal and mechanical hypersensitivity. Pain 158, 1754-1764.

Hong, S., Fan, J., Kemmerer, E. S., Evans, S., Li, Y., Wiley, J. W., 2009. Reciprocal changes in vanilloid (TRPV1) and endocannabinoid (CB1) receptors contribute to visceral hyperalgesia in the water avoidance stressed rat. Gut 58, 202.

Horio, M., Fujita, Y., Hashimoto, K., 2013. Therapeutic effects of metabotropic glutamate receptor 5 positive allosteric modulator CDPPB on phencyclidine-induced cognitive deficits in mice. Fundam. Clin. Pharmacol. 27, 483-488.

Hou, L., Klann, E., 2004. Activation of the phosphoinositide 3-kinase-Akt-mammalian target of rapamycin signaling pathway is required for metabotropic glutamate receptor-dependent long-term depression. J. Neurosci. 24, 6352-6361.

Houamed, K. M., Kuijper, J. L., Gilbert, T. L., Haldeman, B. A., O'Hara, P. J., Mulvihill, E. R., Almers, W., Hagen, F. S., 1991. Cloning, expression, and gene structure of a G protein-coupled glutamate receptor from rat brain. Science 252, 1318-1321.

Hu, H. J., Alter, B. J., Carrasquillo, Y., Qiu, C. S., Gereau, R. W. t., 2007. Metabotropic glutamate receptor 5 modulates nociceptive plasticity via extracellular signal-regulated kinase-Kv4.2 signaling in spinal cord dorsal horn neurons. J. Neurosci. 27, 13181-13191.

Huang, C.-C., Liang, Y.-C., Lee, C.-C., Hsu, K.-S., 2015. Cocaine Withdrawal Impairs mGluR5-Dependent Long-Term Depression in Nucleus Accumbens Shell Neurons of Both Direct and Indirect Pathways. Mol. Neurobiol. 52, 1223-1233.

Huang, S. M., Bisogno, T., Trevisani, M., Al-Hayani, A., De Petrocellis, L., Fezza, F., Tognetto, M., Petros, T. J., Krey, J. F., Chu, C. J., Miller, J. D., Davies, S. N., Geppetti, P., Walker, J. M., Di Marzo, V., 2002. An endogenous capsaicin-like substance with high potency at recombinant and native vanilloid VR1 receptors. Proc. Natl. Acad. Sci. U S A. 99, 8400-8405.

Huber, K. M., Gallagher, S. M., Warren, S. T., Bear, M. F., 2002. Altered synaptic plasticity in a mouse model of fragile X mental retardation. Proc. Natl. Acad. Sci. U S A. 99, 7746-7750.

Huber, K. M., Roder, J. C., Bear, M. F., 2001. Chemical induction of mGluR5- and protein synthesis--dependent long-term depression in hippocampal area CA1. J. Neurophysiol. 86, 321-325.

Hubert, G. W., Paquet, M., Smith, Y., 2001. Differential subcellular localization of mGluR1a and mGluR5 in the rat and monkey Substantia nigra. J. Neurosci. 21, 1838-1847.

Hughes, Z. A., Neal, S. J., Smith, D. L., Sukoff Rizzo, S. J., Pulicicchio, C. M., Lotarski, S., Lu, S., Dwyer, J. M., Brennan, J., Olsen, M., Bender, C. N., Kouranova, E., Andree, T. H., Harrison, J. E., Whiteside, G. T., Springer, D., O'Neil, S. V., Leonard, S. K., Schechter, L. E., Dunlop, J., Rosenzweig-Lipson, S., Ring, R. H., 2013. Negative allosteric modulation of metabotropic glutamate receptor 5 results in

broad spectrum activity relevant to treatment resistant depression. Neuropharmacology 66, 202-214.

Inta, D., Vogt, M. A., Luoni, A., Filipovic, D., Lima-Ojeda, J. M., Pfeiffer, N., Gasparini, F., Riva, M. A., Gass, P., 2013. Significant increase in anxiety during aging in mGlu5 receptor knockout mice. Behav. Brain Res. 241, 27-31.

Irwin, S. A., Idupulapati, M., Gilbert, M. E., Harris, J. B., Chakravarti, A. B., Rogers, E. J., Crisostomo, R. A., Larsen, B. P., Mehta, A., Alcantara, C. J., Patel, B., Swain, R. A., Weiler, I. J., Oostra, B. A., Greenough, W. T., 2002. Dendritic spine and dendritic field characteristics of layer V pyramidal neurons in the visual cortex of fragile-X knockout mice. Am. J. Med. Genet. 111, 140-146.

Iso, Y., Grajkowska, E., Wroblewski, J. T., Davis, J., Goeders, N. E., Johnson, K. M., Sanker, S., Roth, B. L., Tueckmantel, W., Kozikowski, A. P., 2006. Synthesis and structure-activity relationships of 3-[(2-methyl-1,3-thiazol-4-yl)ethynyl]pyridine analogues as potent, noncompetitive metabotropic glutamate receptor subtype 5 antagonists; search for cocaine medications. J. Med. Chem. 49, 1080-1100.

Jacob, W., Gravius, A., Pietraszek, M., Nagel, J., Belozertseva, I., Shekunova, E., Malyshkin, A., Greco, S., Barberi, C., Danysz, W., 2009. The anxiolytic and analgesic properties of fenobam, a potent mGlu5 receptor antagonist, in relation to the impairment of learning. Neuropharmacology 57, 97-108.

Jacobson, K. A., 2015. New paradigms in GPCR drug discovery. Biochem. Pharmacol. 98, 541-555.

Jaeschke, G., Kolczewski, S., Spooren, W., Vieira, E., Bitter-Stoll, N., Boissin, P., Borroni, E., Buttelmann, B., Ceccarelli, S., Clemann, N., David, B., Funk, C., Guba, W., Harrison, A., Hartung, T., Honer, M., Huwyler, J., Kuratli, M., Niederhauser, U., Pahler, A., Peters, J. U., Petersen, A., Prinssen, E., Ricci, A., Rueher, D., Rueher, M., Schneider, M., Spurr, P., Stoll, T., Tannler, D., Wichmann, J., Porter, R. H., Wettstein, J. G., Lindemann, L., 2015. Metabotropic glutamate receptor 5 negative allosteric modulators: discovery of 2-chloro-4-[1-(4-fluorophenyl)-2,5-dimethyl-1H-imidazol-4-ylethynyl]pyridine (basimglurant, RO4917523), a promising novel medicine for psychiatric diseases. J. Med. Chem. 58, 1358-1371.

Jalan-Sakrikar, N., Field, J. R., Klar, R., Mattmann, M. E., Gregory, K. J., Zamorano, R., Engers, D. W., Bollinger, S. R., Weaver, C. D., Days, E. L., Lewis, L. M., Utley, T. J., Hurtado, M., Rigault, D., Acher, F., Walker, A. G., Melancon, B. J., Wood, M. R., Lindsley, C. W., Conn, P. J., Xiang, Z., Hopkins, C. R., Niswender, C. M., 2014. Identification of positive allosteric modulators VU0155094 (ML397) and VU0422288 (ML396) reveals new insights into the biology of metabotropic glutamate receptor 7. ACS Chem. Neurosci. 5, 1221-1237.

Jamison, R. N., Mao, J., 2015. Opioid Analgesics. Mayo Clin. Proc. 90, 957-968.
Jensen, A. A., Brauner-Osborne, H., 2007. Allosteric modulation of the calcium-sensing receptor. Curr. Neuropharmacol. 5, 180-186.

Jerman, J. C., Gray, J., Brough, S. J., Ooi, L., Owen, D., Davis, J. B., Smart, D., 2002. Comparison of effects of anandamide at recombinant and endogenous rat vanilloid receptors. Br. J. Anaesth. 89, 882-887.

Jia, Z., Lu, Y., Henderson, J., Taverna, F., Romano, C., Abramow-Newerly, W., Wojtowicz, J. M., Roder, J., 1998. Selective abolition of the NMDA component of long-term potentiation in mice lacking mGluR5. Learn. Mem. 5, 331-343.

Jin, X., Semenova, S., Yang, L., Ardecky, R., Sheffler, D. J., Dahl, R., Conn, P. J., Cosford, N. D., Markou, A., 2010. The mGluR2 positive allosteric modulator BINA decreases cocaine self-administration and cue-induced cocaine-seeking and counteracts cocaine-induced enhancement of brain reward function in rats. Neuropsychopharmacol. 35, 2021-2036.

Jin, Y. H., Nishioka, H., Wakabayashi, K., Fujita, T., Yonehara, N., 2006. Effect of morphine on the release of excitatory amino acids in the rat hind instep: Pain is modulated by the interaction between the peripheral opioid and glutamate systems. Neuroscience 138, 1329-1339.

Johnson, M. P., Barda, D., Britton, T. C., Emkey, R., Hornback, W. J., Jagdmann, G. E., McKinzie, D. L., Nisenbaum, E. S., Tizzano, J. P., Schoepp, D. D., 2005. Metabotropic glutamate 2 receptor potentiators: receptor modulation, frequency-dependent synaptic activity, and efficacy in preclinical anxiety and psychosis model(s). Psychopharmacol. (Berl) 179, 271-283.

Joly, C., Gomeza, J., Brabet, I., Curry, K., Bockaert, J., Pin, J. P., 1995. Molecular, functional, and pharmacological characterization of the metabotropic glutamate receptor type 5 splice variants: comparison with mGluR1. J. Neurosci. 15, 3970-3981.

Jones, C. K., Engers, D. W., Thompson, A. D., Field, J. R., Blobaum, A. L., Lindsley, S. R., Zhou, Y., Gogliotti, R. D., Jadhav, S., Zamorano, R., Bogenpohl, J., Smith, Y., Morrison, R., Daniels, J. S., Weaver, C. D., Conn, P. J., Lindsley, C. W., Niswender, C. M., Hopkins, C. R., 2011. Discovery, synthesis, and structure-activity relationship development of a series of N-4-(2,5-dioxopyrrolidin-1-yl)phenylpicolinamides (VU0400195, ML182): characterization of a novel positive allosteric modulator of the metabotropic glutamate receptor 4 (mGlu(4)) with oral efficacy in an antiparkinsonian animal model. J. Med. Chem. 54, 7639-7647.

Jong, Y. J., Kumar, V., Kingston, A. E., Romano, C., O'Malley, K. L., 2005. Functional metabotropic glutamate receptors on nuclei from brain and primary cultured striatal neurons. Role of transporters in delivering ligand. J. Biol. Chem. 280, 30469-30480.

Jong, Y. J., Kumar, V., O'Malley, K. L., 2009. Intracellular metabotropic glutamate receptor 5 (mGluR5) activates signaling cascades distinct from cell surface counterparts. J. Biol. Chem. 284, 35827-35838.

Jong, Y. J., Sergin, I., Purgert, C. A., O'Malley, K. L., 2014. Location-dependent signaling of the group 1 metabotropic glutamate receptor mGlu5. Mol. Pharmacol. 86, 774-785.

Jung, J., Shin, J. S., Lee, S. Y., Hwang, S. W., Koo, J., Cho, H., Oh, U., 2004. Phosphorylation of vanilloid receptor 1 by Ca2+/calmodulin-dependent kinase II regulates its vanilloid binding. J. Biol. Chem. 279, 7048-7054.

Kaiser, L. G., Schuff, N., Cashdollar, N., Weiner, M. W., 2005. Age-related glutamate and glutamine concentration changes in normal human brain: (1)H MR spectroscopy study at 4 T. Neurobiol. Aging 26, 665-672.

Kalia, L. V., Lang, A. E., 2015. Parkinson's disease. Lancet 386, 896-912.
Kammermeier, P. J., 2012. Functional and pharmacological characteristics of metabotropic glutamate receptors 2/4 heterodimers. Mol. Pharmacol. 82, 438-447.

Kammermeier, P. J., Ikeda, S. R., 2001. A role for Seven in Absentia Homolog (Siah1a) in metabotropic glutamate receptor signaling. BMC Neurosci. 2, 15.

Kammermeier, P. J., Worley, P. F., 2007. Homer 1a uncouples metabotropic glutamate receptor 5 from postsynaptic effectors. Proc. Natl. Acad. Sci. U S A. 104, 6055-6060.

Kammermeier, P. J., Xiao, B., Tu, J. C., Worley, P. F., Ikeda, S. R., 2000. Homer proteins regulate coupling of group I metabotropic glutamate receptors to N-type calcium and M-type potassium channels. J. Neurosci. 20, 7238-7245.

Karim, F., Bhave, G., Gereau, R. W. t., 2001. Metabotropic glutamate receptors on peripheral sensory neuron terminals as targets for the development of novel analgesics. Mol. Psychiatr. 6, 615-617.

Kato, H. K., Kassai, H., Watabe, A. M., Aiba, A., Manabe, T., 2012. Functional coupling of the metabotropic glutamate receptor, InsP3 receptor and L-type Ca2+ channel in mouse CA1 pyramidal cells. J. Physiol. 590, 3019-3034.

Kawabata, S., Tsutsumi, R., Kohara, A., Yamaguchi, T., Nakanishi, S., Okada, M., 1996. Control of calcium oscillations by phosphorylation of metabotropic glutamate receptors. Nature 383, 89-92.

Kenakin, T., 2004. Principles: receptor theory in pharmacology. Trends Pharmacol. Sci. 25, 186-192.

Kenakin, T., 2009. Quantifying biological activity in chemical terms: a pharmacology primer to describe drug effect. ACS Chem. Biol. 4, 249-260.

Kenakin, T., Christopoulos, A., 2011. Analytical pharmacology: the impact of numbers on pharmacology. Trends Pharmacol. Sci. 32, 189-196.

Kenakin, T., Christopoulos, A., 2013. Signalling bias in new drug discovery: detection, quantification and therapeutic impact. Nat. Rev. Drug Discov. 12, 205-216.

Kenakin, T., Watson, C., Muniz-Medina, V., Christopoulos, A., Novick, S., 2012. A simple method for quantifying functional selectivity and agonist bias. ACS Chem. Neurosci. 3, 193-203.

Keov, P., Sexton, P. M., Christopoulos, A., 2011. Allosteric modulation of G protein-coupled receptors: a pharmacological perspective. Neuropharmacology 60, 24-35.

Kessler, R. C., Aguilar-Gaxiola, S., Alonso, J., Chatterji, S., Lee, S., Ormel, J., Üstün, T. B., Wang, P. S., 2009. The global burden of mental disorders: An update from the WHO World Mental Health (WMH) Surveys. Epidemiologia e psichiatria sociale 18, 23-33.

Kettunen, P., Krieger, P., Hess, D., El Manira, A., 2002. Signaling mechanisms of metabotropic glutamate receptor 5 subtype and its endogenous role in a locomotor network. J. Neurosci. 22, 1868-1873.

Khajehali, E., Malone, D. T., Glass, M., Sexton, P. M., Christopoulos, A., Leach, K., 2015. Biased Agonism and Biased Allosteric Modulation at the CB1 Cannabinoid Receptor. Mol. Pharmacol. 88, 368-379.

Kim, Y. H., Park, C. K., Back, S. K., Lee, C. J., Hwang, S. J., Bae, Y. C., Na, H. S., Kim, J. S., Jung, S. J., Oh, S. B., 2009. Membrane-delimited coupling of TRPV1 and mGluR5 on presynaptic terminals of nociceptive neurons. J. Neurosci. 29, 10000-10009.

Kinney, G. G., Burno, M., Campbell, U. C., Hernandez, L. M., Rodriguez, D., Bristow, L. J., Conn, P. J., 2003. Metabotropic glutamate subtype 5 receptors modulate locomotor activity and sensorimotor gating in rodents. J. Pharmacol. Exp. Ther. 306, 116-123.

Kinney, G. G., O'Brien, J. A., Lemaire, W., Burno, M., Bickel, D. J., Clements, M. K., Chen, T. B., Wisnoski, D. D., Lindsley, C. W., Tiller, P. R., Smith, S., Jacobson, M. A., Sur, C., Duggan, M. E., Pettibone, D. J., Conn, P. J., Williams, D. L., Jr., 2005. A novel selective positive allosteric modulator of metabotropic glutamate receptor subtype 5 has in vivo activity and antipsychotic-like effects in rat behavioral models. J. Pharmacol. Exp. Ther. 313, 199-206.

Klein Herenbrink, C., Sykes, D. A., Donthamsetti, P., Canals, M., Coudrat, T., Shonberg, J., Scammells, P. J., Capuano, B., Sexton, P. M., Charlton, S. J., Javitch, J. A., Christopoulos, A., Lane, J. R., 2016. The role of kinetic context in apparent biased agonism at GPCRs. Nat Commun 7, 10842.

Knoflach, F., Mutel, V., Jolidon, S., Kew, J. N., Malherbe, P., Vieira, E., Wichmann, J., Kemp, J. A., 2001. Positive allosteric modulators of metabotropic glutamate 1 receptor: characterization, mechanism of action, and binding site. Proc. Natl. Acad. Sci. U S A. 98, 13402-13407.

Ko, S. J., Isozaki, K., Kim, I., Lee, J. H., Cho, H. J., Sohn, S. Y., Oh, S. R., Park, S., Kim, D. G., Kim, C. H., Roche, K. W., 2012. PKC phosphorylation regulates mGluR5 trafficking by enhancing binding of Siah-1A. J. Neurosci. 32, 16391-16401.

Kobayashi, K., Fukuoka, T., Obata, K., Yamanaka, H., Dai, Y., Tokunaga, A., Noguchi, K., 2005. Distinct expression of TRPM8, TRPA1, and TRPV1 mRNAs in

rat primary afferent neurons with adelta/c-fibers and colocalization with trk receptors. J. Comp. Neurol. 493, 596-606.

Kohara, A., Toya, T., Tamura, S., Watabiki, T., Nagakura, Y., Shitaka, Y., Hayashibe, S., Kawabata, S., Okada, M., 2005. Radioligand binding properties and pharmacological characterization of 6-amino-N-cyclohexyl-N,3-dimethylthiazolo[3,2-a]benzimidazole-2-carboxamide (YM-298198), a high-affinity, selective, and noncompetitive antagonist of metabotropic glutamate receptor type 1. J. Pharmacol. Exp. Ther. 315, 163-169.

Kolber, B. J., Montana, M. C., Carrasquillo, Y., Xu, J., Heinemann, S. F., Muglia, L. J., Gereau, R. W. t., 2010. Activation of metabotropic glutamate receptor 5 in the amygdala modulates pain-like behavior. J. Neurosci. 30, 8203-8213.

Kotecha, S. A., Jackson, M. F., Al-Mahrouki, A., Roder, J. C., Orser, B. A., MacDonald, J. F., 2003. Co-stimulation of mGluR5 and N-methyl-D-aspartate receptors is required for potentiation of excitatory synaptic transmission in hippocampal neurons. J. Biol. Chem. 278, 27742-27749.

Kubo, Y., Miyashita, T., Murata, Y., 1998. Structural basis for a Ca2+-sensing function of the metabotropic glutamate receptors. Science 279, 1722-1725.

Kumar, J., Hapidin, H., Bee, Y.-T., Ismail, Z., 2013. Effects of the mGluR5 antagonist MPEP on ethanol withdrawal induced anxiety-like syndrome in rats. Behav. Brain Funct. 9, 43.

Kumar, V., Fahey, P. G., Jong, Y. J., Ramanan, N., O'Malley, K. L., 2012. Activation of intracellular metabotropic glutamate receptor 5 in striatal neurons leads to up-regulation of genes associated with sustained synaptic transmission including Arc/Arg3.1 protein. J. Biol. Chem. 287, 5412-5425.

Kumar, V., Jong, Y. J., O'Malley, K. L., 2008. Activated nuclear metabotropic glutamate receptor mGlu5 couples to nuclear Gq/11 proteins to generate inositol 1,4,5-trisphosphate-mediated nuclear Ca2+ release. J. Biol. Chem. 283, 14072-14083.

Kunishima, N., Shimada, Y., Tsuji, Y., Sato, T., Yamamoto, M., Kumasaka, T., Nakanishi, S., Jingami, H., Morikawa, K., 2000. Structural basis of glutamate recognition by a dimeric metabotropic glutamate receptor. Nature 407, 971-977.

Kwiatkowski, D. J., Manning, B. D., 2005. Tuberous sclerosis: a GAP at the crossroads of multiple signaling pathways. Hum. Mol. Genet. 14 Spec No. 2, R251-258.

Lagerstrom, M. C., Schioth, H. B., 2008. Structural diversity of G protein-coupled receptors and significance for drug discovery. Nat. Rev. Drug Discov. 7, 339-357.

Lamb, J. P., Engers, D. W., Niswender, C. M., Rodriguez, A. L., Venable, D. F., Conn, P. J., Lindsley, C. W., 2011. Discovery of molecular switches within the ADX-47273 mGlu5 PAM scaffold that modulate modes of pharmacology to afford potent

mGlu5 NAMs, PAMs and partial antagonists. Bioorg. Med. Chem. Lett. 21, 2711-2714.

Lane, J. R., May, L. T., Parton, R. G., Sexton, P. M., Christopoulos, A., 2017. A kinetic view of GPCR allostery and biased agonism. Nat. Chem. Biol. 13, 929-937.
Langmead, C. J., Christopoulos, A., 2014. Functional and structural perspectives on allosteric modulation of GPCRs. Curr. Opin. Cell. Biol. 27, 94-101.

Latek, D., Modzelewska, A., Trzaskowski, B., Palczewski, K., Filipek, S., 2012. G protein-coupled receptors — recent advances. Acta biochimica Polonica 59, 515-529.

Latif-Hernandez, A., Faldini, E., Ahmed, T., Balschun, D., 2016. Separate Ionotropic and Metabotropic Glutamate Receptor Functions in Depotentiation vs. LTP: A Distinct Role for Group1 mGluR Subtypes and NMDARs. Front. Cell. Neurosci. 10, 252.

Lavreysen, H., Janssen, C., Bischoff, F., Langlois, X., Leysen, J. E., Lesage, A. S., 2003. [3H]R214127: a novel high-affinity radioligand for the mGlu1 receptor reveals a common binding site shared by multiple allosteric antagonists. Mol. Pharmacol. 63, 1082-1093.

Lawand, N. B., McNearney, T., Westlund, K. N., 2000. Amino acid release into the knee joint: key role in nociception and inflammation. Pain 86, 69-74.

Lazareno, S., Birdsall, N. J., 1993. Estimation of competitive antagonist affinity from functional inhibition curves using the Gaddum, Schild and Cheng-Prusoff equations. Br. J. Pharmacol. 109, 1110-1119.

Lazareno, S., Birdsall, N. J., 1995. Detection, quantitation, and verification of allosteric interactions of agents with labeled and unlabeled ligands at G protein-coupled receptors: interactions of strychnine and acetylcholine at muscarinic receptors. Mol. Pharmacol. 48, 362-378.

Le Poul, E., Bolea, C., Girard, F., Poli, S., Charvin, D., Campo, B., Bortoli, J., Bessif, A., Luo, B., Koser, A. J., Hodge, L. M., Smith, K. M., DiLella, A. G., Liverton, N., Hess, F., Browne, S. E., Reynolds, I. J., 2012. A potent and selective metabotropic glutamate receptor 4 positive allosteric modulator improves movement in rodent models of Parkinson's disease. J. Pharmacol. Exp. Ther. 343, 167-177.

Lea, P. M. t., Faden, A. I., 2006. Metabotropic glutamate receptor subtype 5 antagonists MPEP and MTEP. CNS Drug Rev. 12, 149-166.

Leach, K., Gregory, K. J., 2017. Molecular insights into allosteric modulation of Class C G protein-coupled receptors. Pharmacol. Res. 116, 105-118.

Leach, K., Gregory, K. J., Kufareva, I., Khajehali, E., Cook, A. E., Abagyan, R., Conigrave, A. D., Sexton, P. M., Christopoulos, A., 2016. Towards a structural understanding of allosteric drugs at the human calcium-sensing receptor. Cell Research 26, 574-592.

Leach, K., Sexton, P. M., Christopoulos, A., 2007. Allosteric GPCR modulators: taking advantage of permissive receptor pharmacology. Trends Pharmacol. Sci. 28, 382-389.

Leach, K., Wen, A., Cook, A. E., Sexton, P. M., Conigrave, A. D., Christopoulos, A., 2013. Impact of clinically relevant mutations on the pharmacoregulation and signaling bias of the calcium-sensing receptor by positive and negative allosteric modulators. Endocrinology 154, 1105-1116.

Lee, J. H., Lee, J., Choi, K. Y., Hepp, R., Lee, J. Y., Lim, M. K., Chatani-Hinze, M., Roche, P. A., Kim, D. G., Ahn, Y. S., Kim, C. H., Roche, K. W., 2008. Calmodulin dynamically regulates the trafficking of the metabotropic glutamate receptor mGluR5. Proc. Natl. Acad. Sci. U S A. 105, 12575-12580.

Lee, J. S., Ro, J. Y., 2007. Peripheral metabotropic glutamate receptor 5 mediates mechanical hypersensitivity in craniofacial muscle via protein kinase C dependent mechanisms. Neuroscience 146, 375-383.

Levenga, J., Hayashi, S., de Vrij, F. M., Koekkoek, S. K., van der Linde, H. C., Nieuwenhuizen, I., Song, C., Buijsen, R. A., Pop, A. S., Gomezmancilla, B., Nelson, D. L., Willemsen, R., Gasparini, F., Oostra, B. A., 2011. AFQ056, a new mGluR5 antagonist for treatment of fragile X syndrome. Neurobiol. Dis. 42, 311-317.

Li, X., Need, A. B., Baez, M., Witkin, J. M., 2006. Metabotropic glutamate 5 receptor antagonism is associated with antidepressant-like effects in mice. J. Pharmacol. Exp. Ther. 319, 254-259.

Liechti, M. E., Lhuillier, L., Kaupmann, K., Markou, A., 2007. Metabotropic glutamate 2/3 receptors in the ventral tegmental area and the nucleus accumbens shell are involved in behaviors relating to nicotine dependence. J. Neurosci. 27, 9077-9085.

Limame, R., Wouters, A., Pauwels, B., Fransen, E., Peeters, M., Lardon, F., De Wever, O., Pauwels, P., 2012. Comparative Analysis of Dynamic Cell Viability, Migration and Invasion Assessments by Novel Real-Time Technology and Classic Endpoint Assays. PLoS One 7, e46536.

Lindemann, L., Jaeschke, G., Michalon, A., Vieira, E., Honer, M., Spooren, W., Porter, R., Hartung, T., Kolczewski, S., Büttelmann, B., Flament, C., Diener, C., Fischer, C., Gatti, S., Prinssen, E. P., Parrott, N., Hoffmann, G., Wettstein, J. G., 2011. CTEP: A Novel, Potent, Long-Acting, and Orally Bioavailable Metabotropic Glutamate Receptor 5 Inhibitor. J. Pharmacol. Exp.Ther. 339, 474-486.

Lindemann, L., Porter, R. H., Scharf, S. H., Kuennecke, B., Bruns, A., von Kienlin, M., Harrison, A. C., Paehler, A., Funk, C., Gloge, A., Schneider, M., Parrott, N. J., Polonchuk, L., Niederhauser, U., Morairty, S. R., Kilduff, T. S., Vieira, E., Kolczewski, S., Wichmann, J., Hartung, T., Honer, M., Borroni, E., Moreau, J. L., Prinssen, E., Spooren, W., Wettstein, J. G., Jaeschke, G., 2015. Pharmacology of basimglurant (RO4917523, RG7090), a unique metabotropic glutamate receptor 5 negative allosteric modulator in clinical development for depression. J. Pharmacol. Exp. Ther. 353, 213-233.

Lindsley, C. W., Emmitte, K. A., Hopkins, C. R., Bridges, T. M., Gregory, K. J., Niswender, C. M., Conn, P. J., 2016. Practical Strategies and Concepts in GPCR Allosteric Modulator Discovery: Recent Advances with Metabotropic Glutamate Receptors. Chem. Rev. 116, 6707-6741.

Lindsley, C. W., Stauffer, S. R., 2013. Metabotropic glutamate receptor 5-positive allosteric modulators for the treatment of schizophrenia (2004-2012). Pharm. Pat. Anal. 2, 93-108.

Lindsley, C. W., Wisnoski, D. D., Leister, W. H., O'Brien J, A., Lemaire, W., Williams, D. L., Jr., Burno, M., Sur, C., Kinney, G. G., Pettibone, D. J., Tiller, P. R., Smith, S., Duggan, M. E., Hartman, G. D., Conn, P. J., Huff, J. R., 2004. Discovery of positive allosteric modulators for the metabotropic glutamate receptor subtype 5 from a series of N-(1,3-diphenyl-1H- pyrazol-5-yl)benzamides that potentiate receptor function in vivo. J. Med. Chem. 47, 5825-5828.

Litim, N., Morissette, M., Di Paolo, T., 2017. Metabotropic glutamate receptors as therapeutic targets in Parkinson's disease: An update from the last 5 years of research. Neuropharmacology 115, 166-179.

Litschig, S., Gasparini, F., Rueegg, D., Stoehr, N., Flor, P. J., Vranesic, I., Prezeau, L., Pin, J. P., Thomsen, C., Kuhn, R., 1999. CPCCOEt, a noncompetitive metabotropic glutamate receptor 1 antagonist, inhibits receptor signaling without affecting glutamate binding. Mol. Pharmacol. 55, 453-461.

Llansola, M., Felipo, V., 2010. Metabotropic glutamate receptor 5, but not 1, modulates NMDA receptor-mediated activation of neuronal nitric oxide synthase. Neurochem. Int. 56, 535-545.

Lopez, S., Jouve, L., Turle-Lorenzo, N., Kerkerian-Legoff, L., Salin, P., Amalric, M., 2012. Antiparkinsonian action of a selective group III mGlu receptor agonist is associated with reversal of subthalamonigral overactivity. Neurobiol. Dis. 46, 69-77.
Lopez-Llano, J., Campos, L. A., Sancho, J., 2006. Alpha-helix stabilization by alanine relative to glycine: roles of polar and apolar solvent exposures and of backbone entropy. Proteins 64, 769-778.

Lu, W. Y., Xiong, Z. G., Lei, S., Orser, B. A., Dudek, E., Browning, M. D., MacDonald, J. F., 1999. G-protein-coupled receptors act via protein kinase C and Src to regulate NMDA receptors. Nat. Neurosci. 2, 331-338.

Luccini, E., Musante, V., Neri, E., Brambilla Bas, M., Severi, P., Raiteri, M., Pittaluga, A., 2007. Functional interactions between presynaptic NMDA receptors and metabotropic glutamate receptors co-expressed on rat and human noradrenergic terminals. Br. J. Pharmacol. 151, 1087-1094.

Lujan, R., Nusser, Z., Roberts, J. D., Shigemoto, R., Somogyi, P., 1996. Perisynaptic location of metabotropic glutamate receptors mGluR1 and mGluR5 on dendrites and dendritic spines in the rat hippocampus. Eur. J. Neurosci. 8, 1488-1500.

Lundstrom, L., Bissantz, C., Beck, J., Wettstein, J. G., Woltering, T. J., Wichmann, J., Gatti, S., 2011. Structural determinants of allosteric antagonism at metabotropic glutamate receptor 2: mechanistic studies with new potent negative allosteric modulators. Br. J. Pharmacol. 164, 521-537.

Luttrell, L. M., 2014. Minireview: More than just a hammer: ligand "bias" and pharmaceutical discovery. Mol. Endocrinol. 28, 281-294.

Lv, M. M., Cheng, Y. C., Xiao, Z. B., Sun, M. Y., Ren, P. C., Sun, X. D., 2014. Down-regulation of Homer1b/c attenuates group I metabotropic glutamate receptors dependent Ca(2)(+) signaling through regulating endoplasmic reticulum Ca(2)(+) release in PC12 cells. Biochem. Biophys. Res. Commun. 450, 1568-1574.

Mabire, D., Coupa, S., Adelinet, C., Poncelet, A., Simonnet, Y., Venet, M., Wouters, R., Lesage, A. S., Van Beijsterveldt, L., Bischoff, F., 2005. Synthesis, structure-activity relationship, and receptor pharmacology of a new series of quinoline derivatives acting as selective, noncompetitive mGlu1 antagonists. J. Med. Chem. 48, 2134-2153.

Maj, M., Bruno, V., Dragic, Z., Yamamoto, R., Battaglia, G., Inderbitzin, W., Stoehr, N., Stein, T., Gasparini, F., Vranesic, I., Kuhn, R., Nicoletti, F., Flor, P. J., 2003. (-)-PHCCC, a positive allosteric modulator of mGluR4: characterization, mechanism of action, and neuroprotection. Neuropharmacology 45, 895-906.

Malek, N., Mrugala, M., Makuch, W., Kolosowska, N., Przewlocka, B., Binkowski, M., Czaja, M., Morera, E., Di Marzo, V., Starowicz, K., 2015. A multi-target approach for pain treatment: dual inhibition of fatty acid amide hydrolase and TRPV1 in a rat model of osteoarthritis. Pain 156, 890-903.

Malherbe, P., Kratochwil, N., Muhlemann, A., Zenner, M. T., Fischer, C., Stahl, M., Gerber, P. R., Jaeschke, G., Porter, R. H., 2006. Comparison of the binding pockets of two chemically unrelated allosteric antagonists of the mGlu5 receptor and identification of crucial residues involved in the inverse agonism of MPEP. J. Neurochem. 98, 601-615.

Malherbe, P., Kratochwil, N., Zenner, M. T., Piussi, J., Diener, C., Kratzeisen, C., Fischer, C., Porter, R. H., 2003. Mutational analysis and molecular modeling of the binding pocket of the metabotropic glutamate 5 receptor negative modulator 2-methyl-6-(phenylethynyl)-pyridine. Mol. Pharmacol. 64, 823-832.

Mao, L., Yang, L., Tang, Q., Samdani, S., Zhang, G., Wang, J. Q., 2005. The scaffold protein Homer1b/c links metabotropic glutamate receptor 5 to extracellular signal-regulated protein kinase cascades in neurons. J. Neurosci. 25, 2741-2752.

Mao, L. M., Liu, X. Y., Zhang, G. C., Chu, X. P., Fibuch, E. E., Wang, L. S., Liu, Z., Wang, J. Q., 2008. Phosphorylation of group I metabotropic glutamate receptors (mGluR1/5) in vitro and in vivo. Neuropharmacology 55, 403-408.

Marek, G. J., Behl, B., Bespalov, A. Y., Gross, G., Lee, Y., Schoemaker, H., 2010. Glutamatergic (N-methyl-D-aspartate receptor) hypofrontality in schizophrenia: too little juice or a miswired brain? Mol. Pharmacol. 77, 317-326.

Marinelli, S., Di Marzo, V., Florenzano, F., Fezza, F., Viscomi, M. T., van der Stelt, M., Bernardi, G., Molinari, M., Maccarrone, M., Mercuri, N. B., 2007. N-arachidonoyl-dopamine tunes synaptic transmission onto dopaminergic neurons by activating both cannabinoid and vanilloid receptors. Neuropsychopharmacol. 32, 298-308.

Marino, M. J., Williams, D. L., Jr., O'Brien, J. A., Valenti, O., McDonald, T. P., Clements, M. K., Wang, R., DiLella, A. G., Hess, J. F., Kinney, G. G., Conn, P. J., 2003. Allosteric modulation of group III metabotropic glutamate receptor 4: a potential approach to Parkinson's disease treatment. Proc. Natl. Acad. Sci. U S A. 100, 13668-13673.

Martin, L. J., Blackstone, C. D., Huganir, R. L., Price, D. L., 1992. Cellular localization of a metabotropic glutamate receptor in rat brain. Neuron 9, 259-270.

Masu, M., Tanabe, Y., Tsuchida, K., Shigemoto, R., Nakanishi, S., 1991. Sequence and expression of a metabotropic glutamate receptor. Nature 349, 760-765.

Masuoka, T., Kudo, M., Yoshida, J., Ishibashi, T., Muramatsu, I., Kato, N., Imaizumi, N., Nishio, M., 2016. Long-term activation of group I metabotropic glutamate receptors increases functional TRPV1-expressing neurons in mouse dorsal root ganglia. Front. Cell. Neurosci. 10, 79.

Masuoka, T., Nakamura, T., Kudo, M., Yoshida, J., Takaoka, Y., Kato, N., Ishibashi, T., Imaizumi, N., Nishio, M., 2015. Biphasic modulation by mGlu5 receptors of TRPV1-mediated intracellular calcium elevation in sensory neurons contributes to heat sensitivity. Br. J. Pharmacol. 172, 1020-1033.

Matosin, N., Newell, K. A., 2013. Metabotropic glutamate receptor 5 in the pathology and treatment of schizophrenia. Neurosci. Biobehav. Rev. 37, 256-268.

McCool, B. A., Pin, J. P., Harpold, M. M., Brust, P. F., Stauderman, K. A., Lovinger, D. M., 1998. Rat group I metabotropic glutamate receptors inhibit neuronal Ca2+ channels via multiple signal transduction pathways in HEK 293 cells. J. Neurophysiol. 79, 379-391.

Melancon, B. J., Hopkins, C. R., Wood, M. R., Emmitte, K. A., Niswender, C. M., Christopoulos, A., Conn, P. J., Lindsley, C. W., 2012. Allosteric modulation of seven transmembrane spanning receptors: theory, practice, and opportunities for central nervous system drug discovery. J. Med. Chem. 55, 1445-1464.

Michalon, A., Sidorov, M., Ballard, T. M., Ozmen, L., Spooren, W., Wettstein, J. G., Jaeschke, G., Bear, M. F., Lindemann, L., 2012. Chronic pharmacological mGlu5 inhibition corrects fragile X in adult mice. Neuron 74, 49-56.

Millns, P. J., Chapman, V., Kendall, D. A., 2001. Cannabinoid inhibition of the capsaicin-induced calcium response in rat dorsal root ganglion neurones. Br. J. Pharmacol. 132, 969-971.

Mitsukawa, K., Yamamoto, R., Ofner, S., Nozulak, J., Pescott, O., Lukic, S., Stoehr, N., Mombereau, C., Kuhn, R., McAllister, K. H., van der Putten, H., Cryan, J. F., Flor, P. J., 2005. A selective metabotropic glutamate receptor 7 agonist: activation of receptor signaling via an allosteric site modulates stress parameters in vivo. Proc. Natl. Acad. Sci. U S A. 102, 18712-18717.

Moghaddam, B., Adams, B. W., 1998. Reversal of phencyclidine effects by a group II metabotropic glutamate receptor agonist in rats. Science 281, 1349-1352.

Mølck, C., Harpsøe, K., Gloriam, D. E., Clausen, R. P., Madsen, U., Pedersen, L. Ø., Jimenez, H. N., Nielsen, S. M., Mathiesen, J. M., Bräuner-Osborne, H., 2012. Pharmacological Characterization and Modeling of the Binding Sites of Novel 1,3-Bis(pyridinylethynyl)benzenes as Metabotropic Glutamate Receptor 5-Selective Negative Allosteric Modulators. Mol. Pharmacol. 82, 929.

Montana, M. C., Conrardy, B. A., Cavallone, L. F., Kolber, B. J., Rao, L. K., Greco, S. C., Gereau, R. W. t., 2011. Metabotropic glutamate receptor 5 antagonism with fenobam: examination of analgesic tolerance and side effect profile in mice. Anesthesiology 115, 1239-1250.

Morin, N., Gregoire, L., Morissette, M., Desrayaud, S., Gomez-Mancilla, B., Gasparini, F., Di Paolo, T., 2013a. MPEP, an mGlu5 receptor antagonist, reduces the development of L-DOPA-induced motor complications in de novo parkinsonian monkeys: biochemical correlates. Neuropharmacology 66, 355-364.

Morin, N., Morissette, M., Gregoire, L., Gomez-Mancilla, B., Gasparini, F., Di Paolo, T., 2013b. Chronic treatment with MPEP, an mGlu5 receptor antagonist, normalizes basal ganglia glutamate neurotransmission in L-DOPA-treated parkinsonian monkeys. Neuropharmacology 73, 216-231.

Moriyoshi, K., Iijima, K., Fujii, H., Ito, H., Cho, Y., Nakanishi, S., 2004. Seven in absentia homolog 1A mediates ubiquitination and degradation of group 1 metabotropic glutamate receptors. Proc. Natl. Acad. Sci. U S A. 101, 8614-8619.
Morris, B. J., Cochran, S. M., Pratt, J. A., 2005. PCP: from pharmacology to modelling schizophrenia. Curr. Opin. Pharmacol. 5, 101-106.

Moutin, E., Raynaud, F., Roger, J., Pellegrino, E., Homburger, V., Bertaso, F., Ollendorff, V., Bockaert, J., Fagni, L., Perroy, J., 2012. Dynamic remodeling of scaffold interactions in dendritic spines controls synaptic excitability. J. Cell. Biol. 198, 251-263.

Mueller, R., Dawson, E. S., Meiler, J., Rodriguez, A. L., Chauder, B. A., Bates, B. S., Felts, A. S., Lamb, J. P., Menon, U. N., Jadhav, S. B., Kane, A. S., Jones, C. K., Gregory, K. J., Niswender, C. M., Conn, P. J., Olsen, C. M., Winder, D. G., Emmitte, K. A., Lindsley, C. W., 2012. Discovery of 2-(2-benzoxazoyl amino)-4-aryl-5-cyanopyrimidine as negative allosteric modulators (NAMs) of metabotropic

glutamate receptor 5 (mGlu(5)): from an artificial neural network virtual screen to an in vivo tool compound. ChemMedChem 7, 406-414.

Muguruza, C., Meana, J. J., Callado, L. F., 2016. Group II Metabotropic Glutamate Receptors as Targets for Novel Antipsychotic Drugs. Front. Pharmacol. 7, 130.

Muhlemann, A., Ward, N. A., Kratochwil, N., Diener, C., Fischer, C., Stucki, A., Jaeschke, G., Malherbe, P., Porter, R. H., 2006. Determination of key amino acids implicated in the actions of allosteric modulation by 3,3'-difluorobenzaldazine on rat mGlu5 receptors. Eur. J. Pharmacol. 529, 95-104.

Mutel, V., Ellis, G. J., Adam, G., Chaboz, S., Nilly, A., Messer, J., Bleuel, Z., Metzler, V., Malherbe, P., Schlaeger, E. J., Roughley, B. S., Faull, R. L., Richards, J. G., 2000. Characterization of [(3)H]Quisqualate binding to recombinant rat metabotropic glutamate 1a and 5a receptors and to rat and human brain sections. J. Neurochem. 75, 2590-2601.

Muto, T., Tsuchiya, D., Morikawa, K., Jingami, H., 2007. Structures of the extracellular regions of the group II/III metabotropic glutamate receptors. Proc. Natl. Acad. Sci. U S A. 104, 3759-3764.

Nakamoto, M., Nalavadi, V., Epstein, M. P., Narayanan, U., Bassell, G. J., Warren, S. T., 2007. Fragile X mental retardation protein deficiency leads to excessive mGluR5-dependent internalization of AMPA receptors. Proc. Natl. Acad. Sci. U S A. 104, 15537-15542.

Nash, M. S., Schell, M. J., Atkinson, P. J., Johnston, N. R., Nahorski, S. R., Challiss, R. A., 2002. Determinants of metabotropic glutamate receptor-5-mediated Ca2+ and inositol 1,4,5-trisphosphate oscillation frequency. Receptor density versus agonist concentration. J. Biol. Chem. 277, 35947-35960.

Neyman, S., Manahan-Vaughan, D., 2008. Metabotropic glutamate receptor 1 (mGluR1) and 5 (mGluR5) regulate late phases of LTP and LTD in the hippocampal CA1 region in vitro. Eur. J. Neurosci. 27, 1345-1352.

Nickols, H. H., Conn, P. J., 2014. Development of allosteric modulators of GPCRs for treatment of CNS disorders. Neurobiol. Dis. 61, 55-71.

Nickols, H. H., Yuh, J. P., Gregory, K. J., Morrison, R. D., Bates, B. S., Stauffer, S. R., Emmitte, K. A., Bubser, M., Peng, W., Nedelcovych, M. T., Thompson, A., Lv, X., Xiang, Z., Daniels, J. S., Niswender, C. M., Lindsley, C. W., Jones, C. K., Conn, P. J., 2016. VU0477573: Partial Negative Allosteric Modulator of the Subtype 5 Metabotropic Glutamate Receptor with In Vivo Efficacy. J. Pharmacol. Exp. Ther. 356, 123-136.

Nicodemo, A. A., Pampillo, M., Ferreira, L. T., Dale, L. B., Cregan, T., Ribeiro, F. M., Ferguson, S. S., 2010. Pyk2 uncouples metabotropic glutamate receptor G protein signaling but facilitates ERK1/2 activation. Mol. Brain 3, 4.

Nicoletti, F., Bockaert, J., Collingridge, G. L., Conn, P. J., Ferraguti, F., Schoepp, D. D., Wroblewski, J. T., Pin, J. P., 2011a. Metabotropic glutamate receptors: from the workbench to the bedside. Neuropharmacology 60, 1017-1041.

Nicoletti, F., Bockaert, J., Collingridge, G. L., Conn, P. J., Ferraguti, F., Schoepp, D. D., Wroblewski, J. T., Pin, J. P., 2011b. Metabotropic glutamate receptors: From the workbench to the bedside. Neuropharmacology 60, 1017-1041.

Nicoletti, F., Bruno, V., Ngomba, R. T., Gradini, R., Battaglia, G., 2015. Metabotropic glutamate receptors as drug targets: what's new? Curr. Opin. Pharmacol. 20, 89-94.

Nimchinsky, E. A., Oberlander, A. M., Svoboda, K., 2001. Abnormal development of dendritic spines in FMR1 knock-out mice. J. Neurosci. 21, 5139-5146.

Nishi, A., Liu, F., Matsuyama, S., Hamada, M., Higashi, H., Nairn, A. C., Greengard, P., 2003. Metabotropic mGlu5 receptors regulate adenosine A2A receptor signaling. Proc. Natl. Acad. Sci. U S A. 100, 1322-1327.

Niswender, C. M., Conn, P. J., 2010. Metabotropic glutamate receptors: physiology, pharmacology, and disease. Annu. Rev. Pharmacol. Toxicol. 50, 295-322.

Niswender, C. M., Johnson, K. A., Miller, N. R., Ayala, J. E., Luo, Q., Williams, R., Saleh, S., Orton, D., Weaver, C. D., Conn, P. J., 2010. Context-dependent pharmacology exhibited by negative allosteric modulators of metabotropic glutamate receptor 7. Mol. Pharmacol. 77, 459-468.

Noetzel, M. J., Gregory, K. J., Vinson, P. N., Manka, J. T., Stauffer, S. R., Lindsley, C. W., Niswender, C. M., Xiang, Z., Conn, P. J., 2013. A novel metabotropic glutamate receptor 5 positive allosteric modulator acts at a unique site and confers stimulus bias to mGlu5 signaling.[Erratum appears in Mol Pharmacol. 2013 Oct;84(4):654]. Mol. Pharmacol. 83, 835-847.

Noetzel, M. J., Jones, C. K., Conn, P. J., 2012. Emerging approaches for treatment of schizophrenia: modulation of glutamatergic signaling. Discov. Med. 14, 335-343.
Nozadze, I., Tsiklauri, N., Gurtskaia, G., Tsagareli, M. G., 2016. Role of thermo TRPA1 and TRPV1 channels in heat, cold, and mechanical nociception of rats. Behav. pharmacol. 27, 29-36.

Nygaard, R., Frimurer, T. M., Holst, B., Rosenkilde, M. M., Schwartz, T. W., 2009. Ligand binding and micro-switches in 7TM receptor structures. Trends Pharmacol. Sci. 30, 249-259.

O'Brien, J. A., Lemaire, W., Chen, T. B., Chang, R. S., Jacobson, M. A., Ha, S. N., Lindsley, C. W., Schaffhauser, H. J., Sur, C., Pettibone, D. J., Conn, P. J., Williams, D. L., Jr., 2003. A family of highly selective allosteric modulators of the metabotropic glutamate receptor subtype 5. Mol. Pharmacol. 64, 731-740.

O'Brien, J. A., Lemaire, W., Wittmann, M., Jacobson, M. A., Ha, S. N., Wisnoski, D. D., Lindsley, C. W., Schaffhauser, H. J., Rowe, B., Sur, C., Duggan, M. E., Pettibone,

D. J., Conn, P. J., Williams, D. L., Jr., 2004. A novel selective allosteric modulator potentiates the activity of native metabotropic glutamate receptor subtype 5 in rat forebrain. J. Pharmacol. Exp. Ther. 309, 568-577.

O'Hara, P. J., Sheppard, P. O., Thogersen, H., Venezia, D., Haldeman, B. A., McGrane, V., Houamed, K. M., Thomsen, C., Gilbert, T. L., Mulvihill, E. R., 1993. The ligand-binding domain in metabotropic glutamate receptors is related to bacterial periplasmic binding proteins. Neuron 11, 41-52.

Okamoto, T., Sekiyama, N., Otsu, M., Shimada, Y., Sato, A., Nakanishi, S., Jingami, H., 1998. Expression and purification of the extracellular ligand binding region of metabotropic glutamate receptor subtype 1. J. Biol. Chem. 273, 13089-13096.
Olive, M., 2009. Metabotropic glutamate receptor ligands as potential therapeutics for addiction. Curr. Drug Abuse Rev. 2, 83 - 98.

Olsen, C. M., Childs, D. S., Stanwood, G. D., Winder, D. G., 2010. Operant sensation seeking requires metabotropic glutamate receptor 5 (mGluR5). PLoS One 5, e15085.
Omote, K., Kawamata, T., Kawamata, M., Namiki, A., 1998. Formalin-induced release of excitatory amino acids in the skin of the rat hindpaw. Brain Res. 787, 161-164.

Orlando, L. R., Ayala, R., Kett, L. R., Curley, A. A., Duffner, J., Bragg, D. C., Tsai, L. H., Dunah, A. W., Young, A. B., 2009. Phosphorylation of the homer-binding domain of group I metabotropic glutamate receptors by cyclin-dependent kinase 5. J. Neurochem. 110, 557-569.

Osikowicz, M., Mika, J., Makuch, W., Przewlocka, B., 2008. Glutamate receptor ligands attenuate allodynia and hyperalgesia and potentiate morphine effects in a mouse model of neuropathic pain. Pain 139, 117-126.

Osterweil, E. K., Krueger, D. D., Reinhold, K., Bear, M. F., 2010. Hypersensitivity to mGluR5 and ERK1/2 leads to excessive protein synthesis in the hippocampus of a mouse model of fragile X syndrome. J. Neurosci. 30, 15616-15627.

Ouattara, B., Gregoire, L., Morissette, M., Gasparini, F., Vranesic, I., Bilbe, G., Johns, D. R., Rajput, A., Hornykiewicz, O., Rajput, A. H., Gomez-Mancilla, B., Di Paolo, T., 2011. Metabotropic glutamate receptor type 5 in levodopa-induced motor complications. Neurobiol. Aging 32, 1286-1295.

Overington, J. P., Al-Lazikani, B., Hopkins, A. L., 2006. How many drug targets are there? Nat. Rev. Drug Discov. 5, 993-996.

Owens, R. M., Wang, C., You, J. A., Jiambutr, J., Xu, A. S., Marala, R. B., Jin, M. M., 2009. Real-time quantitation of viral replication and inhibitor potency using a label-free optical biosensor. J. Recept. Signal Transduct. Res. 29, 195-201.

Pagano, A., Ruegg, D., Litschig, S., Stoehr, N., Stierlin, C., Heinrich, M., Floersheim, P., Prezeau, L., Carroll, F., Pin, J. P., Cambria, A., Vranesic, I., Flor, P. J., Gasparini, F., Kuhn, R., 2000. The non-competitive antagonists 2-methyl-6-(phenylethynyl)pyridine and 7-hydroxyiminocyclopropan[b]chromen-1a-carboxylic

acid ethyl ester interact with overlapping binding pockets in the transmembrane region of group I metabotropic glutamate receptors. J. Biol. Chem. 275, 33750-33758.

Palucha-Poniewiera, A., Szewczyk, B., Pilc, A., 2014. Activation of the mTOR signaling pathway in the antidepressant-like activity of the mGlu5 antagonist MTEP and the mGlu7 agonist AMN082 in the FST in rats. Neuropharmacology 82, 59-68.

Palucha-Poniewiera, A., Wieronska, J. M., Branski, P., Burnat, G., Chruscicka, B., Pilc, A., 2013. Is the mGlu5 receptor a possible target for new antidepressant drugs? Pharmacol. Rep. 65, 1506-1511.

Pandya, N. J., Klaassen, R. V., van der Schors, R. C., Slotman, J. A., Houtsmuller, A., Smit, A. B., Li, K. W., 2016. Group 1 metabotropic glutamate receptors 1 and 5 form a protein complex in mouse hippocampus and cortex. Proteomics 16, 2698-2705.

Parmentier-Batteur, S., Hutson, P. H., Menzel, K., Uslaner, J. M., Mattson, B. A., O'Brien, J. A., Magliaro, B. C., Forest, T., Stump, C. A., Tynebor, R. M., Anthony, N. J., Tucker, T. J., Zhang, X. F., Gomez, R., Huszar, S. L., Lambeng, N., Faure, H., Le Poul, E., Poli, S., Rosahl, T. W., Rocher, J. P., Hargreaves, R., Williams, T. M., 2014. Mechanism based neurotoxicity of mGlu5 positive allosteric modulators--development challenges for a promising novel antipsychotic target. Neuropharmacology 82, 161-173.

Peavy, R. D., Chang, M. S., Sanders-Bush, E., Conn, P. J., 2001. Metabotropic glutamate receptor 5-induced phosphorylation of extracellular signal-regulated kinase in astrocytes depends on transactivation of the epidermal growth factor receptor. J. Neurosci. 21, 9619-9628.

Peavy, R. D., Conn, P. J., 1998. Phosphorylation of mitogen-activated protein kinase in cultured rat cortical glia by stimulation of metabotropic glutamate receptors. J. Neurochem. 71, 603-612.

Pecknold, J. C., McClure, D. J., Appeltauer, L., Wrzesinski, L., Allan, T., 1982. Treatment of anxiety using fenobam (a nonbenzodiazepine) in a double-blind standard (diazepam) placebo-controlled study. J. Clin. Psychopharmacol. 2, 129-133.

Peters, J., Scofield, M. D., Ghee, S. M., Heinsbroek, J. A., Reichel, C. M., 2016. Perirhinal Cortex mGlu5 Receptor Activation Reduces Relapse to Methamphetamine Seeking by Restoring Novelty Salience. Neuropsychopharmacol. 41, 1477-1485.

Petersen, G., Sørensen, C., Schmid, P. C., Artmann, A., Tang-Christensen, M., Hansen, S. H., Larsen, P. J., Schmid, H. H. O., Hansen, H. S., 2006. Intestinal levels of anandamide and oleoylethanolamide in food-deprived rats are regulated through their precursors. Biochimica et Biophysica Acta (BBA) - Molecular and Cell Biology of Lipids 1761, 143-150.

Picconi, B., Piccoli, G., Calabresi, P., 2012. Synaptic dysfunction in Parkinson's disease. Adv. Exp. Med. Biol. 970, 553-572.

Picker, M. J., Daugherty, D., Henry, F. E., Miller, L. L., Dykstra, L. A., 2011. Metabotropic glutamate antagonists alone and in combination with morphine: Comparison across two models of acute pain and a model of persistent, inflammatory pain. Behav. pharmacol. 22, 785-793.

Pilc, A., Wieronska, J. M., Skolnick, P., 2013. Glutamate-based antidepressants: preclinical psychopharmacology. Biol. Psychiat. 73, 1125-1132.

Pin, J., Duvoisin, R., 1995. The metabotropic glutamate receptors: Structure and functions. Neuropharmacology 34, 1 - 26.

Pin, J.-P., Prézeau, L., 2007. Allosteric Modulators of GABA(B) Receptors: Mechanism of Action and Therapeutic Perspective. Curr. Neuropharmacol. 5, 195-201.

Popoli, P., Pezzola, A., Torvinen, M., Reggio, R., Pintor, A., Scarchilli, L., Fuxe, K., Ferre, S., 2001. The selective mGlu(5) receptor agonist CHPG inhibits quinpirole-induced turning in 6-hydroxydopamine-lesioned rats and modulates the binding characteristics of dopamine D(2) receptors in the rat striatum: interactions with adenosine A(2a) receptors. Neuropsychopharmacol. 25, 505-513.

Porter, R. H., Jaeschke, G., Spooren, W., Ballard, T. M., Buttelmann, B., Kolczewski, S., Peters, J. U., Prinssen, E., Wichmann, J., Vieira, E., Muhlemann, A., Gatti, S., Mutel, V., Malherbe, P., 2005a. Fenobam: a clinically validated nonbenzodiazepine anxiolytic is a potent, selective, and noncompetitive mGlu5 receptor antagonist with inverse agonist activity. J. Pharmacol. Exp.Ther. 315, 711-721.

Porter, R. H., Jaeschke, G., Spooren, W., Ballard, T. M., Buttelmann, B., Kolczewski, S., Peters, J. U., Prinssen, E., Wichmann, J., Vieira, E., Muhlemann, A., Gatti, S., Mutel, V., Malherbe, P., 2005b. Fenobam: a clinically validated nonbenzodiazepine anxiolytic is a potent, selective, and noncompetitive mGlu5 receptor antagonist with inverse agonist activity. J. Pharmacol. Exp. Ther. 315, 711-721.

Potter, W. B., Basu, T., O'Riordan, K. J., Kirchner, A., Rutecki, P., Burger, C., Roopra, A., 2013. Reduced juvenile long-term depression in tuberous sclerosis complex is mitigated in adults by compensatory recruitment of mGluR5 and Erk signaling. PLoS Biol 11, e1001627.

Price, M. R., Baillie, G. L., Thomas, A., Stevenson, L. A., Easson, M., Goodwin, R., McLean, A., McIntosh, L., Goodwin, G., Walker, G., Westwood, P., Marrs, J., Thomson, F., Cowley, P., Christopoulos, A., Pertwee, R. G., Ross, R. A., 2005. Allosteric modulation of the cannabinoid CB1 receptor. Mol. Pharmacol. 68, 1484-1495.

Priestley, R., Glass, M., Kendall, D., 2017. Functional Selectivity at Cannabinoid Receptors. Adv. Pharmacol. 80, 207-221.

Prinster, S. C., Hague, C., Hall, R. A., 2005. Heterodimerization of g protein-coupled receptors: specificity and functional significance. Pharmacol. Rev. 57, 289-298.

Purgert, C. A., Izumi, Y., Jong, Y. J., Kumar, V., Zorumski, C. F., O'Malley, K. L., 2014. Intracellular mGluR5 can mediate synaptic plasticity in the hippocampus. J. Neurosci. 34, 4589-4598.

Quiroz, J. A., Tamburri, P., Deptula, D., Banken, L., Beyer, U., Rabbia, M., Parkar, N., Fontoura, P., Santarelli, L., 2016. Efficacy and Safety of Basimglurant as Adjunctive Therapy for Major Depression: A Randomized Clinical Trial. JAMA Psychiatry 73, 675-684.

Raboisson, P., Breitholtz-Emanuelsson, A., Dahllof, H., Edwards, L., Heaton, W. L., Isaac, M., Jarvie, K., Kers, A., Minidis, A. B., Nordmark, A., Sheehan, S. M., Slassi, A., Strom, P., Terelius, Y., Wensbo, D., Wilson, J. M., Xin, T., McLeod, D. A., 2012. Discovery and characterization of AZD9272 and AZD6538-Two novel mGluR5 negative allosteric modulators selected for clinical development. Bioorg. Med. Chem. Lett. 22, 6974-6979.

Rathee, P. K., Distler, C., Obreja, O., Neuhuber, W., Wang, G. K., Wang, S. Y., Nau, C., Kress, M., 2002. PKA/AKAP/VR-1 module: A common link of Gs-mediated signaling to thermal hyperalgesia. J. Neurosci. 22, 4740-4745.

Ren, B. X., Gu, X. P., Zheng, Y. G., Liu, C. L., Wang, D., Sun, Y. E., Ma, Z. L., 2012. Intrathecal injection of metabotropic glutamate receptor subtype 3 and 5 agonist/antagonist attenuates bone cancer pain by inhibition of spinal astrocyte activation in a mouse model. Anesthesiology 116, 122-132.

Ribeiro, F. M., Devries, R. A., Hamilton, A., Guimaraes, I. M., Cregan, S. P., Pires, R. G., Ferguson, S. S., 2014. Metabotropic glutamate receptor 5 knockout promotes motor and biochemical alterations in a mouse model of Huntington's disease. Hum. Mol. Genet. 23, 2030-2042.

Ribeiro, F. M., Ferreira, L. T., Paquet, M., Cregan, T., Ding, Q., Gros, R., Ferguson, S. S., 2009. Phosphorylation-independent regulation of metabotropic glutamate receptor 5 desensitization and internalization by G protein-coupled receptor kinase 2 in neurons. J. Biol. Chem. 284, 23444-23453.

Ribeiro, F. M., Paquet, M., Cregan, S. P., Ferguson, S. S., 2010a. Group I metabotropic glutamate receptor signalling and its implication in neurological disease. CNS Neurol. Disord. Drug Targets 9, 574-595.

Ribeiro, F. M., Paquet, M., Ferreira, L. T., Cregan, T., Swan, P., Cregan, S. P., Ferguson, S. S., 2010b. Metabotropic glutamate receptor-mediated cell signaling pathways are altered in a mouse model of Huntington's disease. J. Neurosci. 30, 316-324.

Richardson, J. D., Vasko, M. R., 2002. Cellular mechanisms of neurogenic inflammation. J. Pharmacol. Exp. Ther. 302, 839-845.

Rodrigues, R. J., Alfaro, T. M., Rebola, N., Oliveira, C. R., Cunha, R. A., 2005. Co-localization and functional interaction between adenosine A(2A) and metabotropic

group 5 receptors in glutamatergic nerve terminals of the rat striatum. J. Neurochem. 92, 433-441.

Rodriguez, A. L., Grier, M. D., Jones, C. K., Herman, E. J., Kane, A. S., Smith, R. L., Williams, R., Zhou, Y., Marlo, J. E., Days, E. L., Blatt, T. N., Jadhav, S., Menon, U. N., Vinson, P. N., Rook, J. M., Stauffer, S. R., Niswender, C. M., Lindsley, C. W., Weaver, C. D., Conn, P. J., 2010a. Discovery of novel allosteric modulators of metabotropic glutamate receptor subtype 5 reveals chemical and functional diversity and in vivo activity in rat behavioral models of anxiolytic and antipsychotic activity. Mol. Pharmacol. 78, 1105-1123.

Rodriguez, A. L., Nong, Y., Sekaran, N. K., Alagille, D., Tamagnan, G. D., Conn, P. J., 2005a. A close structural analog of 2-methyl-6-(phenylethynyl)-pyridine acts as a neutral allosteric site ligand on metabotropic glutamate receptor subtype 5 and blocks the effects of multiple allosteric modulators. Mol. Pharmacol. 68, 1793-1802.

Rodriguez, A. L., Nong, Y., Sekaran, N. K., Alagille, D., Tamagnan, G. D., Conn, P. J., 2005b. A close structural analog of 2-methyl-6-(phenylethynyl)-pyridine acts as a neutral allosteric site ligand on metabotropic glutamate receptor subtype 5 and blocks the effects of multiple allosteric modulators. Mol. Pharmacol. 68, 1793-1802.

Rodriguez, A. L., Tarr, J. C., Zhou, Y., Williams, R., Gregory, K. J., Bridges, T. M., Daniels, J. S., Niswender, C. M., Conn, P. J., Lindsley, C. W., Stauffer, S. R., 2010b. Identification of a glycine sulfonamide based non-MPEP site positive allosteric potentiator (PAM) of mGlu5. Probe Reports from the NIH Molecular Libraries Program. National Center for Biotechnology Information (US), Bethesda (MD).

Rohrer, D. K., Kobilka, B. K., 1998. G protein-coupled receptors: functional and mechanistic insights through altered gene expression. Physiol. Rev. 78, 35-52.

Romano, C., Miller, J. K., Hyrc, K., Dikranian, S., Mennerick, S., Takeuchi, Y., Goldberg, M. P., O'Malley, K. L., 2001. Covalent and noncovalent interactions mediate metabotropic glutamate receptor mGlu5 dimerization. Mol. Pharmacol. 59, 46-53.

Romano, C., Yang, W. L., O'Malley, K. L., 1996. Metabotropic glutamate receptor 5 is a disulfide-linked dimer. J. Biol. Chem. 271, 28612-28616.

Romano, C., Van den Pol, A. N., O;Malley, K. L., 1996. Enhanced early developmental expression of the metabotropic glutamate receptor mGluR5 in rat brain: Protein, mRNA splice variants, and regional distribution. J. Comp. Neurol. 367, 403-412.

Rondard, P., Liu, J., Huang, S., Malhaire, F., Vol, C., Pinault, A., Labesse, G., Pin, J. P., 2006. Coupling of agonist binding to effector domain activation in metabotropic glutamate-like receptors. J. Biol. Chem. 281, 24653-24661.

Ronesi, J. A., Collins, K. A., Hays, S. A., Tsai, N. P., Guo, W., Birnbaum, S. G., Hu, J. H., Worley, P. F., Gibson, J. R., Huber, K. M., 2012. Disrupted Homer scaffolds

mediate abnormal mGluR5 function in a mouse model of fragile X syndrome. Nat. Neurosci. 15, 431-440, s431.

Rook, J. M., Noetzel, M. J., Pouliot, W. A., Bridges, T. M., Vinson, P. N., Cho, H. P., Zhou, Y., Gogliotti, R. D., Manka, J. T., Gregory, K. J., Stauffer, S. R., Dudek, F. E., Xiang, Z., Niswender, C. M., Daniels, J. S., Jones, C. K., Lindsley, C. W., Conn, P. J., 2013. Unique signaling profiles of positive allosteric modulators of metabotropic glutamate receptor subtype 5 determine differences in in vivo activity. Biol. Psychiat. 73, 501-509.

Rook, J. M., Xiang, Z., Lv, X., Ghoshal, A., Dickerson, J. W., Bridges, T. M., Johnson, K. A., Foster, D. J., Gregory, K. J., Vinson, P. N., Thompson, A. D., Byun, N., Collier, R. L., Bubser, M., Nedelcovych, M. T., Gould, R. W., Stauffer, S. R., Daniels, J. S., Niswender, C. M., Lavreysen, H., Mackie, C., Conde-Ceide, S., Alcazar, J., Bartolome-Nebreda, J. M., Macdonald, G. J., Talpos, J. C., Steckler, T., Jones, C. K., Lindsley, C. W., Conn, P. J., 2015. Biased mGlu5-Positive Allosteric Modulators Provide In Vivo Efficacy without Potentiating mGlu5 Modulation of NMDAR Currents. Neuron 86, 1029-1040.

Rosenbaum, T., Simon, S. A., 2007. TRPV1 Receptors and Signal Transduction. In: Liedtke, W. B., Heller, S., (Eds), TRP Ion Channel Function in Sensory Transduction and Cellular Signaling Cascades. CRC Press/Taylor & Francis
Taylor & Francis Group, LLC., Boca Raton (FL).

Ross, R. A., 2003. Anandamide and vanilloid TRPV1 receptors. Br. J. Pharmacol. 140, 790-801.

Rovira, X., Malhaire, F., Scholler, P., Rodrigo, J., Gonzalez-Bulnes, P., Llebaria, A., Pin, J. P., Giraldo, J., Goudet, C., 2015. Overlapping binding sites drive allosteric agonism and positive cooperativity in type 4 metabotropic glutamate receptors. Faseb j 29, 116-130.

Rush, A. M., Wu, J., Rowan, M. J., Anwyl, R., 2002. Group I metabotropic glutamate receptor (mGluR)-dependent long-term depression mediated via p38 mitogen-activated protein kinase is inhibited by previous high-frequency stimulation and activation of mGluRs and protein kinase C in the rat dentate gyrus in vitro. J. Neurosci. 22, 6121-6128.

Rylander, D., Iderberg, H., Li, Q., Dekundy, A., Zhang, J., Li, H., Baishen, R., Danysz, W., Bezard, E., Cenci, M. A., 2010. A mGluR5 antagonist under clinical development improves L-DOPA-induced dyskinesia in parkinsonian rats and monkeys. Neurobiol. Dis. 39, 352-361.

Sagar, D. R., Smith, P. A., Millns, P. J., Smart, D., Kendall, D. A., Chapman, V., 2004. TRPV1 and CB(1) receptor-mediated effects of the endovanilloid/endocannabinoid N-arachidonoyl-dopamine on primary afferent fibre and spinal cord neuronal responses in the rat. Eur. J. Neurosci. 20, 175-184.

Sahin, M., 2012. Targeted treatment trials for tuberous sclerosis and autism: no longer a dream. Curr. Opin. Neurobiol. 22, 895-901.

Sanacora, G., Treccani, G., Popoli, M., 2012. Towards a glutamate hypothesis of depression: An emerging frontier of neuropsychopharmacology for mood disorders. Neuropharmacology 62, 63-77.

Sarramegna, V., Talmont, F., Demange, P., Milon, A., 2003. Heterologous expression of G-protein-coupled receptors: comparison of expression systems from the standpointof large-scale production and purification. Cell. Mol. Life Sci. 60, 1529-1546.

Schaffhauser, H., Rowe, B. A., Morales, S., Chavez-Noriega, L. E., Yin, R., Jachec, C., Rao, S. P., Bain, G., Pinkerton, A. B., Vernier, J. M., Bristow, L. J., Varney, M. A., Daggett, L. P., 2003. Pharmacological characterization and identification of amino acids involved in the positive modulation of metabotropic glutamate receptor subtype 2. Mol. Pharmacol. 64, 798-810.

Schepers, R. J., Ringkamp, M., 2009. Thermoreceptors and thermosensitive afferents. Neurosci. Biobehav. Rev. 33, 205-212.

Schoepp, D. D., Goldsworthy, J., Johnson, B. G., Salhoff, C. R., Baker, S. R., 1994. 3,5-dihydroxyphenylglycine is a highly selective agonist for phosphoinositide-linked metabotropic glutamate receptors in the rat hippocampus. J. Neurochem. 63, 769-772.
Schoepp, D. D., Wright, R. A., Levine, L. R., Gaydos, B., Potter, W. Z., 2003. LY354740, an mGlu2/3 receptor agonist as a novel approach to treat anxiety/stress. Stress 6, 189-197.

Schroder, H., Wu, D. F., Seifert, A., Rankovic, M., Schulz, S., Hollt, V., Koch, T., 2009. Allosteric modulation of metabotropic glutamate receptor 5 affects phosphorylation, internalization, and desensitization of the micro-opioid receptor. Neuropharmacology 56, 768-778.

Schroeder, J. P., Spanos, M., Stevenson, J. R., Besheer, J., Salling, M., Hodge, C. W., 2008. Cue-induced reinstatement of alcohol-seeking behavior is associated with increased ERK1/2 phosphorylation in specific limbic brain regions: blockade by the mGluR5 antagonist MPEP. Neuropharmacology 55, 546-554.

Schulz, B., Fendt, M., Gasparini, F., Lingenhohl, K., Kuhn, R., Koch, M., 2001. The metabotropic glutamate receptor antagonist 2-methyl-6-(phenylethynyl)-pyridine (MPEP) blocks fear conditioning in rats. Neuropharmacology 41, 1-7.

Seese, R. R., Maske, A. R., Lynch, G., Gall, C. M., 2014. Long-term memory deficits are associated with elevated synaptic ERK1/2 activation and reversed by mGluR5 antagonism in an animal model of autism. Neuropsychopharmacol. 39, 1664-1673.
Sengmany, K., Gregory, K. J., 2016. Metabotropic glutamate receptor subtype 5: molecular pharmacology, allosteric modulation and stimulus bias. Br. J. Pharmacol. 173, 3001-3017.

Sengmany, K., Singh, J., Stewart, G. D., Conn, P. J., Christopoulos, A., Gregory, K. J., 2017. Biased allosteric agonism and modulation of metabotropic glutamate

receptor 5: Implications for optimizing preclinical neuroscience drug discovery. Neuropharmacology 115, 60-72.

Serafini, G., Pompili, M., Innamorati, M., Dwivedi, Y., Brahmachari, G., Girardi, P., 2013. Pharmacological properties of glutamatergic drugs targeting NMDA receptors and their application in major depression. Curr. Pharm. Des. 19, 1898-1922.
Serrano, L., Neira, J. L., Sancho, J., Fersht, A. R., 1992. Effect of alanine versus glycine in alpha-helices on protein stability. Nature 356, 453-455.

Sevastyanova, T. N., Kammermeier, P. J., 2014a. Cooperative signaling between homodimers of metabotropic glutamate receptors 1 and 5. Molecular Pharmacology 86, 492-504.

Sevastyanova, T. N., Kammermeier, P. J., 2014b. Cooperative signaling between homodimers of metabotropic glutamate receptors 1 and 5. Mol. Pharmacol. 86, 492-504.

Sharma, S., Kedrowski, J., Rook, J. M., Smith, R. L., Jones, C. K., Rodriguez, A. L., Conn, P. J., Lindsley, C. W., 2009. Discovery of molecular switches that modulate modes of metabotropic glutamate receptor subtype 5 (mGlu5) pharmacology in vitro and in vivo within a series of functionalized, regioisomeric 2- and 5-(phenylethynyl)pyrimidines. J. Med. Chem. 52, 4103-4106.

Sharma, S., Rodriguez, A. L., Conn, P. J., Lindsley, C. W., 2008. Synthesis and SAR of a mGluR5 allosteric partial antagonist lead: unexpected modulation of pharmacology with slight structural modifications to a 5-(phenylethynyl)pyrimidine scaffold. Bioorg. Med. Chem. Lett. 18, 4098-4101.

She, W. C., Quairiaux, C., Albright, M. J., Wang, Y. C., Sanchez, D. E., Chang, P. S., Welker, E., Lu, H. C., 2009. Roles of mGluR5 in synaptic function and plasticity of the mouse thalamocortical pathway. Eur. J. Neurosci. 29, 1379-1396.

Sheffler, D. J., Gregory, K. J., Rook, J. M., Conn, P. J., 2011. Allosteric modulation of metabotropic glutamate receptors. Adv. Pharmacol. 62, 37-77.

Sheffler, D. J., Wenthur, C. J., Bruner, J. A., Carrington, S. J., Vinson, P. N., Gogi, K. K., Blobaum, A. L., Morrison, R. D., Vamos, M., Cosford, N. D., Stauffer, S. R., Daniels, J. S., Niswender, C. M., Conn, P. J., Lindsley, C. W., 2012. Development of a novel, CNS-penetrant, metabotropic glutamate receptor 3 (mGlu3) NAM probe (ML289) derived from a closely related mGlu5 PAM. Bioorg. Med. Chem. Lett. 22, 3921-3925.

Shi, L., Liapakis, G., Xu, R., Guarnieri, F., Ballesteros, J. A., Javitch, J. A., 2002. Beta2 adrenergic receptor activation. Modulation of the proline kink in transmembrane 6 by a rotamer toggle switch. J. Biol. Chem. 277, 40989-40996.
Shigemoto, R., Nomura, S., Ohishi, H., Sugihara, H., Nakanishi, S., Mizuno, N., 1993. Immunohistochemical localization of a metabotropic glutamate receptor, mGluR5, in the rat brain. Neurosci. Lett. 163, 53-57.

Shiina, T., Arai, K., Tanabe, S., Yoshida, N., Haga, T., Nagao, T., Kurose, H., 2001. Clathrin box in G protein-coupled receptor kinase 2. J. Biol. Chem. 276, 33019-33026.

Soliman, A. C., Yu, J. S., Coderre, T. J., 2005. mGlu and NMDA receptor contributions to capsaicin-induced thermal and mechanical hypersensitivity. Neuropharmacology 48, 325-332.
Sorensen, S. D., Conn, P. J., 2003. G protein-coupled receptor kinases regulate metabotropic glutamate receptor 5 function and expression. Neuropharmacology 44, 699-706.

Spooren, W., Ballard, T., Gasparini, F., Amalric, M., Mutel, V., Schreiber, R., 2003. Insight into the function of Group I and Group II metabotropic glutamate (mGlu) receptors: behavioural characterization and implications for the treatment of CNS disorders. Behav. pharmacol. 14, 257-277.

Spooren, W. P., Gasparini, F., Salt, T. E., Kuhn, R., 2001. Novel allosteric antagonists shed light on mglu(5) receptors and CNS disorders. Trends Pharmacol. Sci. 22, 331-337.

Spooren, W. P., Vassout, A., Neijt, H. C., Kuhn, R., Gasparini, F., Roux, S., Porsolt, R. D., Gentsch, C., 2000. Anxiolytic-like effects of the prototypical metabotropic glutamate receptor 5 antagonist 2-methyl-6-(phenylethynyl)pyridine in rodents. J. Pharmacol. Exp. Ther. 295, 1267-1275.

Stallaert, W., Dorn, J. F., van der Westhuizen, E., Audet, M., Bouvier, M., 2012. Impedance responses reveal beta(2)-adrenergic receptor signaling pluridimensionality and allow classification of ligands with distinct signaling profiles. PLoS One 7, e29420.

Starowicz, K., Makuch, W., Osikowicz, M., Piscitelli, F., Petrosino, S., Di Marzo, V., Przewlocka, B., 2012. Spinal anandamide produces analgesia in neuropathic rats: possible CB(1)- and TRPV1-mediated mechanisms. Neuropharmacology 62, 1746-1755.

Stephenson, R. P., 1956. A modification of receptor theory. Br. J. Pharm. Chemoth. 11, 379-393.

Stoker, A. K., Olivier, B., Markou, A., 2012. Involvement of metabotropic glutamate receptor 5 in brain reward deficits associated with cocaine and nicotine withdrawal and somatic signs of nicotine withdrawal. Psychopharmacol. (Berl) 221, 317-327.

Suardíaz, M., Estivill-Torrús, G., Goicoechea, C., Bilbao, A., Rodríguez de Fonseca, F., 2007. Analgesic properties of oleoylethanolamide (OEA) in visceral and inflammatory pain. Pain 133, 99-110.

Suratman, S., Leach, K., Sexton, P., Felder, C., Loiacono, R., Christopoulos, A., 2011. Impact of species variability and 'probe-dependence' on the detection and in vivo validation of allosteric modulation at the M4 muscarinic acetylcholine receptor. Br. J. Pharmacol. 162, 1659-1670.

Suzuki, G., Kimura, T., Satow, A., Kaneko, N., Fukuda, J., Hikichi, H., Sakai, N., Maehara, S., Kawagoe-Takaki, H., Hata, M., Azuma, T., Ito, S., Kawamoto, H., Ohta, H., 2007. Pharmacological characterization of a new, orally active and potent allosteric metabotropic glutamate receptor 1 antagonist, 4-[1-(2-fluoropyridin-3-yl)-5-methyl-1H-1,2,3-triazol-4-yl]-N-isopropyl-N-methyl- 3,6-dihydropyridine-1(2H)-carboxamide (FTIDC). J. Pharmacol. Exp. Ther. 321, 1144-1153.
Swanson, C. J., Bures, M., Johnson, M. P., Linden, A. M., Monn, J. A., Schoepp, D. D., 2005. Metabotropic glutamate receptors as novel targets for anxiety and stress disorders. Nat. Rev. Drug Discov. 4, 131-144.

Swedberg, M. D., Ellgren, M., Raboisson, P., 2014. mGluR5 antagonist-induced psychoactive properties: MTEP drug discrimination, a pharmacologically selective non-NMDA effect with apparent lack of reinforcing properties. J. Pharmacol. Exp. Ther. 349, 155-164.

Swedberg, M. D., Raboisson, P., 2014. AZD9272 and AZD2066: selective and highly central nervous system penetrant mGluR5 antagonists characterized by their discriminative effects. J. Pharmacol. Exp. Ther. 350, 212-222.

Sykes, D. A., Moore, H., Stott, L., Holliday, N., Javitch, J. A., Lane, J. R., Charlton, S. J., 2017. Extrapyramidal side effects of antipsychotics are linked to their association kinetics at dopamine D2 receptors. Nat. Commun. 8, 763.

Tatarczynska, E., Klodzinska, A., Chojnacka-Wojcik, E., Palucha, A., Gasparini, F., Kuhn, R., Pilc, A., 2001. Potential anxiolytic- and antidepressant-like effects of MPEP, a potent, selective and systemically active mGlu5 receptor antagonist. Br. J. Pharmacol. 132, 1423 - 1430.

Tebano, M. T., Martire, A., Pepponi, R., Domenici, M. R., Popoli, P., 2006. Is the functional interaction between adenosine A(2A) receptors and metabotropic glutamate 5 receptors a general mechanism in the brain? Differences and similarities between the striatum and the hippocampus. Purinerg. Signal. 2, 619-625.

Tebano, M. T., Martire, A., Rebola, N., Pepponi, R., Domenici, M. R., Gro, M. C., Schwarzschild, M. A., Chen, J. F., Cunha, R. A., Popoli, P., 2005. Adenosine A2A receptors and metabotropic glutamate 5 receptors are co-localized and functionally interact in the hippocampus: a possible key mechanism in the modulation of N-methyl-D-aspartate effects. J. Neurochem. 95, 1188-1200.

Thabuis, C., Tissot-Favre, D., Bezelgues, J. B., Martin, J. C., Cruz-Hernandez, C., Dionisi, F., Destaillats, F., 2008. Biological functions and metabolism of oleoylethanolamide. Lipids 43, 887-894.

Tham, A., Jonsson, U., Andersson, G., Soderlund, A., Allard, P., Bertilsson, G., 2016. Efficacy and tolerability of antidepressants in people aged 65 years or older with major depressive disorder - A systematic review and a meta-analysis. J. Affect. Disord. 205, 1-12.

Thandi, S., Blank, J. L., Challiss, R. A., 2002. Group-I metabotropic glutamate receptors, mGlu1a and mGlu5a, couple to extracellular signal-regulated kinase (ERK) activation via distinct, but overlapping, signalling pathways. J. Neurochem. 83, 1139-1153.

Thompson, G. L., Canals, M., Poole, D. P., 2014. Biological redundancy of endogenous GPCR ligands in the gut and the potential for endogenous functional selectivity. Front. Pharmacol. 5, 262.
Thompson, G. L., Lane, J. R., Coudrat, T., Sexton, P. M., Christopoulos, A., Canals, M., 2015. Biased Agonism of Endogenous Opioid Peptides at the mu-Opioid Receptor. Mol. Pharmacol. 88, 335-346.

Tison, F., Keywood, C., Wakefield, M., Durif, F., Corvol, J. C., Eggert, K., Lew, M., Isaacson, S., Bezard, E., Poli, S. M., Goetz, C. G., Trenkwalder, C., Rascol, O., 2016. A Phase 2A Trial of the Novel mGluR5-Negative Allosteric Modulator Dipraglurant for Levodopa-Induced Dyskinesia in Parkinson's Disease. Mov. Disord. 31, 1373-1380.

Trenkwalder, C., Stocchi, F., Poewe, W., Dronamraju, N., Kenney, C., Shah, A., von Raison, F., Graf, A., 2016. Mavoglurant in Parkinson's Patients With l-Dopa-Induced Dyskinesias: Two Randomized Phase 2 Studies. Mov. Disord. 31, 1054-1058.

Tu, J. C., Xiao, B., Naisbitt, S., Yuan, J. P., Petralia, R. S., Brakeman, P., Doan, A., Aakalu, V. K., Lanahan, A. A., Sheng, M., Worley, P. F., 1999. Coupling of mGluR/Homer and PSD-95 complexes by the Shank family of postsynaptic density proteins. Neuron 23, 583-592.

Turlington, M., Noetzel, M. J., Bridges, T. M., Vinson, P. N., Steckler, T., Lavreysen, H., Mackie, C., Bartolome-Nebreda, J. M., Conde-Ceide, S., Tong, H. M., Macdonald, G. J., Daniels, J. S., Jones, C. K., Niswender, C. M., Conn, P. J., Lindsley, C. W., Stauffer, S. R., 2014. Discovery and SAR of a novel series of metabotropic glutamate receptor 5 positive allosteric modulators with high ligand efficiency. Bioorg. Med. Chem. Lett. 24, 3641-3646.

Turlington, M., Noetzel, M. J., Chun, A., Zhou, Y., Gogliotti, R. D., Nguyen, E. D., Gregory, K. J., Vinson, P. N., Rook, J. M., Gogi, K. K., Xiang, Z., Bridges, T. M., Daniels, J. S., Jones, C., Niswender, C. M., Meiler, J., Conn, P. J., Lindsley, C. W., Stauffer, S. R., 2013. Exploration of allosteric agonism structure-activity relationships within an acetylene series of metabotropic glutamate receptor 5 (mGlu5) positive allosteric modulators (PAMs): discovery of 5-((3-fluorophenyl)ethynyl)-N-(3-methyloxetan-3-yl)picolinamide (ML254). J. Med. Chem. 56, 7976-7996.

Tzschentke, T. M., Schmidt, W. J., 2003. Glutamatergic mechanisms in addiction. Mol. Psychiatr. 8, 373-382.

Uematsu, K., Heiman, M., Zelenina, M., Padovan, J., Chait, B. T., Aperia, A., Nishi, A., Greengard, P., 2015. Protein kinase A directly phosphorylates metabotropic glutamate receptor 5 to modulate its function. J. Neurochem. 132, 677-686.

Urban, J. D., Vargas, G. A., von Zastrow, M., Mailman, R. B., 2007. Aripiprazole has functionally selective actions at dopamine D2 receptor-mediated signaling pathways. Neuropsychopharmacol. 32, 67-77.

Valant, C., Felder, C. C., Sexton, P. M., Christopoulos, A., 2012. Probe dependence in the allosteric modulation of a G protein-coupled receptor: implications for detection and validation of allosteric ligand effects. Mol. Pharmacol. 81, 41-52.
Valenti, O., Conn, P. J., Marino, M. J., 2002. Distinct physiological roles of the Gq-coupled metabotropic glutamate receptors Co-expressed in the same neuronal populations. J. Cell. Physiol. 191, 125-137.

Valerio, A., Rizzonelli, P., Paterlini, M., Moretto, G., Knopfel, T., Kuhn, R., Memo, M., Spano, P., 1997. mGluR5 metabotropic glutamate receptor distribution in rat and human spinal cord: a developmental study. Neurosci. Res. 28, 49-57.

Varney, M. A., Gereau, R. W. t., 2002. Metabotropic glutamate receptor involvement in models of acute and persistent pain: prospects for the development of novel analgesics. Curr. Drug Targets CNS Neurol. Disord. 1, 283-296.

Veerman, S. R., Schulte, P. F., de Haan, L., 2014. The Glutamate Hypothesis: A Pathogenic Pathway from which Pharmacological Interventions have Emerged. Pharmacopsychiatry 47, 121-130.

Vilar, B., Busserolles, J., Ling, B., Laffray, S., Ulmann, L., Malhaire, F., Chapuy, E., Aissouni, Y., Etienne, M., Bourinet, E., Acher, F., Pin, J. P., Eschalier, A., Goudet, C., 2013. Alleviating pain hypersensitivity through activation of type 4 metabotropic glutamate receptor. J. Neurosci. 33, 18951-18965.

Vincent, K., Cornea, V. M., Jong, Y. J., Laferriere, A., Kumar, N., Mickeviciute, A., Fung, J. S., Bandegi, P., Ribeiro-da-Silva, A., O'Malley, K. L., Coderre, T. J., 2016. Intracellular mGluR5 plays a critical role in neuropathic pain. Nat. Commun. 7, 10604.

Violin, J. D., Crombie, A. L., Soergel, D. G., Lark, M. W., 2014. Biased ligands at G-protein-coupled receptors: promise and progress. Trends Pharmacol. Sci. 35, 308-316.
Viwatpinyo, K., Chongthammakun, S., 2009. Activation of group I metabotropic glutamate receptors leads to brain-derived neurotrophic factor expression in rat C6 cells. Neurosci. Lett. 467, 127-130.

Volk, L. J., Daly, C. A., Huber, K. M., 2006. Differential roles for group 1 mGluR subtypes in induction and expression of chemically induced hippocampal long-term depression. J. Neurophysiol. 95, 2427-2438.

Vyklicky, L., Novakova-Tousova, K., Benedikt, J., Samad, A., Touska, F., Vlachova, V., 2008. Calcium-dependent desensitization of vanilloid receptor TRPV1: a mechanism possibly involved in analgesia induced by topical application of capsaicin. Physiol. Res. 57 Suppl 3, S59-68.

Walker, K., Reeve, A., Bowes, M., Winter, J., Wotherspoon, G., Davis, A., Schmid, P., Gasparini, F., Kuhn, R., Urban, L., 2001. mGlu5 receptors and nociceptive

function II. mGlu5 receptors functionally expressed on peripheral sensory neurones mediate inflammatory hyperalgesia. Neuropharmacology 40, 10-19.

Wang, H., Westin, L., Nong, Y., Birnbaum, S., Bendor, J., Brismar, H., Nestler, E., Aperia, A., Flajolet, M., Greengard, P., 2009. Norbin is an endogenous regulator of metabotropic glutamate receptor 5 signaling. Science 326, 1554-1557.
Wang, J. Q., Fibuch, E. E., Mao, L., 2007. Regulation of mitogen-activated protein kinases by glutamate receptors. J. Neurochem. 100, 1-11.

Wang, S., Joseph, J., Ro, J. Y., Chung, M. K., 2015. Modality-specific mechanisms of protein kinase C-induced hypersensitivity of TRPV1: S800 is a polymodal sensitization site. Pain 156, 931-941.

Wang, X., Miyares, R. L., Ahern, G. P., 2005. Oleoylethanolamide excites vagal sensory neurones, induces visceral pain and reduces short-term food intake in mice via capsaicin receptor TRPV1. J. Physiol. 564, 541-547.

Watterson, L. R., Kufahl, P. R., Nemirovsky, N. E., Sewalia, K., Hood, L. E., Olive, M. F., 2013. Attenuation of reinstatement of methamphetamine-, sucrose-, and food-seeking behavior in rats by fenobam, a metabotropic glutamate receptor 5 negative allosteric modulator. Psychopharmacol. (Berl) 225, 151-159.

Waung, M. W., Huber, K. M., 2009. Protein translation in synaptic plasticity: mGluR-LTD, Fragile X. Curr. Opin. Neurobiol. 19, 319-326.

Wieronska, J. M., Pilc, A., 2013. Glutamate-based anxiolytic ligands in clinical trials. Expert Opin. Investig. Drugs 22, 1007-1022.

Wieronska, J. M., Zorn, S. H., Doller, D., Pilc, A., 2016. Metabotropic glutamate receptors as targets for new antipsychotic drugs: Historical perspective and critical comparative assessment. Pharmacol. Ther. 157, 10-27.

Wijetunge, L. S., Till, S. M., Gillingwater, T. H., Ingham, C. A., Kind, P. C., 2008. mGluR5 regulates glutamate-dependent development of the mouse somatosensory cortex. J. Neurosci. 28, 13028-13037.

Williams, J. T., Ingram, S. L., Henderson, G., Chavkin, C., von Zastrow, M., Schulz, S., Koch, T., Evans, C. J., Christie, M. J., 2013. Regulation of mu-opioid receptors: desensitization, phosphorylation, internalization, and tolerance. Pharmacol. Rev. 65, 223-254.

Wise, A., Gearing, K., Rees, S., 2002. Target validation of G-protein coupled receptors. Drug Discov. Today 7, 235-246.

Wisler, J. W., DeWire, S. M., Whalen, E. J., Violin, J. D., Drake, M. T., Ahn, S., Shenoy, S. K., Lefkowitz, R. J., 2007. A unique mechanism of beta-blocker action: carvedilol stimulates beta-arrestin signaling. Proc. Natl. Acad. Sci. U S A. 104, 16657-16662.

Wisniewski, K., Car, H., 2002. (S)-3,5-DHPG: a review. CNS Drug Rev. 8, 101-116.

Wood, M. R., Hopkins, C. R., Brogan, J. T., Conn, P. J., Lindsley, C. W., 2011. "Molecular switches" on mGluR allosteric ligands that modulate modes of pharmacology. Biochemistry 50, 2403-2410.

Woods, J. H., Katz, J. L., Winger, G., 1992. Benzodiazepines: use, abuse, and consequences. Pharmacol. Rev. 44, 151-347.
Woolf, C. J., Salter, M. W., 2000. Neuronal plasticity: increasing the gain in pain. Science 288, 1765-1769.

Wootten, D., Christopoulos, A., Sexton, P. M., 2013. Emerging paradigms in GPCR allostery: implications for drug discovery. Nat. Rev. Drug Discov. 12, 630-644.

Wright, R. A., Johnson, B. G., Zhang, C., Salhoff, C., Kingston, A. E., Calligaro, D. O., Monn, J. A., Schoepp, D. D., Marek, G. J., 2013. CNS distribution of metabotropic glutamate 2 and 3 receptors: transgenic mice and [(3)H]LY459477 autoradiography. Neuropharmacology 66, 89-98.

Wu, H., Wang, C., Gregory, K. J., Han, G. W., Cho, H. P., Xia, Y., Niswender, C. M., Katritch, V., Meiler, J., Cherezov, V., Conn, P. J., Stevens, R. C., 2014. Structure of a class C GPCR metabotropic glutamate receptor 1 bound to an allosteric modulator. Science 344, 58-64.

Wullschleger, S., Loewith, R., Hall, M. N., 2006. TOR signaling in growth and metabolism. Cell 124, 471-484.

Xiao, B., Tu, J. C., Petralia, R. S., Yuan, J. P., Doan, A., Breder, C. D., Ruggiero, A., Lanahan, A. A., Wenthold, R. J., Worley, P. F., 1998. Homer regulates the association of group 1 metabotropic glutamate receptors with multivalent complexes of homer-related, synaptic proteins. Neuron 21, 707-716.

Xiao, X. L., Ma, D. L., Wu, J., Tang, F. R., 2013. Metabotropic glutamate receptor 5 (mGluR5) regulates proliferation and differentiation of neuronal progenitors in the developmental hippocampus. Brain. Res. 1493, 1-12.

Xu, J., Zhu, Y., Contractor, A., Heinemann, S. F., 2009. mGluR5 has a critical role in inhibitory learning. J. Neurosci. 29, 3676-3684.

Yan, Q. J., Rammal, M., Tranfaglia, M., Bauchwitz, R. P., 2005. Suppression of two major Fragile X Syndrome mouse model phenotypes by the mGluR5 antagonist MPEP. Neuropharmacology 49, 1053-1066.

Yin, S., Noetzel, M. J., Johnson, K. A., Zamorano, R., Jalan-Sakrikar, N., Gregory, K. J., Conn, P. J., Niswender, C. M., 2014. Selective actions of novel allosteric modulators reveal functional heteromers of metabotropic glutamate receptors in the CNS. J. Neurosci. 34, 79-94.

Zhang, Y., Rodriguez, A. L., Conn, P. J., 2005. Allosteric potentiators of metabotropic glutamate receptor subtype 5 have differential effects on different signaling pathways in cortical astrocytes. J. Pharmacol. Exp. Ther. 315, 1212-1219.

Zhou, Q., Wang, J., Zhang, X., Zeng, L., Wang, L., Jiang, W., 2013. Effect of metabotropic glutamate 5 receptor antagonists on morphine efficacy and tolerance in rats with neuropathic pain. Eur. J. Pharmacol. 718, 17-23.

Zhu, C. Z., Hsieh, G., Ei-Kouhen, O., Wilson, S. G., Mikusa, J. P., Hollingsworth, P. R., Chang, R., Moreland, R. B., Brioni, J., Decker, M. W., Honore, P., 2005. Role of central and peripheral mGluR5 receptors in post-operative pain in rats. Pain 114, 195-202.

Appendix 1

Allosteric modulation of DHPG-mediated iCa^{2+} mobilisation by DPFE, VU29 and VU0409551 at mutant $mGlu_5$ receptors (Chapter 4)

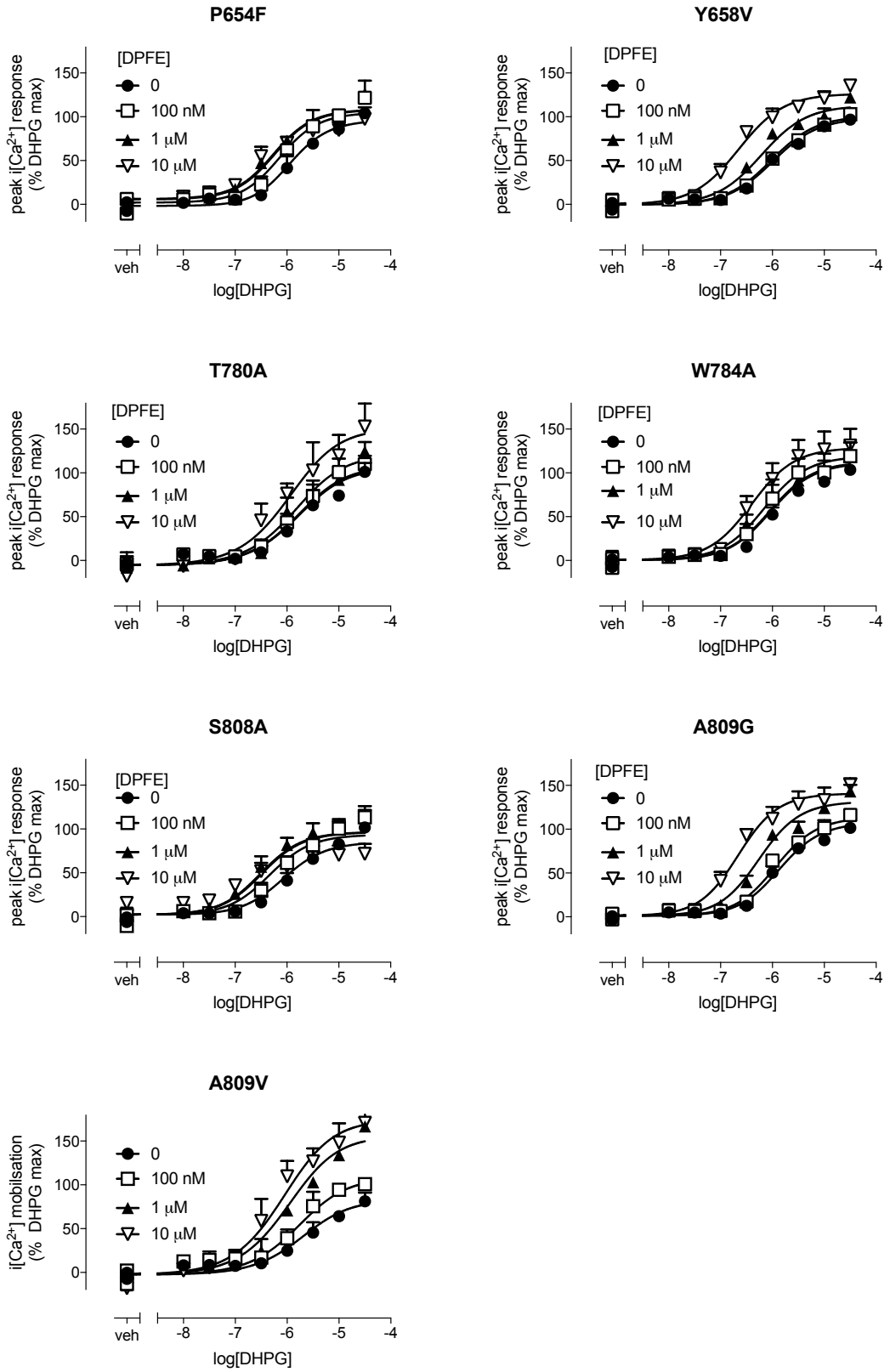

Appendix Fig 1. Allosteric modulation of DHPG-mediated iCa^{2+} mobilisation by DPFE at mutant $mGlu_5$ receptors. Data are expressed as mean ± SEM of n=3-5 independent experiments performed in duplicate.

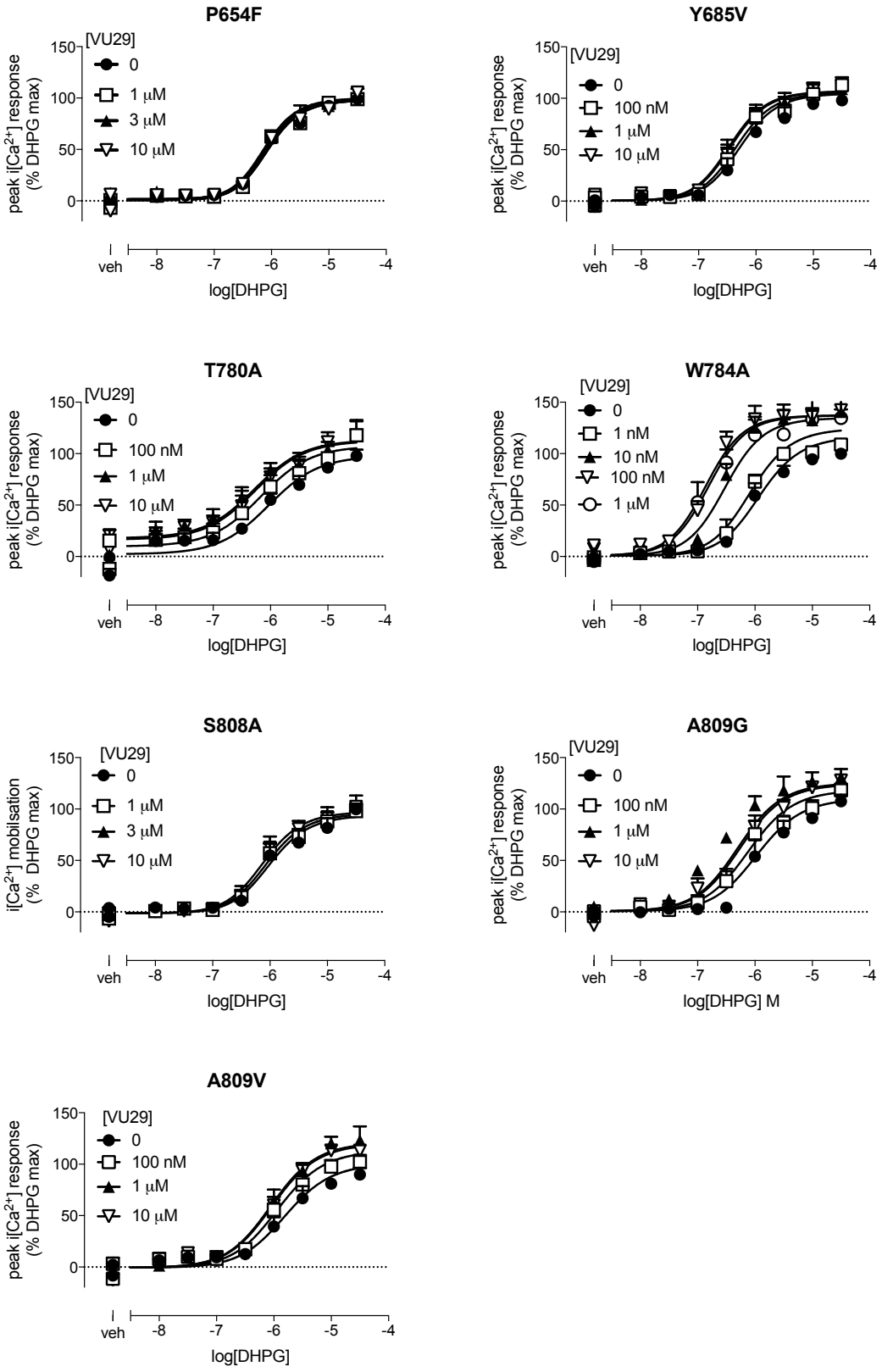

Appendix Fig 2. Allosteric modulation of DHPG-mediated iCa^{2+} mobilisation by VU29 at mutant $mGlu_5$ receptors. Data are expressed as mean ± SEM of n=3-5 independent experiments performed in duplicate.

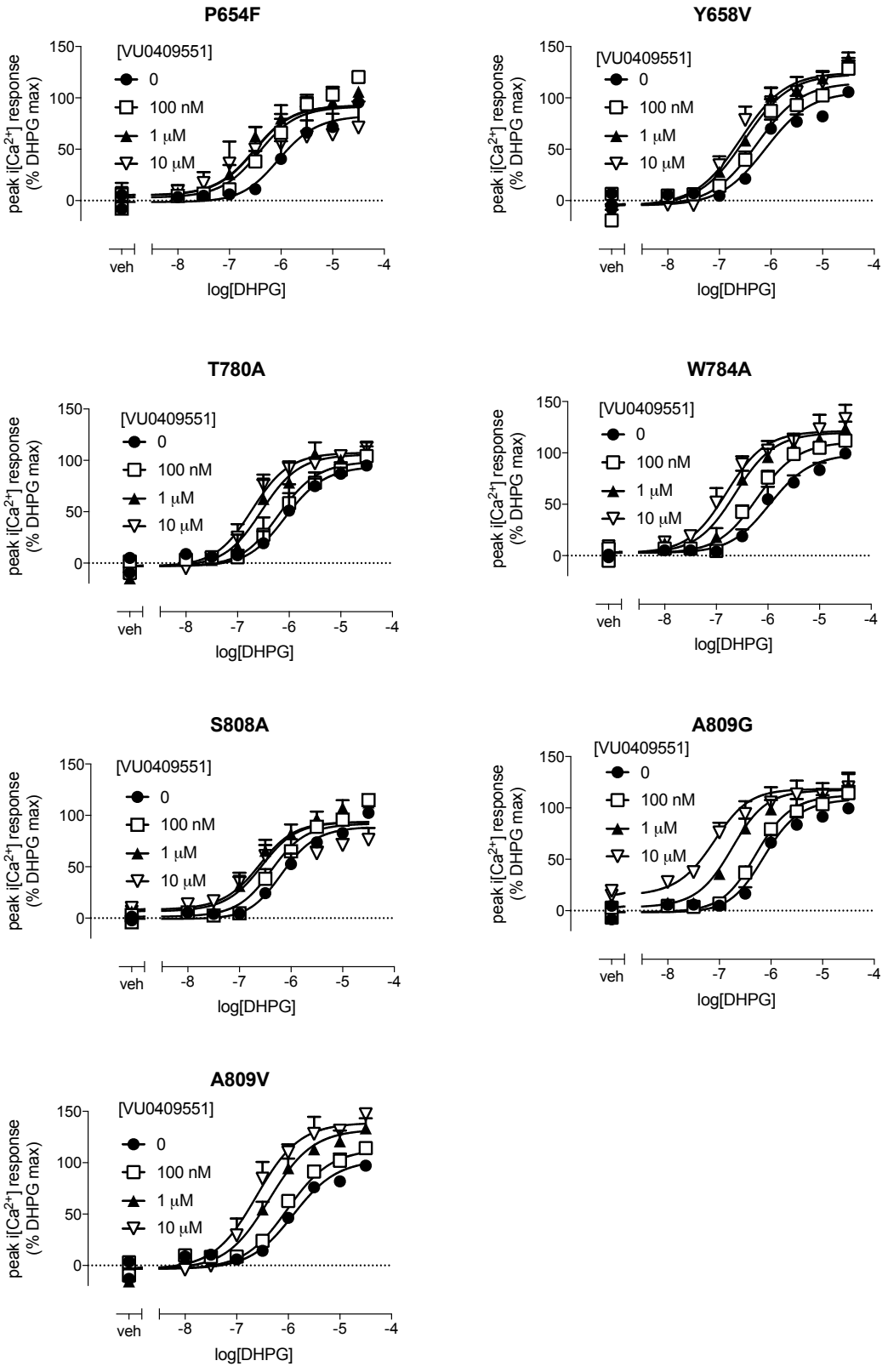

Appendix Fig 3. Allosteric modulation of DHPG-mediated iCa^{2+} mobilisation by VU0409551 at mutant $mGlu_5$ receptors. Data are expressed as mean ± SEM of n=3-5 independent experiments performed in duplicate.